ANALYSIS AND CONTROL OF MARINE CABLE SYSTEMS

Shan Huang

A thesis submitted for the degree of
Doctor of Philosophy

Department of Ship and Marine Technology
University of Strathclyde
United Kingdom
1992

For mother

SUMMARY

The thesis deals with systems consisting of marine cables and subsea units Such systems have wide applications in offshore subsea operations.

After a general introduction, the thesis sets out to analyse both the stati and dynamic behaviours of the system under various environmental and operationa conditions. It endeavours to pursue a fundamental approach in order to reveal th basic characteristics of the system, in addition to developing numerical algorithms fo predicting performance. The analysis of behaviour of marine cables consists of th following parts:

- Statics A semi-analytic approach is developed to predict the equilibriur configurations of marine cables.

- One-dimensional dynamics Using a coordinate transformation, the metho can predict the unsteady dynamic behaviour of systems where the length c cable varies.

- Two-dimensional dynamics The methodology adopted in the one-dimension analysis is extended to a more general case.

- Three-dimensional dynamics An alternative approach based upon a lumpe

mass model is developed. Mathematical analysis reveals many interesting characteristics of the model.

By applying modern control theory, a novel heave compensation mechanism is developed for marine systems of cables and subsea units. This mechanism involves an actively controlled winch system. A framework of optimal stochastic control is outlined for integrating all the elements of surface supported subsea operations.

The thesis presents a variety of numerical examples in domenstrating the validity of the approaches adopted, along with discussions. Further developments are also recommended.

Table of Contents

SUMMARY i

TABLE OF CONTENTS iii

1 INTRODUCTION 1

1.1 GENERAL REMARKS 1

1.2 BACKGROUND: SUBSEA NATURAL RESOURCES 2

1.2.1 Oil and Gas 2

1.2.2 Mineral Deposits 3

1.2.3 Miscellaneous 5

1.3 SCOPE OF THE THESIS: TETHERED SUBSEA UNITS 5

1.4 THE PRESENT INVESTIGATION 10

1.5 A BRIEF REMARK ON THE CHOSEN TOPICS 11

1.6 AIMS OF THE THESIS 14

1.7 AN OUTLINE OF THE THESIS 15

2 THREE DIMENSIONAL STATICS 19

2.1 GENERAL REMARKS 19

2.2 MATHEMATICAL MODELLING 23

2.2.1 Fundamental Assumptions 23
2.2.2 Coordinate System and Discretisation 24
2.2.3 Equilibrium Equation 25
2.2.4 Boundary Conditions 26
2.3 PARAMETRIC ANALYTIC SOLUTION 28
2.3.1 Submerged Cable 30
2.3.2 Towing Cable 31
2.3.3 Mooring Cable 31
2.4 DRAG FORCE 32
2.5 NUMERICAL ITERATION 33
2.6 NUMERICAL EXAMPLES 34
2.7 CONCLUDING REMARKS 35

3 ONE DIMENSIONAL DYNAMICS **42**
3.1 GENERAL REMARKS 42
3.2 MATHEMATICAL FORMULATION 46
3.2.1 Governing Equation 46
3.2.2 Boundary Conditions 46
3.2.3 Initial Conditions 47
3.2.4 Variable Transformation and Important Relations 47
3.2.5 Transformed Governing Equation and Boundary Conditions . 48
3.2.6 Finite Difference Discretisation 50
3.3 NUMERICAL EXAMPLES & DISCUSSION 52
3.3.1 Example One 52
3.3.2 Example Two 53

3.3.3 Example Three 54
3.3.4 Example Four 55
3.3.5 Example Five 56
3.4 CONCLUDING REMARKS 59

4 TWO DIMENSIONAL DYNAMICS 82

4.1 GENERAL REMARKS 82
4.2 EQUATIONS OF MOTION 84
4.3 PROBLEM CHARACTERISTICS 86
4.4 FORMULATION AND NUMERICAL DISCRETISATION 90
4.4.1 Boundary Conditions 90
4.4.2 Initial Conditions 91
4.4.3 Variable Transformation 92
4.4.4 Transformed Equations of Motion and Boundary Conditions 92
4.4.5 Finite Difference Discretisation 94
4.5 NUMERICAL EXAMPLES & DISCUSSION 95
4.5.1 Example One 95
4.5.2 Example Two 96
4.5.3 Example Three 97
4.5.4 Example Four 97
4.5.5 Example Five 98
4.6 CONCLUDING REMARKS 99

5 THREE DIMENSIONAL DYNAMICS 113

5.1 GENERAL REMARKS 113

5.2 FORMULATION 116
5.2.1 Governing Equations 116
5.2.2 Boundary Conditions 120
5.2.3 Initial Conditions 122
5.3 PROBLEM CHARACTERISTICS 123
5.3.1 Governing Equations 123
5.3.2 Effects of the Discretisation 125
5.4 FINITE-DIFFERENCE SOLUTION IN TIME DOMAIN 130
5.5 STABILITY OF THE NUMERICAL SCHEME 134
5.6 COMPUTATIONAL ASPECTS 139
5.6.1 Procedure 139
5.6.2 Geometrical Discretisation 139
5.7 NUMERICAL EXAMPLES 139
5.7.1 Convergence 140
5.7.2 Effect of the Current 141
5.7.3 Effect of the Excitation Frequency 142
5.7.4 Loop Turn 142
5.8 CONCLUDING REMARKS 143

6 HEAVE COMPENSATION **154**

6.1 GENERAL REMARKS 154
6.1.1 Statement of the Problem 154
6.1.2 Aim 156
6.1.3 Problem Characteristics 156
6.1.4 Approaches 157

6.1.5 Concerns of the Chapter 160
6.2 MODELLING AND DESIGN OF A REGULATOR 162
6.2.1 An Explanation of the Problem 162
6.2.2 Modelling of the winch 164
6.2.3 Modelling of the cable 166
6.2.4 Optimal control: the design of the control law 168
6.2.5 Account of the time delay 170
6.2.6 Numerical examples 172
6.3 STOCHASTIC CONTROL: AN OVERALL APPROACH 173
6.3.1 Modelling of sea waves 174
6.3.2 Modelling of vessel dynamics 176
6.3.3 Modelling of the cable/subsea unit and the winch 178
6.3.4 Stochastic optimal control design 178
6.3.5 Optimization 180
6.3.6 Numerical examples 183
6.4 DISCUSSION 184
6.5 CONCLUDING REMARKS 186

7 DISCUSSION **202**

7.1 GENERAL REMARKS 202
7.2 CONTRIBUTIONS OF THE THESIS 203
7.2.1 Statics 203
7.2.2 Dynamics 203
7.2.3 Heave Compensation 204
7.3 RECOMMENDATIONS FOR FURTHER STUDIES 204

8 CONCLUSIONS 207

9 REFERENCES 209

10 NOMENCLATURE 225

11 ACKNOWLEDGEMENT 230

12 APPENDIX: INTRODUCTION TO EQUATIONS OF MARINE CABLE DYNAMICS 231

12.1 GENERAL REMARKS 231

12.2 FORCES ON A CABLE ELEMENT 232

12.3 EQUATION OF MOTION 234

12.4 ANALYSIS IN A CARTESIAN COORDINATE SYSTEM 236

12.4.1 Cable Equations 236

12.4.2 Characteristics 237

12.4.3 Ordinary Differential equations 241

12.4.4 Propagation of Discontinuities 244

12.4.5 Linearisation 247

12.4.6 Effects of Bending Stiffness 252

12.5 ANALYSIS IN A NATURAL COORDINATE SYSTEM 254

12.5.1 Cable Equations 254

12.5.2 Characteristics 259

12.5.3 Ordinary Differential Equations 267

Chapter 1

INTRODUCTION

Roll on, thou deep and dark blue ocean – roll!
Ten thousand fleets sweep over thee in vain;
Man marks the earth with ruin – his control
Stops with the shore.

Lord Byron: *Childe Harold's Pilgrimage*

1.1 GENERAL REMARKS

Had Lord Byron lived today, he would surely have penned some different lines in place of this pessimistic sigh. The sea has never ceased to be either an inspiration source of poets, or a frontier of temptation for human beings on this rather watery planet. Having mapped the water surface and excluded all possibility of any 'Treasure Island', men delve into the water deeper and deeper beneath its surface.

Though occasionally, man dives into the deep sea out of inherent heroism or adventure, the true reason for mankind's massive march into the subsea world

has never failed to be economic. Even in ancient times people dwelling near the shore knew how to earn a living by deriving salt from the ocean. As mankind consumes inland natural resources at an ever increasing rate and new kinds of technology are constantly developing at high speed, it has become obvious that the present industrial growth cannot be met by land-based resources alone, and we both have to and are able to turn to the sea as a possible source of additional materials. Although for the time being exploitation has been confined principally to continental shelf areas where water depth is low, there is little doubt that when needed in the future, it will be moved into the deep sea region.

1.2 BACKGROUND: SUBSEA NATURAL RESOURCES

Subsea natural resources include oil and gas, which of course top the resource list in terms of value for the moment, and consolidated mineral deposits.

1.2.1 Oil and Gas

Oil and gas, which exist beneath the sea bed, can be extracted through boreholes. The history of marine drilling for oil goes back to 1938 when the Creole field was discoved in the Gulf of Mexico, but it was from the mid-1950s that offshore exploitation got its real impetus, spreading to the waters off Mexico, Brazil and Brunei. In the 1960s, the more challenging North Sea became the major battlefield between modern technology and the harsh sea. Today the oil industry has expanded to offshore waters all over the world.

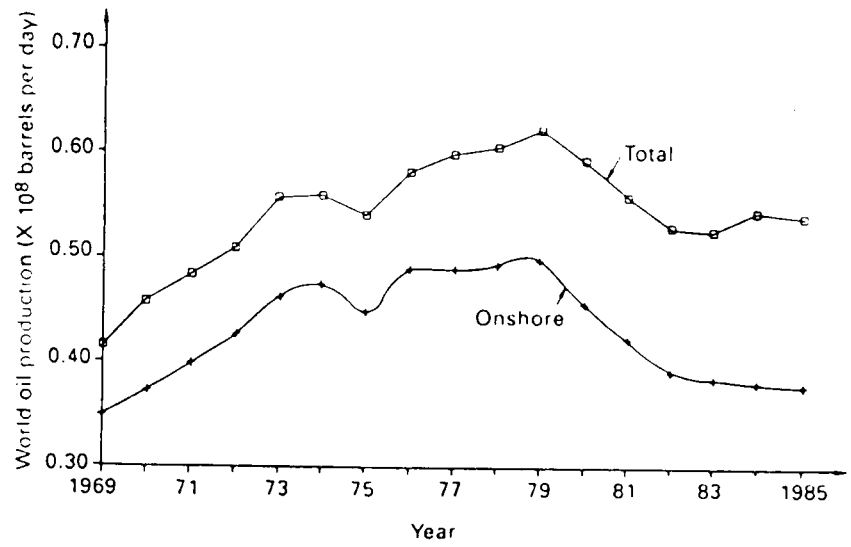

Figure 1.1: Growth of onshore and total oil production (from Patel, 1989)

production. Bearing in mind that most drilling so far has been restricted principally to near shore waters, this contribution could turn out to be even greater in the future.

1.2.2 Mineral Deposits

The subsea consolidated minerals include coal, iron ore, nickel, copper, tin, sand and gravel. As the land reserves of these materials become limited, it is quite natural for industry to move offshore to secure its need. For example, sand and gravel are extensively used in construction work. Table 1.1 shows the estimated land and marine resources and the estimated demand. Apparently, exploitation of marine resources is in this case essential if demand is to be met.

marine resources is in this case essential if demand is to be met.

Table 1.1 Comparison Between (apparent) Marine Sand and Gravel Deposits and (apparent) Land-Based Sand and Gravel Deposits

Variable	U.S.	World
Annual demand (1970)	1.02	7.45
Cumulative demand to 2000	76.70	535.00
Apparent land resources	67.00	333.00
Apparent marine resources	1690.00	31000.00

Source. Cruickshank and Hess (1976)
Note. The units represent gross market values in billions of 1972 dollars. They do not indicate economic reserves; instead, they are used for comparative purposes.

The main classes of minerals on and beneath the ocean floor occur in variou forms, from nodules and encrustations to soft-layered deposits, and are as follows.

1. Manganese nodules. These dark, potato-sized lumps which contain copper nickel, cobalt and other important metals have been identified as a potentiall large resource.

2. Cobalt crusts. This mineral is potentially more valuable. However, th prospect of exploitation is limited in the shorter term.

3. Polymetallic sulphide accumulations. These contain iron, copper, zinc an manganese in various chemical forms. Exploitation and surveying will brin more reserves to light.

4. Phosphorites. These are minerals of calcium phosphate that can be forme from decaying organisms on the sea floor. Fluorine and uranium deposits ar often associated with phosphorites, and are potentially important by-product

1.2.3 Miscellaneous

Other major types of subsea resource are:

1. Renewable energy from the thermal gradients between the surface and deeper layers of the ocean in tropic and sub-tropic areas. The process to extract the energy is known as ocean thermal energy conversion (OTEC).

2. In the future, underwater currents such as the Gulf stream and Kuroshio may also become a source of energy, extracted using an equivalent of windmills.

3. An ever-increasing world population requires the sea to play a major role in providing food resources. One example is mariculture. Though for the time being most fish farms involve conventional floating cages, concepts have been proposed to submerge the cages in deep water.

1.3 SCOPE OF THE THESIS: TETHERED SUBSEA UNIT

Tempted by such a huge resource and potential for economic gain, the development of materials, structures and equipment for use in the harsh environment of the oceans has been expanded rapidly in the past few decades. Among the various technical achievements, tethered subsea units have played an important role and are widely used in practice to fulfill certain tasks such as:

1. Mapping the Exclusive Economic Zones

   Before the deep sea and the sea bed can be utilized, it will be necessary to have a comprehensive and accurate picture of the physical, chemical and geological characteristics of the environment.

2. Pipeline Surveying

   This includes inspection to identify whether the pipeline is damaged or not and to locate any stresses which might cause it to fail. Also before laying the pipeline, it is necessary to survey the seabed to determine a suitable route.

3. Offshore Platform Inspection, Repair and Maintenance

   To assess the safety of older platforms and maintain standards in order to comply with governmental regulations, it is imperative to inspect the submerged parts of platforms frequently.

4. Seabed Object Detection and Classification

   There is growing effort to detect, classify and recover items from the seabed in deep water. Such items may include crash debris and shipwrecked articles. The skills involved in performing such tasks also have military applications such as mine detection.

5. Subsea Construction and Destruction

   As production moves into deeper water where divers can no longer reach, tethered subsea units have to play a more important role in constructing seabed structures. A similar task is the decommissioning of abandoned subsea installa-

tions which have ceased operating, as awareness of environmental conservatio increases.

6. Deep Sea Rescue

   This task includes rescuing divers in detached diving vessels, or crews in th case of submarine accidents.

7. Environmental Monitoring

   Tethered subsea units are used to monitor the marine environment. Specia attention is paid to over-enrichment or depletion of oxygen in coastal waters the physical modification of sea bed habitats, pollution damage to fish an shellfish, and coastal erosion.

There is no question that as exploitation and production moves into deepe water, we will observe a continued increase in tethered subsea unit intervention.

However, frequent accidents during operations resulting in the loss of th subsea units and an inability to carry out designated tasks accurately indicate demand for better understanding of the whole system. Daunting and comple problems are still to be solved. These problems can be categorised as follows:

1. Surface Support

   Though the use of submersible support vessels has been suggested, most sub sea interventions are controlled from conventional surface vessels. As it i often required that the surface support vessel should remain sensibly statio ary, various techniques have been applied in holding such vessels against th

forces of environment. Since the first dynamically positioned ship, *The Glomar Challenger*, around 1970, numerous dynamically positioned vessels have been constructed. The idea of dynamical positioning is to match the mean loadings imposed by the environment with counter forces exerted by the onboard thrusters. However, efforts are still needed as the methods available to estimate these mean hydrodynamic loadings are not entirely satisfactory, especially with regard to high order wave forces.

2. Marine Cable Statics and Dynamics

   The importance of the cable is manifested by the fact that it is the sole link between the surface support vessel and the subsea unit. Any failure occurring to it, such as breakage due to excessive tension in the cable, almost inevitably means the loss of the subsea unit. Furthermore, as the subsea unit is linked to the cable, its performance can be significantly influenced by the presence of the cable.

3. Subsea Unit Design

   The design of the subsea unit is still a formidable task because of its complex dynamic behaviour in interaction with the surrounding fluid medium. The external shape of the unit is an important factor which principally determines the hydrodynamic characteristics and, therefore, has great effect upon the crucial operational abilities of the subsea unit such as stability, manoeuvrability and speed.

4. Control and Communication

Control and communication are indispensable in subsea intervention. The manoeuvring of the subsea unit in deep water is entirely dependent upon the control of the thruster forces. Communication between the tethered subsea unit and the surface supporting vessel is another crucial factor which becomes both more necessary and more difficult as the operational depth of the subsea unit increases. Due to signal attenuation over the transmission line and the requirements for higher speed data transmission and multiple video systems, the linking cable grows to excessive diameter and weight. As a result, novel methods of communication need to be developed.

5. Relevant Problems

There are some problems arising from the integration of the different parts described above into a coherent operational system. For example, the deployment of a subsea unit requires a handling system through which the supporting vessel introduces disturbances to the cable, sometimes resulting in snap loadings. Such snap loadings can greatly increase the amount of cable tension and therefore can be detrimental. Hence, it is necessary to introduce a motion compensation mechanism which will reduce the dynamic vessel disturbance to the cable in a given sea state and extend the range of sea states in which operations can continue.

Other relevant problems include the interaction between the subsea unit and the vessel when the subsea unit is heavy enough to influence the vessel dynamics.

1.4 THE PRESENT INVESTIGATION

Needless to say, this thesis can not cover all the problems identified in the previous section arising from subsea intervention using tethered subsea units. We confine ourselves to the following two areas:

- Behaviour of marine cables (including cable-unit systems).
- Heave compensation.

The selection of these two topics is based upon the following considerations:

1. The fact that a cable links the subsea unit to the support vessel is the essential feature of the subsea operation. This justifies the selection of the marine cable as an appropriate starting point for the whole theoretical conquest of operations involving tethered subsea units deployed from a floating vessel.

2. Once we have a firm grasp of the behaviour of marine cables, the next step forward is naturally to consider the integration of the cable-unit system with the floating vessel and the auxiliary handling systems, assuming that the available theories on the mechanics of offshore floating vessels can adequately describe their motion. It is at this stage that we begin to consider the heave compensation.

The selection of research areas dictates the structure of the present investigation. Following the conventional rule, we shall first proceed to deal with simpler problems, and gradually move to more general and difficult areas. This idea and the structure of the present investigation is illustrated in Figure 1.2.

1.5 A BRIEF REMARK ON THE CHOSEN TOPICS

Research on cables in the air is almost as old as our civilisation, first attracting attention because of their use in stringed musical instruments. Pythagoras in the 6th century B.C. and Aristotle in 3rd century B.C. knew quantitatively the relation between frequency, tension and length of a taut chord. Since the Renaissance, cable research work bears the names of great mathematicians and scientists such as Leonardo da Vinci, Galileo, the Bernoullis, Leibnitz and Euler. In the early 18th century, the vibration of taut cables attracted much interest from many great mathematicians. 'To the mathematicians', wrote Lord Rayleigh, 'they must always possess a peculiar interest as the battlefield on which were fought out the controversies of D'Alembert, Euler, Bernoulli and Lagrange, relating to the nature of the solution of partial differential equations.' (Lord Rayleigh, 1945).

In our modern time, cables and cable networks in the air medium still remain a research topic, especially in the fields of civil engineering and architecture (Otto, 1967; Argyris et al, 1974; Buchholdt, 1985).

By comparison, research on marine cables started much later. Probably

the first event to attract the attention of leading scientists to this problem was the failure of the laying of the first trans-Atlantic cable in 1857 when amongst others Lord Kelvin and G. B. Airy considered its analysis (Lord Kelvin, 1857; Airy, 1858; Gravatt, 1858; Woolhouse, 1860).

However, it was only several decades ago that the previously sporadic research into marine cables moved into a new phase of progressive and systematic research as the increasing subsea activities involved in offshore oil and gas exploitation required a good understanding of their statics and dynamics. The main research areas concerned can be conveniently separated into the following groups:

1. Effects of the surrounding fluid medium

The difference between a cable in air and one in water lies in the fact that for the former, the effects of the surrounding fluid medium are often negligible whilst for the latter this is not so. This indicates that a good understanding of the effects imposed by the surrounding fluid medium, namely water, upon the cable and the subsea unit is a prerequisite to the analysis of the cable. This partially explains the reason why research on marine cables could only be sporadic before the advent of modern hydrodynamics theory in this century. Although we are now much better equipped with the theory of hydrodynamics, to fully understand, and therefore to predict the hydrodynamic effects on marine cables remains as daunting as ever. The complex phenomenon of fluid passing around a cable involves a laminar boundary, flow separation, vortex shedding, turbulence and other factors. A complete theoretical method is en-

tirely untenable, at least for the time being. This untidy state forces us to rely upon empirical formulae.

2. Statics

   Though there can be hardly a marine cable system which remains static in the ever changing environment of the sea, a static analysis can nevertheless be a fair approximation to many practical problems, especially when only a quick estimation is required. Needless to say, the static problem is normally far easier than the corresponding dynamic one in terms of both theoretical analysis and numerical computation.

3. Dynamics

   Due to environmental disturbances, such as water surface waves and current, systems of cables are continuously subject to dynamic loading. Traditionally, the dynamic behaviour of a marine cable was not regarded as an important aspect of its practical design and operation, dynamic loading being covered by a safety factor based upon the static analysis. However, in the last decade or so the dynamic behaviour has gained increasing interest for the following reasons:

   - It is desired to reduce the frequency of cable breakages.
   - New types of system with new materials are being proposed. These systems are expected to exhibit dynamic behaviour which is different from that found in traditional systems.

- With increasing awareness of risk the demand for reliability assessment is increasing.
- Development of the computer and advanced computation methods has brought the cost of dynamic analysis down to a moderate level.

As for theoretical work on heave compensation, this remains almost untouched with a heavy emphasis on empirical design. Heave compensation is however useful if the subsea intervention requires either or both of the following:

1. Decoupling of the subsea unit from the supporting vessel's heave motion.
2. Reduction of the tension in the cable.

1.6 AIMS OF THE THESIS

The present thesis aims to take on the following tasks:

1. To assess the state of research in the fields of marine cable analysis and heave compensation in order to identify areas to which the present endeavour should be directed.
2. To establish the governing equations for a three dimensional marine cable, and to conduct a general mathematical analysis in order to explore the fundamental characteristics of the equations.
3. To develop numerical solutions of the governing equations to predict static and dynamic behaviour of marine cables.

4. Based upon the accomplishment of the three tasks above, to develop a feasible active control mechanism, which can effectively compensate the heave motion, by using modern control theory.

5. To seek as much available experimental information as possible to verify the methods developed.

6. To summarise and recommend future developments.

1.7 AN OUTLINE OF THE THESIS

The thesis can be seen as a nine-piece jigsaw assembled logically to meet the aims defined in the previous section and to reflect the structure depicted in Figure 1.2. The nine parts are the present chapter which defines the problem and route to solution, Chapters 2 to 6 which form the core of the thesis, Chapters 7 and 8, and an appendix which contains the derivation of the governing equations for marine cable dynamics as a foundation of both static and dynamic analyses.

Chapters 2 to 6 form the central part of the thesis. Each of these contains basically three parts. The first part states the problem, carries out a review on relevant past work and defines the strategy. The second part is the core of the chapter. It sets out to develop a theoretical approach to solve the problem stated. The final part presents numerical examples along with discussions. Further modifications are also suggested in this part.

In Chapter 2, a method to solve static marine cable problems is developed.

This method avoids solving a large number of simultaneous algebraic equations by exploiting the analytical properties of the governing equation, resulting in a robust approach which needs solve no more than three simultaneous equations. In addition, it can handle different types of boundary conditions easily.

In Chapter 3, one-dimensional dynamic behaviour of marine cables is investigated by invoking the finite difference method. By introducing a coordinate transformation, unsteady dynamics where the length of cable is varying and the steady dynamics where the length is fixed can be solved in a uniform manner.

In Chapter 4, the method developed in Chapter 3 is extended to the two-dimensional case. Analysis is provided to show the relation between the previous model and the two-dimensional one, hence indicating which model should be employed in any given circumstance.

In Chapter 5, the steady dynamics of marine cables is analysed in three dimensions using a lumped-mass model. A great deal of theoretical analysis is carried out to reveal the basic characteristics of the model. The numerical solution is based upon the finite difference approximation and the Fourier stability method is employed to analyse the stability of the numerical scheme developed.

In Chapter 6, a theoretical approach for heave compensation is developed. After properly modelling each element of the system, which includes the cable, the winch and the motion of the vessel due to waves, modern control theory is then applied to design a feedback control system.

In Chapter 7, the contributions of the thesis are summarised, and further

developments are recommended. The thesis is concluded in chapter Chapter 8.

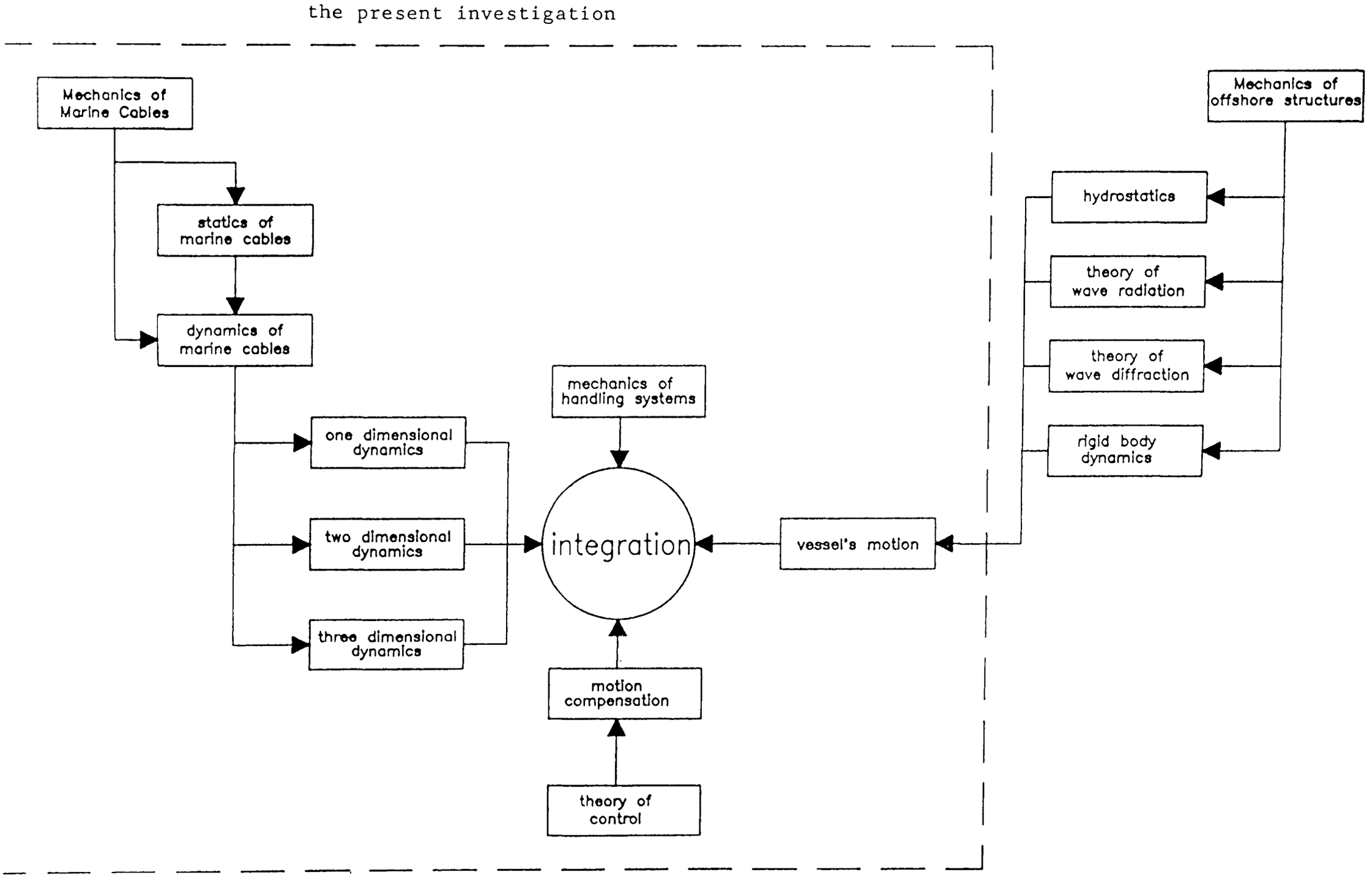
the present investigation
Mechanics of Marine Cables
statics of marine cables
dynamics of marine cables
one dimensional dynamics
two dimensional dynamics
three dimensional dynamics
mechanics of handling systems
integration
motion compensation
theory of control
vessel's motion
Mechanics of offshore structures
hydrostatics
theory of wave radiation
theory of wave diffraction
rigid body dynamics

Figure 1.2

Chapter 2

THREE DIMENSIONAL STATICS

But his little daughter whispered
As she took his icy hand
'Isn't God upon the ocean
Just the same as on the land?'

James T. Fields: *The ballad of the Tempest*

2.1 GENERAL REMARKS

Neglecting dynamic excitation due to wave action on a moored structure or support vessel and variation of underwater current in the time domain, the cable system can be treated as a static one under the action of steady underwater current and/or steady thruster forces acting on the subsea unit.

In addition to its tensile properties, tether cable often serves to contain items necessary for subsea operations such as power conductors, instrumentation lines and

lines and fibre optics. As a result, the diameter of the cable is increased such that the hydrodynamic drag effect of the underwater current can not be ignored and the cable can no longer be treated as a catenary in air. In fact the static performance of a marine cable is severely limited by drag, especially so when it works in deep water or under strong current.

There are four different types of marine cable system which can be tackled by a static theory. They are shown in Figure 2.1:

1. Submerged Cable System

   The cable is fixed at both ends to stationary structures. It is necessary to evaluate the variation in cable tension along its length and the configuration of the cable. This system also has aeronautical applications for glider cables and in-flight refuelling lines where the drag force can not be neglected due to the high speed.

2. Towing Cable System

   The upper end is joined to an advancing ship on the ocean surface. The lower end is connected to a subsea unit. The unit itself may have its own propulsion system. In this case it is necessary to know the location of the subsea unit. This is of practical importance for subsea operations as it can show whether certain locations can be reached or not.

3. Mooring Cable System

   The upper end of the cable is connected to a floating vessel or a buoy on the

surface, while the lower end is fixed upon the sea floor by an anchor. Tension in the cable and position of the moored body are the primary concerns in this case.

4. Footprint Problem

   For reasons such as underwater inspection and maintenance, a tethered subsea unit is often required to crawl over an area of the sea bed by means of thruster force. The so-called footprint of the unit is defined as the outer boundary of the operational area of the unit on the ocean floor under given operational conditions.

The importance of the static analysis of marine cables is three-fold:

1. Many questions of practical importance can be answered without a full dynamic analysis which is undoubtedly more expensive.

2. When dynamic analysis is needed, it is often linearized as a perturbation problem around the static solution. In this case, the static analysis becomes a prerequisite to the dynamic analysis.

3. Static modelling and theoretical prediction provides a cheap and quick technique through which the interaction between the various parameters can be understood and a better design achieved. It is especially useful for the preliminary design.

A number of different approaches have been adopted to solve the static problem under various assumptions and simplifications (Eames, 1968; Ferriss, 1979; Every,

1982; Sayer, 1989; Macgregor, 1990). Most assumptions are made regarding the following aspects:

1. Dimension

   Quite a few practical problems can be modelled as two-dimensional problems which, needless to say, are easier than three-dimensional ones.

2. Elasticity

   A lot of static problems involve little elastic deformation which provides a sound basis for the treatment of the cable as an inelastic one. The governing equations for an inelastic cable are slightly simpler than those for an elastic cable.

3. Nature of the drag

   The drag caused by the current passing around the cable is still an unsolved problem. Hence, it is an area open to different manipulations with no one having more theoretical justifications than others.

The cable analysis is basically a two point boundary value problem where some or all of the boundary values are known at either end of the cable. Dependent upon the types of practical problem, boundary conditions of different kinds are imposed. A common flaw lying in most available methods is the inability to handle the different types of boundary conditions in a uniform manner. For example, the method by Macgregor (1990) can only solve the towing cable system described above readily and effectively. Another feature of the existing research is that while most authors have experimented with different numerical techniques in solving the governing

equations, they have failed to explore the analytic properties, rendering the numerical solutions both less efficient and less accurate.

In comparison with the numerous applications of cables in marine operations the theoretical research work is hardly proportional, and the experimental research work is even less so. Little work has been done specifically on the equilibrium configuration of marine cables, especially in the three-dimensional case. As a result, it is difficult to verify and confirm theoretical results against experimental ones.

In this chapter a rather general semi-analytical method has been developed. The basic idea is to consider a three-dimensional cable under a given distribution of many point loads. A compact exact solution is derived as a function of three parameters only which can be solved numerically by implementing different kinds of boundary condition. The real marine cable, where the drag load can not be given beforehand, is solved by using an iterative procedure.

2.2 MATHEMATICAL MODELLING

2.2.1 Fundamental Assumptions

The modelling is based upon the following assumptions:

1. Zero torsional stiffness. Though kinking and twisting may occur in practice, torsion can be ignored for most situations.

2. Zero bending stiffness. The cable is assumed to be completely flexible. Therefore, the cable sustains no internal force other than tension.

3. The tension is non-negative.

4. The cable is uniform.

5. Hydrodynamic loading acting on an element of the cable depends only upon the dimensions of that element, the angle of that element to the current and the current speed, and is not affected by neighbouring elements. The loading can be resolved into two components of normal and tangential forces which are dependent upon the normal component and the tangential component of the current velocity respectively.

2.2.2 Coordinate System and Discretisation

We define a Cartesian coordinate system (x, y, z), as shown in Figure 2.2. Let s and p be the unstrained and the strained arc lengths along the cable, respectively. Maintaining generality, it is possible to let one end of the cable stay at the origin of the coordinate system.

Conceptually, a continuous marine cable can be discretised into many small segments each under one point load which as a whole represent the distributed drag force along the cable. The end points of the segments and the point loads are numbered by index i which runs from 0 at one end to N at the other.

2.2.3 Equilibrium Equation

The statement of equilibrium at a point P between the coordinates p_n and p_{n+1} on the strained cable profile gives:

$$T\frac{dx}{dp} = -V_x - \sum_{i=0}^{n} F_x^i \tag{2.1}$$

$$T\frac{dy}{dp} = -V_y - \sum_{i=0}^{n} F_y^i \tag{2.2}$$

$$T\frac{dz}{dp} = -V_z - \sum_{i=0}^{n} F_z^i - \frac{W}{L}s \tag{2.3}$$

where T is the cable tension. V_x, V_y and V_z are the three components of the force acting on the end $s = 0$. F_x^i, F_y^i and F_z^i are the external force components acting on the i-th cable segment. L is the unstrained length of the whole cable and W is its weight in the fluid.

In addition to the force equilibrium, the cable must satisfy the compatibility relation and the constitutive relation. They are:

- Compatibility relation:

$$(\frac{dx}{dp})^2 + (\frac{dy}{dp})^2 + (\frac{dz}{dp})^2 = 1 \tag{2.4}$$

- Constitutive relation: which is a mathematical expression of Hooke's law

$$T = EA(\frac{dp}{ds} - 1) \tag{2.5}$$

where E is Young's modulus. A is the cross-sectional area of the cable in the unstrained profile.

2.2.4 Boundary Conditions

The mathematical formulation of the problem is completed by the addition of the boundary conditions. Corresponding to the four types of marine cable system, there are four sets of boundary conditions:

1. Both ends of the cable are fixed at known points, i.e.,

$$x(0) = y(0) = z(0) = 0 \tag{2.6}$$

and

$$x(L) = x_L, y(L) = y_L, z(L) = z_L \tag{2.7}$$

where coordinates x_L, y_L and z_L are given.

2. One end is fixed, the other subjected to known force components, i.e.,

$$x(0) = y(0) = z(0) = 0 \tag{2.8}$$

and

$$T\frac{dx}{dp}|_{s=L} = T_x \tag{2.9}$$

$$T\frac{dy}{dp}|_{s=L} = T_y \tag{2.10}$$

$$T\frac{dz}{dp}|_{s=L} = T_z \tag{2.11}$$

where T_x, T_y and T_z are given.

3. Mooring Cable. The boundary conditions are a combination of the two above, i.e.,

$$x(0) = y(0) = z(0) = 0 \tag{2.12}$$

and

$$T\frac{dx}{dp}|_{s=L} = T_x \tag{2.13}$$

$$T\frac{dy}{dp}|_{s=L} = T_y \tag{2.14}$$

$$z(L) = z_L \tag{2.15}$$

4. Footprint. In this case, setting the boundary condition becomes a maximization problem with equality and inequality constraints. It could be defined as the following:

$$x(0) = y(0) = z(0) = 0 \tag{2.16}$$

and

$$Max[(x(L) - x(0))^2 + (y(L) - y(0))^2] \tag{2.17}$$

under the constraints:

$$0 < \quad L \quad \leq L_{max}$$

$$0 \leq \quad T_x \quad \leq T_{xmax}$$

$$0 \leq \quad T_y \quad \leq T_{ymax}$$

$$0 \leq \quad T_z \quad \leq T_{zmax}$$

$$z(L) = z_L$$

$$x(L) - x(0) = c_1 cos(\vartheta)$$

[1] In general T_x and T_y, being dependent upon the tension T, can not be given beforehand. An iterative scheme is usually required.

$$y(L) - y(0) = c_1 sin(\vartheta)$$

for all the ϑ in the range $[0, 2\pi]$. The parameters of the operational conditions $L_{max}, T_{xmax}, T_{ymax}, T_{zmax}$ are all given, and c_1 is arbitrary.

2.3 PARAMETRIC ANALYTIC SOLUTION

We are now in a position to derive the parametric solution that describes the strained cable profile.

By invoking the following relations:

$$\frac{dx}{ds} = \frac{dx}{dp}\frac{dp}{ds} \tag{2.18}$$

$$\frac{dy}{ds} = \frac{dy}{dp}\frac{dp}{ds} \tag{2.19}$$

$$\frac{dz}{ds} = \frac{dz}{dp}\frac{dp}{ds} \tag{2.20}$$

and noting that $\frac{dp}{ds}$ is given as a function of the tension T through Eq. (2.5), we have:

$$\frac{dx}{ds} = -\frac{1}{T}(V_x + \sum_{i=0}^{n} F_x^i)(\frac{T}{EA} + 1) \tag{2.21}$$

$$\frac{dy}{ds} = -\frac{1}{T}(V_y + \sum_{i=0}^{n} F_y^i)(\frac{T}{EA} + 1) \tag{2.22}$$

$$\frac{dz}{ds} = -\frac{1}{T}(V_z + \sum_{i=0}^{n} F_z^i + \frac{W}{L}s)(\frac{T}{EA} + 1) \tag{2.23}$$

where T is given as the following by squaring Eqs.(2.1), (2.2) and (2.3) and substituting them into the compatibility relation:

$$T = \sqrt{(V_x + \sum_{i=0}^{n} F_x^i)^2 + (V_y + \sum_{i=0}^{n} F_y^i)^2 + (V_z + \sum_{i=0}^{n} F_z^i + \frac{W}{L}s)^2} \tag{2.24}$$

Integrating these equations over the interval $[s_n, s_{n+1}]$ gives:

$$x(s_{n+1}) = x(s_n) + \int_{s_n}^{s_{n+1}} \frac{dx}{ds} ds = x(s_n) + \triangle x(s_n) \tag{2.25}$$

$$y(s_{n+1}) = y(s_n) + \int_{s_n}^{s_{n+1}} \frac{dy}{ds} ds = y(s_n) + \triangle y(s_n) \tag{2.26}$$

$$z(s_{n+1}) = z(s_n) + \int_{s_n}^{s_{n+1}} \frac{dz}{ds} ds = z(s_n) + \triangle z(s_n) \tag{2.27}$$

where

$$\triangle x(s_n) = \int_{s_n}^{s_{n+1}} \frac{dx}{ds} ds \tag{2.28}$$

$$\triangle y(s_n) = \int_{s_n}^{s_{n+1}} \frac{dy}{ds} ds \tag{2.29}$$

$$\triangle z(s_n) = \int_{s_n}^{s_{n+1}} \frac{dz}{ds} ds \tag{2.30}$$

After some mathematical manipulation, the integrations result in the following:

$$\begin{aligned} \triangle x(s_n) &= -\frac{V_x + \sum_{i=0}^{n} F_x^i}{EA}(s_{n+1} - s_n) + \frac{L(V_x + \sum_{i=0}^{n} F_x^i)}{W}[\\ &\quad sinh^{-1}\frac{-(V_z + \sum_{i=0}^{n} F_z^i + \frac{W}{L}s_{n+1})}{\sqrt{(V_x + \sum_{i=0}^{n} F_x^i)^2 + (V_y + \sum_{i=0}^{n} F_y^i)^2}} - \\ &\quad sinh^{-1}\frac{-(V_z + \sum_{i=0}^{n} F_z^i + \frac{W}{L}s_n)}{\sqrt{(V_x + \sum_{i=0}^{n} F_x^i)^2 + (V_y + \sum_{i=0}^{n} F_y^i)^2}}] \end{aligned} \tag{2.31}$$

$$\begin{aligned} \triangle y(s_n) &= -\frac{V_y + \sum_{i=0}^{n} F_y^i}{EA}(s_{n+1} - s_n) + \frac{L(V_y + \sum_{i=0}^{n} F_y^i)}{W}[\\ &\quad sinh^{-1}\frac{-(V_z + \sum_{i=0}^{n} F_z^i + \frac{W}{L}s_{n+1})}{\sqrt{(V_x + \sum_{i=0}^{n} F_x^i)^2 + (V_y + \sum_{i=0}^{n} F_y^i)^2}} - \\ &\quad sinh^{-1}\frac{-(V_z + \sum_{i=0}^{n} F_z^i + \frac{W}{L}s_n)}{\sqrt{(V_x + \sum_{i=0}^{n} F_x^i)^2 + (V_y + \sum_{i=0}^{n} F_y^i)^2}}] \end{aligned} \tag{2.32}$$

$$\begin{aligned} \triangle z(s_n) &= \frac{L}{2WEA}[(V_z + \sum_{i=0}^{n} F_z^i + \frac{W}{L}s_n)^2 - \\ &\quad (V_z + \sum_{i=0}^{n} F_z^i + \frac{W}{L}s_{n+1})^2] + \frac{L}{W}[\end{aligned} \tag{2.33}$$

$$\sqrt{(V_x+\sum_{i=0}^{n}F_x^i)^2+(V_y+\sum_{i=0}^{n}F_y^i)^2+(V_z+\sum_{i=0}^{n}F_z^i+\frac{W}{L}s_n)^2}-$$
$$\sqrt{(V_x+\sum_{i=0}^{n}F_x^i)^2+(V_y+\sum_{i=0}^{n}F_y^i)^2+(V_z+\sum_{i=0}^{n}F_z^i+\frac{W}{L}s_{n+1})^2}]$$

These analytical solutions are given as functions of three unknown parameters, i.e., V_x, V_y and V_z. The remaining part of this section is concerned with the solution of them. In doing so, we shall confine ourselves to the submerged cable, the towing cable and the mooring cable. To seek direct solution of the footprint problem would not be easy. It can, however, be achieved through solving the less difficult towing cable problem iteratively (Sayer et al, 1989).

2.3.1 Submerged Cable

By using Eqs. (2.25), (2.26) and (2.27) repeatedly, we have:

$$\sum_{i=0}^{N-1}\triangle x(s_i)=x(L)-x(0) \tag{2.34}$$

$$\sum_{i=0}^{N-1}\triangle y(s_i)=y(L)-y(0) \tag{2.35}$$

$$\sum_{i=0}^{N-1}\triangle z(s_i)=z(L)-z(0) \tag{2.36}$$

The solution of this nonlinear algebraic equation system gives the answer for the three unknowns.

Once V_x, V_y and V_z are known, the coordinates of any points between s_n and s_{n+1} on the strained cable profile are given by:

$$x(s)=x(0)+\sum_{i=0}^{n-1}\triangle x(s_i)+\int_{s_n}^{s}\frac{dx}{ds}ds \tag{2.37}$$

$$y(s) = y(0) + \sum_{i=0}^{n-1} \Delta y(s_i) + \int_{s_n}^{s} \frac{dy}{ds} ds \tag{2.38}$$

$$z(s) = z(0) + \sum_{i=0}^{n-1} \Delta z(s_i) + \int_{s_n}^{s} \frac{dz}{ds} ds \tag{2.39}$$

and the tension is given by Eq. (2.24).

2.3.2 Towing Cable

This is an easier situation. The unknowns V_x, V_y and V_z can be calculated directly by the following relations:

$$V_x = -T_x - \sum_{i=0}^{N} F_x^i \tag{2.40}$$

$$V_y = -T_y - \sum_{i=0}^{N} F_y^i \tag{2.41}$$

$$V_z = -T_z - \sum_{i=0}^{N} F_z^i - W \tag{2.42}$$

2.3.3 Mooring Cable

In this case, two force components can be found readily from:

$$V_x = -T_x - \sum_{i=0}^{N} F_x^i \tag{2.43}$$

$$V_y = -T_y - \sum_{i=0}^{N} F_y^i \tag{2.44}$$

and the third one V_z is solved from

$$\sum_{i=0}^{N-1} \Delta z(s_i) = z(L) - z(0) \tag{2.45}$$

2.4 DRAG FORCE

In this section the hydrodynamic drag force acting on one segment is detailed.

Let $\mathbf{U} = \{U_x, U_y, U_z\}$ represent the averaged current velocity vector at the i-th cable segment which has two end points with coordinates (x_i, y_i, z_i) and $(x_{i-1}, y_{i-1}, z_{i-1})$. The normal drag component $\mathbf{F}_N$ and the tangential drag component $\mathbf{F}_\tau$ are given by:

$$\mathbf{F}_N = \frac{1}{2}\rho C_N dl |\mathbf{U}_N| \mathbf{U}_N \tag{2.46}$$

$$\mathbf{F}_\tau = \frac{\pi}{2}\rho C_\tau dl |\mathbf{U}_\tau| \mathbf{U}_\tau \tag{2.47}$$

where C_N and C_τ are the normal and the tangential drag coefficients respectively. d is the diameter of the cable and ρ is the density of the fluid. $l, \mathbf{U}_\tau, \mathbf{U}_N$ are given by:

$$l = \sqrt{(x_i - x_{i-1})^2 + (y_i - y_{i-1})^2 + (z_i - z_{i-1})^2}$$

$$\begin{aligned}
\mathbf{U}_\tau &= \{U_{\tau x}, U_{\tau y}, U_{\tau z}\} \\
&= \{\frac{1}{l^2}[U_x(x_i - x_{i-1})^2 + U_y(x_i - x_{i-1})(y_i - y_{i-1}) + U_z(x_i - x_{i-1})(z_i - z_{i-1})], \\
&\quad \frac{1}{l^2}[U_x(x_i - x_{i-1})(y_i - y_{i-1}) + U_y(y_i - y_{i-1})^2 + U_z(y_i - y_{i-1})(z_i - z_{i-1})], \\
&\quad \frac{1}{l^2}[U_x(x_i - x_{i-1})(z_i - z_{i-1}) + U_y(y_i - y_{i-1})(z_i - z_{i-1}) + U_z(z_i - z_{i-1})^2]\}
\end{aligned}$$

$$\mathbf{U}_N = \{U_x - U_{\tau x}, U_y - U_{\tau y}, U_z - U_{\tau z}\}$$

2.5 NUMERICAL ITERATION

To calculate the cable profile by using Eqs. (2.37), (2.38) and (2.39), F_x^i, F_y^i and F_z^i $(i = 0, 1, 2, ..., N)$ must be known. These drag forces, however, depend upon the cable profile, and they can not be known beforehand. In fact they are one part of the solution themselves. As a result, an iterative scheme must be used to solve the problem, as shown in Figure 2.3.

Inside this global iteration, there exists another smaller iterative loop to solve the nonlinear algebraic equation system of Eqs. (2.34), (2.35) and (2.36) or Eq. (2.45), if the submerged cable problem or mooring cable problem is to be solved. The Newton-Raphson method is used here to seek the solution by solving a succession of linear equation systems.

As is always true for a nonlinear problem involving an iterative solution procedure, the initial estimation plays an important role. A bad starting estimate can either deteriorate the overall efficiency or make the procedure totally unworkable. In the present study the initial approximation is based upon the zero hydrodynamic load situation. This is good for the cases where the cable experiences a light drag force in comparison with its own weight in the fluid. When the drag force becomes dominant, however, more iterations are needed to increase the current speed step by step until the prescribed value. The results of the previous iteration serve as the starting estimate of the present iteration.

2.6 NUMERICAL EXAMPLES

The above analysis forms a suite of programs which predicts the equilibrium profile of a marine cable. In this section we present some results to demonstrate the validity of the method.

Figure 2.4 shows an elastic steel catenary configuration in air predicted by the present method. It is suspended between two rigid supports which are not at the same level. Shown on the same figure is the exact analytic solution (Irvine, 1981). They agree with each other very well.

Figure 2.5 shows the change in configuration of a hanging cable in air under the action of a point load.

Figures 2.6 and 2.7 show theoretical predictions of marine cables in ocean current against the results of experimental measurements. In Figure 2.6 the cable is 350m long and in Figure 2.7 it is 300m long. Both have a diameter of 0.032m, Young's modulus of $2 \times 10^{11} N/m^2$, and the same weight distribution in water of $2.25 N/m$. The results correspond to a current speed of 0.514m/sec for both cases. The agreement between the theoretical results and the experimental ones is good. Also shown on the two figures is the effect of the ocean current through illustration of the different cable configurations at different current speeds. It is clear that the current plays a significant role.

Figure 2.8 shows the results for a three-dimensional submerged cable. A verification of the results is not possible since no report on three-dimensional experi-

mental work is available.

2.7 CONCLUDING REMARKS

1. The approach developed in this chapter is of practical importance, with the capacity to answer a variety of questions arising from subsea interventions involving cable systems. In addition to this, the semi-analytic method, within the limitations of all assumptions made, is highly accurate and efficient.

2. Further efforts can be focussed on the following aspects:

   - Solution algorithm for the nonlinear equations

     The Newton-Raphson iteration, which only guarantees local convergence, depends upon a good initial guess of the solution. However, a sufficiently good estimation may not always be available. New algorithms which can globally track the solution, such as continuation techniques, should be introduced (Allgower and Georg, 1990).

   - Non-uniform cables

     The present method can be extended into non-uniform marine cables consisting of a series of uniform sections.

   - Static marine cable network

     The present method has the potential to solve problems involving marine cable networks, such as the trawling of fishing nets.

submerged
cable

towing
cable

mooring
cable

footprint
problem

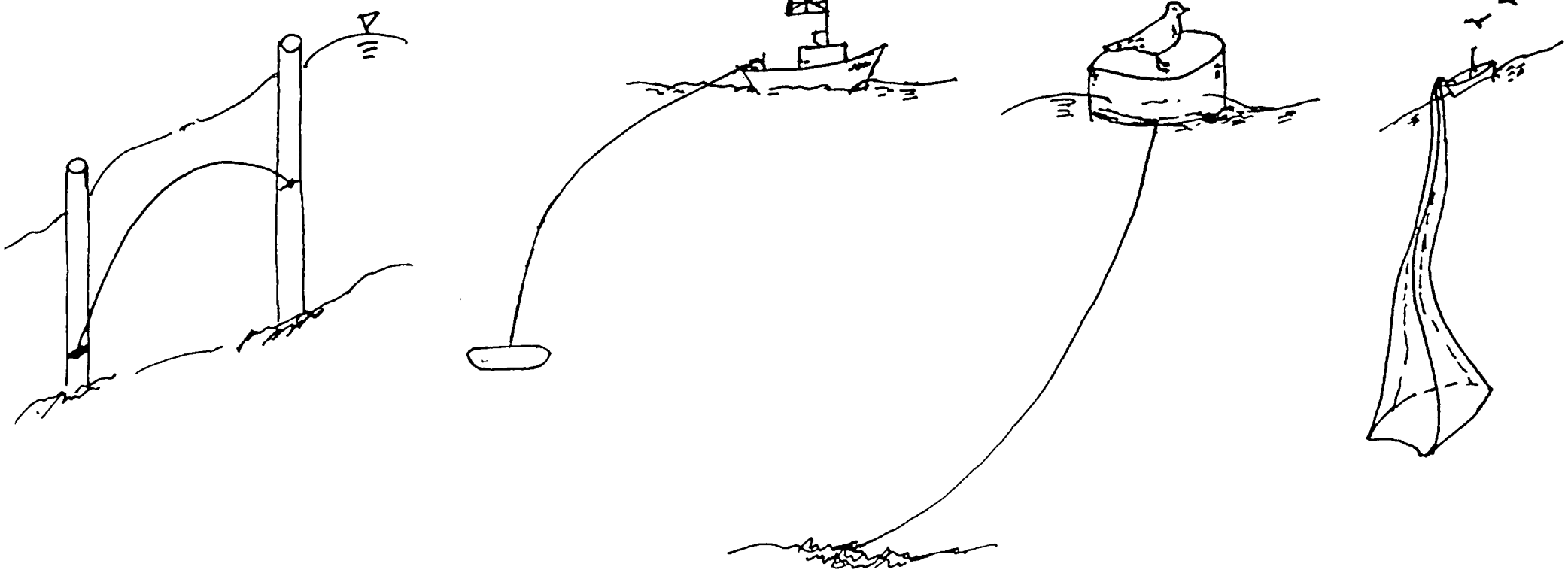

Figure 2.1

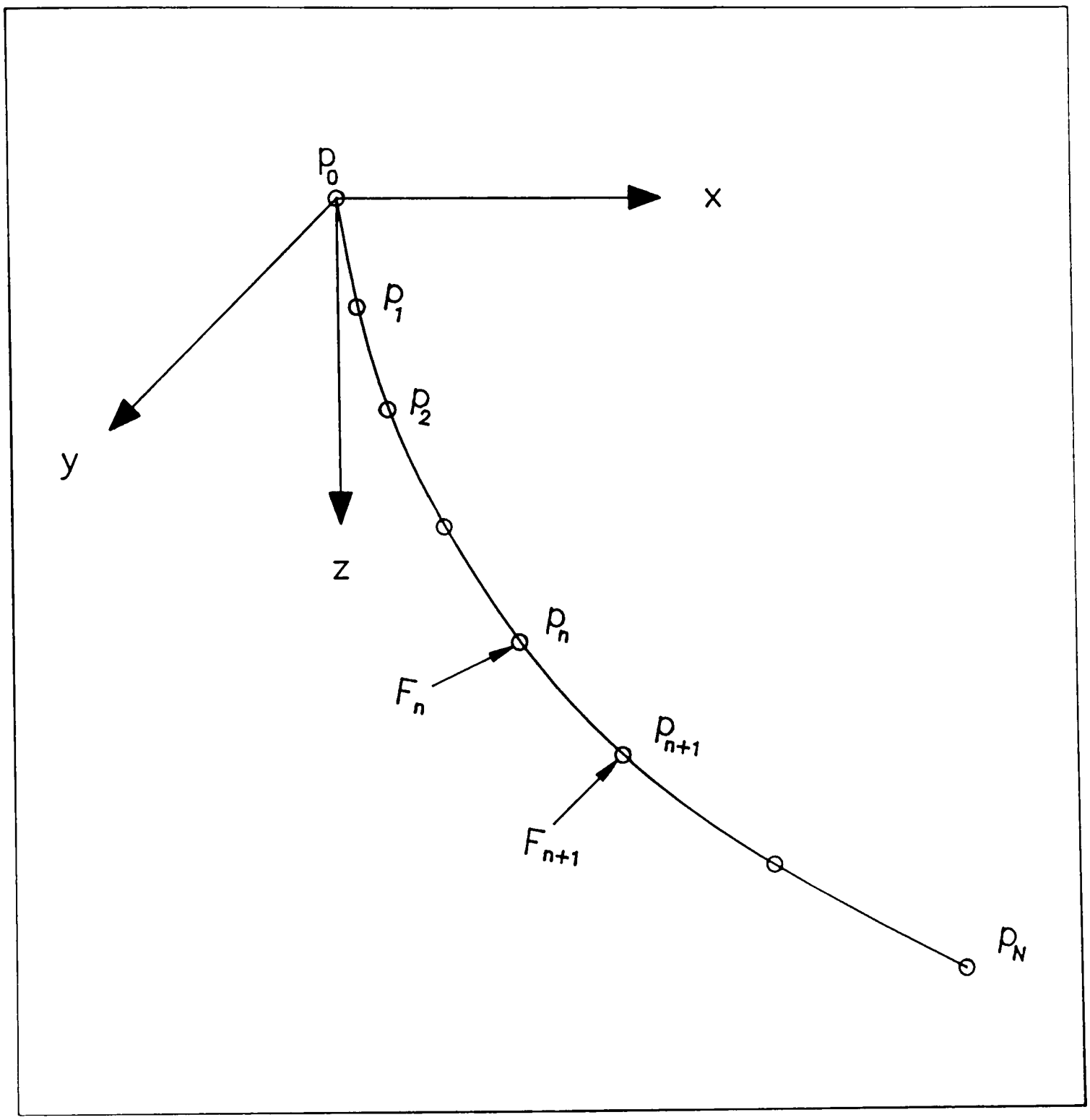

Figure 2.2

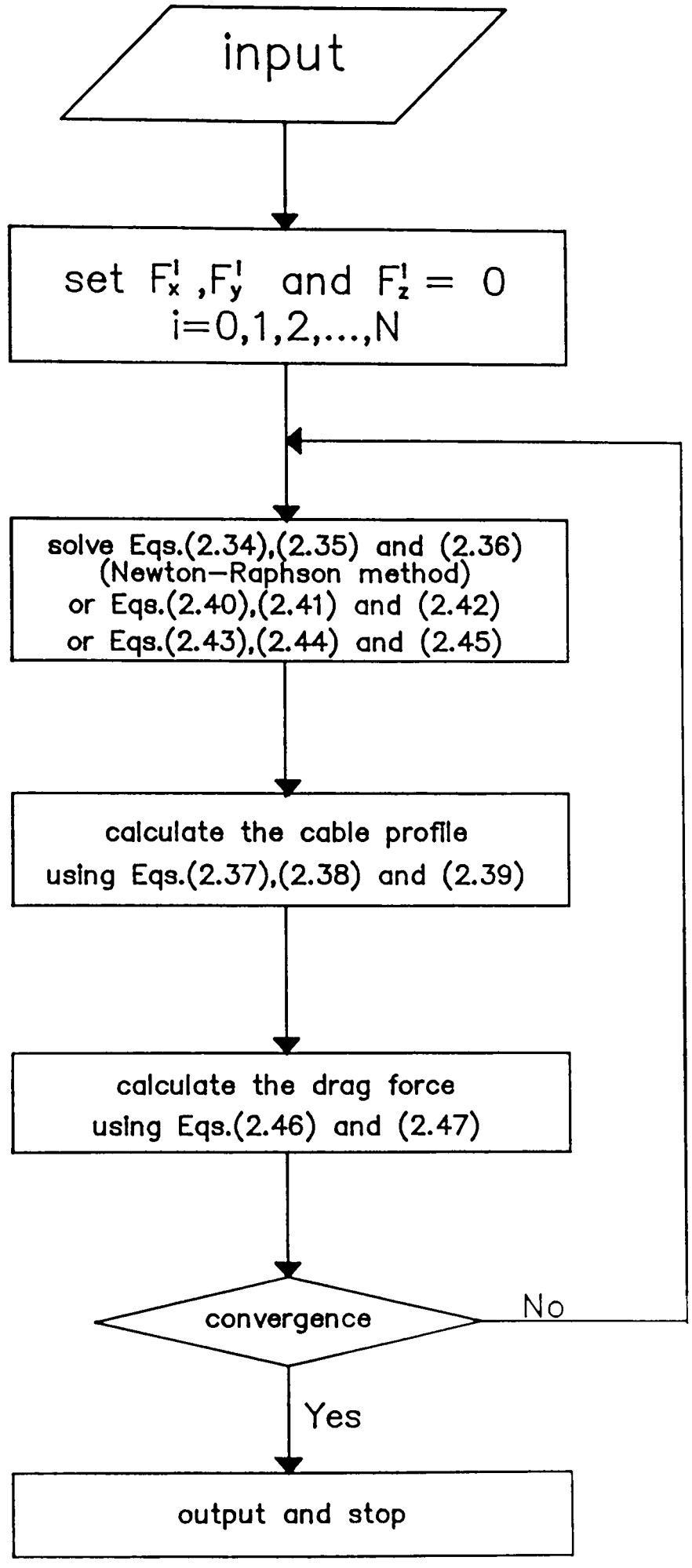
input
set F_x^i, F_y^i and F_z^i = 0
i=0,1,2,...,N
solve Eqs.(2.34),(2.35) and (2.36)
(Newton–Raphson method)
or Eqs.(2.40),(2.41) and (2.42)
or Eqs.(2.43),(2.44) and (2.45)
calculate the cable profile
using Eqs.(2.37),(2.38) and (2.39)
calculate the drag force
using Eqs.(2.46) and (2.47)
convergence
No
Yes
output and stop

Figure 2.3

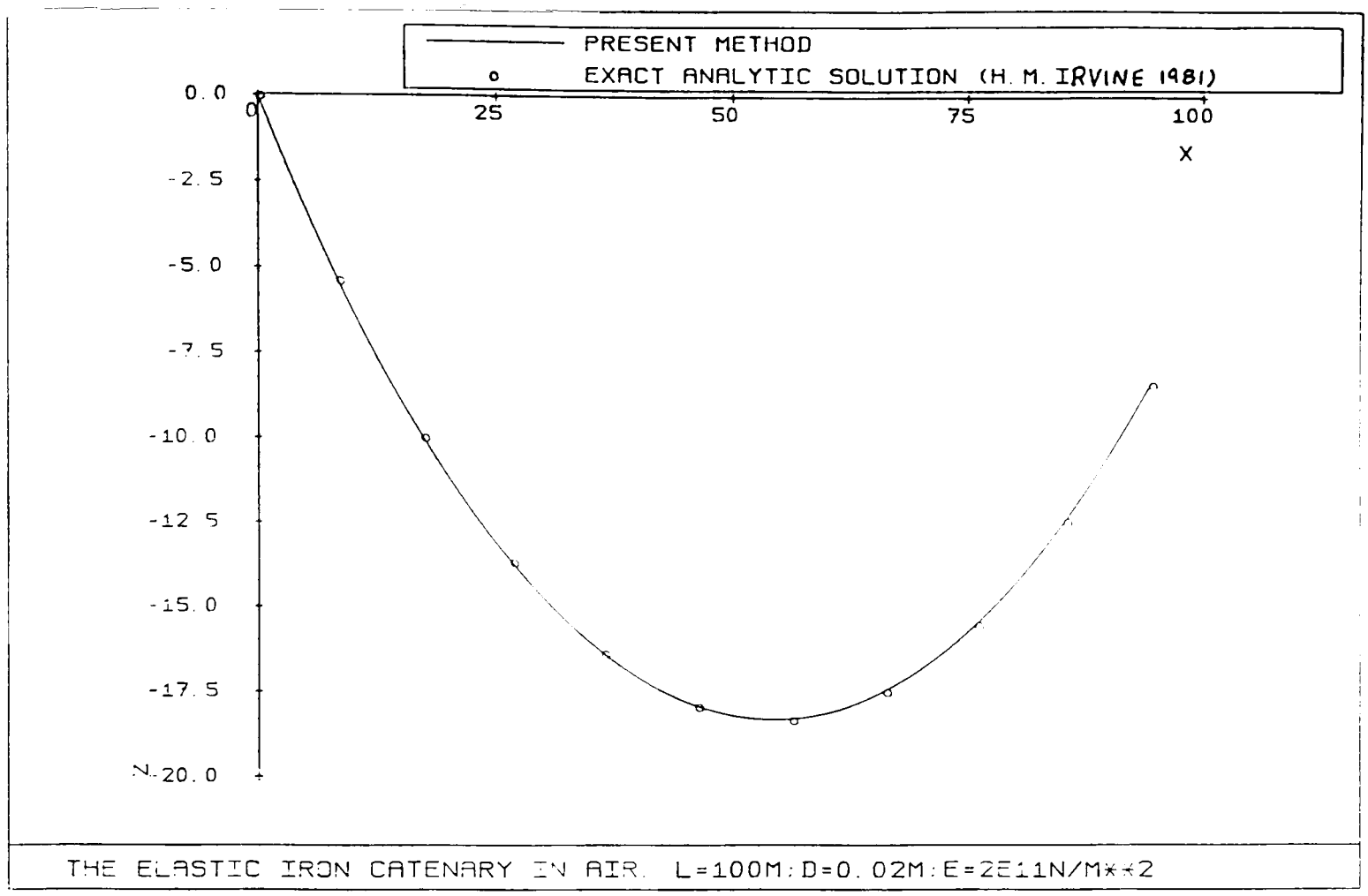

Figure 2.4

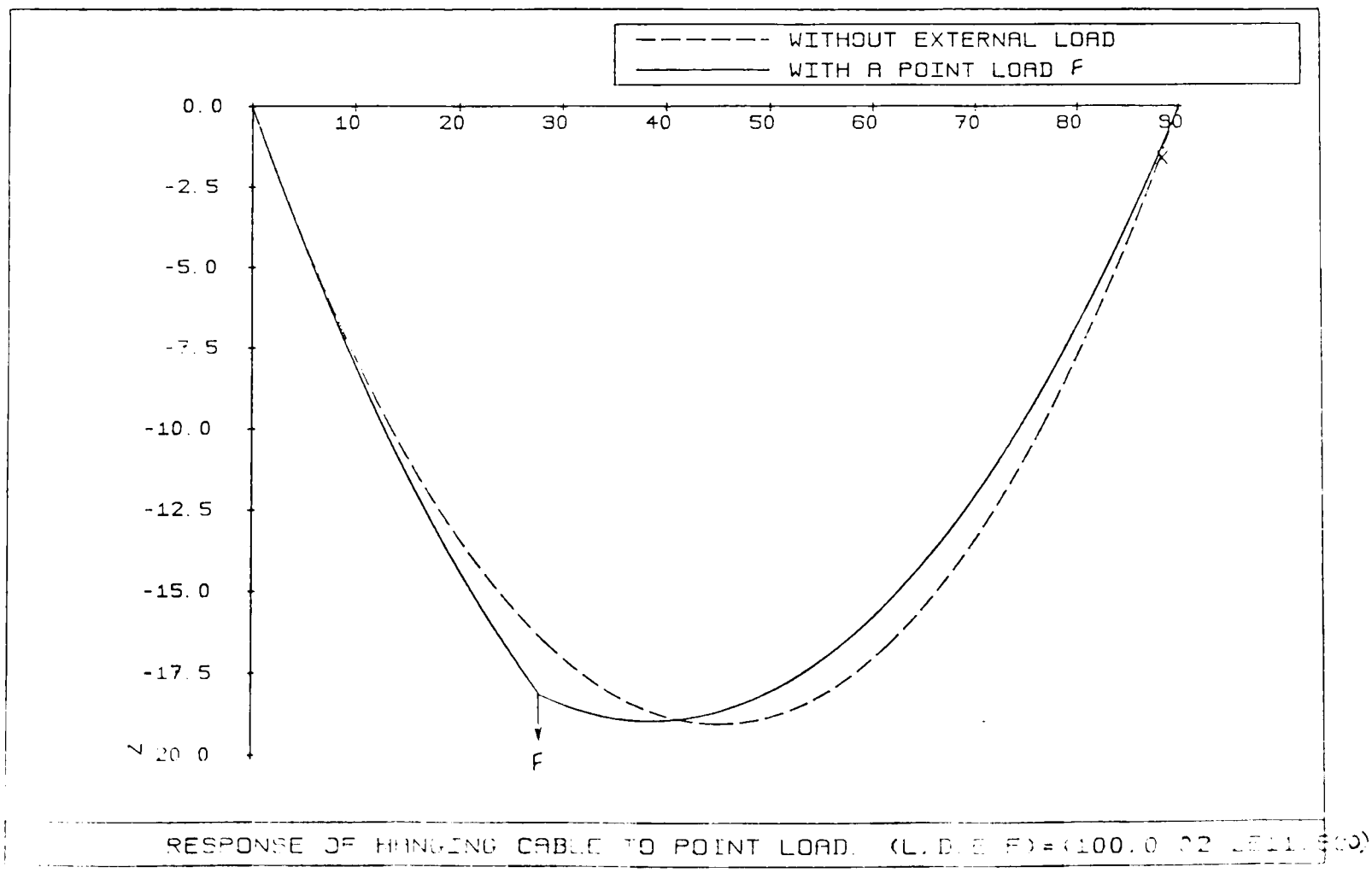

Figure 2.5

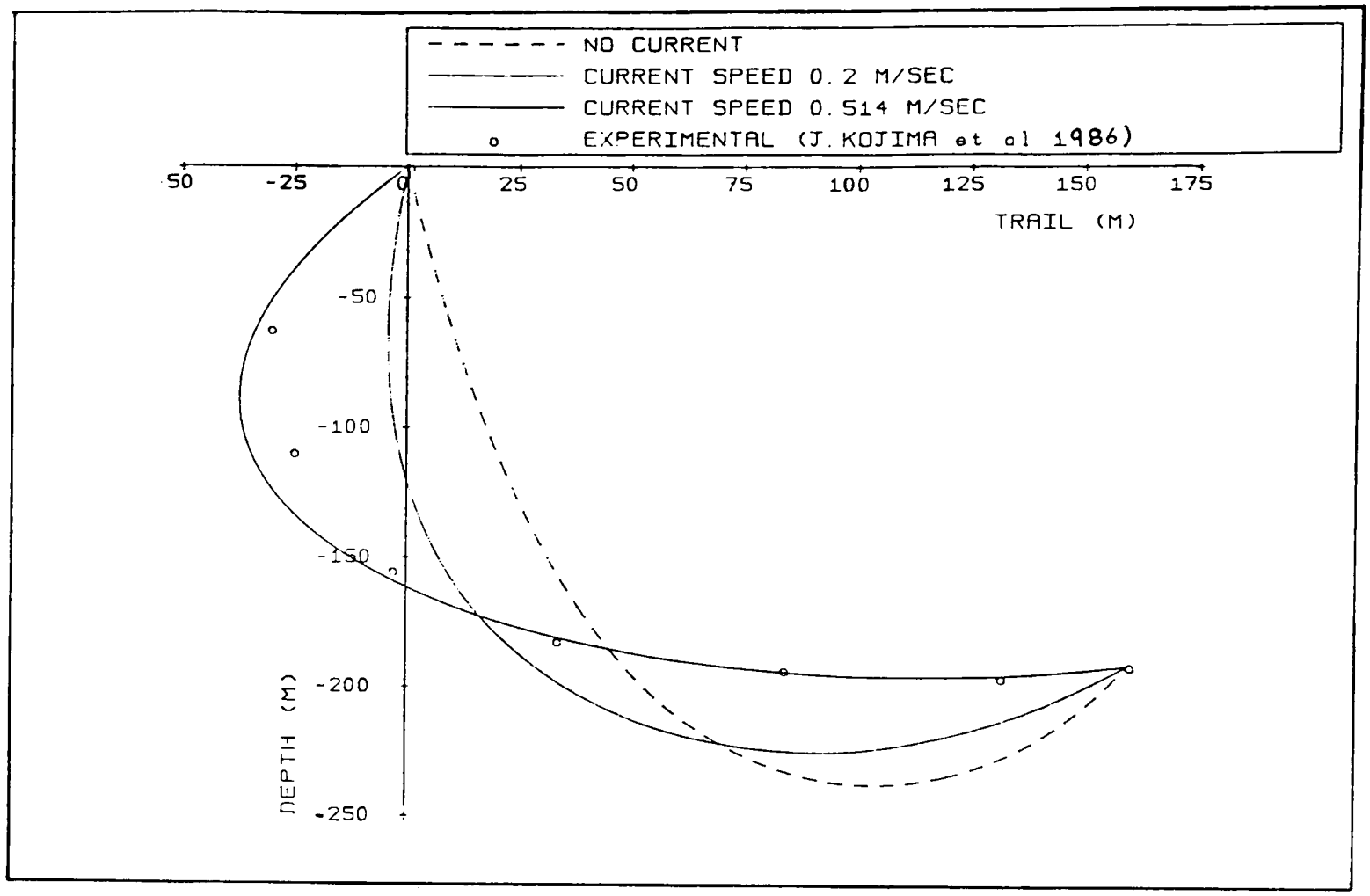
NO CURRENT
CURRENT SPEED 0.2 M/SEC
CURRENT SPEED 0.514 M/SEC
EXPERIMENTAL (J.KOJIMA et al 1986)
-50
-25
0
25
50
75
100
125
150
175
TRAIL (M)
-50
-100
-150
-200
-250
DEPTH (M)

Figure 2.6

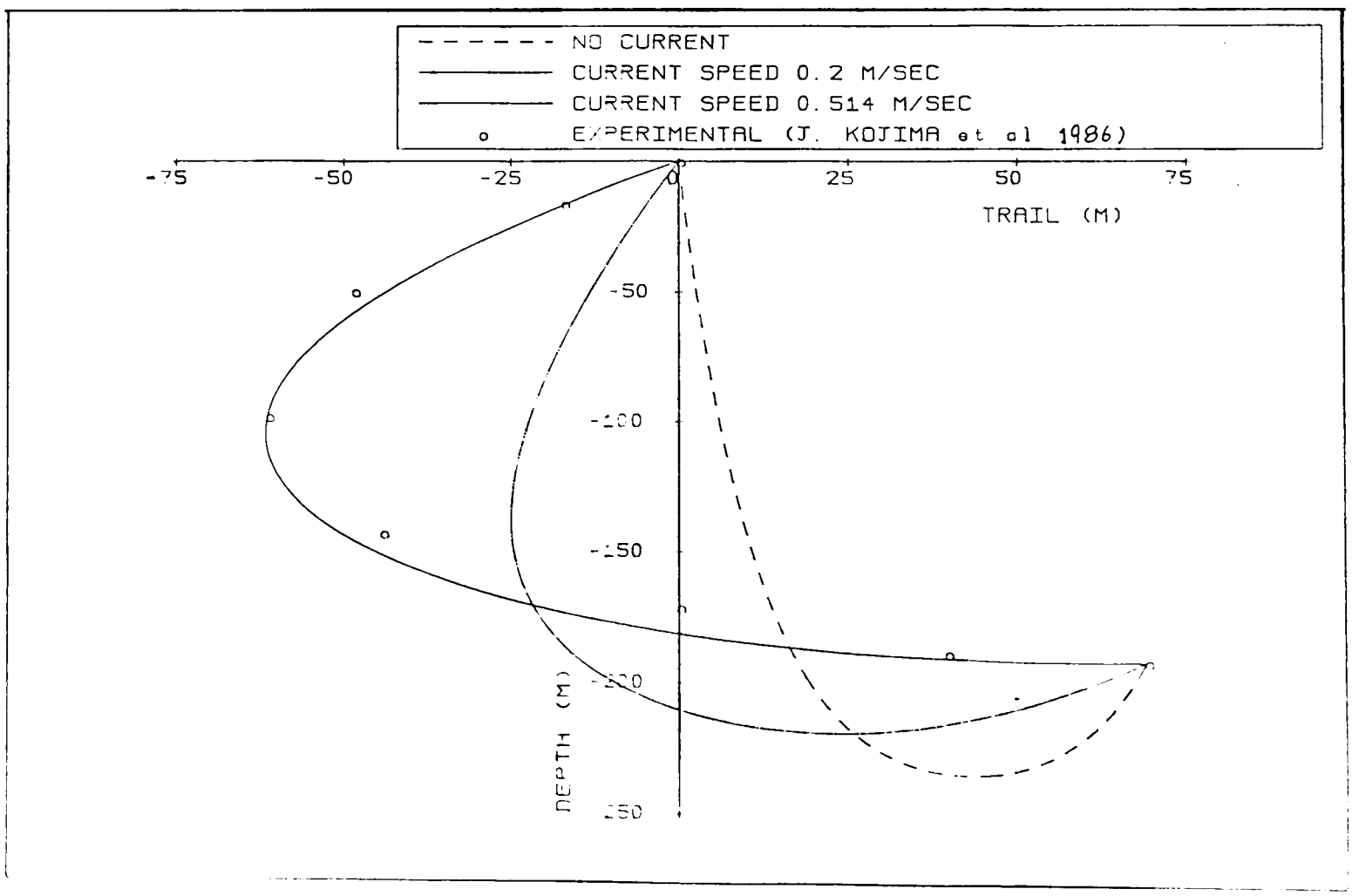
NO CURRENT
CURRENT SPEED 0.2 M/SEC
CURRENT SPEED 0.514 M/SEC
EXPERIMENTAL (J. KOJIMA et al 1986)
-75
-50
-25
0
25
50
75
TRAIL (M)
-50
-100
-150
DEPTH (M)

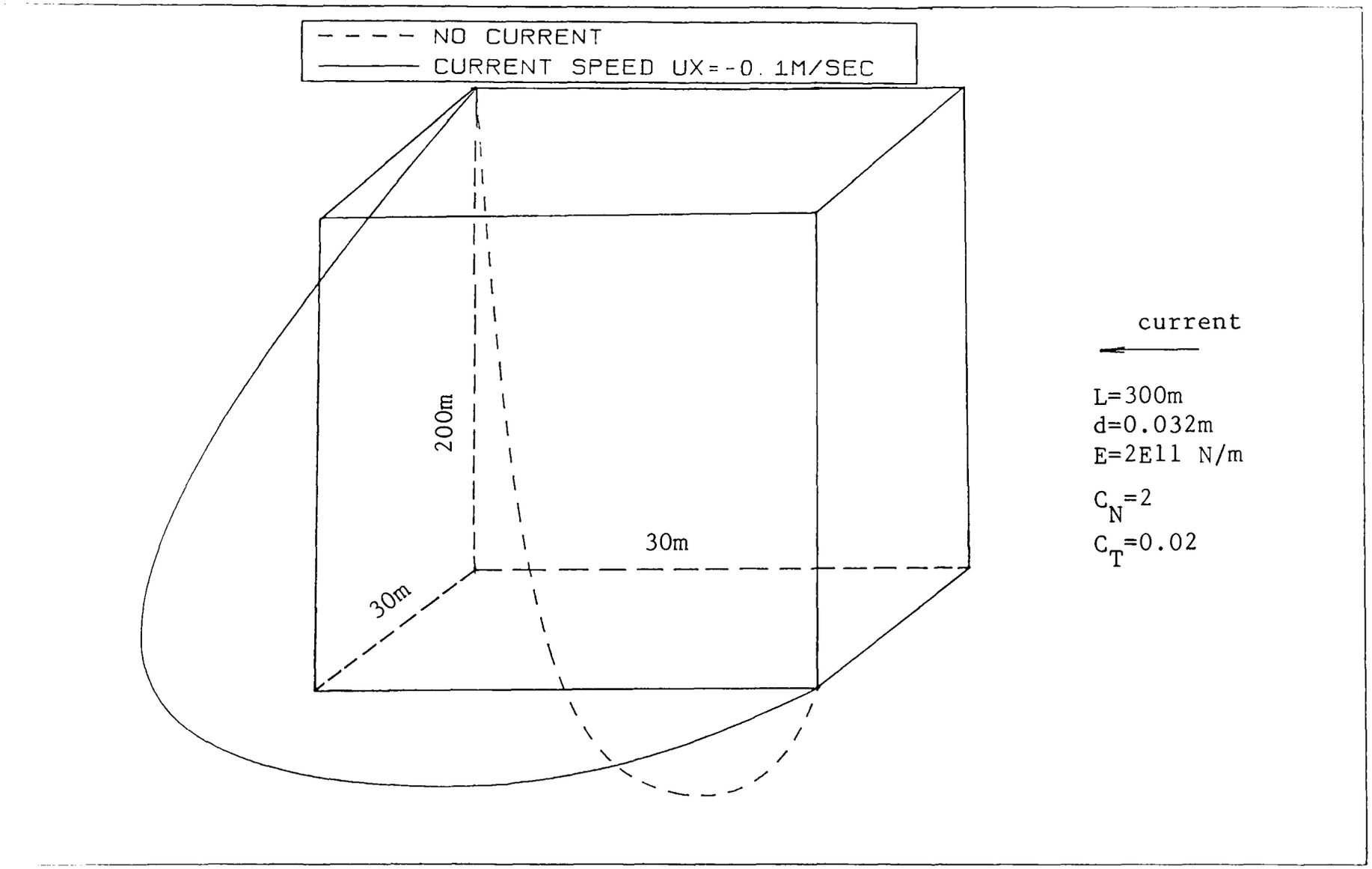
NO CURRENT
CURRENT SPEED UX=-0.1M/SEC
200m
30m
30m
current
L=300m
d=0.032m
E=2E11 N/m
C_N=2
C_T=0.02

Figure 2.8

Chapter 3

ONE DIMENSIONAL DYNAMICS

He goes a great voyage that goes to the bottom of the sea.

Thomas Fuller: *Gnomologia*

3.1 GENERAL REMARKS

The processes involved in the launch, operation, and recovery of a tethered subsea unit consist of four rather distinct stages:

1. Passage through the air gap. During this stage, the pendulum motion of the subsea unit in air, which is often excited by the motion of the vessel, may cause difficulties in control. Generally, the gap between handling systems on deck, such as cranes or A-frames, and the water surface is very small. Nevertheless care must be taken to prevent possible collision with other structures nearby.

2. Transition through the splash zone. This is often a crucial phase of the process involving very complicated hydrodynamic phenomena (Dutta, 1986; Greenhow et al, 1987; Oritsland et al, 1989). Deploying massive units with little buoyancy or surface area is relatively easy since they sink through this zone quickly. Neutrally buoyant systems present a more difficult problem: as soon as they are submerged there is no sinking force on the units. This may cause wave impact loading on the subsea unit and/or snap loading in the cable . However, due to the exponential decay of the wave forces on the subsea unit as it is being lowered, the depth of this zone is much less than the total length of the cable.

3. Lowering to the working depth, or lifting from the working depth to the splash zone. This stage covers most of the time of the deployment and retrieval phase, especially in deep waters. During this phase, resonance may be encountered due to the change in natural frequency of the system.

4. Operation at a certain depth to fulfil the designated tasks.

The handling system of a tethered subsea unit is subjected to the motions of the support vessel resulting from the environmental forces. Among them the most critical one is the heave motion. If a subsea unit is deployed in a weak current, or is constrained by taut vertical guide lines, the whole system can then be approximated as a one-dimensional problem.

Among the many design considerations, one of the major ones centres on the system's heave motion as the vertical oscillation can be amplified significantly

at the bottom end of the cable. The subsequent large amplitude heave motion will severely influence the design and operational requirements and cause unacceptable tension force in the cable which could result in the loss of subsea units.

A number of papers have been published addressing this topic, using different techniques and producing encouraging results (Chung, 1983; Sparks et al, 1983; Dutta, 1986; Niedzwecki et al, 1988; Schellin et al, 1989; Macgregor, 1990). However, a common flaw of these papers lies in the assumption that the top end of the cable is suspended on the floating vessel, therefore the unsteady dynamics during the deployment and retrieval phase associated with Stage 3 can only be tackled with a quasi-steady approach, i.e., performing a dynamic analysis at one fixed length and repeating it for several different lengths of the cable.

The interesting subject of oscillation of a subsea unit involving a time-varying length of cable has not yet been fully investigated. Relevant research on strings or shafts or beams in air has been reported occasionally by several authors (Schaffers, 1961; Kotera, 1978; Zajaczkowski and Yamada, 1980; Tagata, 1983). The various functions which have been used for the time-varying length $L(t)$ are as follows:

1. Linear function

$$L(t) = L_0 + vt$$

where L_0 is the initial length. v is the constant speed; when $v > 0$, the length increases with time, and when $v < 0$, the length decreases.

2. Quadratic function

$$L(t) = L_0 + vt + \frac{1}{2}at^2$$

where a is the acceleration.

3. Periodic function

$$L(t) = L_0 + psin(\omega t)$$

where p is the amplitude, and ω is the frequency.

Due to the time-dependent length, the rather classic oscillation problem cannot be solved easily. Variable transformation is often used to fix the changing domain by a suitable choice of new space coordinate, leading to a fixed domain problem at the expense of complicating the original governing equations (Crank, 1984).

In this chapter a general approach is presented to treat the dynamics of the unsteady phase when the cable is being paid out or hauled in via a handling system on deck. The steady dynamic case where the cable is fixed to the vessel at its top is only a special case incorporated in this general model. The approach is based on the continuous system rather than the various spring-lumped-mass approximations. The hydrodynamic added mass and damping are dealt with in accordance with the common practice. Available experimental data are then compared with numerical results in order to validate the developed program. The various results calculated are of direct design or operational concern.

3.2 MATHEMATICAL FORMULATION

3.2.1 Governing Equation

The governing equation can be derived by balancing different forces acting on a cable element under some general assumptions (Appendix). The resulting governing equation can be expressed as

$$E\frac{\partial}{\partial z}(A\frac{\partial u}{\partial z}) = (m + m_a)\frac{\partial^2 u}{\partial t^2} + \frac{\pi}{2}\rho d C_\tau |\frac{\partial u}{\partial t}|\frac{\partial u}{\partial t} - w_1 \tag{3.1}$$

where u is the displacement of the cable element, A the cross-section area, E the Young's modulus of elasticity, C_τ the tangential viscous damping coefficient of the cable, m the mass distribution, m_a the hydrodynamic added mass per unit length, d the diameter of the cable, and w_1 its weight in water per unit length. The coordinate system is defined in Figure 3.1.

3.2.2 Boundary Conditions

Two boundary conditions are to be satisfied:

1. At $z = 0$, where the cable is attached to the handling system on deck, the boundary condition is

$$u(0, t) = vt + R(t) \tag{3.2}$$

where v is the speed of paying out or hauling in, and $R(t)$ is the heave motion due to the wave excitation on the support vessel.

2. At $z = L_0 + vt$, the lower end of the cable where a subsea unit is attached, the boundary condition is:

$$EA\frac{\partial u}{\partial z} + (M_s + M_a)\frac{\partial^2 u}{\partial t^2} + \frac{\rho}{2}S_P C_D|\frac{\partial u}{\partial t}|\frac{\partial u}{\partial t} - w_2 = 0 \qquad (3.3)$$

where M_s is the mass of the subsea unit, M_a its added mass, C_D the viscous damping coefficient, S_P the projected area of the subsea unit, and w_2 its weight in water. L_0 here is the initial length of the cable.

3.2.3 Initial Conditions

Initial conditions must be specified for both u and $\partial u/\partial t$, however, they are not very important since we are interested in long term motions rather than the initial transient ones which die out quickly due to the damping in the system.

3.2.4 Variable Transformation and Important Relations

Eq. (3.1), together with the boundary conditions Eqs. (3.2) and (3.3), defines a moving boundary problem. It is inconvenient to seek a numerical solution on a time-variant computation domain. To cope with the difficulty, a set of variable transformations is developed here to fix the computation domain in the transformed space.

The transformation is given by:

$$\begin{aligned} U &= u - vt \\ T &= t \end{aligned} \qquad (3.4)$$

$$y = \frac{z}{L_0 + vt}$$

It is evident that the lower end of the cable which is moving in the physical space is fixed on $y = 1$ in the transformed domain.

The following relations of the first and second derivatives can be derived through application of the chain-rule:

$$\begin{aligned}
\frac{\partial}{\partial t} &= \frac{\partial}{\partial T} - \frac{vy}{L_0 + vT}\frac{\partial}{\partial y} \\
\frac{\partial}{\partial z} &= \frac{1}{L_0 + vT}\frac{\partial}{\partial y} \\
\frac{\partial^2}{\partial t^2} &= \frac{\partial^2}{\partial T^2} + \frac{2v^2 y}{(L_0 + vT)^2}\frac{\partial}{\partial y} \\
&\quad - \frac{2vy}{L_0 + vT}\frac{\partial^2}{\partial y \partial T} + \frac{v^2 y^2}{(L_0 + vT)^2}\frac{\partial^2}{\partial y^2} \\
\frac{\partial^2}{\partial z^2} &= \frac{1}{(L_0 + vT)^2}\frac{\partial^2}{\partial y^2}
\end{aligned}$$

3.2.5 Transformed Governing Equation and Boundary Conditions

Using the transformations and the derivative relations, the governing equation Eq. (3.1) transforms to

$$A\frac{\partial^2 U}{\partial y^2} + B\frac{\partial^2 U}{\partial T^2} + C\frac{\partial^2 U}{\partial y \partial T} + D\frac{\partial U}{\partial y} + F\frac{\partial U}{\partial T} + G = 0 \qquad (3.5)$$

where

$$\begin{aligned}
A &= (m + m_a)\frac{v^2 y^2}{(L_0 + vT)^2} - \frac{EA}{(L_0 + vT)^2} \\
B &= m + m_a \\
C &= -2(m + m_a)\frac{vy}{L_0 + vT}
\end{aligned}$$

$$
\begin{aligned}
D &= 2(m+m_a)\frac{v^2 y}{(L_0+vT)^2} - \\
&\quad \frac{\pi\rho d C_\tau v y}{2(L_0+vT)}\left|\frac{\partial U}{\partial T} - \frac{vy}{L_0+vT}\frac{\partial U}{\partial y} + v\right| \\
F &= \frac{\pi}{2}\rho d C_\tau\left|\frac{\partial U}{\partial T} - \frac{vy}{L_0+vT}\frac{\partial U}{\partial y} + v\right| \\
G &= v\frac{\pi}{2}\rho d C_\tau\left|\frac{\partial U}{\partial T} - \frac{vy}{L_0+vT}\frac{\partial U}{\partial y} + v\right| - w_1
\end{aligned}
$$

The new boundary conditions are:

1. At $y = 0$

$$U(0,T) = R(T) \tag{3.6}$$

2. At $y = 1$

$$A'\frac{\partial^2 U}{\partial y^2} + B'\frac{\partial^2 U}{\partial T^2} + C'\frac{\partial^2 U}{\partial y \partial T} + D'\frac{\partial U}{\partial y} + F'\frac{\partial U}{\partial T} + G' = 0 \tag{3.7}$$

where

$$
\begin{aligned}
A' &= (M_s+M_a)\frac{v^2}{(L_0+vT)^2} \\
B' &= M_s + M_a \\
C' &= -2(M_s+M_a)\frac{v}{L_0+vT} \\
D' &= 2(M_s+M_a)\frac{v^2}{(L_0+vT)^2} + \frac{EA}{L_0+vT} - \\
&\quad \frac{v\rho S_P C_D}{2(L_0+vT)}\left|\frac{\partial U}{\partial T} - \frac{v}{L_0+vT}\frac{\partial U}{\partial y} + v\right| \\
F' &= \frac{1}{2}\rho S_P C_D\left|\frac{\partial U}{\partial T} - \frac{v}{L_0+vT}\frac{\partial U}{\partial y} + v\right| \\
G' &= \frac{v}{2}\rho S_P C_D\left|\frac{\partial U}{\partial T} - \frac{v}{L_0+vT}\frac{\partial U}{\partial y} + v\right| - w_2
\end{aligned}
$$

3.2.6 Finite Difference Discretisation

The finite difference method is used here for the numerical solution. With reference to the even mesh in the computational domain of Figure 3.2, and denoting $\triangle y$ and $\triangle T$ as the horizontal and vertical intervals respectively, suitable approximations at node $(i, j+1)$ are:

$$
\begin{aligned}
(\frac{\partial U}{\partial y})_i^{j+1} &= \frac{1}{2\triangle y}(U_{i+1}^{j+1} - U_{i-1}^{j+1}) + O(\triangle y^2) \\
(\frac{\partial U}{\partial T})_i^{j+1} &= \frac{1}{2\triangle T}(3U_i^{j+1} + U_i^{j-1} - 4U_i^j) + O(\triangle T^2) \\
(\frac{\partial^2 U}{\partial y^2})_i^{j+1} &= \frac{1}{\triangle y^2}(U_{i+1}^{j+1} + U_{i-1}^{j+1} - 2U_i^{j+1}) + O(\triangle y^2) \\
(\frac{\partial^2 U}{\partial T^2})_i^{j+1} &= \frac{1}{\triangle T^2}(2U_i^{j+1} + 4U_i^{j-1} - 5U_i^j - U_i^{j-2}) + O(\triangle T^2) \\
(\frac{\partial^2 U}{\partial y \partial T})_i^{j+1} &= \frac{1}{4\triangle T\triangle y}(3U_{i+1}^{j+1} + U_{i+1}^{j-1} - 4U_{i+1}^j - 3U_{i-1}^{j+1} - U_{i-1}^{j-1} + 4U_{i-1}^j) \\
&\quad + O(\triangle T^2, \triangle y^2)
\end{aligned}
$$

The boundary condition of Dirichlet type at $y = 0$ can be readily utilized whilst the boundary condition at $y = 1$ is discretised using similar approximations to the one given above.

As a result of the discretisation and linearization, a linear algebraic simultaneous equation system is derived for the $(N-1)$ unknown variables at $(j+1)$ time level:

$$p_i^{j+1}U_{i+1}^{j+1} + q_i^{j+1}U_i^{j+1} + r_i^{j+1}U_{i-1}^{j+1} = e_i^{j+1}, \quad 1 < i < N \tag{3.8}$$

with

$$U_1^{j+1} = R[(j+1)\triangle T] \tag{3.9}$$

and

$$p_N^{j+1}U_N^{j+1} + q_N^{j+1}U_{N-1}^{j+1} + r_N^{j+1}U_{N-2}^{j+1} + s_N^{j+1}U_{N-3}^{j+1} = e_N^{j+1} \tag{3.10}$$

where

$$\begin{aligned}
p_i^{j+1} &= \frac{A_i^{j+1}}{\triangle y^2} + \frac{3C_i^{j+1}}{4\triangle y\triangle T} + \frac{D_i^{j+1}}{2\triangle y} \\
q_i^{j+1} &= -\frac{2A_i^{j+1}}{\triangle y^2} + \frac{2B_i^{j+1}}{\triangle T^2} + \frac{3F_i^{j+1}}{2\triangle T} \\
r_i^{j+1} &= \frac{A_i^{j+1}}{\triangle y^2} - \frac{3C_i^{j+1}}{4\triangle y\triangle T} - \frac{D_i^{j+1}}{2\triangle y} \\
e_i^{j+1} &= -G_i^{j+1} - \frac{B_i^{j+1}}{\triangle T^2}(-5U_i^j + 4U_i^{j-1} - U_i^{j-2}) \\
&\quad -\frac{C_i^{j+1}}{4\triangle y\triangle T}(U_{i+1}^{j-1} - 4U_{i+1}^j - U_{i-1}^{j-1} + 4U_{i-1}^j) \\
&\quad -\frac{F_i^{j+1}}{2\triangle T}(U_i^{j-1} - 4U_i^j)
\end{aligned}$$

$$\begin{aligned}
p_N^{j+1} &= \frac{2A'^{j+1}}{\triangle y^2} + \frac{2B'^{j+1}}{\triangle T^2} + \frac{9C'^{j+1}}{4\triangle y\triangle T} + \frac{3D'^{j+1}}{2\triangle y} + \frac{3F'^{j+1}}{2\triangle T} \\
q_N^{j+1} &= \frac{-5A'^{j+1}}{\triangle y^2} - \frac{3C'^{j+1}}{\triangle y\triangle T} - \frac{2D'^{j+1}}{\triangle y} \\
r_N^{j+1} &= \frac{4A'^{j+1}}{\triangle y^2} + \frac{3C'^{j+1}}{4\triangle y\triangle T} + \frac{D'^{j+1}}{2\triangle y} \\
s_N^{j+1} &= -\frac{A'^{j+1}}{\triangle y^2} \\
e_N^{j+1} &= -G'^{j+1} - \frac{B'^{j+1}}{\triangle T^2}(-5U_N^j + 4U_N^{j-1} - U_N^{j-2}) \\
&\quad -\frac{C'^{j+1}}{4\triangle y\triangle T}(3U_N^{j-1} + U_{N-2}^{j-1} - 4U_{N-1}^{j-1} - 12U_N^j - 4U_{N-2}^j + 16U_{N-1}^j) \\
&\quad -\frac{F'^{j+1}}{2\triangle T}(U_N^{j-1} - 4U_N^j)
\end{aligned}$$

The solution is marching forward in the time domain. It is stable due to the implicit scheme used here.

3.3 NUMERICAL EXAMPLES & DISCUSSION

As for any theoretical method, it is essential to compare the theoretical results obtained with experimental ones in order to establish the credibility of the mathematical model and enhance confidence in the results which the model produces. A series of numerical simulations has been completed, and the results have been compared with the experimental data available. Due to the fact that little experimental work has been reported on the unsteady deployment or retrieval phase involving time-varying length, only the steady cases are verified against published experimental data.

3.3.1 Example One

The particulars of the cable are as follows:

construction:	3 strand prestretched polyester rope
diameter:	$0.003m$
length:	$4.573m$
Young's modulus:	$3.38\times10^{9}N/m^{2}$
mass distribution:	$8.067\times10^{-3}kg/m$

The particulars of the subsea unit are given by:

construction:	wooden sphere
diameter:	$0.2032m$
mass:	$4.722kg$

The experiment was carried out with the cable/subsea unit system being suspended in air. The top end of suspension of the cable was subjected to forced sinusoidal motion along a vertical line with amplitude equal to $50mm$ (Dutta, 1986).

Both the experimental results and the theoretical prediction of the present

method are presented in Figure 3.3 in the form of maximum tension in the cable *versus* excitation frequency. Also shown in the same figure is the theoretical result based upon a lump-mass-and-spring model by D. Dutta (Dutta, 1986)

The theoretical results agree remarkably well with the experimental data.

3.3.2 Example Two

The particulars of the cable are as follows:

construction:	8-plait standard polyester rope
diameter:	$0.002m$
length:	$4.573m$
Young's modulus:	$2.445\times10^{9}N/m^{2}$
mass distribution:	$4.155\times10^{-3}kg/m$

The subsea unit is the same as that in the last example.

Again the experiment was performed in air. The top end was subject to a larger sinusoidal excitation of $100mm$ amplitude. The theoretical simulation was carried out using the experimental set-up as input data. Both results are shown in Figure 3.4. Compared with Example One, the agreement here between the theoretical results and the experiment ones is less satisfactory. This is due to the larger excitation amplitude. As a result, the cable behaviour may no longer be linear elastic. Polyester rope often exhibits appreciable hysteresis loops during the loading/unloading process, and the stiffness increases with increasing loading.

At the higher frequency region, the agreement becomes even poorer, as expected. At this region, cable snatching occurs which results in an impact load in the cable following initiation of slack in the cable, which the present model can not

handle.

3.3.3 Example Three

Both the experiments in Example One and Example Two were performed in frequency regions away from the respective natural frequencies. Further effort is made here to demonstrate that the present method is also capable of predicting resonance.

The tests were performed in air on nylon rope in a similar manner (Goeller and Laura, 1971). The main particulars of the cable are as follows:

diameter:	$0.00635m$
length:	$22.25m$
Young's modulus:	$2.67\times10^{8}N/m^{2}$
mass distribution:	$3.23\times10^{-2}kg/m$

The main particulars of the subsea unit are given by:

construction:	solid aluminium sphere
diameter	$0.2032m$
mass:	$12.65kg$
added mass in water:	$2.3kg$
weight in water	$83.68N$

The results are presented in Figure 3.5 by plotting the nondimensionalized tension $(T_{max} - T_{static})/Kx_0$ *versus* the nondimensionalized frequency ω/ω_{nc}, where K is the spring constant, x_0 is the amplitude of the sinusoidal excitation at the top end of the cable, ω_{nc} is a measured frequency. These are given by:

$$K = 380N/m$$

$$x_0 = 0.0254m$$

$$\omega_{nc} = 1.1Hz$$

The comparison again shows a good agreement between the theoretical predictions and the experimental results. Even at the resonant frequency they still agree with each other remarkably well. It was observed in both the test and the theoretical simulation that the elongation of the cable was relatively small, even at the resonance. As a result, the cable behaved almost linearly throughout the frequency interval.

3.3.4 Example Four

No hydrodynamic damping is present in the foregoing three examples. The system would behave differently in water because of the presence of viscous damping. This subsection examines its effects.

The same experimental set-up as the one in Example Three is employed here, except this time the experiment was performed in water instead of in air (Goeller and Laura, 1971). The input to the theoretical simulation is adapted accordingly. The results are given in Figures 3.6 and 3.7 for two different excitation amplitudes. In Figure 3.6, $x_0 = 0.0254m$, whilst in Figure 3.7, $x_0 = 0.0508m$.

After comparison of Figures 3.5, 3.6 and 3.7, the following features were observed:

1. Good agreement has been achieved. Throughout the simulation, both C_D and C_τ are assumed to be constant, which appears to be reasonable.

2. Water has a significant effect in reducing the dimensionless tension ratio, especially in the vicinity of resonance. Also due to the presence of the external fluid medium the ω_{nc} has shifted from $1.1Hz$ to $0.72Hz$.

3. In the present nonlinear model, damping introduces an amplitude dependent loading on the system. As a result, the nondimensional tension ratio shall be dependent upon the excitation amplitude, which is clearly demonstrated in Figures 3.6 and 3.7. This would not happen if the model were linear.

3.3.5 Example Five

The unsteady dynamics is examined in this example. During the deployment or retrieval phase, key influential factors may include the following:

1. Heave motion at the top
2. Deploying or retrieving speed and acceleration
3. Weight and shape of the subsea unit
4. Elasticity of the cable.

A number of theoretical simulations in the time domain have been carried out on a system during its launching process. The particulars of the cable and the subsea unit are

initial length:	50m
Young's modulus:	$9.05 \times 10^9 N/m^2$
diameter of the cable :	0.047m
cable mass distribution:	7.2 kg/m
mass of subsea unit:	5000 kg
added mass:	8000 kg

The initial length is assumed to be $50m$ so as to exclude any wave forces on the subsea unit. There are four different speeds and four different frequencies given by:

$v_1 = 0.5$ m/s $\quad v_2 = 1.0$ m/s
$v_3 = 2.0$ m/s $\quad v_4 = 3.0$ m/s

and

$\omega_1 = 0.4189$ rad/s $\quad \omega_2 = 0.628$ rad/s
$\omega_3 = 0.8380$ rad/s $\quad \omega_4 = 1.260$ rad/s

The different combinations give a total of 16 different situations. The time domain simulation results are given in Figure 3.8 through to Figure 3.23. In each figure the lower time record is the vessel heave motion, whilst the upper one gives the motion of the subsea unit. The motions due to the static elongation and the steady lowering are excluded.

The following features have been observed:

1. Deploying speed has a significant effect on the subsea unit motion. The higher the speed, the less the motion, especially through the resonance region.

2. Higher deploying speed means a greater drag force on both the subsea unit and the cable per unit length. Furthermore, as the cable is becoming longer, the total drag force on the cable becomes greater. As a result, the cable experiences an appreciable degree of compression, especially when the deploying speed is high and the cable is long, as shown in Figures 3.20 through 3.23. Of course, this compression is smaller than the static elongation; otherwise, the cable would become slack.

3. A quasi-steady approach, which is not capable of taking the speed of deployment or retrieval into account, would predict a critical length of the cable at which the system experiences the largest heave response for a given situation. However, the results here show the critical length not fixed but a function of the speed for a given system under given conditions. The higher the speed, the longer the critical length.

4. The excitation frequency also has an apparent effect on the response of the subsea unit. This effect will be dependent upon the relationship between the excitation frequency and the natural frequency of the system which is constantly changing in the course of deployment or retrieval.

5. For a rough estimation of the cable length L at which resonance occurs, the following model can be used

$$L = \frac{EA}{\omega^2(M + M_a)}$$

where ω is the excitaion frequency. This estimation is valid when the deployment speed is low.

In the last figure of this chapter, Figure 3.24, the impulsive motion of the subsea unit when the deployment is suddenly suspended is shown. The system goes through a transient phase of large amplitude motion. Beyond that, a steady motion builts up.

3.4 CONCLUDING REMARKS

1. An excellent agreement has been achieved between the available experimental data and the theoretical predictions based upon the present method.

2. For the unsteady dynamics, the present method produces convincing results.

3. The suite of computer programs provides an effective tool for investigating the degree of influence of the various factors in cable/subsea unit systems. The theoretical research here has direct application to the enhancement of safety and effectiveness of subsea operations, and in assisting the design of efficient handling systems.

4. Although this study focuses on the analysis of cable/subsea unit systems, the methodology presented here may be applied to other deep water systems such as long vertical deep-sea drill pipes held at their tops at ships' moonpools.

5. Further effort can be made to address the following aspects:

   - Nonlinearity of the cable material

     Throughout the present chapter, a linear relation between the tension T and the strain ε is assumed:

     $$T = EA\varepsilon$$

     To take the nonlinearity of the cable material into account, a more general constitutive relation should be utilized such as

     $$T = T(\varepsilon)$$

or

$$T = T(\varepsilon, \frac{\partial \varepsilon}{\partial t})$$

- General form of the time-varying length function $L(t)$

  It is envisaged that the acceleration of deployment might be a factor of importance. The extension from the present linear function to a quadratic form should not pose great difficulty; indeed, the present methodology allows an arbitrary form of $L(t)$.

- Stochastic analysis

  Stochastic analysis can be performed by using a random input $R(t)$. The output of the subsea unit motion, which is random in nature, can then be processed to give stochastic descriptions of the motion.

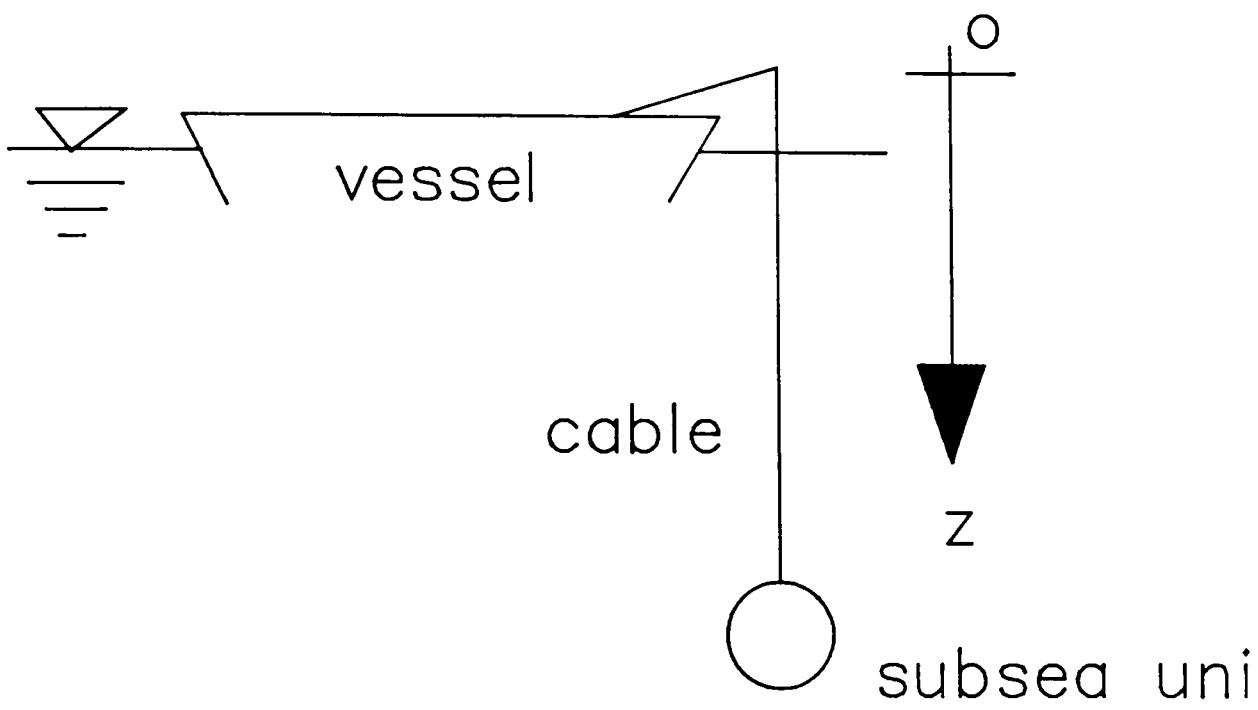

Figure 3.1

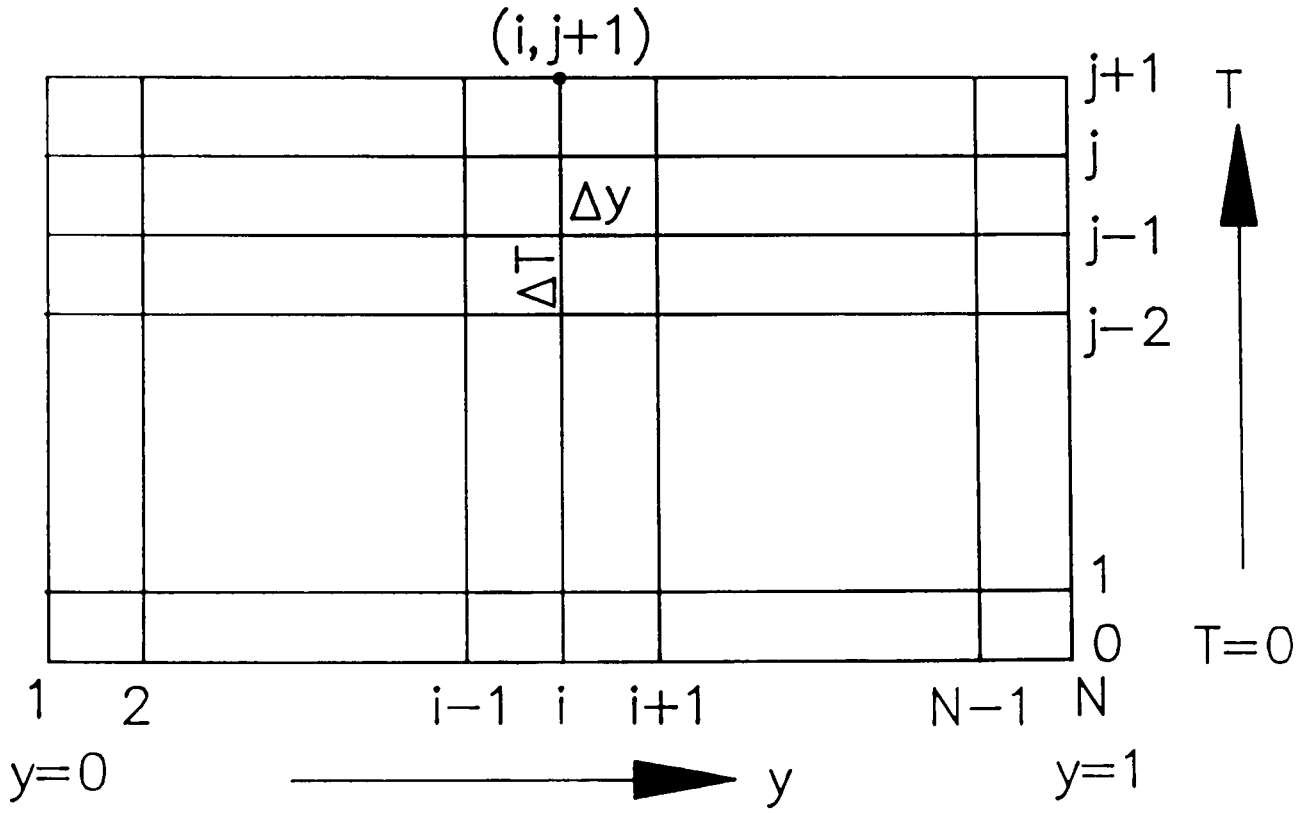

Figure 3.2

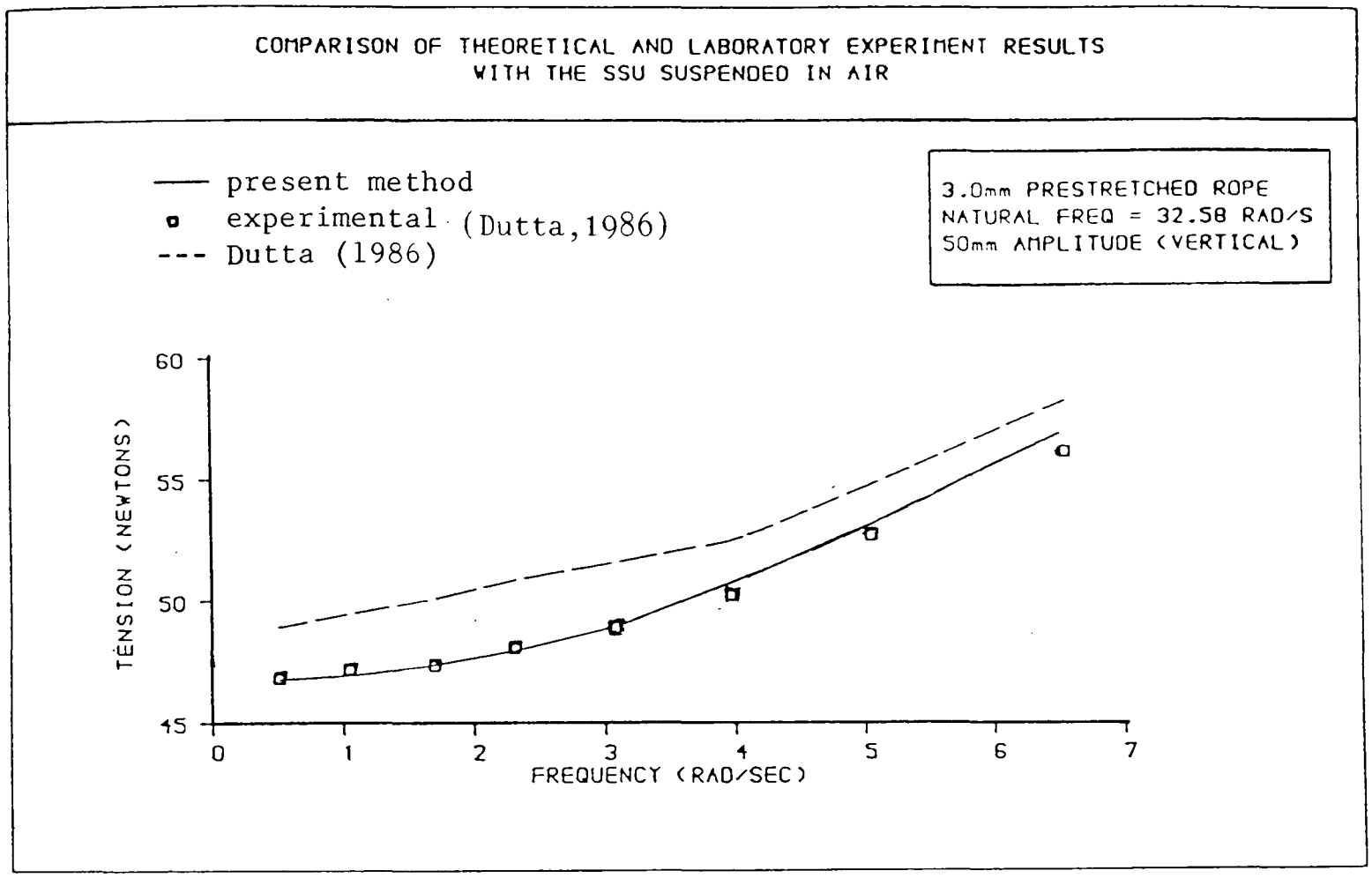
COMPARISON OF THEORETICAL AND LABORATORY EXPERIMENT RESULTS
WITH THE SSU SUSPENDED IN AIR
present method
experimental (Dutta,1986)
Dutta (1986)
3.0mm PRESTRETCHED ROPE
NATURAL FREQ = 32.58 RAD/S
50mm AMPLITUDE (VERTICAL)
TENSION (NEWTONS)
60
55
50
45
0
1
2
3
4
5
6
7
FREQUENCY (RAD/SEC)

Figure 3.3

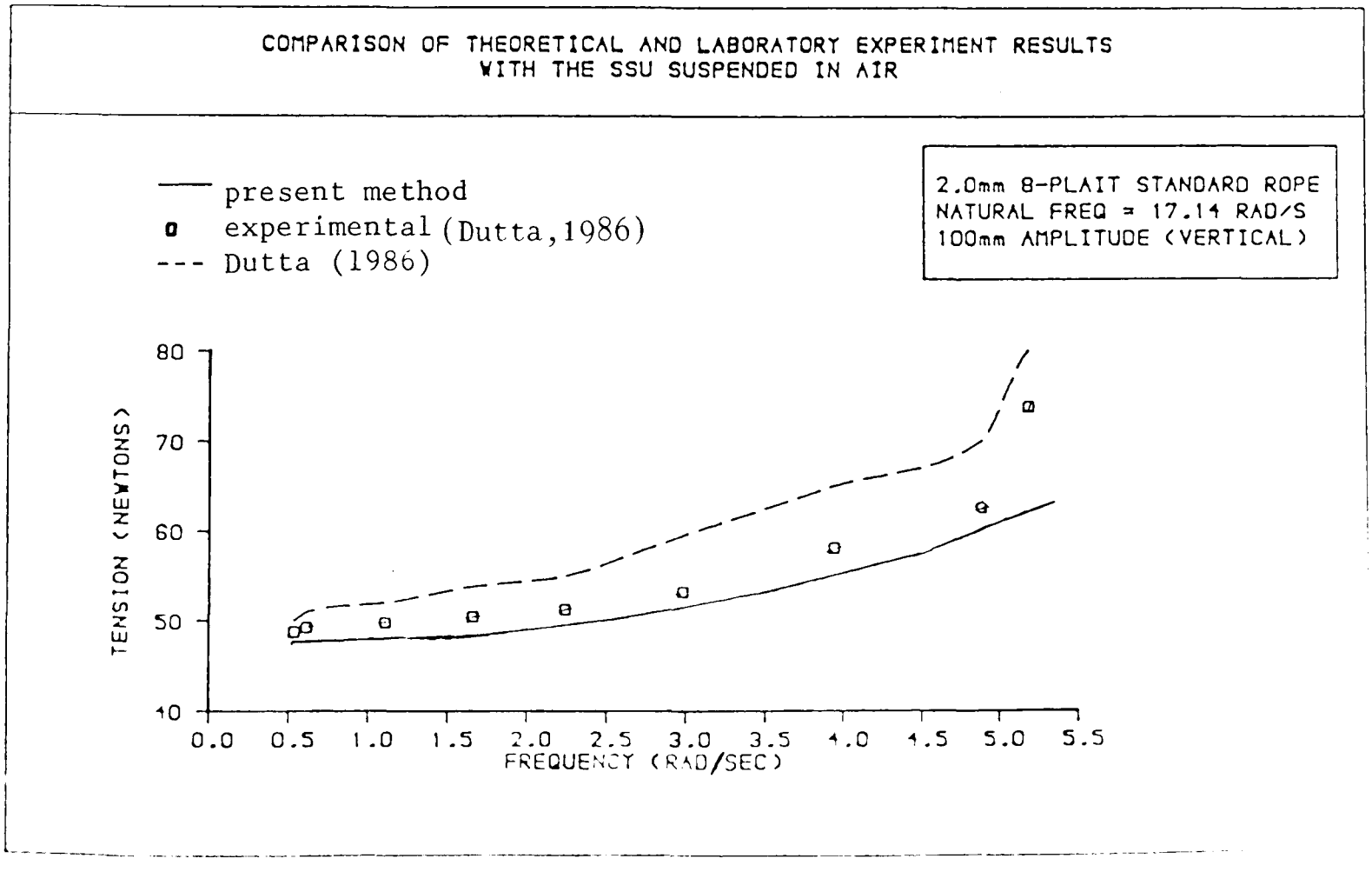
COMPARISON OF THEORETICAL AND LABORATORY EXPERIMENT RESULTS
WITH THE SSU SUSPENDED IN AIR
present method
experimental (Dutta,1986)
Dutta (1986)
2.0mm 8-PLAIT STANDARD ROPE
NATURAL FREQ = 17.14 RAD/S
100mm AMPLITUDE (VERTICAL)
TENSION (NEWTONS)
80
70
60
50
40
0.0
0.5
1.0
1.5
2.0
2.5
3.0
3.5
4.0
4.5
5.0
5.5
FREQUENCY (RAD/SEC)

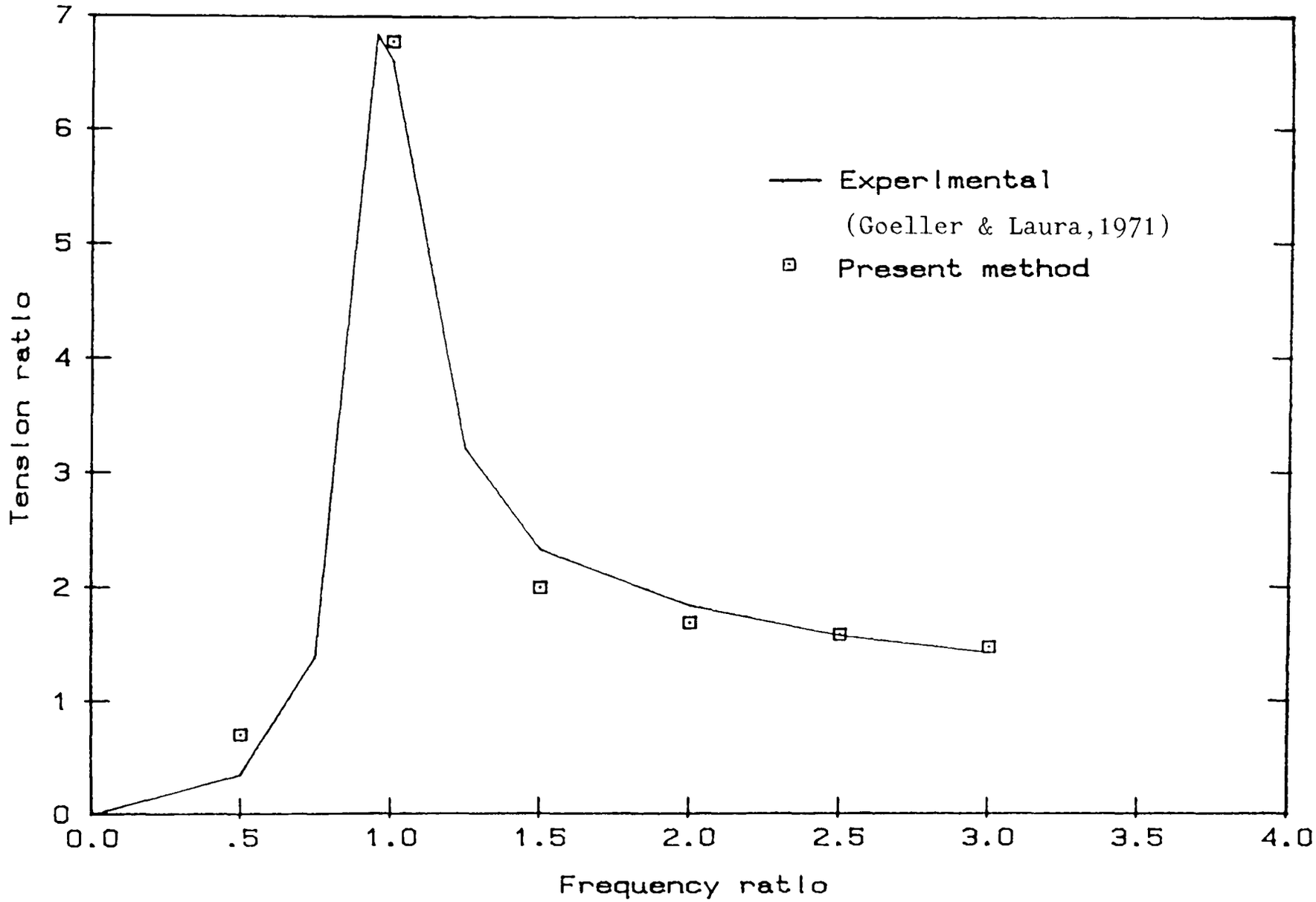
Tension ratio
Frequency ratio
Experimental
(Goeller & Laura, 1971)
Present method
0
1
2
3
4
5
6
7
0.0
.5
1.0
1.5
2.0
2.5
3.0
3.5
4.0

Figure 3.5

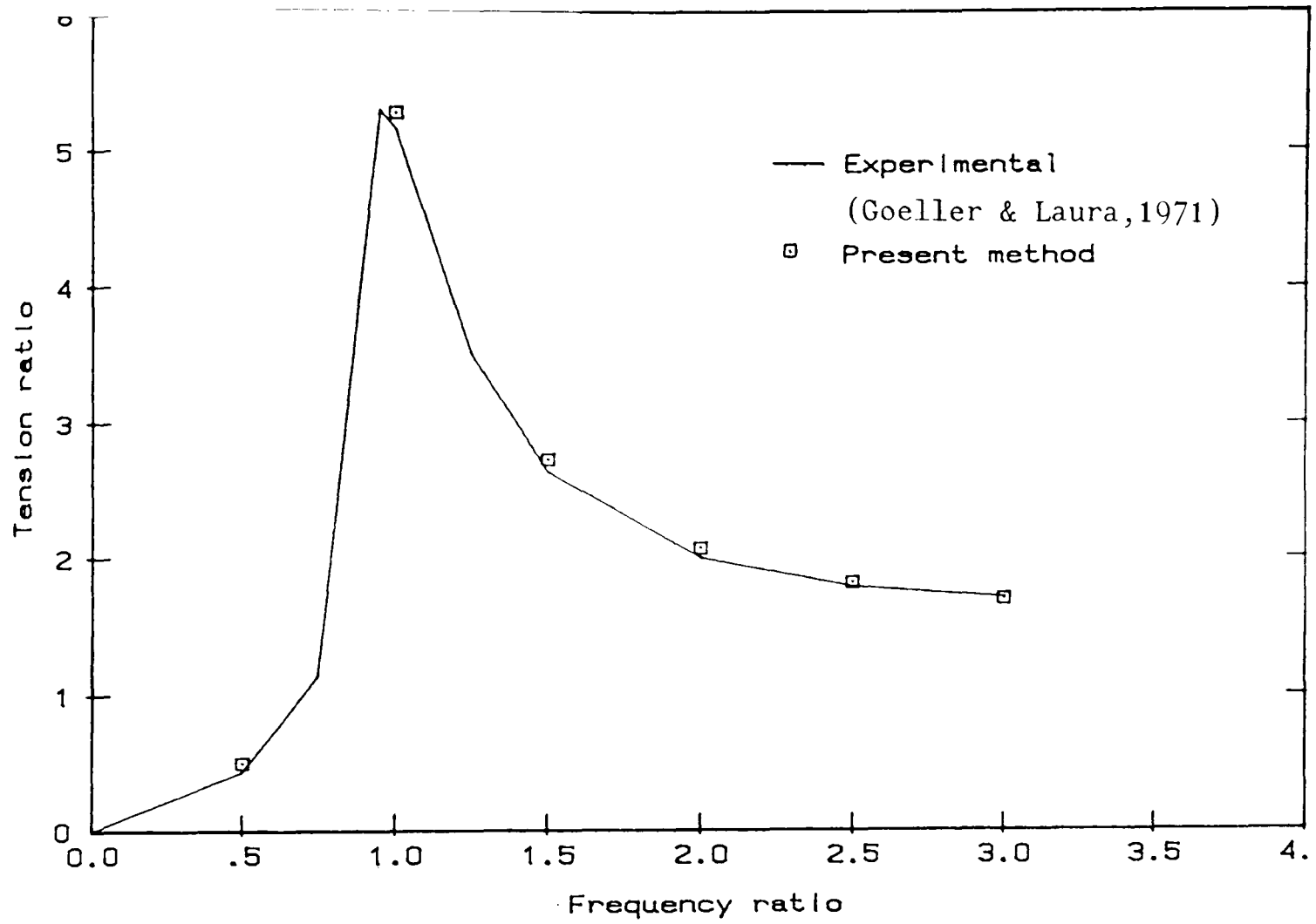

Figure 3.6

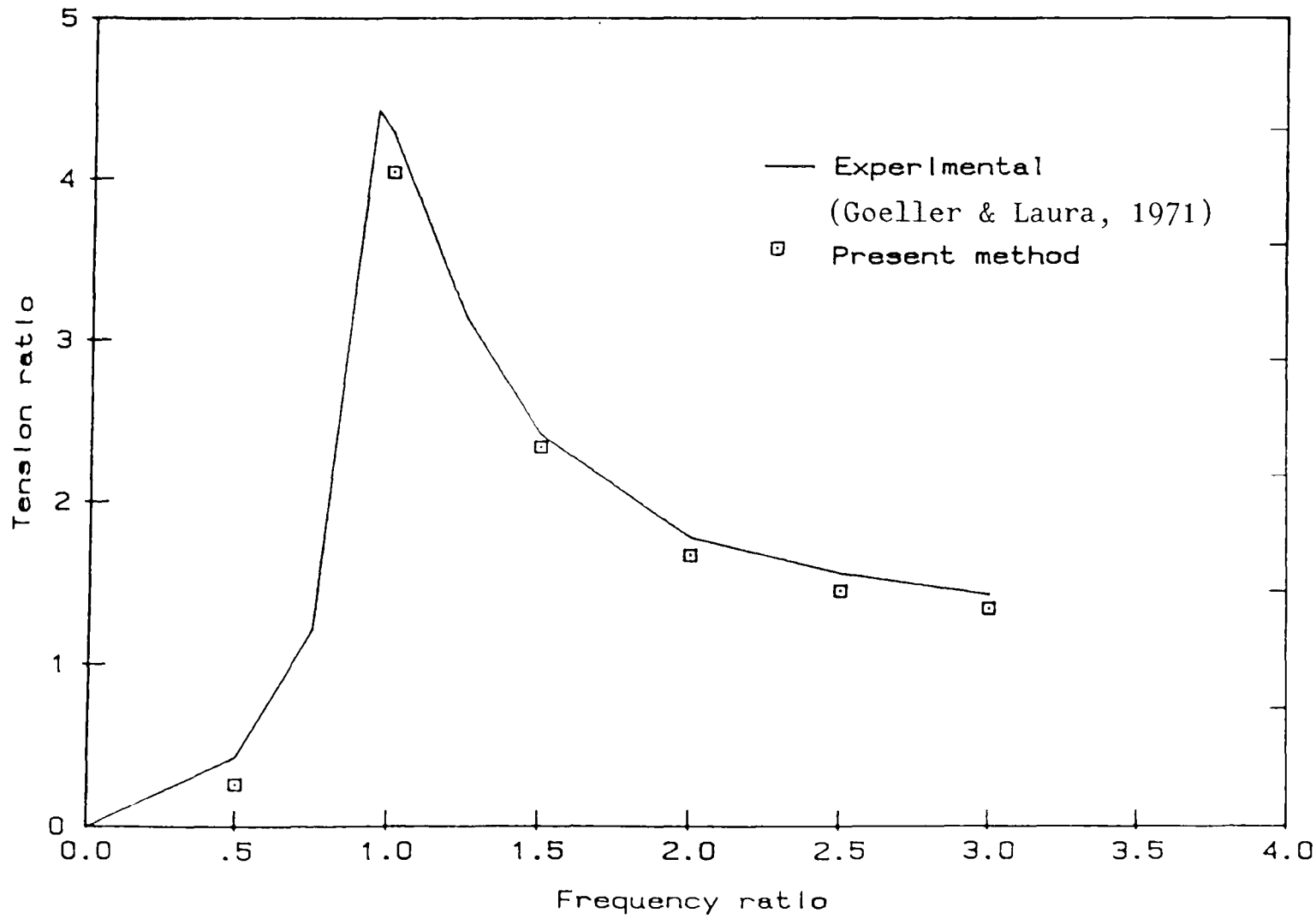

Figure 3.7

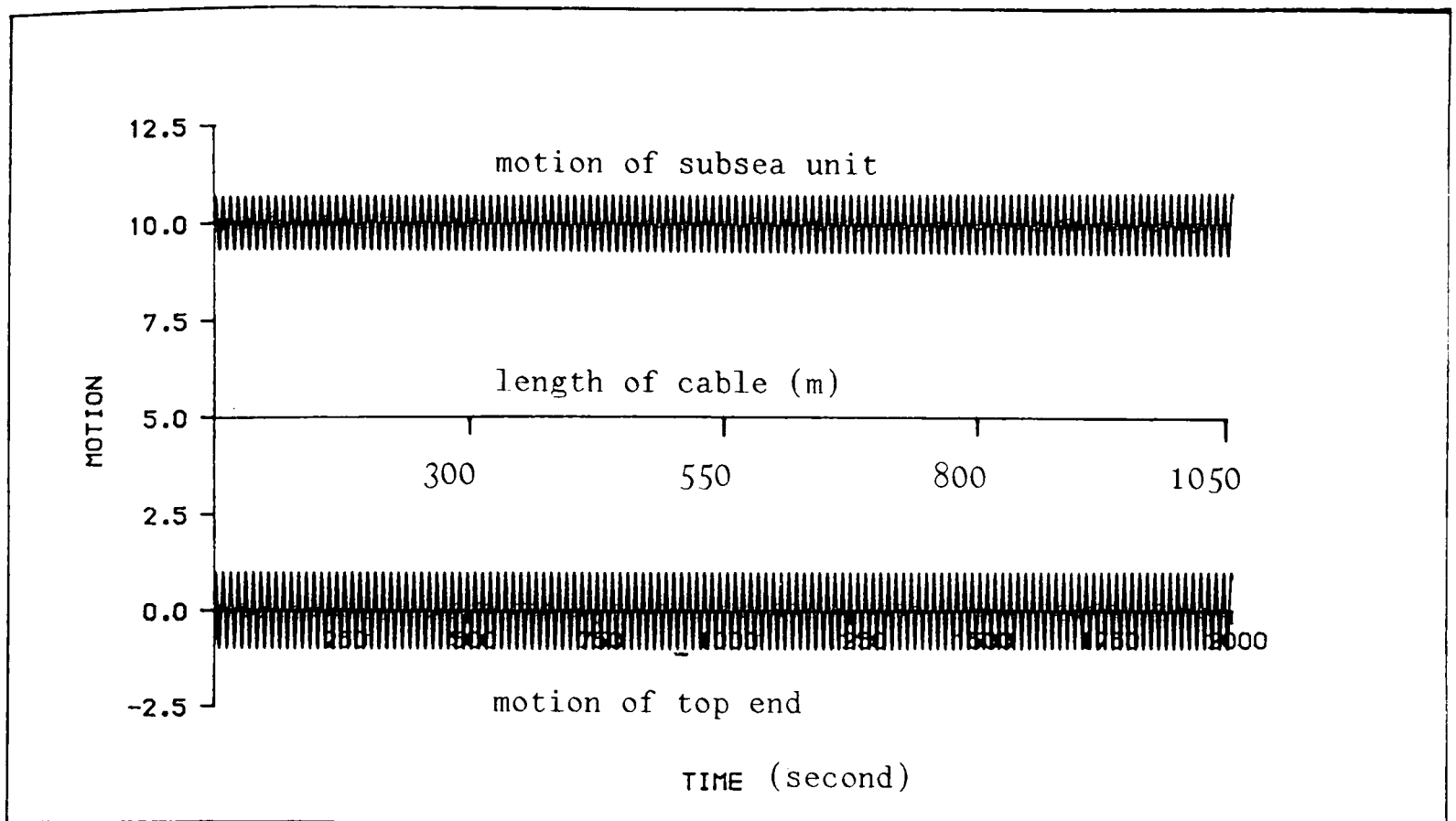

initial length 50m, frequency 0.4189rad/s, launch speed 0.5m/s

(a)

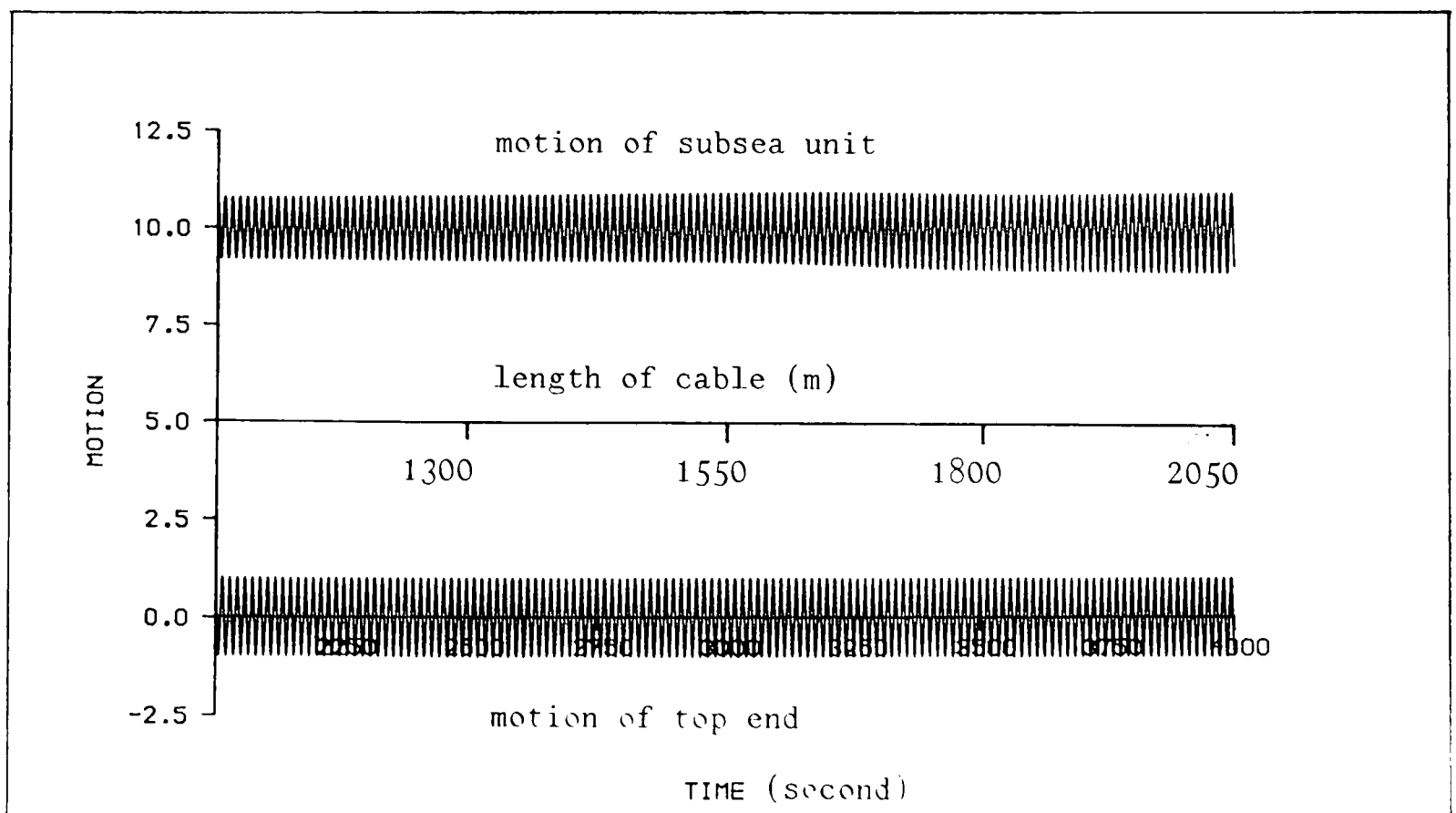

continuation of the graph above: time 2000-4000 s.

(b)

Figure 3.5

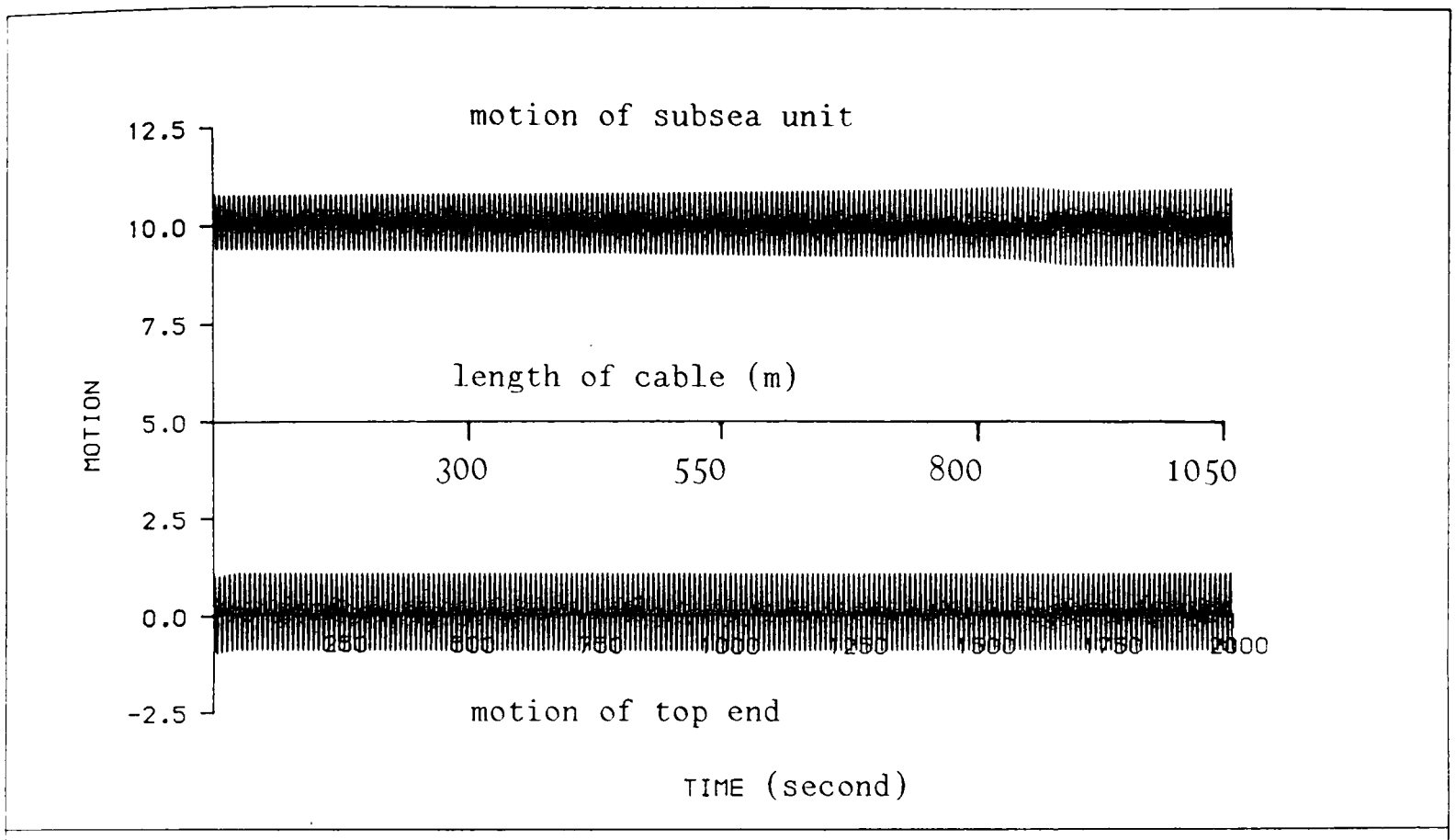

initial length 50m, frequency 0.628rad/s, launch speed 0.5m/s

(a)

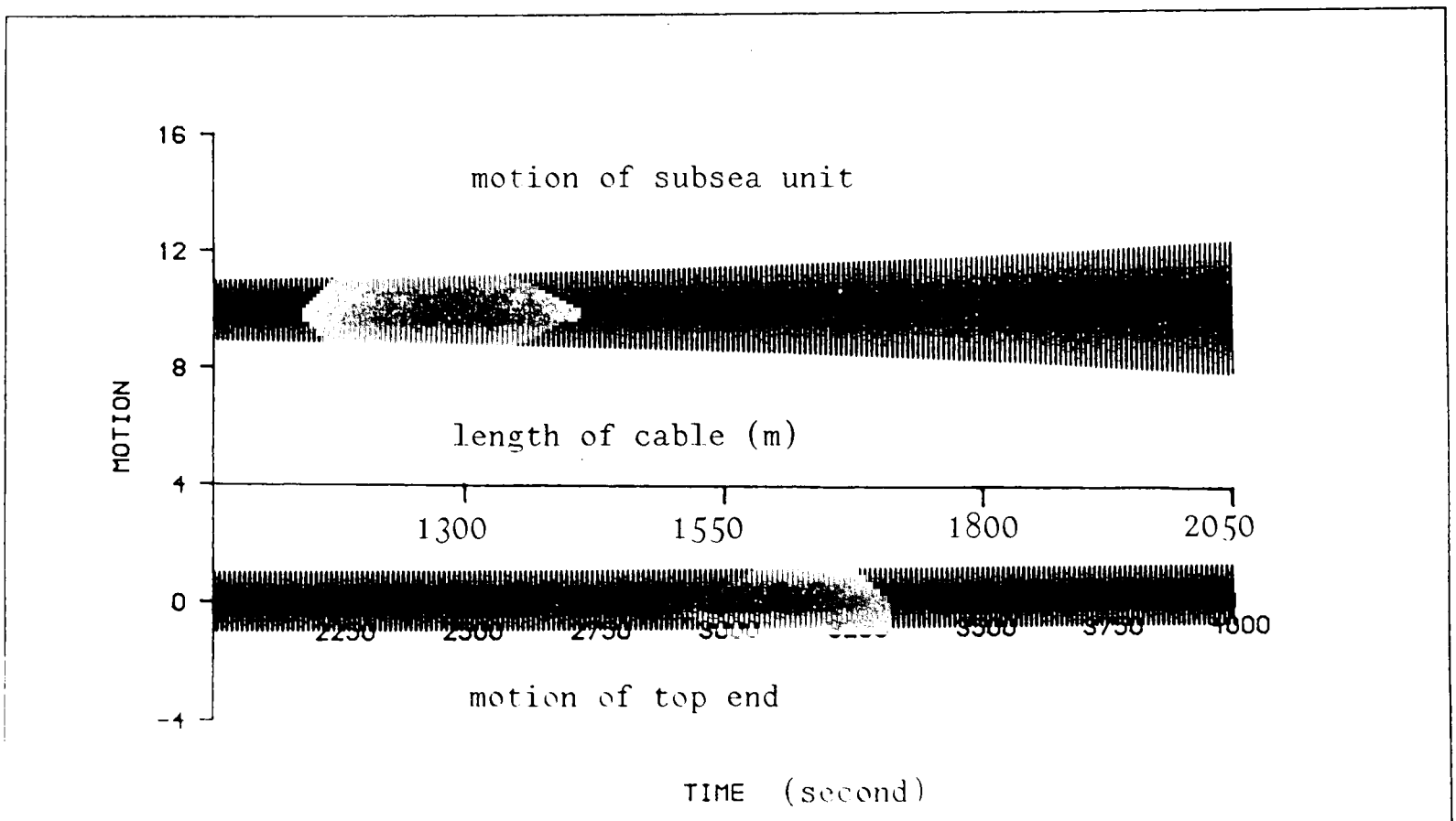

continuation of the graph above: time 2000-4000 s.

(b)

Figure 3.9

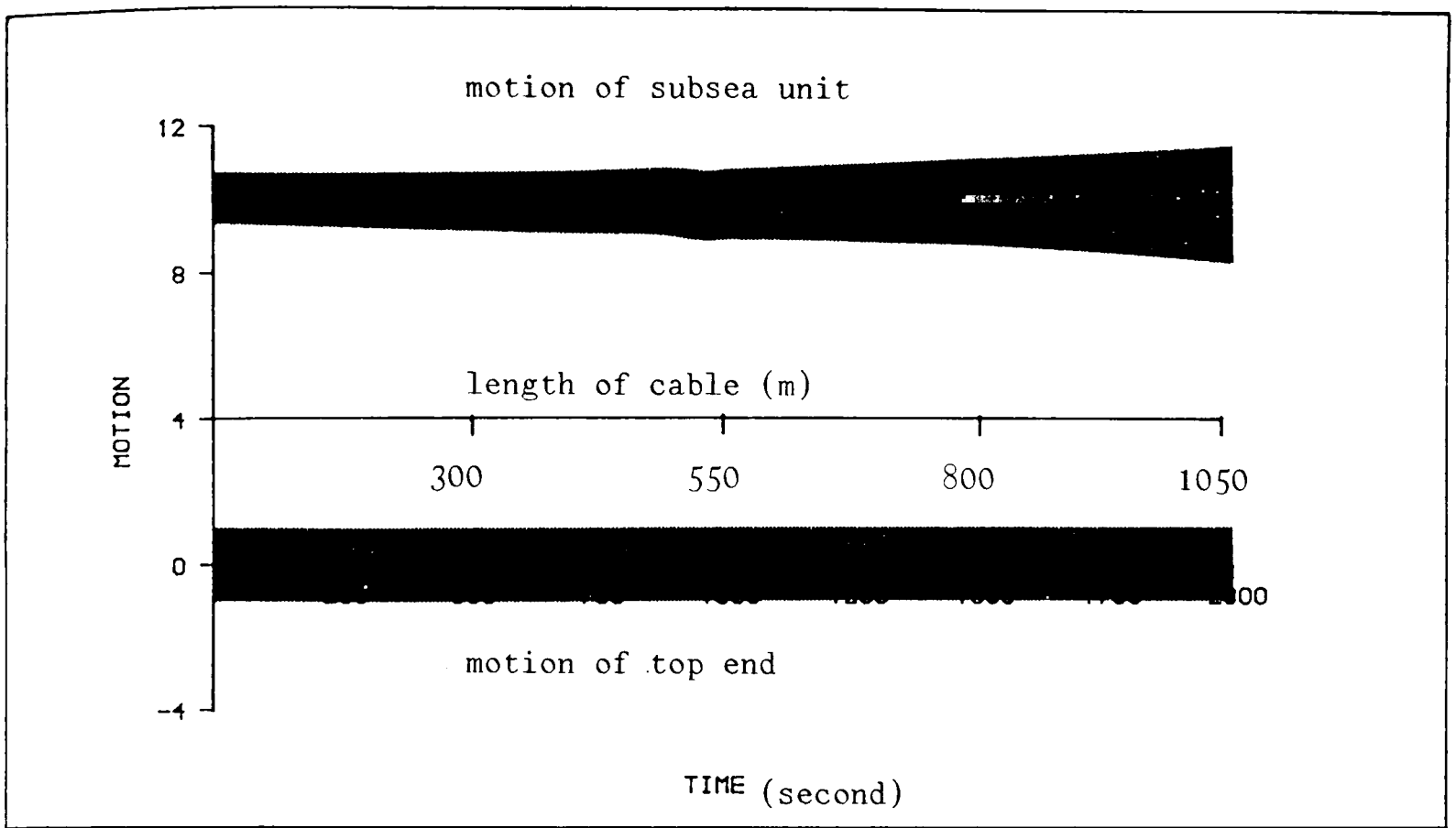

initial length 50m, freqency 0.838 rad/s, launch speed 0.5m/s

(a)

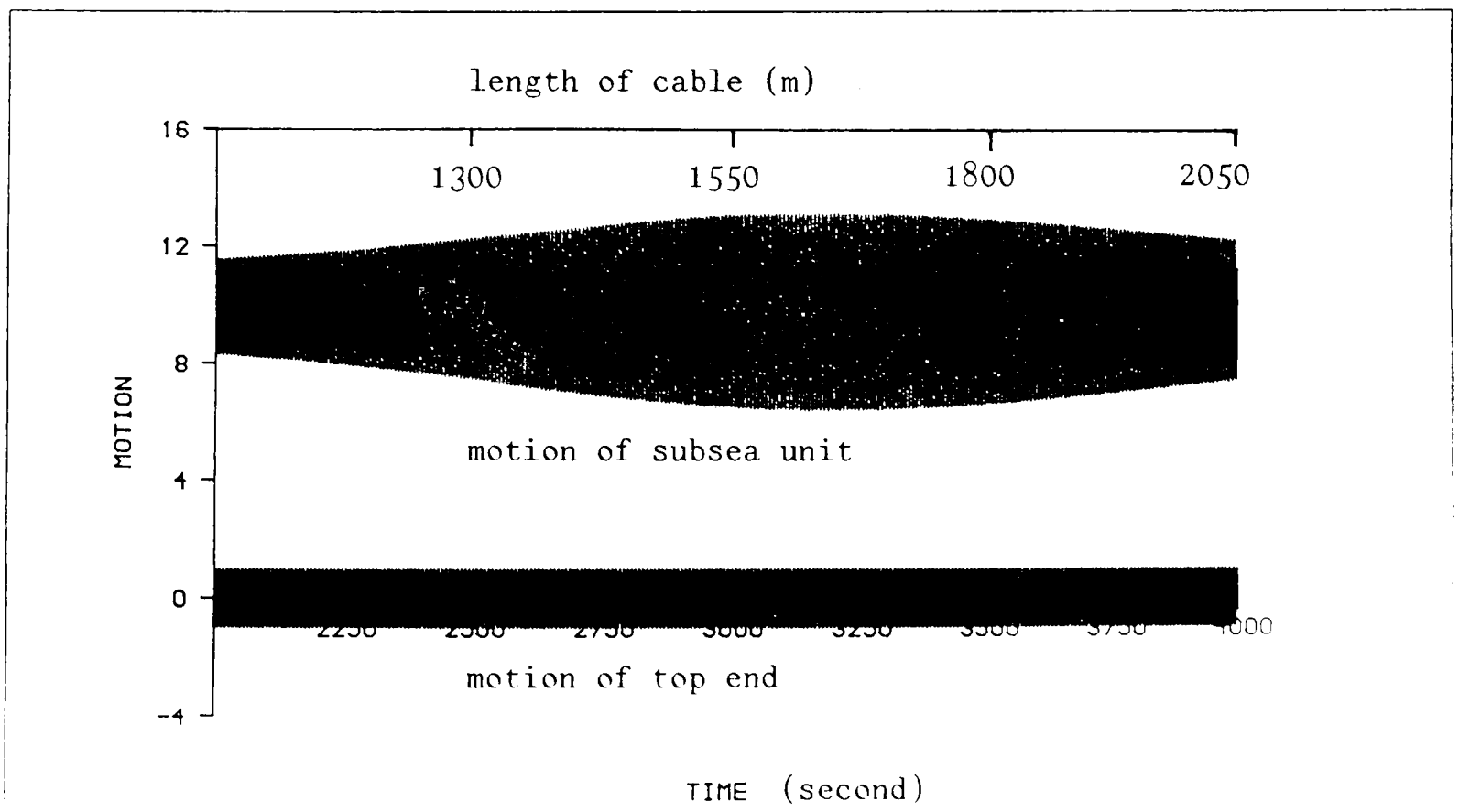

continuation of the graph above: time 2000-4000 s.

(b)

Figure 3.10

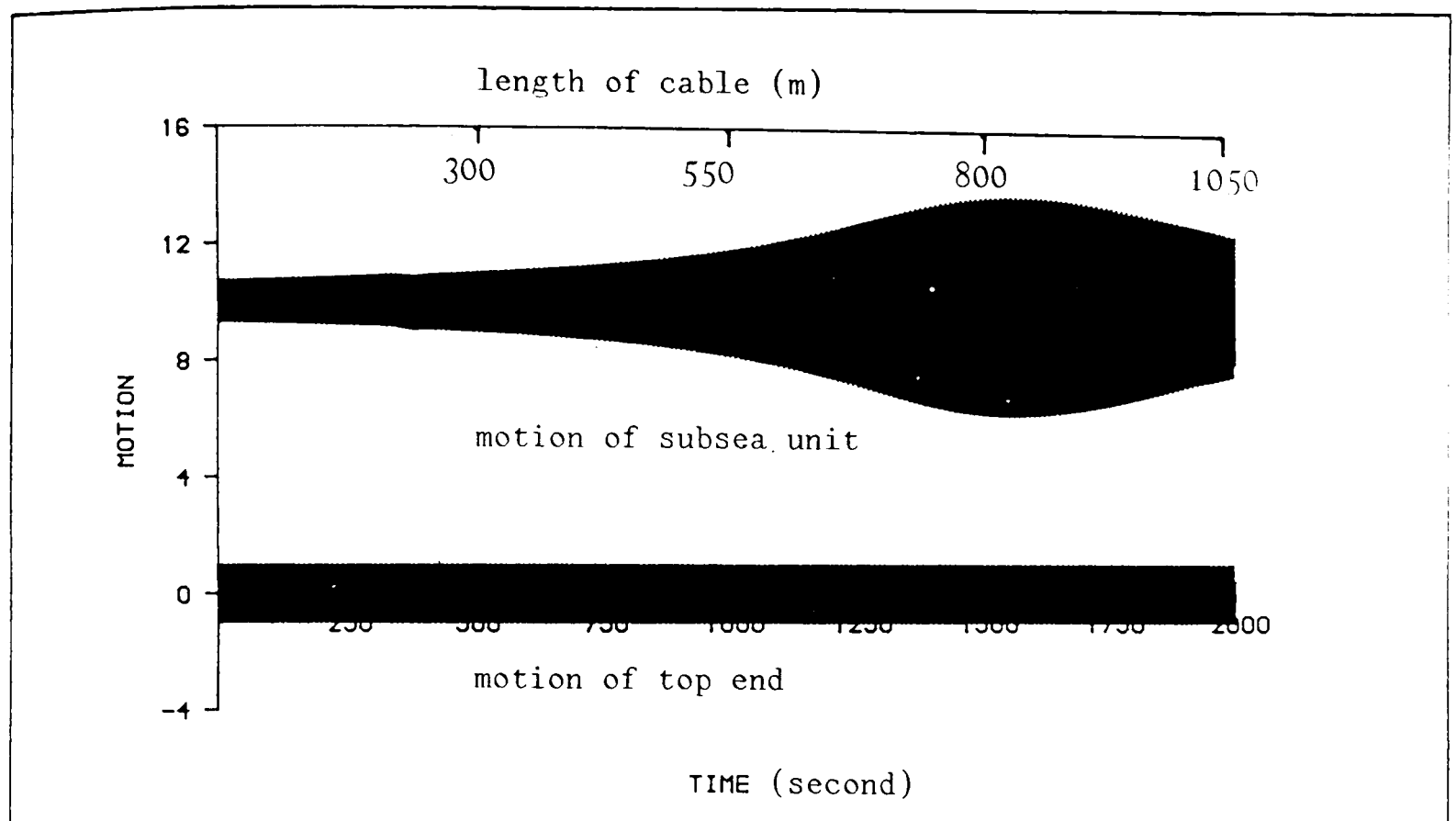

initial length 50m, frequency 1.26rad/s, launch speed 0.5m/s

(a)

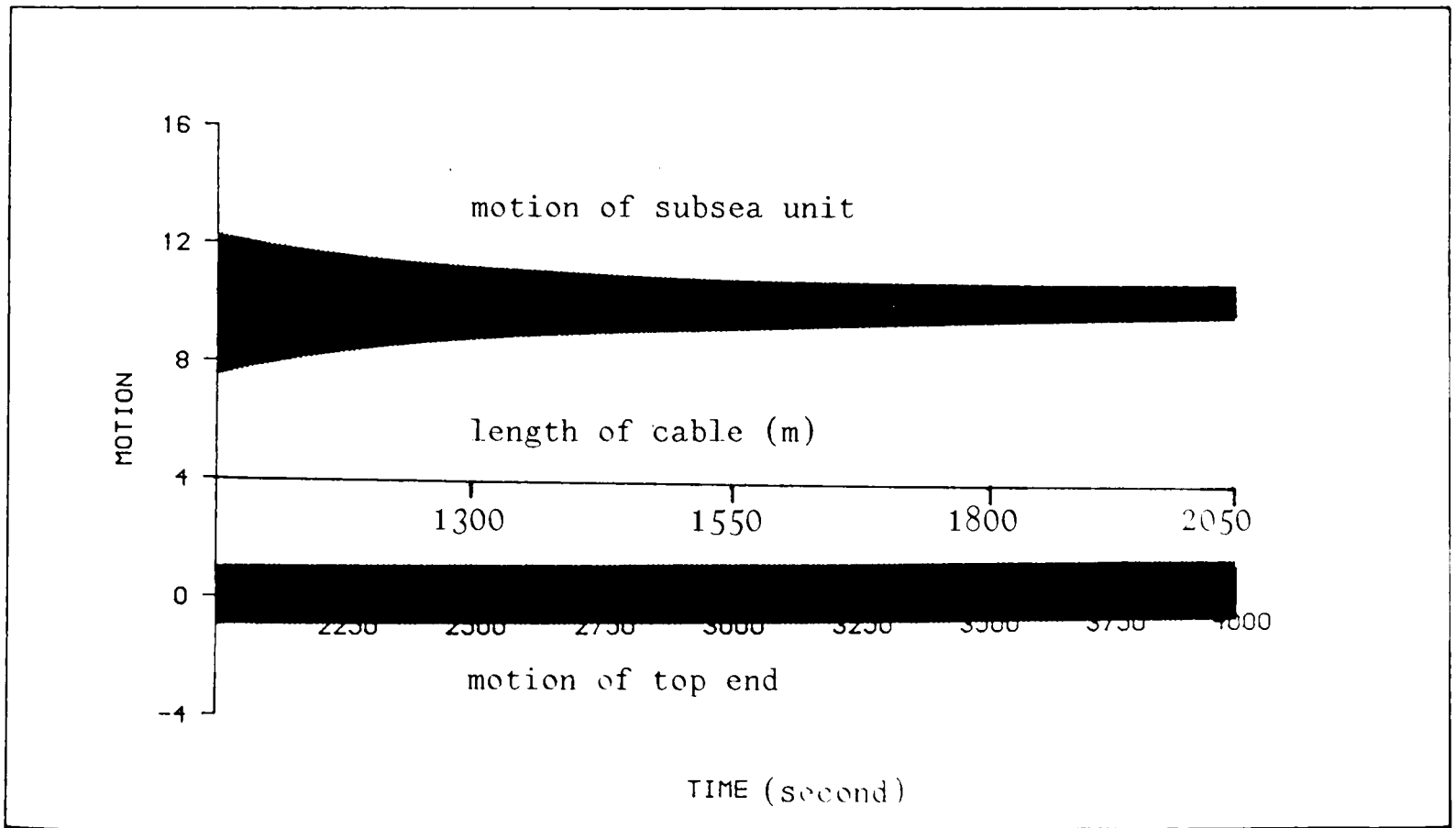

continuation of the graph above: time 2000-4000 s.

(b)

Figure 3.11

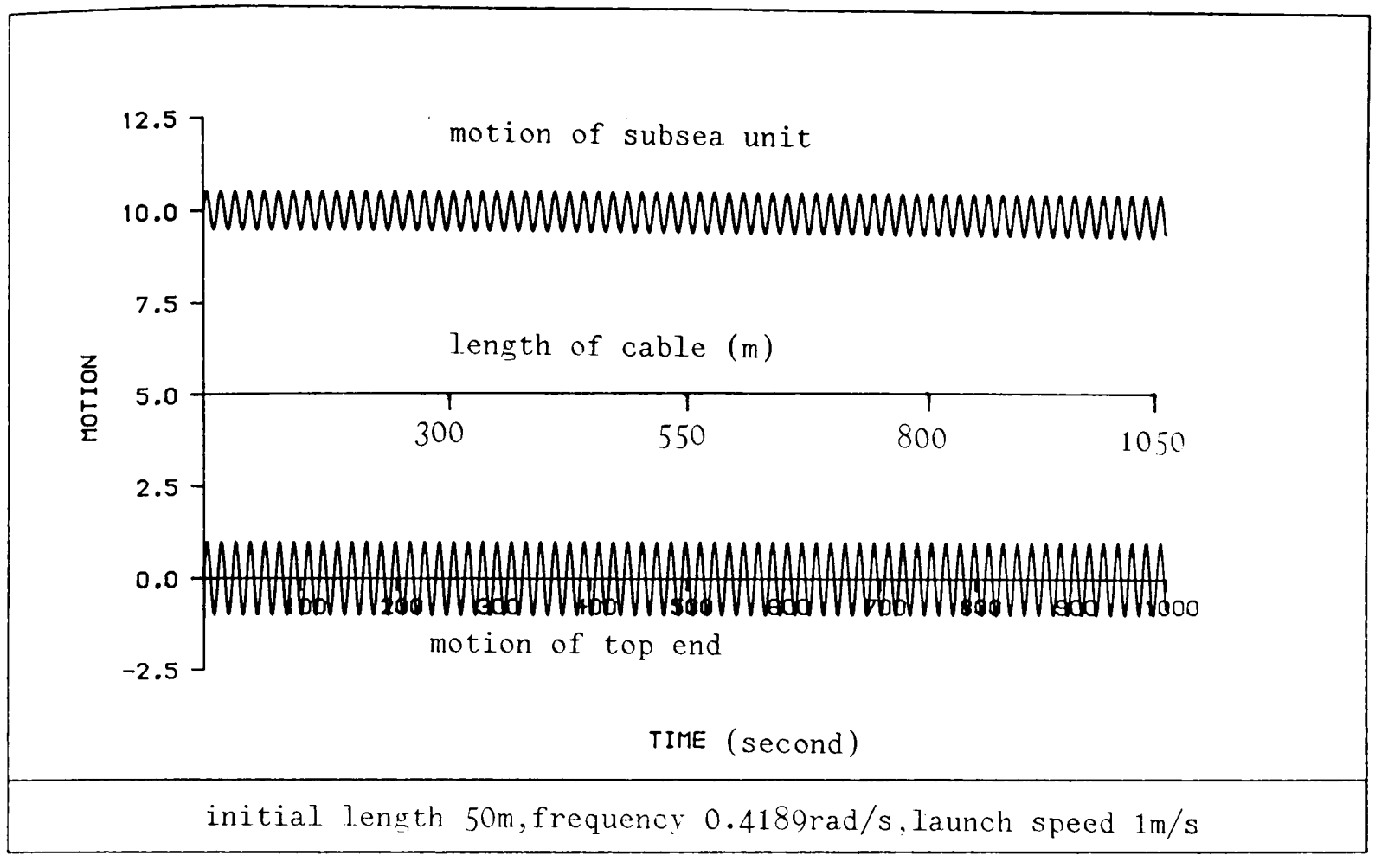

initial length 50m, frequency 0.4189rad/s, launch speed 1m/s

(a)

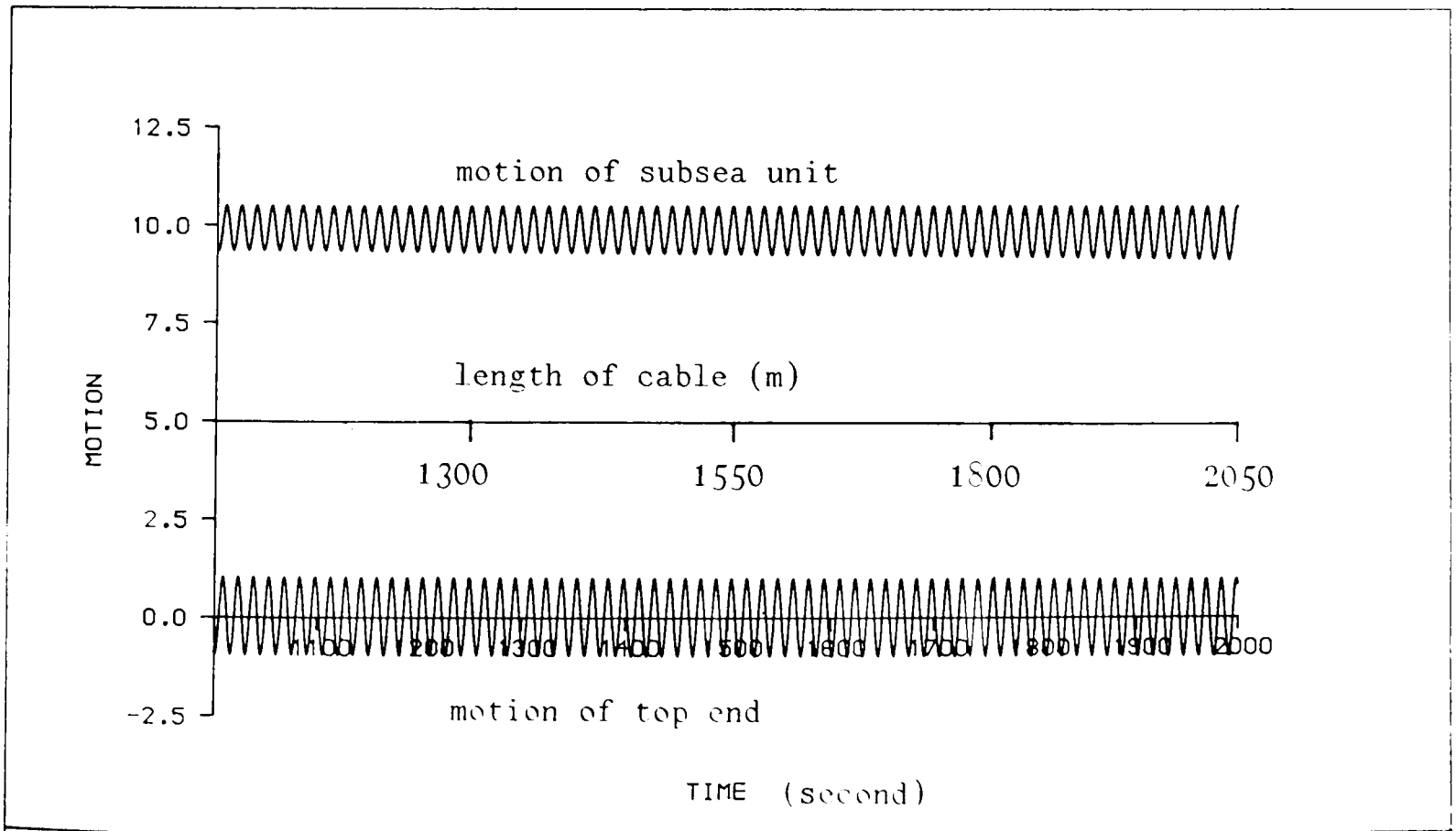

continuation of the graph above; time 1000-2000 s.

(b)

Figure 3.12

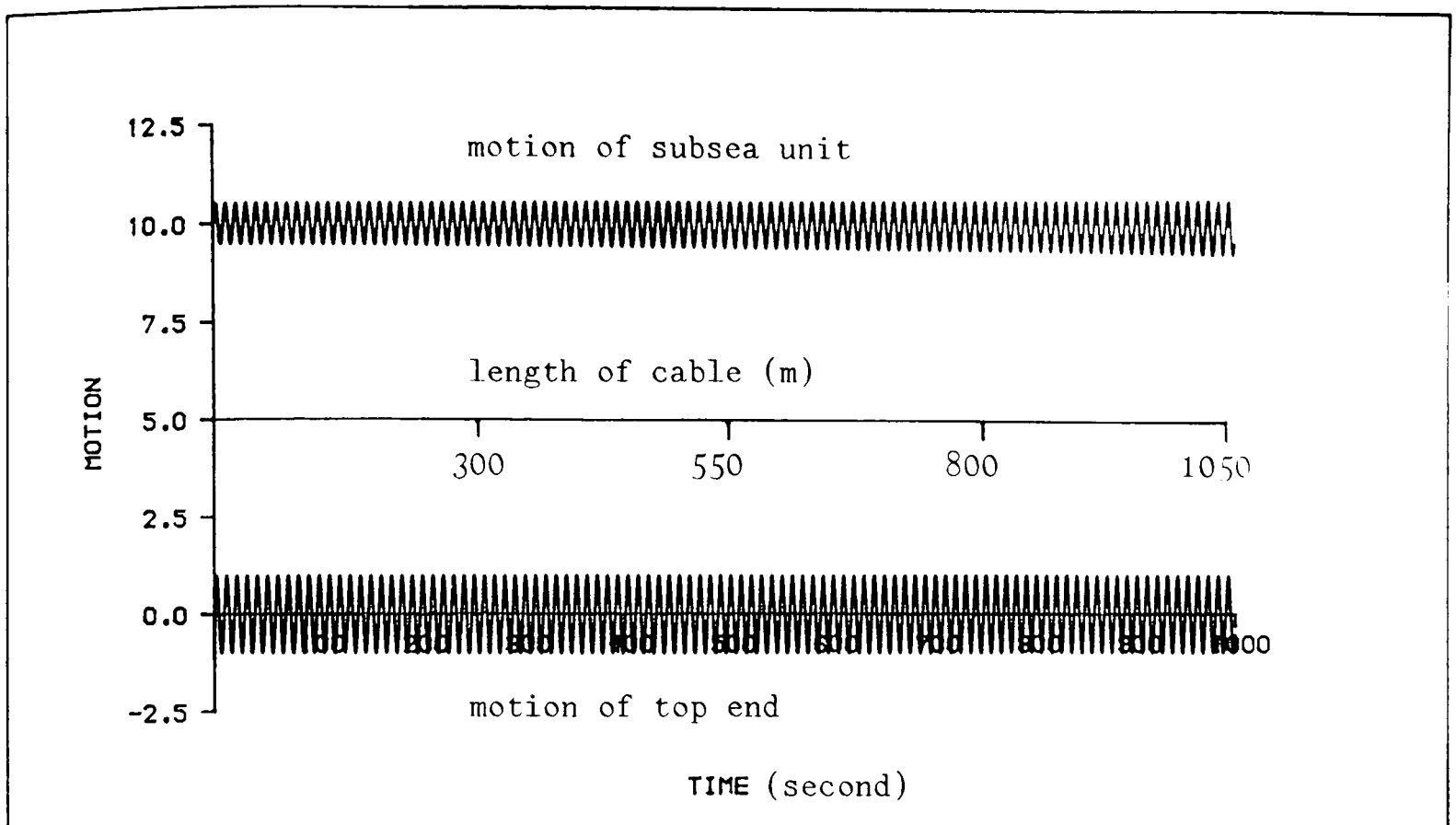

initial length 50m, frequency 0.628rad/s, launch speed 1m/s

(a)

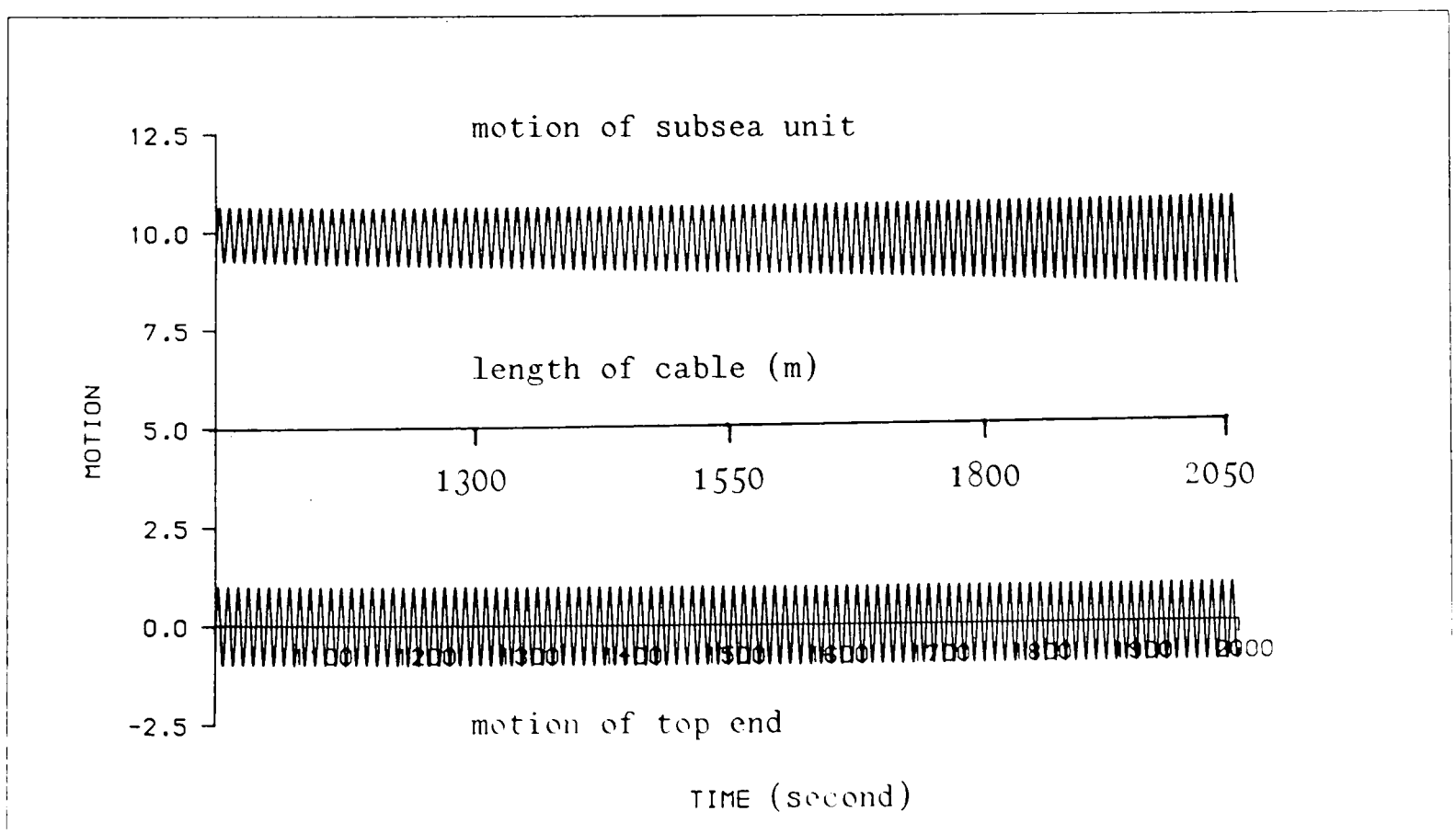

continuation of the graph above: time 1000-2000 s.

(b)

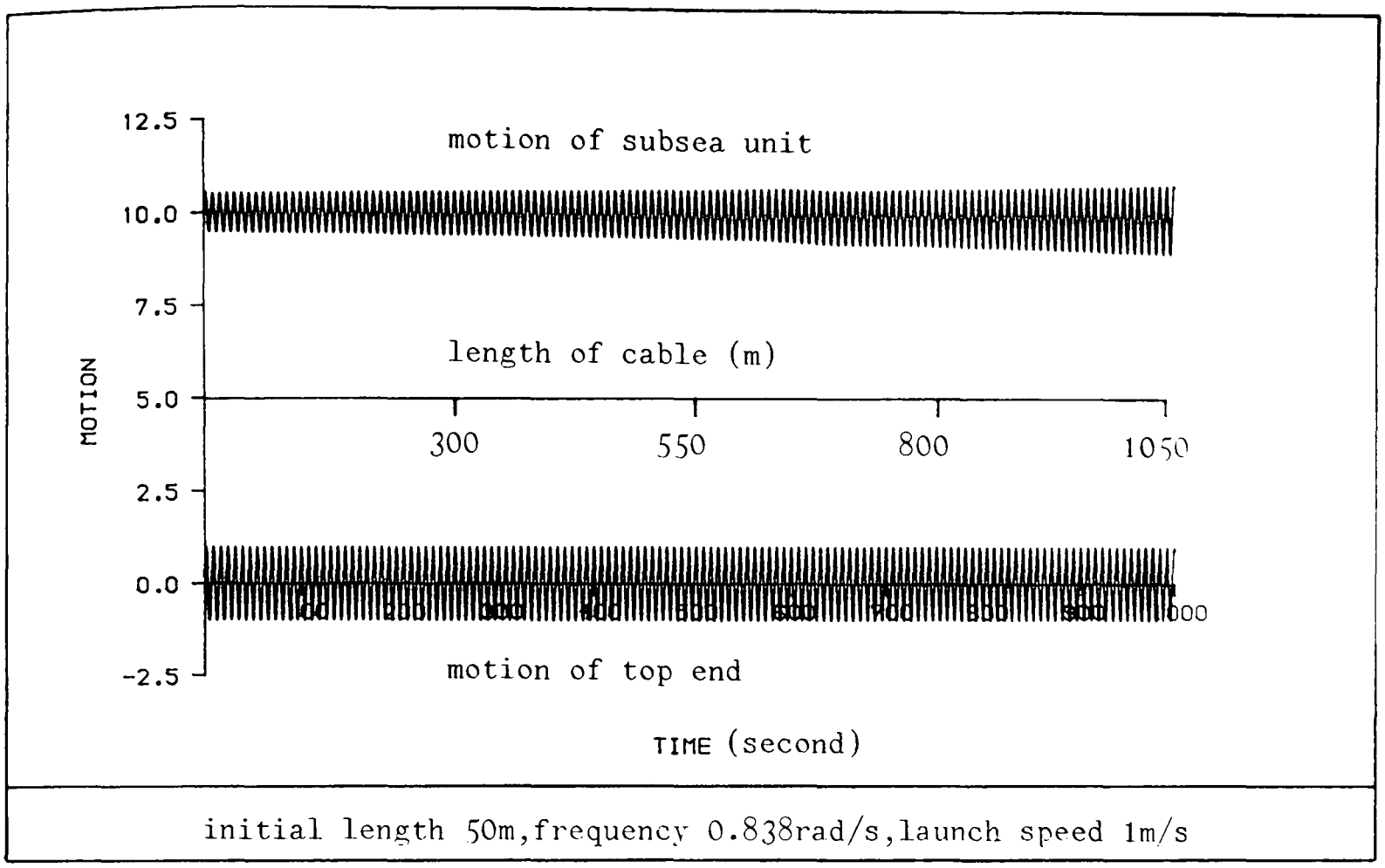

initial length 50m, frequency 0.838rad/s, launch speed 1m/s

(a)

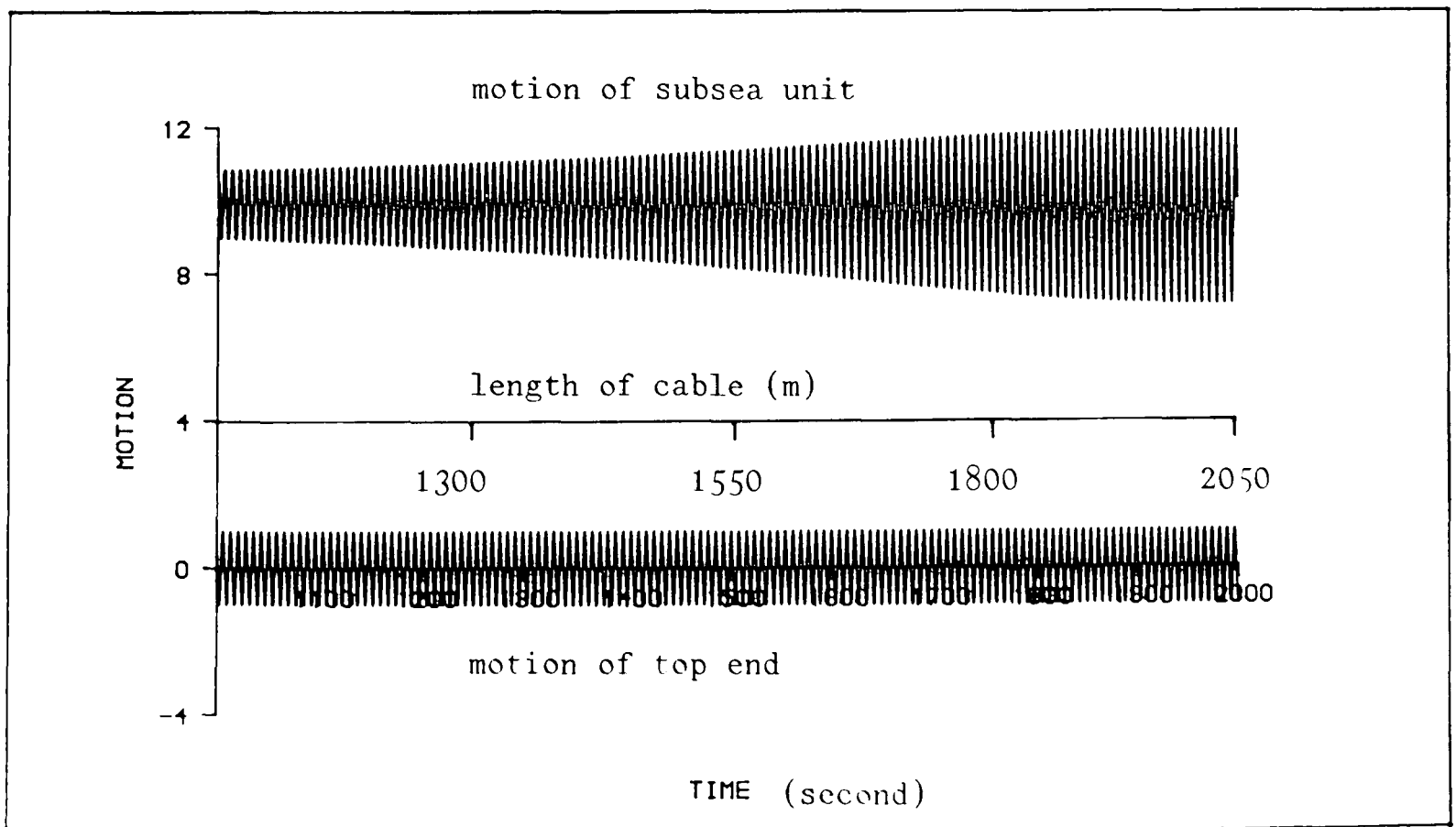

continuation of the graph above; time 1000-2000 s.

(b)

Figure 3.14

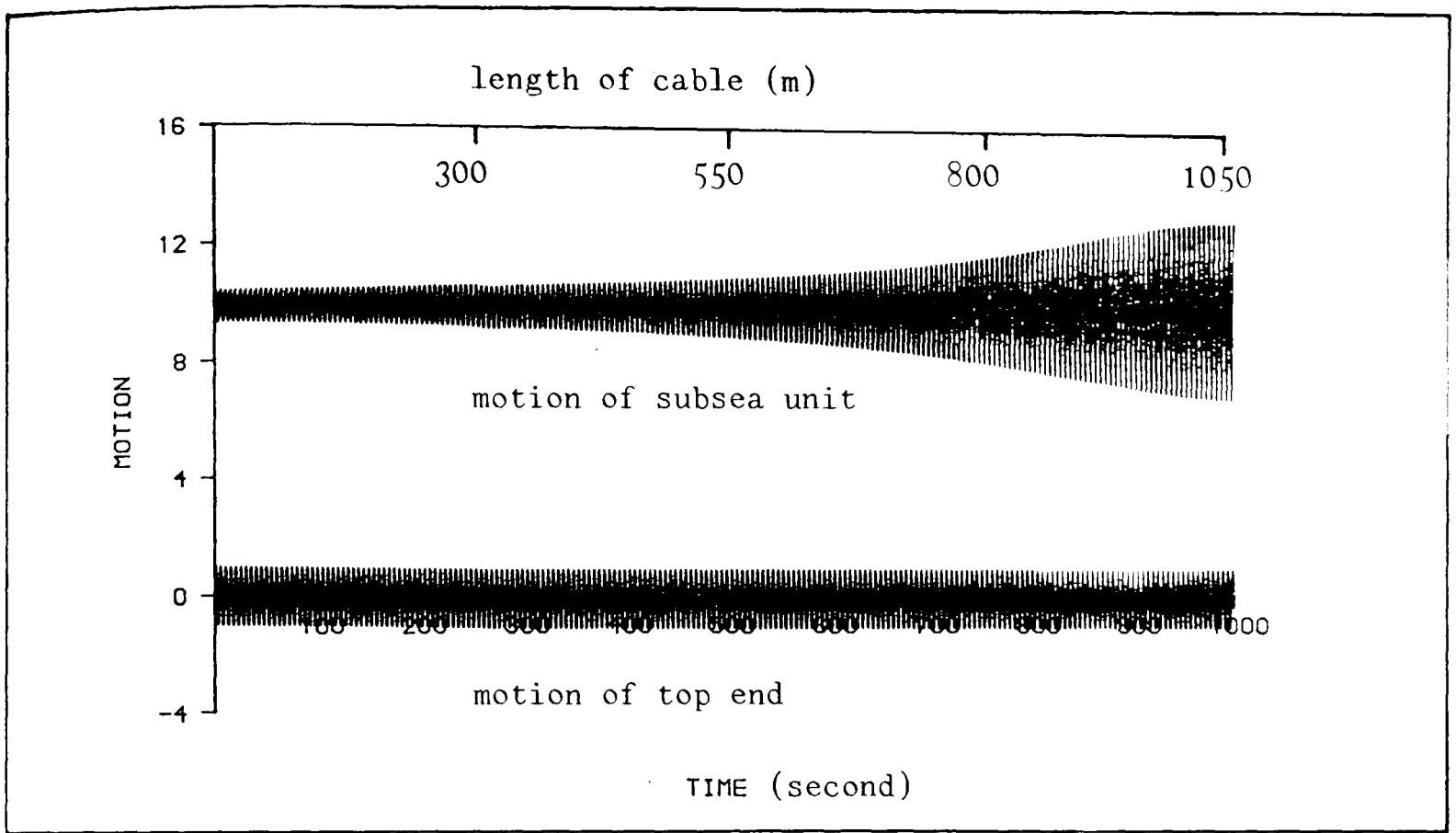

initial length 50m, frequency 1.26rad/s, launch speed 1m/s

(a)

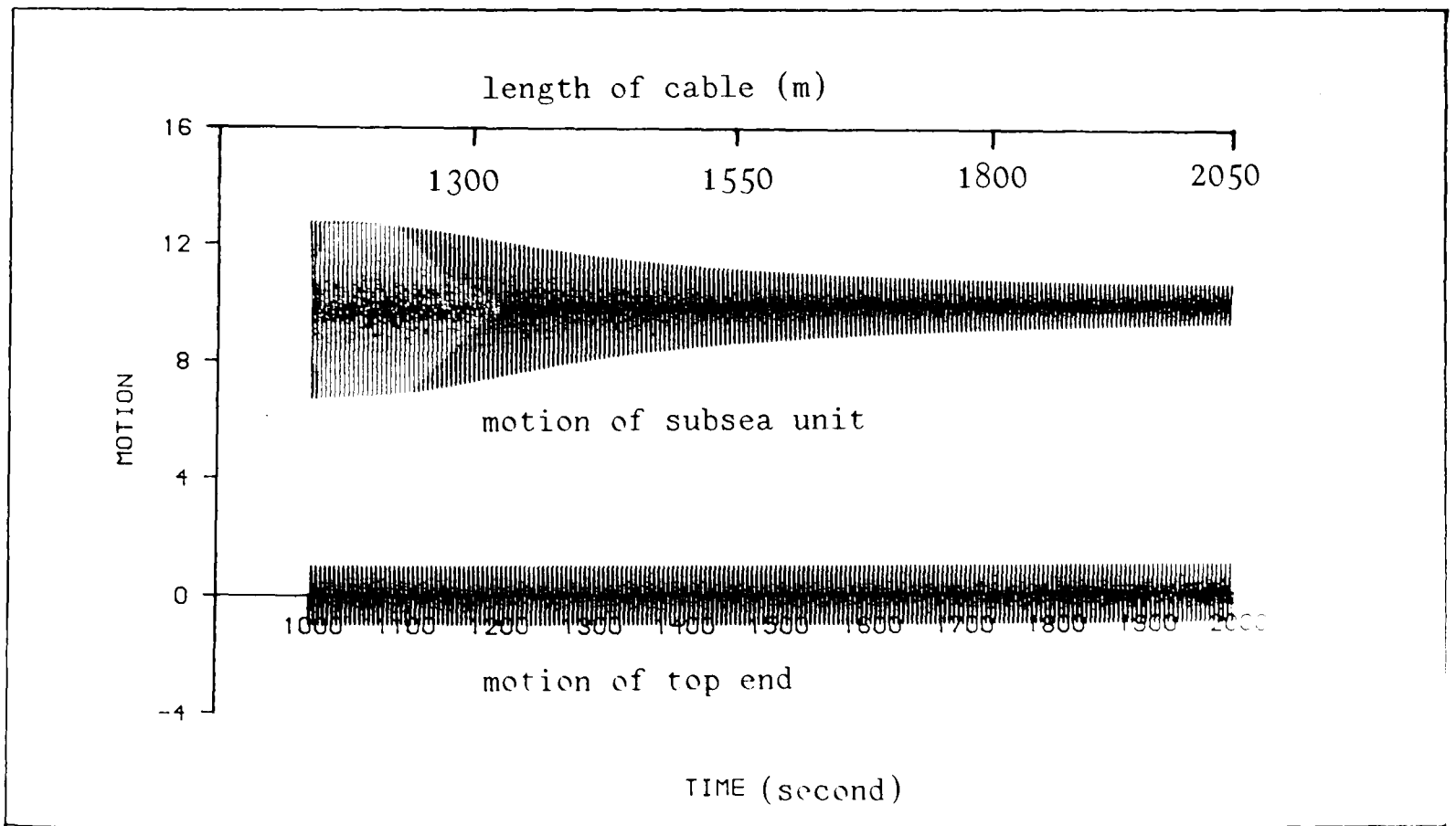

continuation of the graph above: time 1000-2000 s.

(b)

Figure 3.15

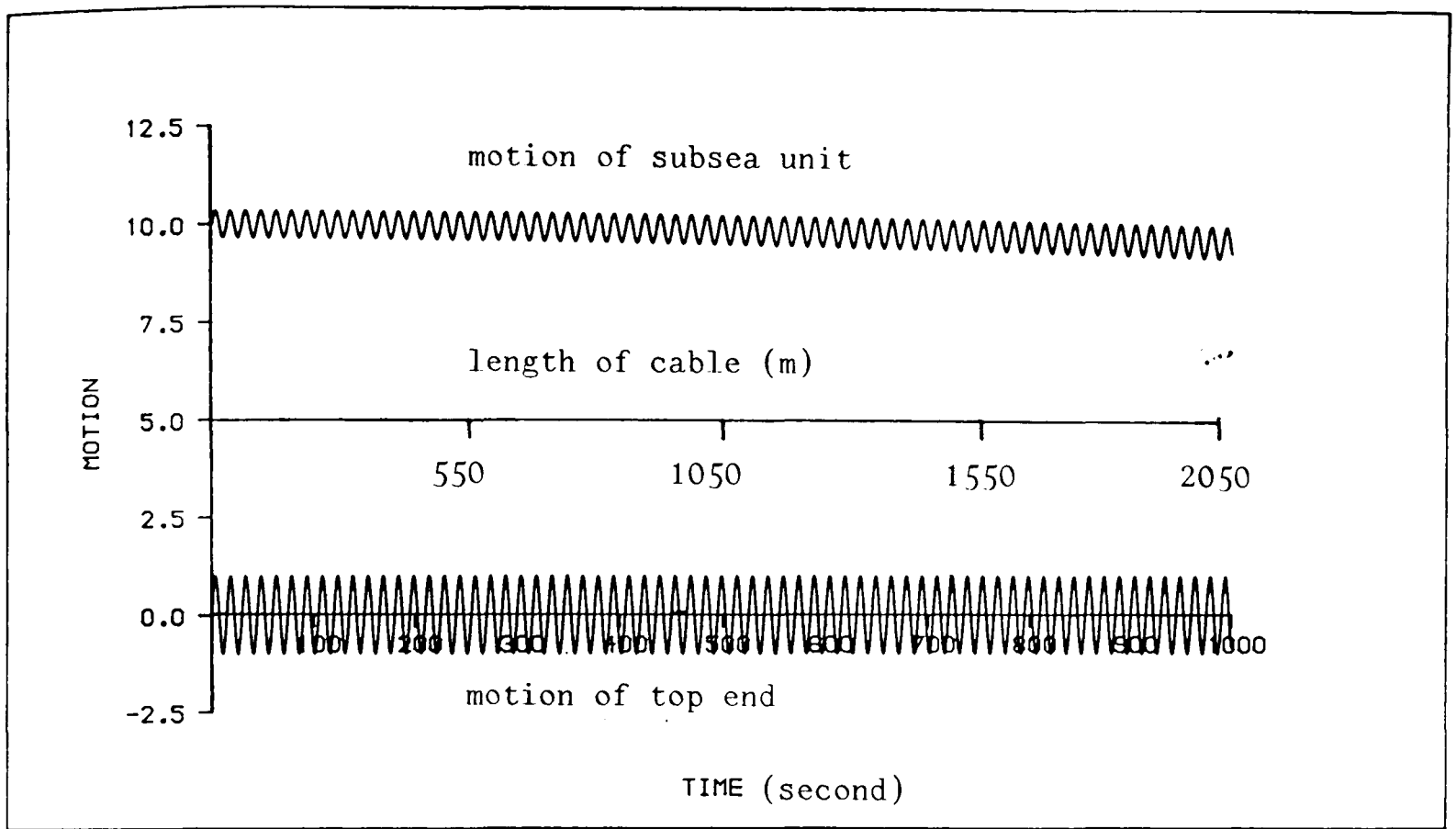

initial length 50m, frequency 0.4189rad/s, launch speed 2m/s

(a)

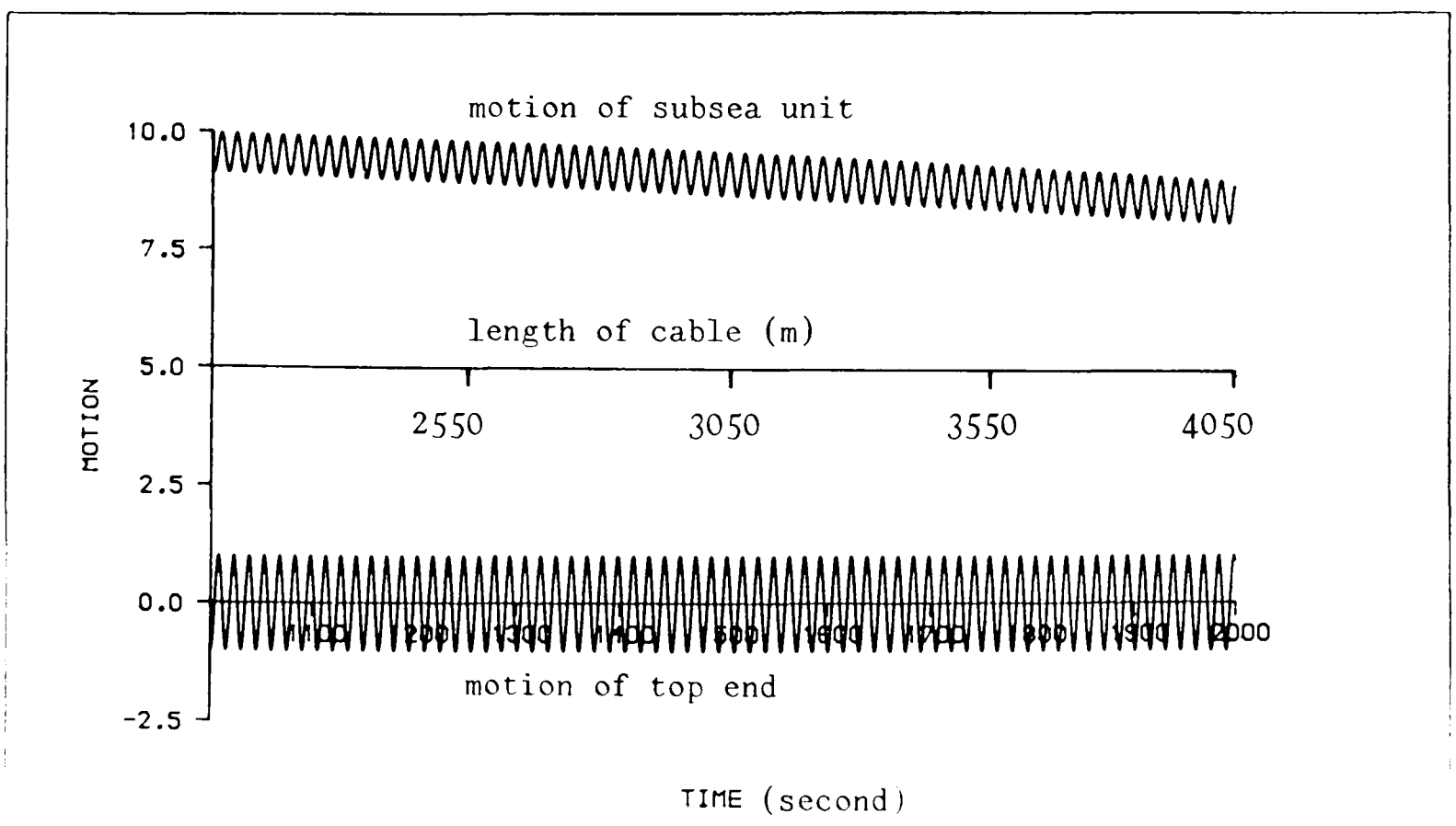

continuation of the graph above: time 1000-2000 s.

(b)

Figure 3.1

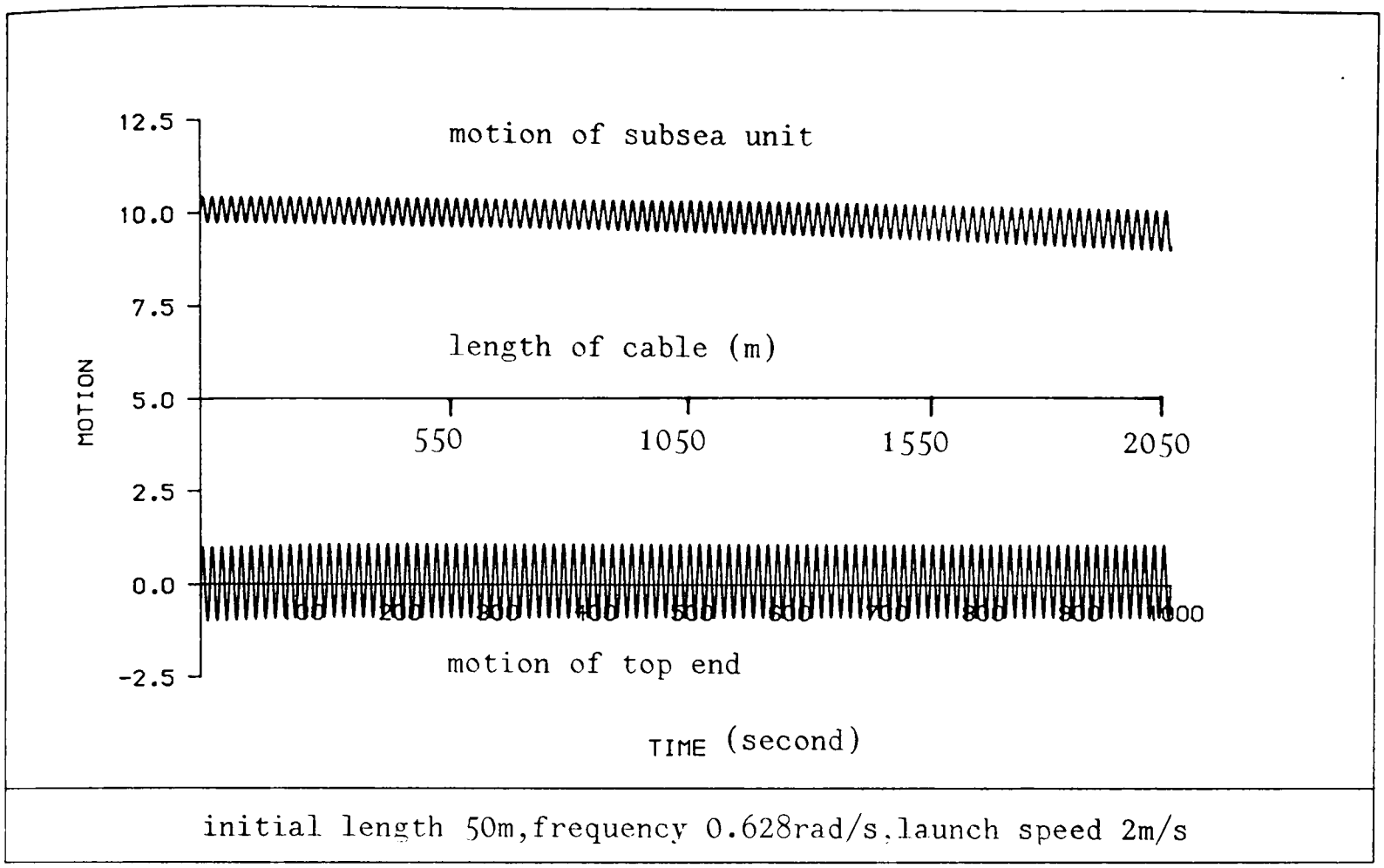

initial length 50m, frequency 0.628rad/s, launch speed 2m/s

(a)

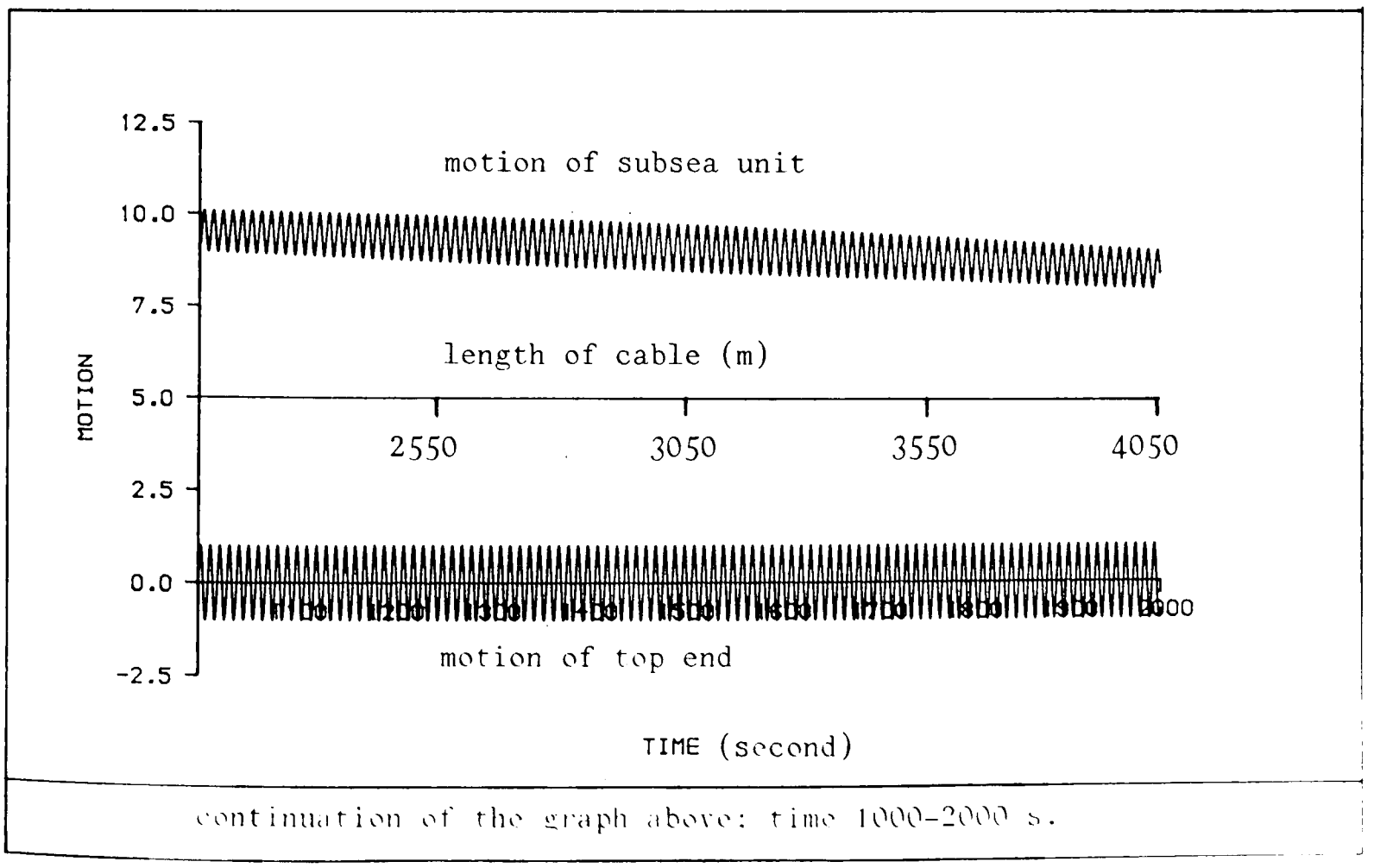

continuation of the graph above: time 1000-2000 s.

(b)

Figure 3.17

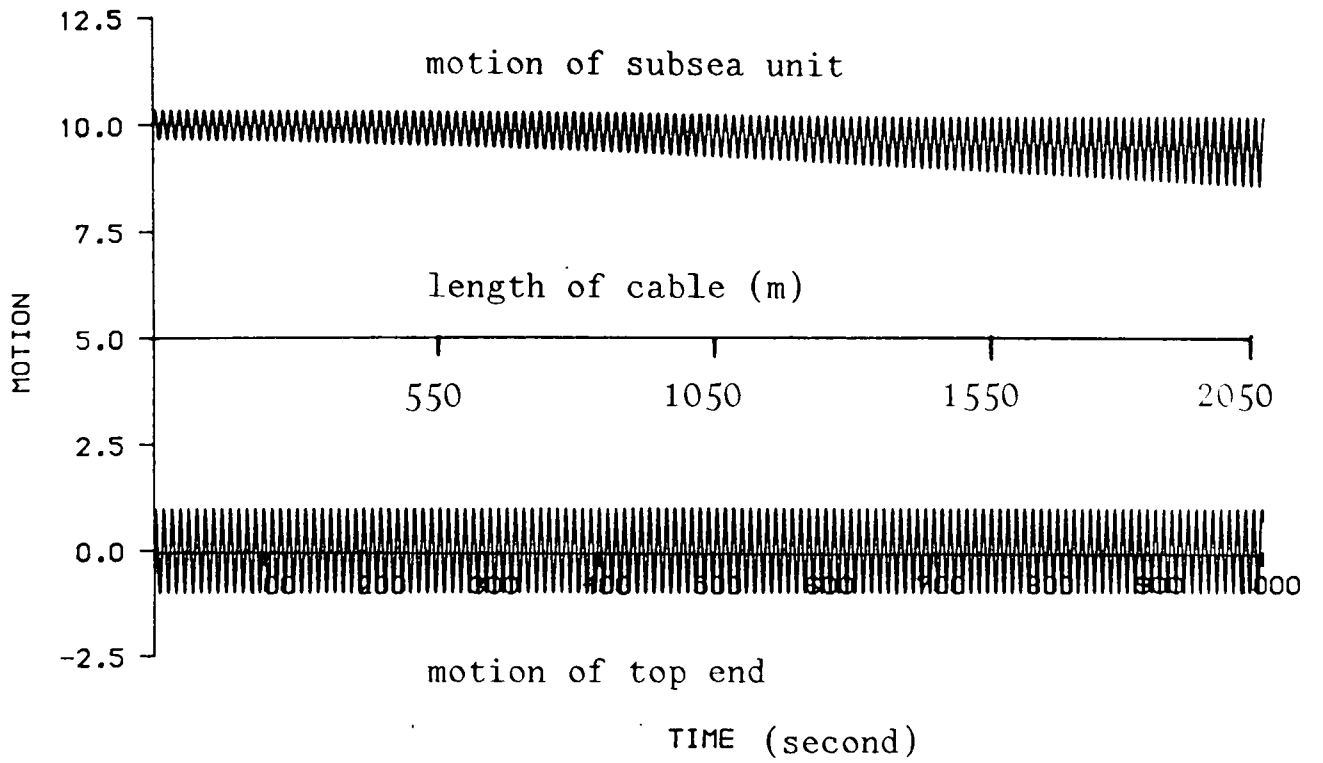

initial length 50m, frequency 0.838rad/s, launch speed 2m/s

(a)

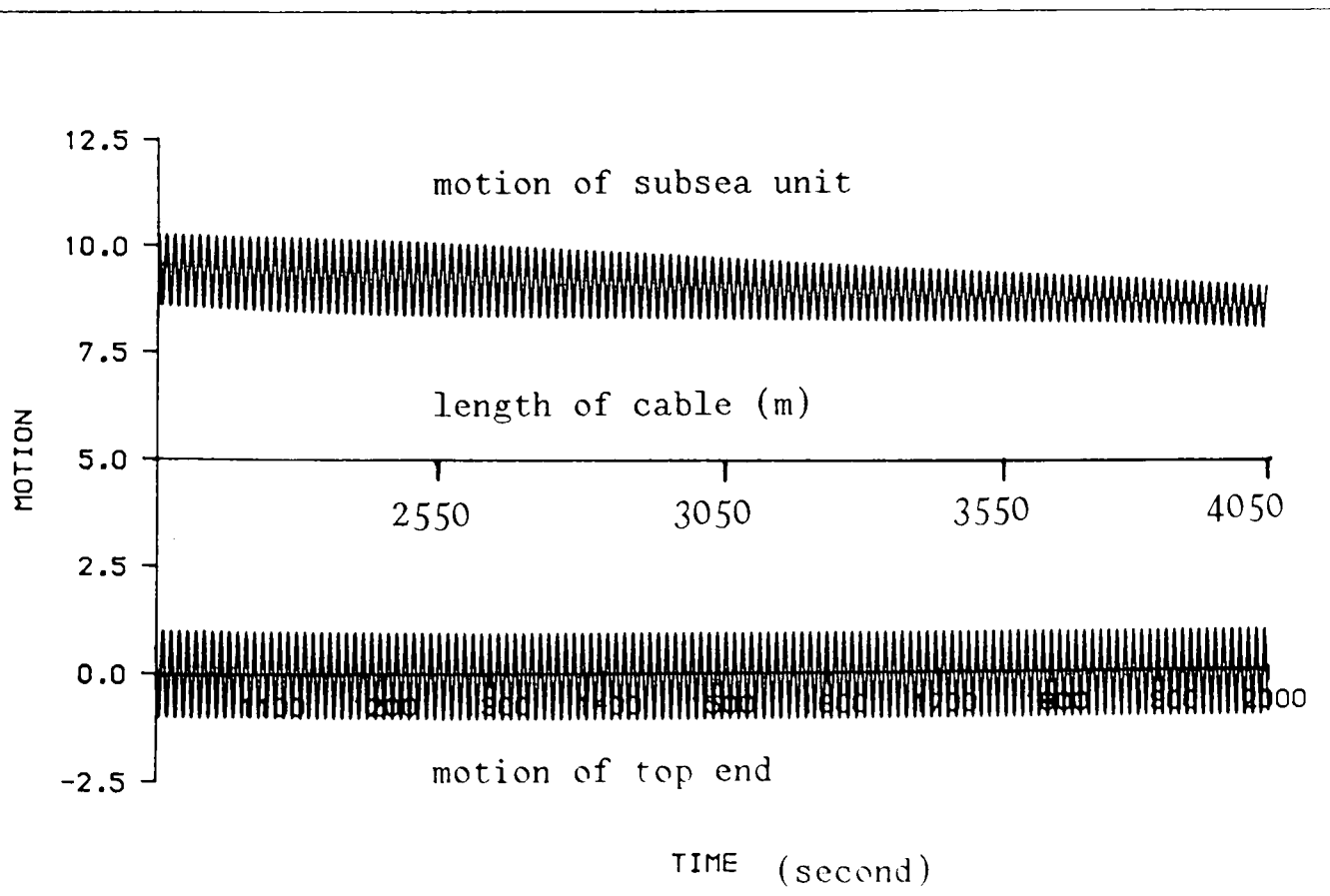

continuation of the graph above: time 1000-2000 s.

(b)

Figure 3.16

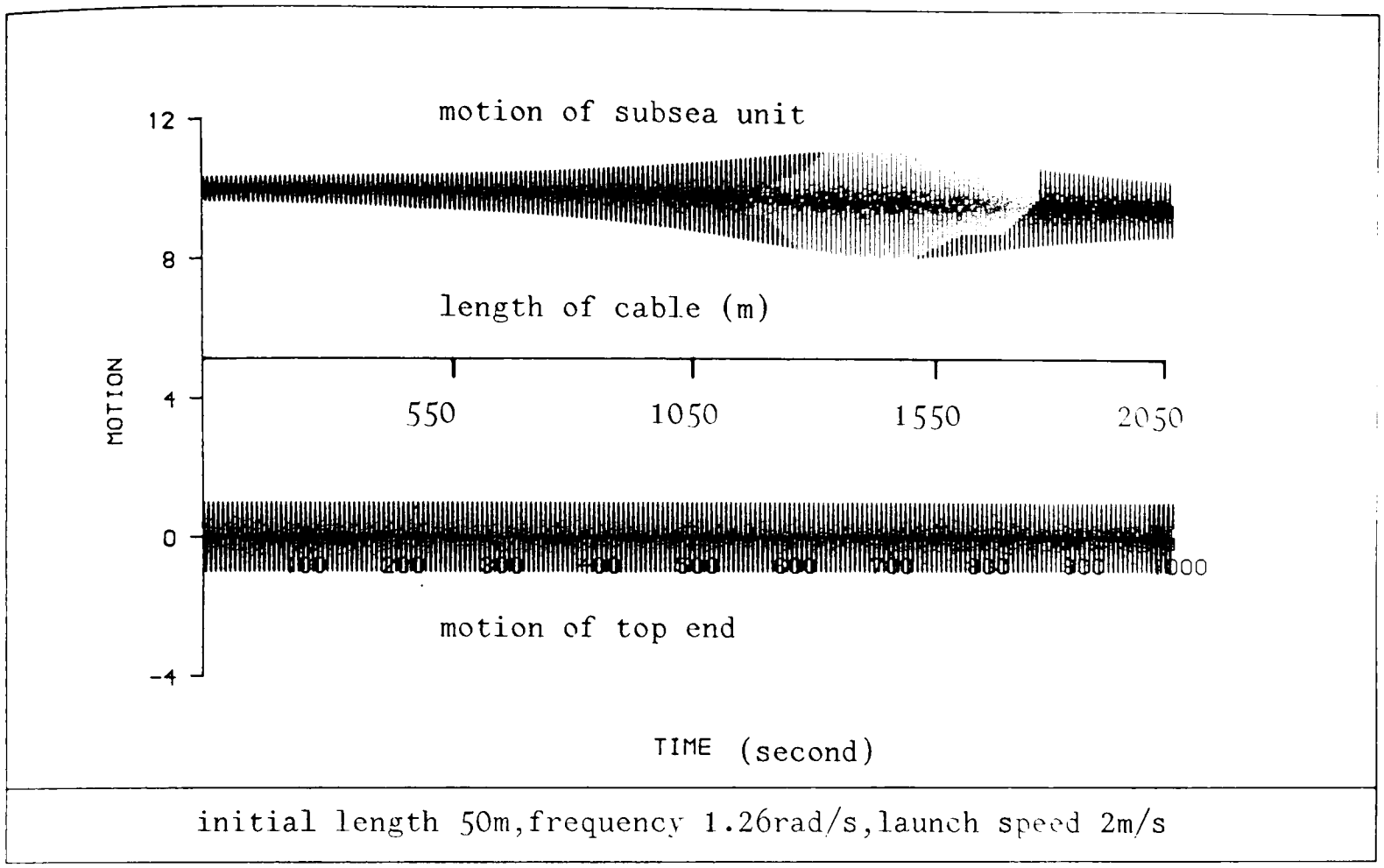

initial length 50m, frequency 1.26rad/s, launch speed 2m/s

(a)

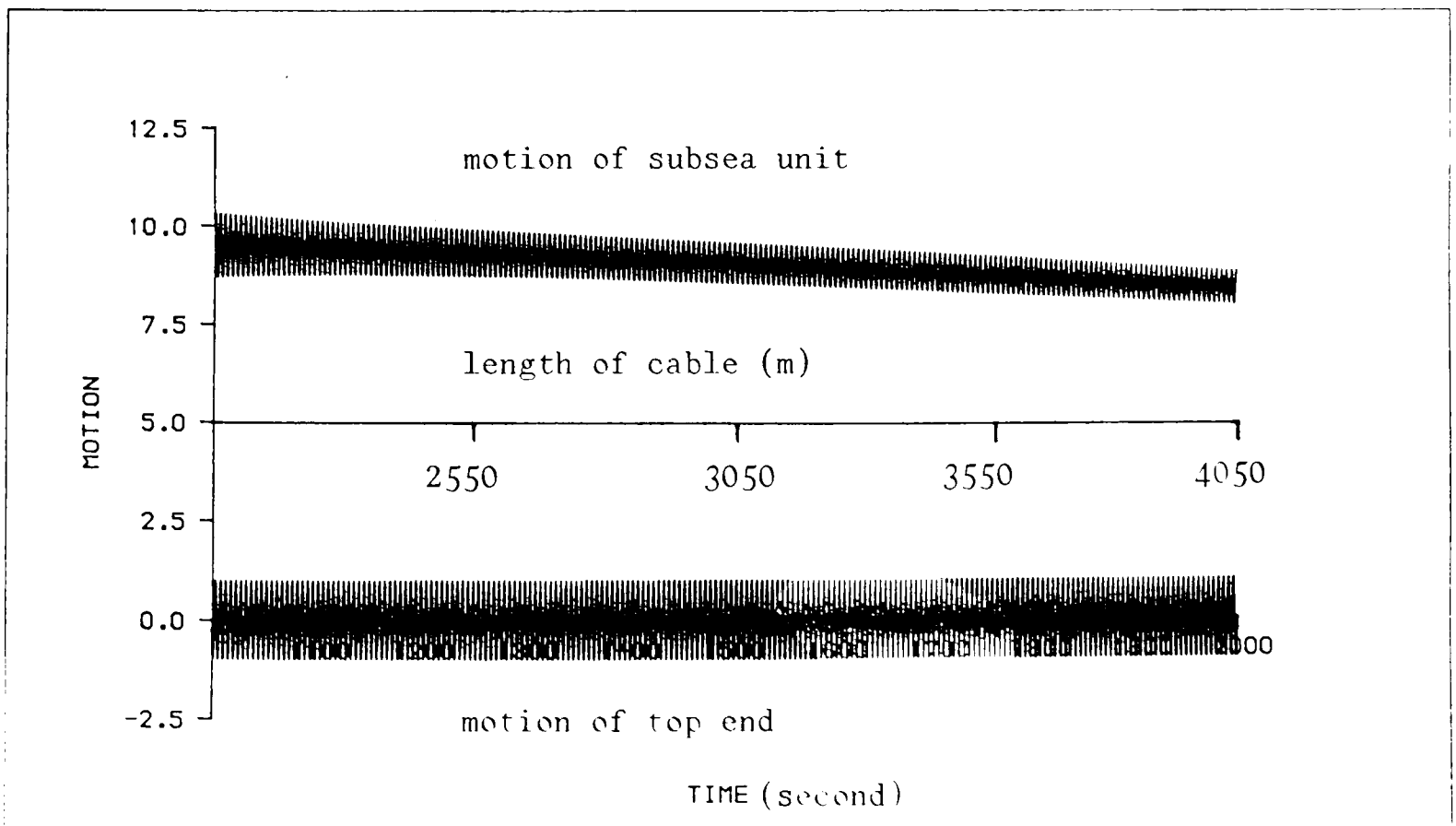

continuation of the graph above; time 1000-2000 s.

(b)

Figure 3.19

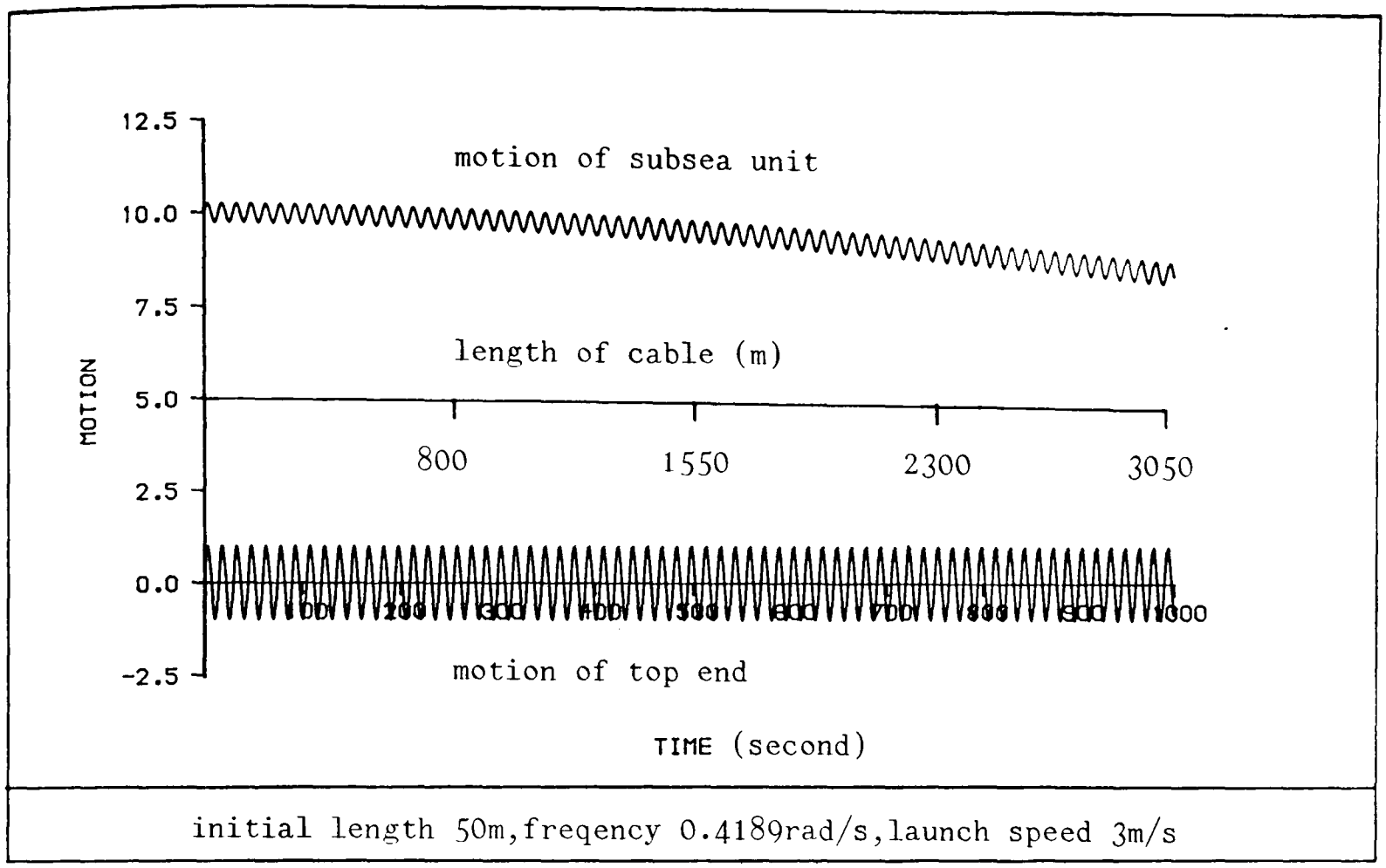

initial length 50m, freqency 0.4189rad/s, launch speed 3m/s

(a)

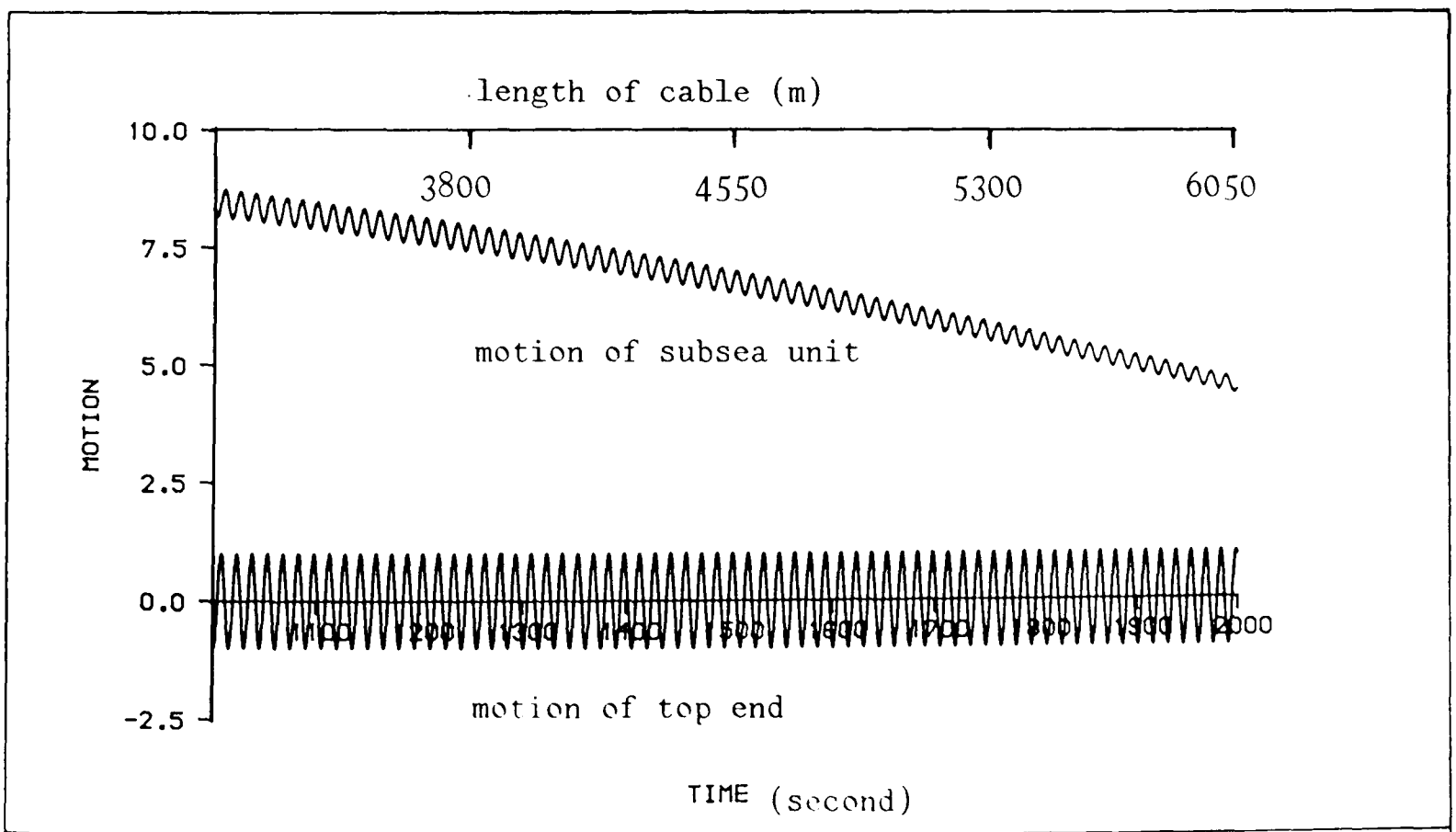

continuation of the graph above: time 1000-2000 s.

(b)

Figure 3.20

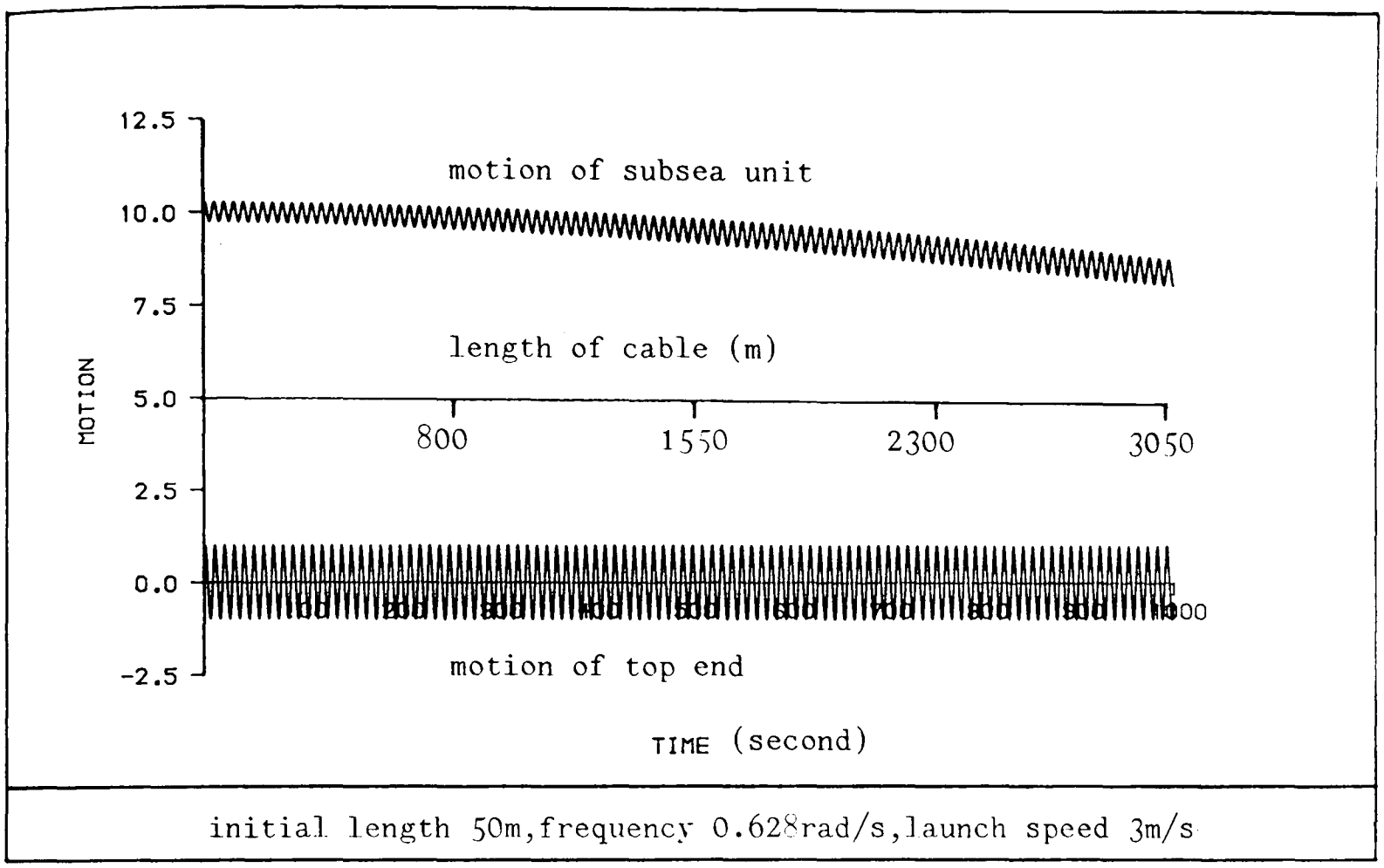

initial length 50m, frequency 0.628rad/s, launch speed 3m/s

(a)

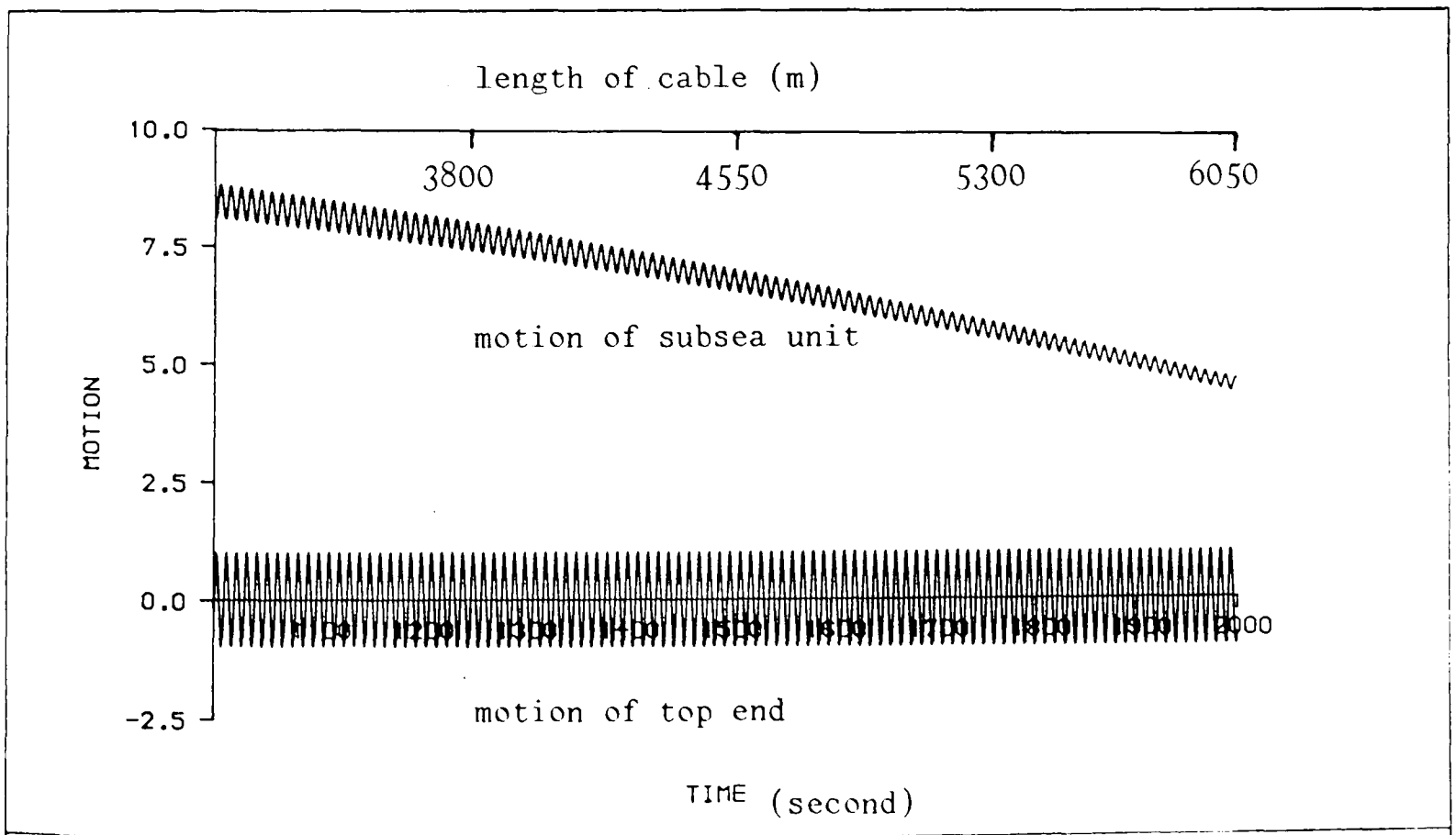

continuation of the graph above; time 1000-2000 s.

(b)

Figure 3.21

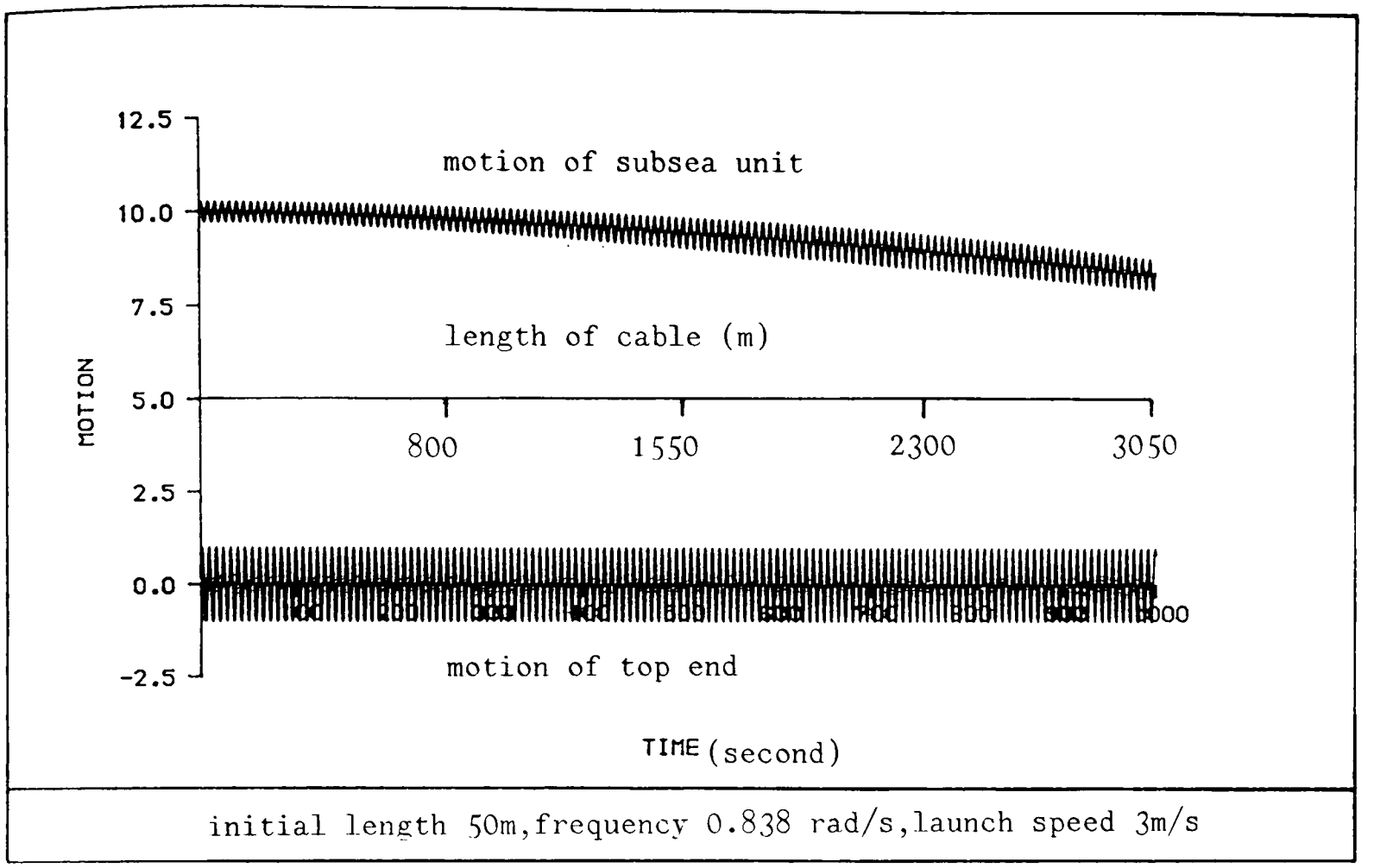

initial length 50m, frequency 0.838 rad/s, launch speed 3m/s

(a)

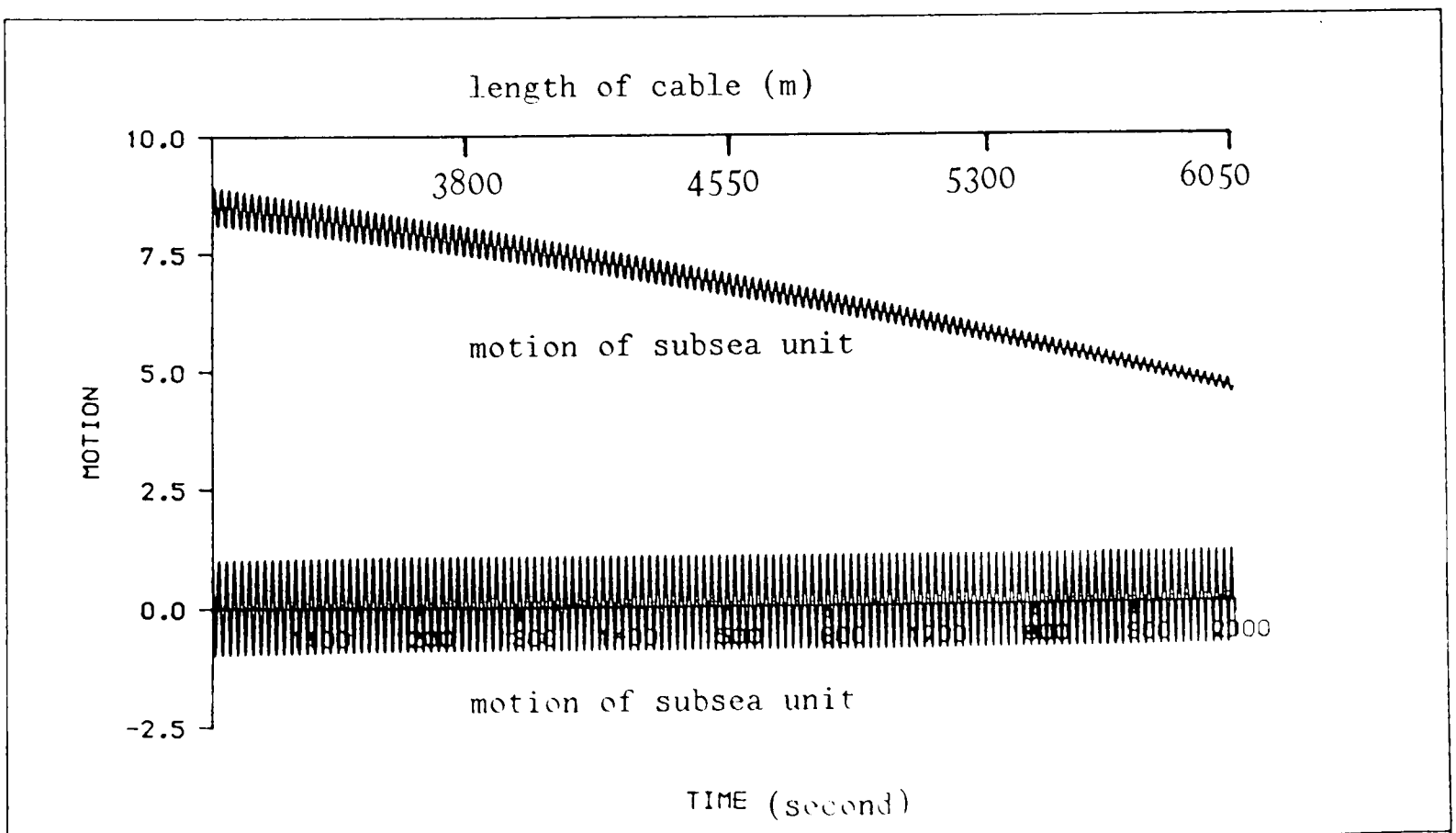

continuation of the graph above: time 1000-2000 s.

(b)

ure 3.22

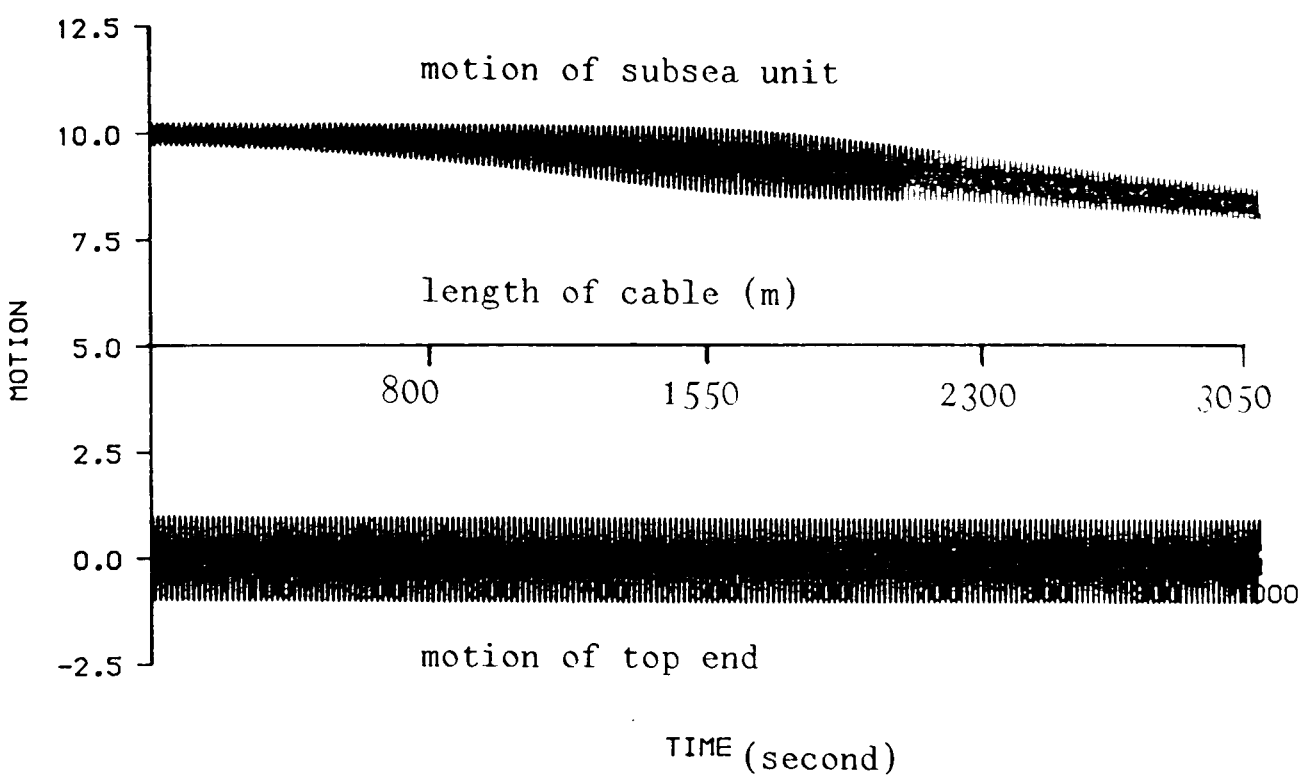

initial length 50m, frequency 1.26rad/s, launch speed 3m/s

(a)

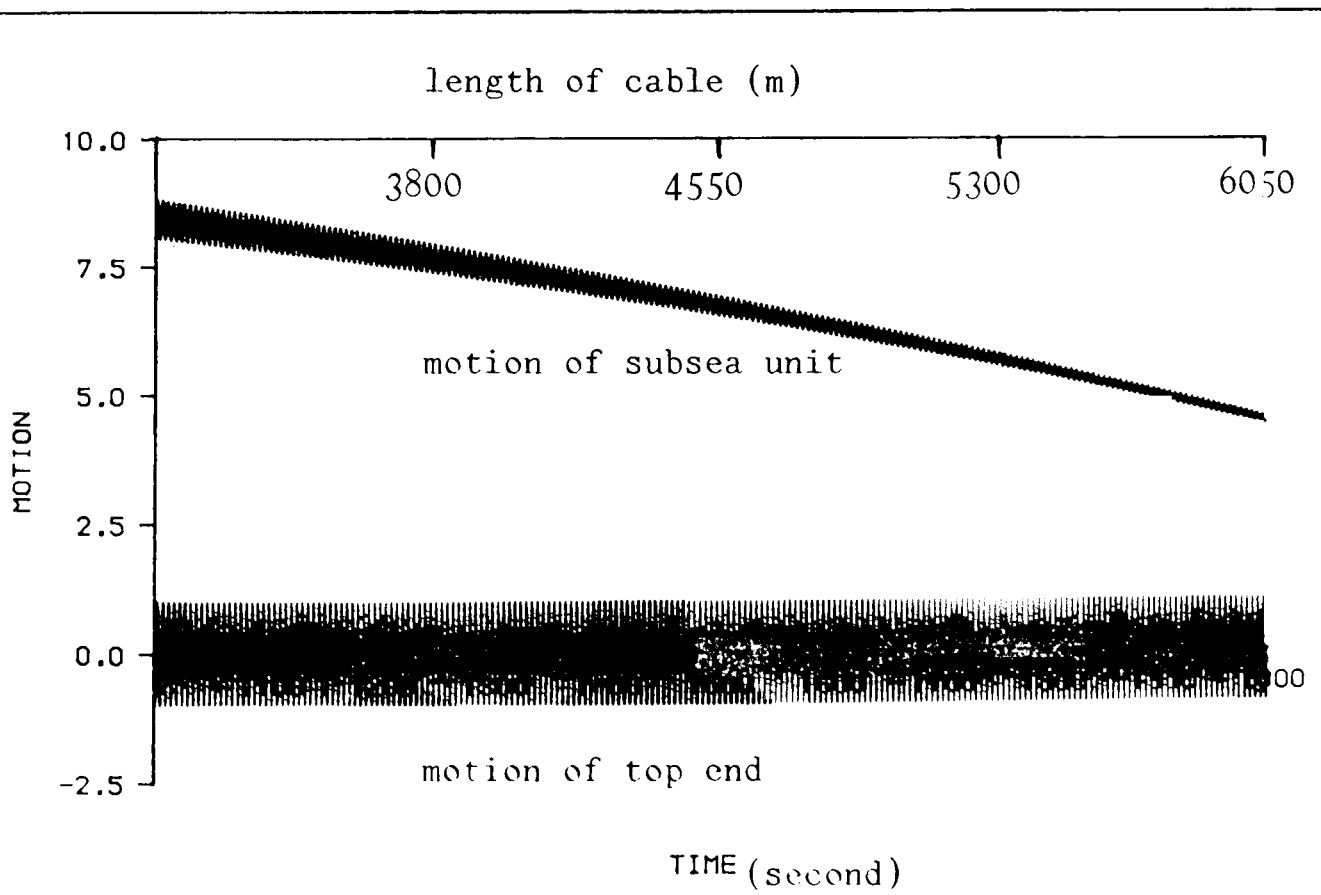

continuation of the graph above: time 1000-2000 s.

(b)

Figure 3.23

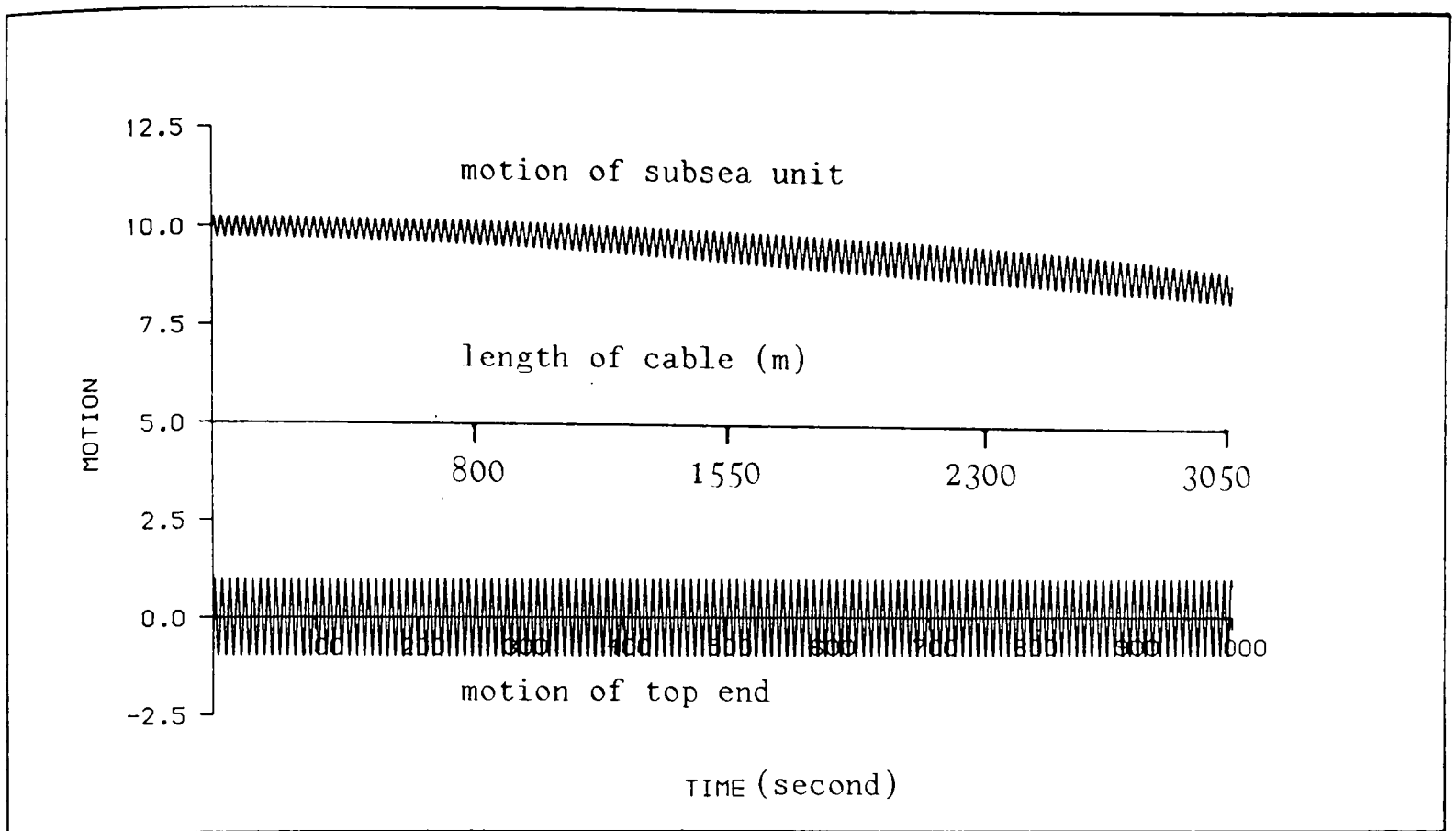

initial length 50m, frequency 0.838rad/s, launch speed 3m/s

(a)

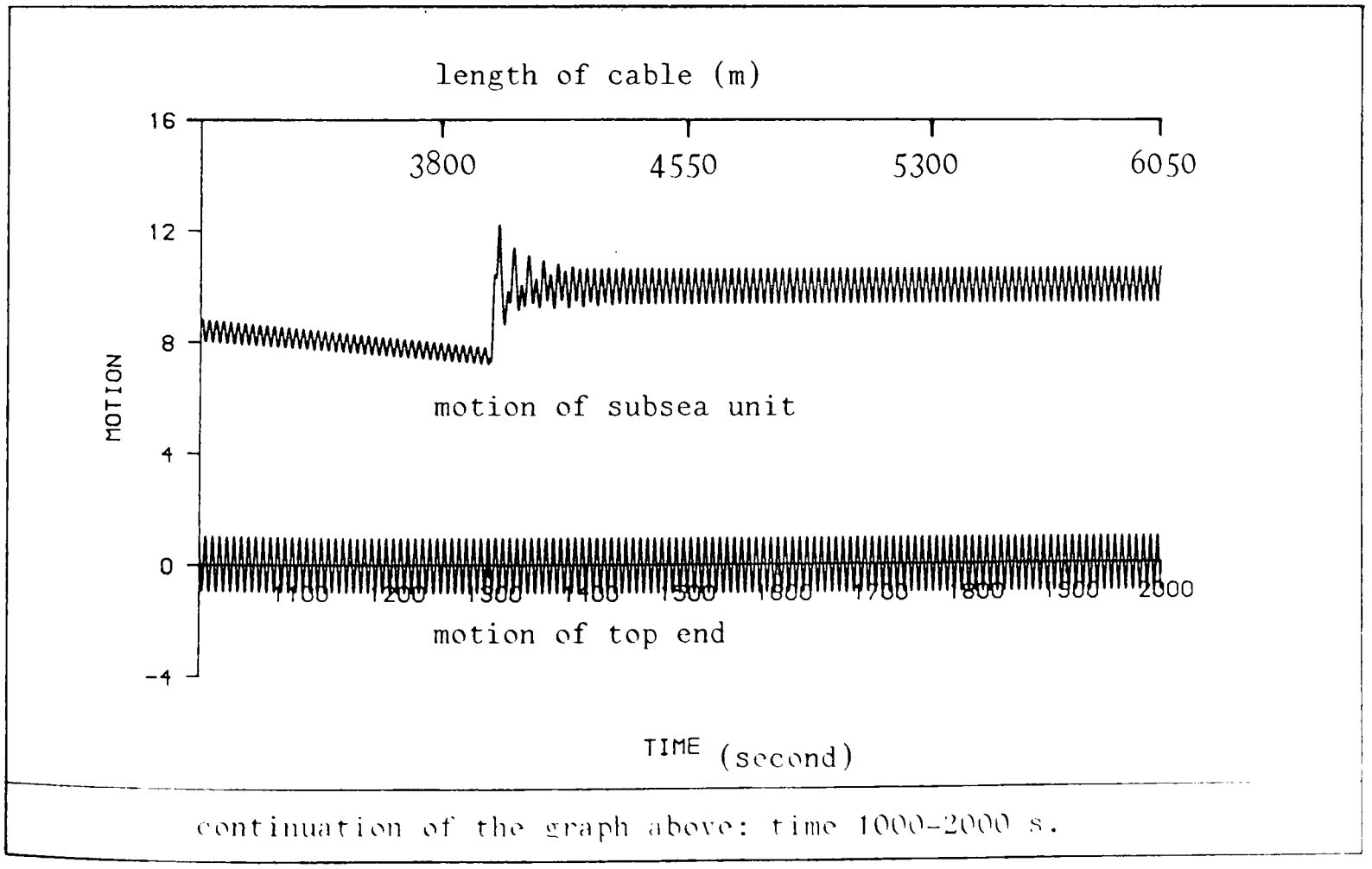

continuation of the graph above: time 1000-2000 s.

(b)

Figure 3.24

Chapter 4

TWO DIMENSIONAL DYNAMICS

Two are better than one.

Ecclesiastes

4.1 GENERAL REMARKS

In certain cases, as for example in the presence of a strong horizontally unidirectional underwater current, the assumption of a one-dimensional configuration of the cable/subsea unit system is clearly no longer tenable. We consider therefore in this chapter the case where the system lies not in a vertical line, but in a vertical plane, i.e., a two-dimensional model.

In addition to the underwater current, there are other factors which can swing the system out of a vertical line position such as motion at the top end of the

cable, pendulous motion, and an asymmetric shape of subsea unit.

In recent years, a substantial amount of research has been conducted in pursuing numerical solutions of the two-dimensional cable dynamics. The prevalent methods include:

1. Finite Difference Method (Ablow and Schechter, 1983; Howell, 1991; Burgess, 1991). The nonlinear hyperbolic equations, which govern the motions of the cable, are approximated by finite differences. This general method allows great flexibility such as the inclusion of bending stiffness. However, it may require a great deal of processing time.

2. Spectral Method (Burgess, 1985; Triantafyllou et al, 1986; Hover et al, 1990). This method takes advantage of the smoothness of the cable, assuming the solution to be a sum of a series of basic models. It may provide good results with a significant reduction in processing time over the finite difference method.

3. Lump Mass Method (Larsen and Fylling, 1982; van den Boom, 1985; Dutta, 1986; Wang, 1988; Ahmadi-Kashani, 1989; Macgregor, 1990). The governing equations become ordinary differential equations after lumping the distributed mass of the cable. Numerical integration is then performed. The method is widely applied because of its simplicity and versatility. However, it is less elegant mathematically.

4. Analytical Method (DeLaurier, 1970; Kennedy and Strahan, 1981; Triantaffyllou, 1982; Triantaffyllou and Bliek, 1983; Benedettini and Rega, 1987; Perkins,

1991). Due to the nonlinear and coupled nature of the governing equations, analytical solutions are only available in simplified cases such as small sagged cables.

Along with this variety of techniques there are a variety of different assumptions made in the formulation of the problem. This means that most methods have their own inherent weaknesses.

The main purpose of this chapter is to generalize the methodology in the previous chapter into a more general situation, i.e., the two-dimensional case.

4.2 EQUATIONS OF MOTION

To establish the equations of motion, we use a Cartesian coordinate system as shown in Figure 4.1. We assume that the cable is flexible and the motion is planar. Therefore the governing equation of motion can be written as (Appendix):

$$\begin{aligned}(m+m_a)\frac{\partial^2 \mathbf{r}}{\partial t^2} &= g(m-\rho A)\mathbf{j} + \\ &+\frac{1}{2}\rho C_{DN} d\sqrt{1+\varepsilon}|\mathbf{V}_N - \mathbf{U}_N|(\mathbf{V}_N - \mathbf{U}_N) \\ &+\frac{\pi}{2}\rho C_{D\tau} d\sqrt{1+\varepsilon}|\mathbf{V}_\tau - \mathbf{U}_\tau|(\mathbf{V}_\tau - \mathbf{U}_\tau) \\ &+\frac{\partial}{\partial s}\left(\frac{T}{1+\varepsilon}\frac{\partial \mathbf{r}}{\partial s}\right) \end{aligned} \tag{4.1}$$

where $\mathbf{r}$ is the vector from the origin to a point on the cable. m and m_a are the mass and added-mass per unit length of the cable. A is the cross section area of the cable. ρ is the density of the fluid medium. C_{DN} and $C_{D\tau}$ are the normal and tangential drag coefficients respectively. $\mathbf{i}$ and $\mathbf{j}$ are the unit vectors along the x and y axes.

Letting

$$\mathbf{r} = (p+s)\mathbf{j} + q\mathbf{i}$$

and using Hooke's law

$$T = EA\varepsilon = EA(|\frac{\partial \mathbf{r}}{\partial s}| - 1) \quad \varepsilon \geq 0$$

we have the following two components of Eq. (4.1):

$$(m+m_{ap})\frac{\partial^2 p}{\partial t^2} - EA\{1 - \frac{(\frac{\partial q}{\partial s})^2}{[(1+\frac{\partial p}{\partial s})^2 + (\frac{\partial q}{\partial s})^2]^{3/2}}\}\frac{\partial^2 p}{\partial s^2}$$

$$- EA\frac{(1+\frac{\partial p}{\partial s})\frac{\partial q}{\partial s}}{[(1+\frac{\partial p}{\partial s})^2 + (\frac{\partial q}{\partial s})^2]^{3/2}}\frac{\partial^2 q}{\partial s^2} = F_p \tag{4.2}$$

$$(m+m_{aq})\frac{\partial^2 q}{\partial t^2} - EA\{1 - \frac{(1+\frac{\partial p}{\partial s})^2}{[(1+\frac{\partial p}{\partial s})^2 + (\frac{\partial q}{\partial s})^2]^{3/2}}\}\frac{\partial^2 q}{\partial s^2}$$

$$- EA\frac{(1+\frac{\partial p}{\partial s})\frac{\partial q}{\partial s}}{[(1+\frac{\partial p}{\partial s})^2 + (\frac{\partial q}{\partial s})^2]^{3/2}}\frac{\partial^2 p}{\partial s^2} = F_q \tag{4.3}$$

where p and q are the vertical and transverse displacements of a point of the cable.

F_p and F_q are given by:

$$\begin{aligned}
F_p &= g(m-\rho A) + \\
&\quad \frac{1}{2}\rho C_{DN} d\sqrt{1+\varepsilon}|\mathbf{V}_N - \mathbf{U}_N|(\mathbf{V}_N - \mathbf{U}_N)\cdot\mathbf{j} + \\
&\quad \frac{\pi}{2}\rho C_{D\tau} d\sqrt{1+\varepsilon}|\mathbf{V}_\tau - \mathbf{U}_\tau|(\mathbf{V}_\tau - \mathbf{U}_\tau)\cdot\mathbf{j} \\
F_q &= \frac{1}{2}\rho C_{DN} d\sqrt{1+\varepsilon}|\mathbf{V}_N - \mathbf{U}_N|(\mathbf{V}_N - \mathbf{U}_N)\cdot\mathbf{i} + \\
&\quad \frac{\pi}{2}\rho C_{D\tau} d\sqrt{1+\varepsilon}|\mathbf{V}_\tau - \mathbf{U}_\tau|(\mathbf{V}_\tau - \mathbf{U}_\tau)\cdot\mathbf{i}
\end{aligned}$$

4.3 PROBLEM CHARACTERISTICS

Before pursuing a numerical solution, some basic characteristics of the problem are examined here in this section.

For most underwater operations involving cables and subsea units, the surface supporting vessel is kept at a designated working place. The wave action gives rise to motions of the boom tip which can be theoretically two-dimensional, for example when the handling system aboard is at the stern region while the vessel is in heading sea situation. The cable and the subsea unit is swung out of the vertical line by the underwater current yet remains in the same plane formed by the boom tip motions. This idealised case also includes some other seemingly different situations such as when the supporting vessel is sailing along a straight line.

Intuitively, one might expect that the transverse motion of the boom tip is of secondary importance to the vertical motion (heave motion) from the perspective of their effects on tension in the cable. The following part of this section aims to prove that this conjecture is only true in a special situation.

The tension T is given by:

$$T = EA(|\frac{\partial \mathbf{r}}{\partial s}| - 1) = EA[\sqrt{(1 + \frac{\partial p}{\partial s})^2 + (\frac{\partial q}{\partial s})^2} - 1] \tag{4.4}$$

We write the displacements and the tension as sums of their stationary components and the dynamic perturbations:

$$\begin{aligned} p &= p_0 + \epsilon p_1 + \epsilon^2 p_2 + \cdots \\ q &= q_0 + \epsilon q_1 + \epsilon^2 q_2 + \cdots \end{aligned} \tag{4.5}$$

$$T = T_0 + eT_1 + e^2T_2 + \cdots$$

where e is a parameter of small quantity which is less than unity.

Substituting Eq. (4.5) into Eq. (4.4) and equating like powers of e , we have

$$T_0 = EA(\sqrt{(1+\frac{\partial p_0}{\partial s})^2+(\frac{\partial q_0}{\partial s})^2}-1)$$

$$T_1 = EA\frac{(1+\frac{\partial p_0}{\partial s})\frac{\partial p_1}{\partial s}+\frac{\partial q_0}{\partial s}\frac{\partial q_1}{\partial s}}{\sqrt{(1+\frac{\partial p_0}{\partial s})^2+(\frac{\partial q_0}{\partial s})^2}}$$

$$T_2 = EA\{\frac{[(1+\frac{\partial p_0}{\partial s})^2+(\frac{\partial q_0}{\partial s})^2][(\frac{\partial p_1}{\partial s})^2+2(1+\frac{\partial p_0}{\partial s})\frac{\partial p_2}{\partial s}+2\frac{\partial q_0}{\partial s}\frac{\partial q_2}{\partial s}+(\frac{\partial q_1}{\partial s})^2]}{2[(1+\frac{\partial p_0}{\partial s})^2+(\frac{\partial q_0}{\partial s})^2]\sqrt{(1+\frac{\partial p_0}{\partial s})^2+(\frac{\partial q_0}{\partial s})^2}}$$

$$-\frac{[(1+\frac{\partial p_0}{\partial s})\frac{\partial p_1}{\partial s}+\frac{\partial q_0}{\partial s}\frac{\partial q_1}{\partial s}]^2}{2[(1+\frac{\partial p_0}{\partial s})^2+(\frac{\partial q_0}{\partial s})^2]\sqrt{(1+\frac{\partial p_0}{\partial s})^2+(\frac{\partial q_0}{\partial s})^2}}\}$$

This indicates:

1. The stationary tension is a function of stationary displacements only.

2. There is a coupling between the vertical and horizontal motions.

3. Displacements of lower order affect all the tensions of equal or higher order.

Now consider a special case where the system has no stationary transverse deflection, i.e.,

$$\frac{\partial q_0}{\partial s} = 0$$

In this case, the tensions T_0, T_1 and T_2 can be simplified as (Zajac, 1957):

$$T_0 = EA\frac{\partial p_0}{\partial s}$$

$$T_1 = EA\frac{\partial p_1}{\partial s}$$
$$T_2 = EA[\frac{\partial p_2}{\partial s} + \frac{(\frac{\partial q_1}{\partial s})^2}{2(1+\frac{\partial p_0}{\partial s})}]$$

It can be seen that the leading term of the dynamic tension T_1 is only related to the vertical motion whilst the leading dynamic transverse displacement q_1 affects tension of higher order. This provides a theoretical foundation for the one-dimensional dynamics approximation to a cable/subsea unit system deployed in a no-current or weak-current environment, even though the boom tip is subjected to horizontal motion as well as heave motion.

This conclusion can be further justified from a motion viewpoint. Intuitively one may expect the hydrodynamic damping to cause the transverse motion to die out as it travels downwards. This proves to be true. To make the theoretical analysis tractable, we make the following assumptions:

1. The hydrodynamic force is linearly dependent upon the relative velocities. Since there is no underwater current, the relative velocities are the cable's vibrating velocities themselves.

2. There is no wave reflection from the bottom end.

Under the first assumption, the transverse component of Eq. (4.1) can be written as:

$$(m+m_{aq})\frac{\partial^2 q}{\partial t^2} + c_1\sqrt{1+\varepsilon}\{\frac{\partial q}{\partial t} - \frac{1}{(1+\varepsilon)^2}[\frac{\partial q}{\partial t}\frac{\partial q}{\partial s} + \frac{\partial p}{\partial t}(1+\frac{\partial p}{\partial s})]\frac{\partial q}{\partial s}\}$$
$$+ c_2\frac{1}{(1+\varepsilon)^{3/2}}[\frac{\partial q}{\partial t}\frac{\partial q}{\partial s} + \frac{\partial p}{\partial t}(1+\frac{\partial p}{\partial s})]\frac{\partial q}{\partial s} - \frac{\partial}{\partial s}(\frac{T}{1+\varepsilon}\frac{\partial q}{\partial s}) = 0 \qquad (4.6)$$

where c_1 and c_2 represent the linearised drag coefficients.

Substituting Eq. (4.5) into the above one, and noticing the following relations:

$$q_0 = 0$$

$$1 + \varepsilon \approx 1$$

we have the governing equation for the leading term of the transverse motion q_1:

$$(m + m_{aq})\frac{\partial^2 q_1}{\partial t^2} + c_1\frac{\partial q_1}{\partial t} - \frac{\partial}{\partial s}(T_0\frac{\partial q_1}{\partial s}) = 0 \tag{4.7}$$

Further assume:

$$\frac{\partial}{\partial s}(T_0) = 0$$

Eq. (4.7) then is reduced to:

$$(m + m_{aq})\frac{\partial^2 q_1}{\partial t^2} + c_1\frac{\partial q_1}{\partial t} - T_0\frac{\partial^2 q_1}{\partial s^2} = 0 \tag{4.8}$$

For forced vibration, the solution of this equation can be written as:

$$q_1 = Re[\bar{q}_1(s)exp(\sqrt{-1}\omega t)] \tag{4.9}$$

where $Re(\Phi)$ means the real part of any complex expression Φ.

Substituting Eq. (4.9) into Eq. (4.8) it follows that

$$T_0\frac{d^2\bar{q}_1}{ds^2} + [\omega^2(m + m_{aq}) - \sqrt{-1}\omega c_1]\bar{q}_1 = 0$$

For an out-going wave – the second assumption – $\bar{q}_1(s)$ is given by:

$$\bar{q}_1(s) = \tilde{q}_1 exp(-\sqrt{-\frac{\omega^2(m + m_{aq}) - \sqrt{-1}\omega c_1}{T_0}}s) \tag{4.10}$$

where $\tilde{q}_1$ is a constant which can be determined by implementing a boundary condition.

Eq. (4.10) shows that $|\bar{q}_1(s)|$, which represents the amplitude of the transverse motion, decreases exponentially as s increases.

If $c_1 = 0$, corresponding to the case where there is no hydrodynamic damping, we have:

$$q_1 = Re\{\tilde{q}_1 exp[\sqrt{-1}\omega(t - s/\sqrt{\frac{T_0}{m + m_{aq}}})]\}$$

In this case, the transverse wave travels with a constant profile and at a speed of $\sqrt{\frac{T_0}{m+m_{aq}}}$.

4.4 FORMULATION AND NUMERICAL DISCRETISATION

4.4.1 Boundary Conditions

At the cable's top end:

$$\begin{aligned} p(0,t) &= R(t) + vt \\ q(0,t) &= O(t) \end{aligned}$$

where v is the speed of paying out or hauling in. $R(t)$ and $O(t)$ are the two components of the boom tip motion.

At cable's bottom end:

$$(M_s + M_a)\frac{\partial^2 \mathbf{r}}{\partial t^2} = EA\frac{|\frac{\partial \mathbf{r}}{\partial s}| - 1}{|\frac{\partial \mathbf{r}}{\partial s}|}\frac{\partial \mathbf{r}}{\partial s} + w_2\mathbf{j} +$$

$$\frac{1}{2}\rho C_D S_P|\mathbf{U} - \frac{\partial \mathbf{r}}{\partial t}|(\mathbf{U} - \frac{\partial \mathbf{r}}{\partial t})$$

Under the assumption that the hydrodynamic forces on the subsea unit can be decomposed into two components along the axes, each as a function of the relative velocity and the acceleration in that direction, just as it was done with the hydrodynamic drag force on the cable, the above vector equation can be resolved into the following two components:

$$(M_s + M_{ap})\frac{\partial^2 p}{\partial t^2} + EA\frac{\sqrt{(1+\frac{\partial p}{\partial s})^2 + (\frac{\partial q}{\partial s})^2} - 1}{\sqrt{(1+\frac{\partial p}{\partial s})^2 + (\frac{\partial q}{\partial s})^2}}(1 + \frac{\partial p}{\partial s}) - w_2$$

$$- \frac{1}{2}\rho C_{Dy} S_y |U_y - \frac{\partial p}{\partial t}|(U_y - \frac{\partial p}{\partial t}) = 0 \qquad (4.11)$$

$$(M_s + M_{aq})\frac{\partial^2 p}{\partial t^2} + EA\frac{\sqrt{(1+\frac{\partial p}{\partial s})^2 + (\frac{\partial q}{\partial s})^2} - 1}{\sqrt{(1+\frac{\partial p}{\partial s})^2 + (\frac{\partial q}{\partial s})^2}}\frac{\partial q}{\partial s}$$

$$- \frac{1}{2}\rho C_{Dx} S_x |U_x - \frac{\partial p}{\partial t}|(U_x - \frac{\partial p}{\partial t}) = 0 \qquad (4.12)$$

where M_s is the mass of the subsea unit, w_2 is its weight in water. (M_{ap}, M_{aq}), (C_{Dy}, C_{Dx}) and (S_y, S_x) are respectively added masses, drag coefficients and projected areas of the subsea unit along the directions of the two axes.

4.4.2 Initial Conditions

Initial conditions need to be assigned to $p(s,0)$, $q(s,0)$, $\frac{\partial p}{\partial t}(s,0)$ and $\frac{\partial q}{\partial t}(s,0)$. however, because there is viscous damping and we are concerned with the long term motions, they are not very important. In the following computation, in its initial state the cable/subsea unit system is assumed to be in a vertical position hanging from the boom tip.

4.4.3 Variable Transformation

The transformation is given by:

$$\begin{aligned} T &= t \\ y &= \frac{s}{L_0 + vt} \\ P &= p - vt \\ Q &= q \end{aligned}$$

A set of relations between the derivatives in the old and new space-time domains, similar to that in the previous chapter, can be derived.

4.4.4 Transformed Equations of Motion and Boundary Conditions

In the new space-time domain (y, T), the equations of motion become:

$$A_1 \frac{\partial^2 P}{\partial T^2} + B_1 \frac{\partial^2 P}{\partial T \partial y} + C_1 \frac{\partial^2 P}{\partial y^2} + D_1 \frac{\partial P}{\partial y} + G_1 \frac{\partial^2 Q}{\partial y^2} = H_1 \qquad (4.13)$$

and

$$A_2 \frac{\partial^2 Q}{\partial T^2} + B_2 \frac{\partial^2 Q}{\partial T \partial y} + C_2 \frac{\partial^2 Q}{\partial y^2} + D_2 \frac{\partial Q}{\partial y} + G_2 \frac{\partial^2 P}{\partial y^2} = H_2 \qquad (4.14)$$

where

$$\begin{aligned} A_1 &= m + m_{ap} \\ A_2 &= m + m_{aq} \\ B_1 &= -\frac{2vy}{L_0 + vt}(m + m_{ap}) \\ B_2 &= -\frac{2vy}{L_0 + vt}(m + m_{aq}) \end{aligned}$$

$$
\begin{aligned}
C_1 &= \frac{v^2y^2}{(L_0+vt)^2}(m+m_{ap}) - \\
&\quad \frac{EA}{(L_0+vt)^2}\{1-\frac{(L_0+vt)(\frac{\partial Q}{\partial y})^2}{[(L_0+vt+\frac{\partial P}{\partial y})^2+(\frac{\partial Q}{\partial y})^2]^{3/2}}\} \\
C_2 &= \frac{v^2y^2}{(L_0+vt)^2}(m+m_{aq}) - \frac{EA}{(L_0+vt)^2} \\
D_1 &= \frac{2v^2y}{(L_0+vt)^2}(m+m_{ap}) \\
D_2 &= \frac{2v^2y}{(L_0+vt)^2}(m+m_{aq}) \\
G_1 &= G_2 = -\frac{EA}{L_0+vt}\frac{(L_0+vt+\frac{\partial P}{\partial y})\frac{\partial Q}{\partial y}}{[(L_0+vt+\frac{\partial P}{\partial y})^2+(\frac{\partial Q}{\partial y})^2]^{3/2}} \\
H_1 &= F_p \\
H_2 &= F_q - \frac{EA}{L_0+vt}\frac{(L_0+vt+\frac{\partial P}{\partial y})^2}{[(L_0+vt+\frac{\partial P}{\partial y})^2+(\frac{\partial Q}{\partial y})^2]^{3/2}}\frac{\partial^2 Q}{\partial y^2}
\end{aligned}
$$

The associated new boundary conditions at the cable's top end, where $y = 0$, are:

$$P(0,T) = R(T) \tag{4.15}$$

$$Q(0,T) = O(T) \tag{4.16}$$

and at the bottom, where $y = 1$, they are given by:

$$\bar{A}_1\frac{\partial^2 P}{\partial T^2} + \bar{B}_1\frac{\partial^2 P}{\partial T\partial y} + \bar{C}_1\frac{\partial^2 P}{\partial y^2} + \bar{D}_1\frac{\partial P}{\partial y} + \bar{G}_1\frac{\partial P}{\partial T} = \bar{H}_1 \tag{4.17}$$

and

$$\bar{A}_2\frac{\partial^2 Q}{\partial T^2} + \bar{B}_2\frac{\partial^2 Q}{\partial T\partial y} + \bar{C}_2\frac{\partial^2 Q}{\partial y^2} + \bar{D}_2\frac{\partial Q}{\partial y} + \bar{G}_2\frac{\partial Q}{\partial T} = \bar{H}_2 \tag{4.18}$$

where

$$\bar{A}_1 = M_s + M_{ap}$$

$$
\begin{aligned}
\bar{A}_2 &= M_s + M_{aq} \\
\bar{B}_1 &= -\frac{2v}{L_0 + vt}(M_s + M_{ap}) \\
\bar{B}_2 &= -\frac{2v}{L_0 + vt}(M_s + M_{aq}) \\
\bar{C}_1 &= \frac{v^2}{(L_0 + vt)^2}(M_s + M_{ap}) \\
\bar{C}_2 &= \frac{v^2}{(L_0 + vt)^2}(M_s + M_{aq}) \\
\bar{D}_1 &= \frac{2v^2}{(L_0 + vt)^2}(M_s + M_{ap}) + \frac{EA}{L_0 + vt} \\
&\quad -\frac{v\rho C_{Dy} S_y}{2(L_0 + vt)}|U_y - v - \frac{\partial P}{\partial T} - \frac{v}{L_0 + vt}\frac{\partial P}{\partial y}| \\
\bar{D}_2 &= \frac{2v^2}{(L_0 + vt)^2}(M_s + M_{aq}) + \frac{EA}{L_0 + vt} \\
&\quad -\frac{v\rho C_{Dx} S_x}{2(L_0 + vt)}|U_x - \frac{\partial Q}{\partial T} - \frac{v}{L_0 + vt}\frac{\partial Q}{\partial y}| \\
\bar{G}_1 &= \frac{1}{2}\rho C_{Dy} S_y |U_y - v - \frac{\partial P}{\partial T} - \frac{v}{L_0 + vt}\frac{\partial P}{\partial y}| \\
\bar{G}_2 &= \frac{1}{2}\rho C_{Dx} S_x |U_x - \frac{\partial Q}{\partial T} - \frac{v}{L_0 + vt}\frac{\partial Q}{\partial y}| \\
\bar{H}_1 &= w_2 - EA[1 - \frac{L_0 + vt + \frac{\partial P}{\partial y}}{\sqrt{(L_0 + vt + \frac{\partial P}{\partial y})^2 + (\frac{\partial Q}{\partial y})^2}}] \\
&\quad +\frac{1}{2}\rho C_{Dy} S_y |U_y - v - \frac{\partial P}{\partial T} - \frac{v}{L_0 + vt}\frac{\partial P}{\partial y}|U_y \\
\bar{H}_2 &= EA\frac{\frac{\partial Q}{\partial y}}{\sqrt{(L_0 + vt + \frac{\partial P}{\partial y})^2 + (\frac{\partial Q}{\partial y})^2}} \\
&\quad +\frac{1}{2}\rho C_{Dy} S_y |U_x - \frac{\partial Q}{\partial T} - \frac{v}{L_0 + vt}\frac{\partial Q}{\partial y}|U_x
\end{aligned}
$$

4.4.5 Finite Difference Discretisation

The differential equations Eqs. (4.13) and (4.14), together with the boundary conditions Eqs. (4.15), (4.16), (4.17) and (4.18), are approximated using finite differences. The procedure of the discretisation is very much similar to the one

described in the previous chapter.

4.5 NUMERICAL EXAMPLES & DISCUSSION

In this section, results of a series of numerical examples are presented. Available experimental data are used to check the mathematical model. In the first three examples given below, steady dynamics is examined, whilst the unsteady dynamics is investigated in the rest of the examples.

4.5.1 Example One

The particulars of the cable and the subsea unit are the same as the ones described in Example One of the previous chapter. In the present case, however, the top end of the cable is subjected to forced horizontal or circular motions, hence the whole system moved in a two-dimensional space.

In Figure 4.2 the top end of the cable is forced to move sinusoidally along a horizontal line with amplitude equal to 0.15m. The whole system oscillates in air, therefore no external force needs to be considered. The theoretical predictions agree very well with the experimental results except at resonance.

In Figure 4.3, hydrodynamic drag force has been taken into account as the system is oscillating in water. As a whole, the agreement is quite good.

Figures 4.4 and 4.5 show results for the system in air and in water respectively. In both cases, the top end is subjected to circular motions with different amplitudes at different frequencies. It can be seen that in the frequency range con-

sidered the agreement between the theoretical results and the experimental results is extremely good for all the amplitudes when the system is forced to move in air. However, when the system moves in water, cable slack appears when the excitation amplitude is large and/or the excitation frequency is high. This explains the discrepancy between the theoretical results and the experimental results observed in Figure 4.5. Though the results of the present method become invalid when slack appears, the method can be used to predict when and where cable slack occurs. For example, at a frequency of 2.5 rad/sec for the 0.15m amplitude curve, there is a sharp increase in tension observed in the experiment. Corresponding to this, the theoretical method predicted the existence of negative tension in the cable, although the maximum tension still remained positive.

4.5.2 Example Two

The particulars of the cable and the subsea unit are the same as the ones given in Example Two of the previous chapter. Calculations were carried out for the system in air and in water respectively. The top end of the cable was subjected to circular motion with an amplitude equal to 0.1m. Again due to cable slack, poor agreement between the theoretical predictions and the experimental results has been observed in the high frequency region when the system is oscillating in water, as shown in Figure 4.6. When slack appears, the tension in the cable should increase sharply due to the impact load, as indicated by the experimental results.

4.5.3 Example Three

This example shows the effects of an underwater current on the steady dynamics of a tethered subsea unit system.

The particulars of the cable are:

diameter:	$0.02m$
length:	$300m$
Young's modulus:	$4\times10^9 N/m^2$
mass distribution:	$5.2\ kg/m$

The main particulars of the subsea unit are given by:

mass:	$1900kg$
added mass in water:	$1600kg$
weight in water	$15000N$

Figure 4.7 shows the mean position of the subsea unit as a function of the strength of the underwater current. As the current is increased, so is the horizontal distance between the subsea unit and the initial vertical line. In addition to this, the mean vertical position of the subsea unit also changes as the current varies.

Figures 4.8 and 4.9 show the changes in the two amplitudes of the vertical motion and horizontal motion respectively.

4.5.4 Example Four

From this example onwards, a variety of results relating to the unsteady dynamics are presented.

The particulars of the cable are:

diameter:	$0.047m$
initial length:	$200m$
Young's modulus:	$9.05\times10^9 N/m^2$
mass distribution:	$5.2kg/m$

The subsea unit remains the same as the one in the previous example.

In Figures 4.10 and 4.11 the subsea unit sway motions are simulated when it is being lowered to a greater depth at two different speeds. The top end in both cases is subjected to sinusoidal horizontal motion with amplitude equal to 5m. Generally speaking, the longer the cable is, the smaller the sway motion. High launching speed means less time for the building up of larger amplitude motion when the cable is short, therefore, it helps to reduce the sway motion. This is true for the two cases presented here.

4.5.5 Example Five

In this example, the subsea unit response is examined as it is passing through the resonant region.

The system is the same as the one in Example Three of this chapter, with initial cable length of 200m. At the top end the condition is set by

$$P(0,t) = sint$$

$$Q(0,t) = 1 - cost$$

Figures 4.12 to 4.19 show the simulated motions of the subsea unit as it is being lowered down at different speeds. The vertical motion presented here is the

dynamic part of the subsea unit motion which is given by

$$P(1,T) - \frac{L_0 + vt}{EA} w_2 - \frac{1}{2EA} g(m - \rho A)(L_0 + vt)^2$$

In general, high launching speed will help to reduce the motion of the subsea unit since the higher the speed, the shorter the duration of the subsea unit in the resonant zone. On the other hand, the tangential friction force on the cable and the vertical drag force on the subsea unit both increase as a consequence of the increase in launching speed. Both forces tend to compress the cable, which is clearly indicated in Figures 4.12, 4.14, 4.16 and 18.

In the last two figures of this chapter, namely Figures 4.20 and 4.21, the effect of current on the unsteady dynamics is examined when the system is deployed in a weak horizontal current. It can be seen that the effect of the current is mainly upon the horizontal motion. As the cable becomes longer and longer, the subsea unit deviates further and further from the vertical line which passes through the mean position of the top end.

4.6 CONCLUDING REMARKS

1. The perturbation analysis shows in which circumstances a two-dimensional mathematical model must be used to examine the dynamics of a cable system.

2. The methodology adopted in the previous chapter has been extended to the two-dimensional case.

3. The various examples given either show a good agreement between the theoretical results and the experimental results, or indicate a convincing trend.

4. Further efforts to be recommended include checking the experimental data in Figures 4.2 and 4.3 through repetition of the experiments.

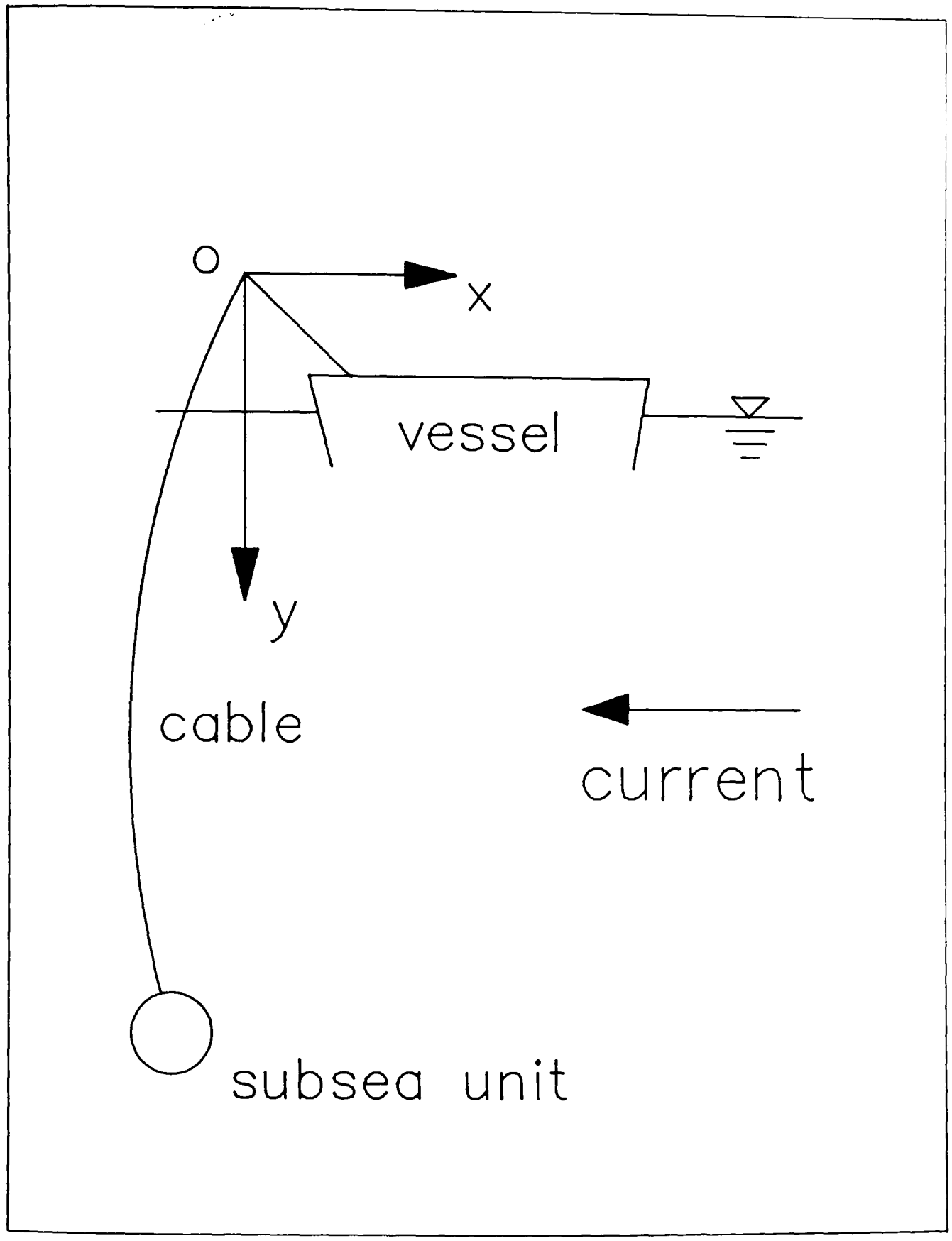

Figure 4.1

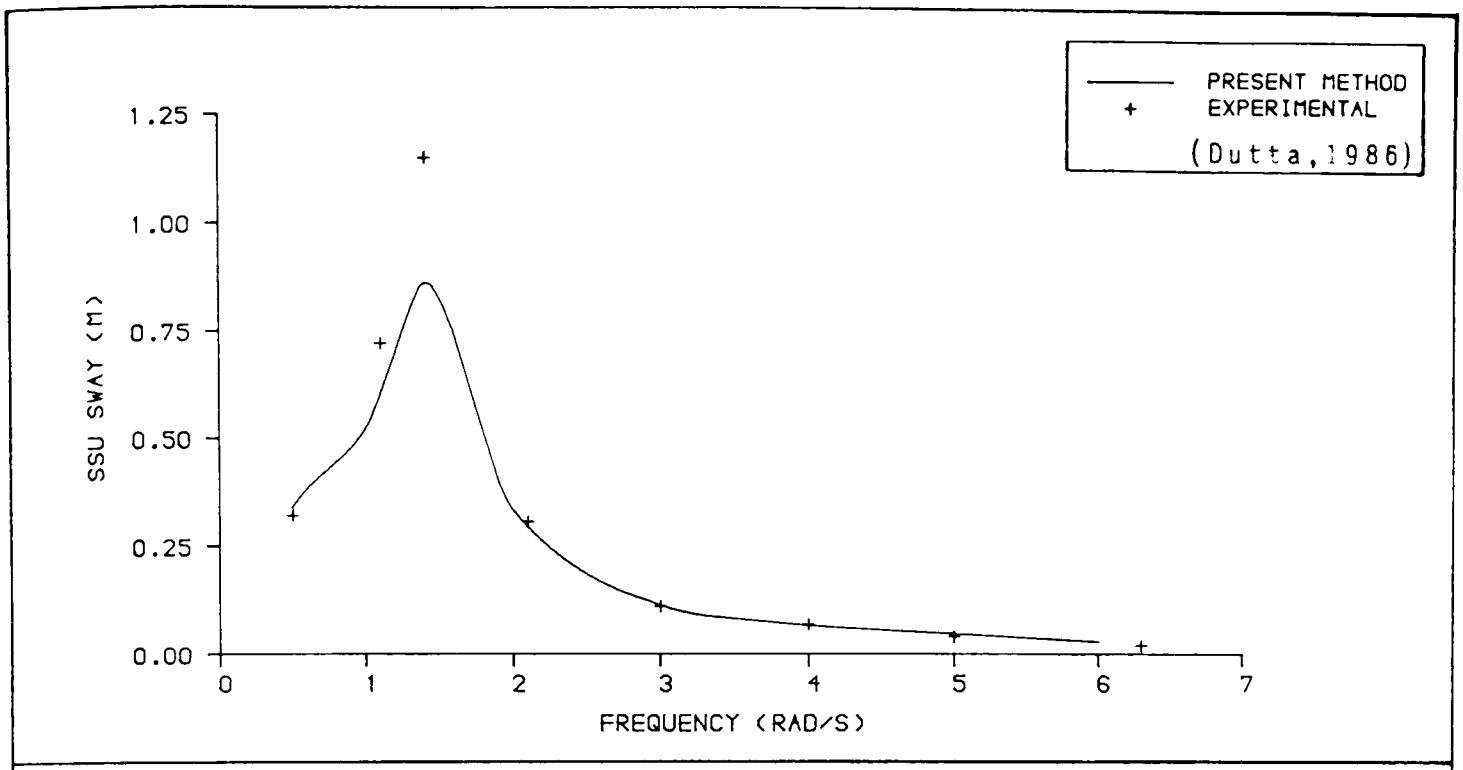

COMPARISON OF THEORETICAL AND EXPERIMENTAL RESULTS
FOR SSU SWAY IN AIR (3mm PRESTRETCHED ROPE)
NATURAL FREQ. = 1.4 RAD/S; AMPLITUDE 0.15m (HORIZONTAL)

Figure 4.2

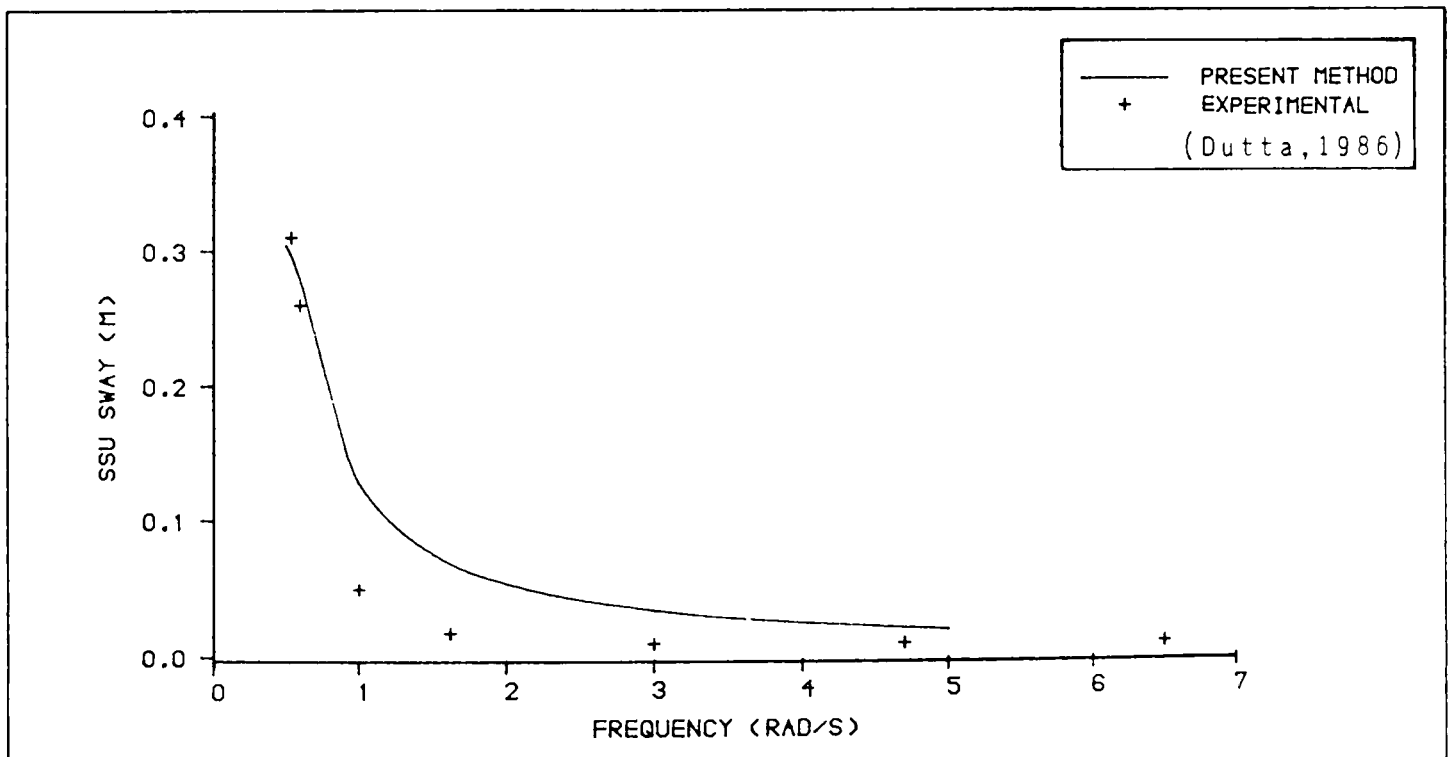

COMPARISON OF THEORETICAL AND EXPERIMENTAL RESULTS
FOR SSU SWAY IN WATER (3mm PRESTRETCHED ROPE)
NATURAL FREQ. = 0.5 RAD/S; AMPLITUDE 0.15m (HORIZONTAL)

Figure 4.3

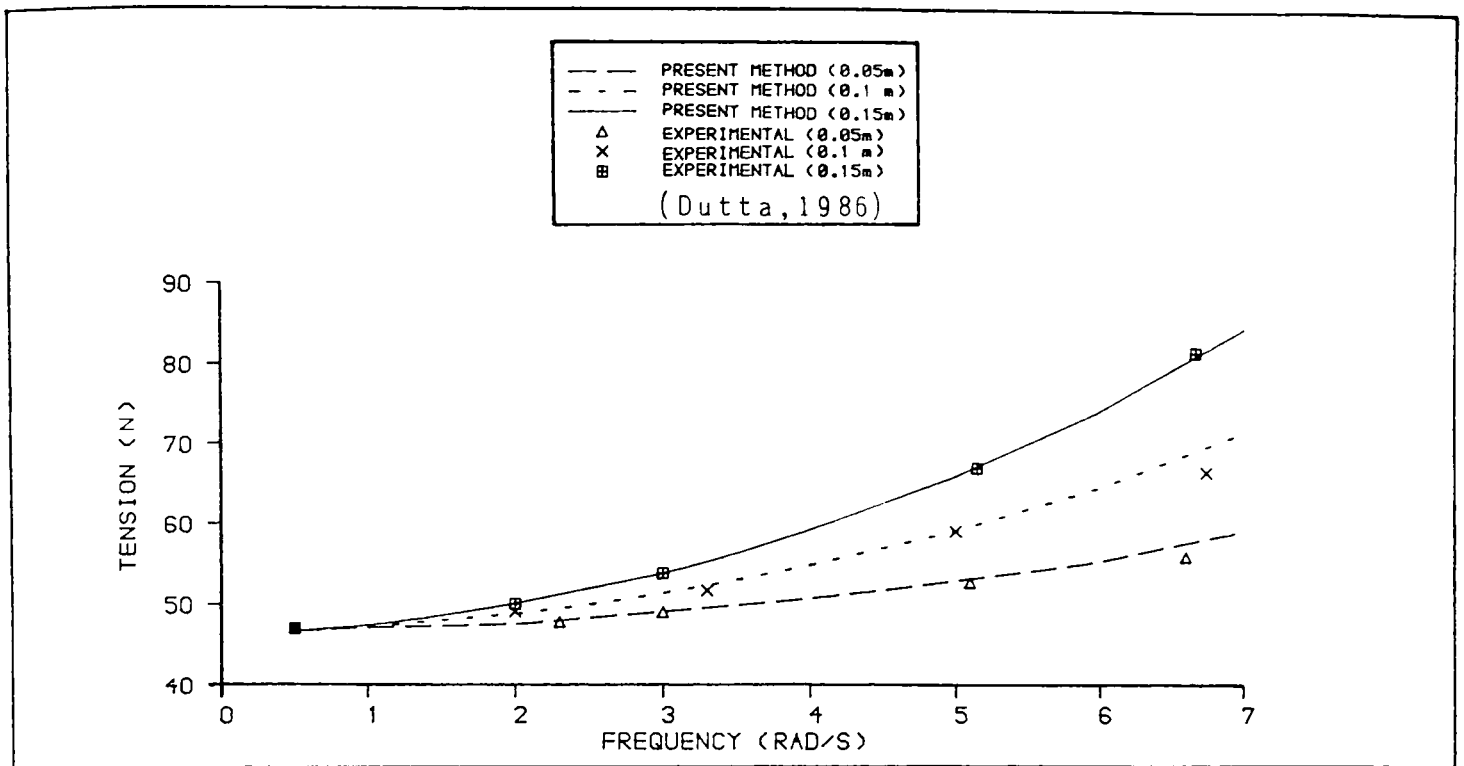

COMPARISON OF THEORETICAL AND EXPERIMENTAL RESULTS
WITH SSU IN AIR (3mm PRESTRETCHED ROPE)
CIRCULAR MOTION AT TOP (AMPLITUDE: 0.05m, 0.1m and 0.15m)

Figure 4.4

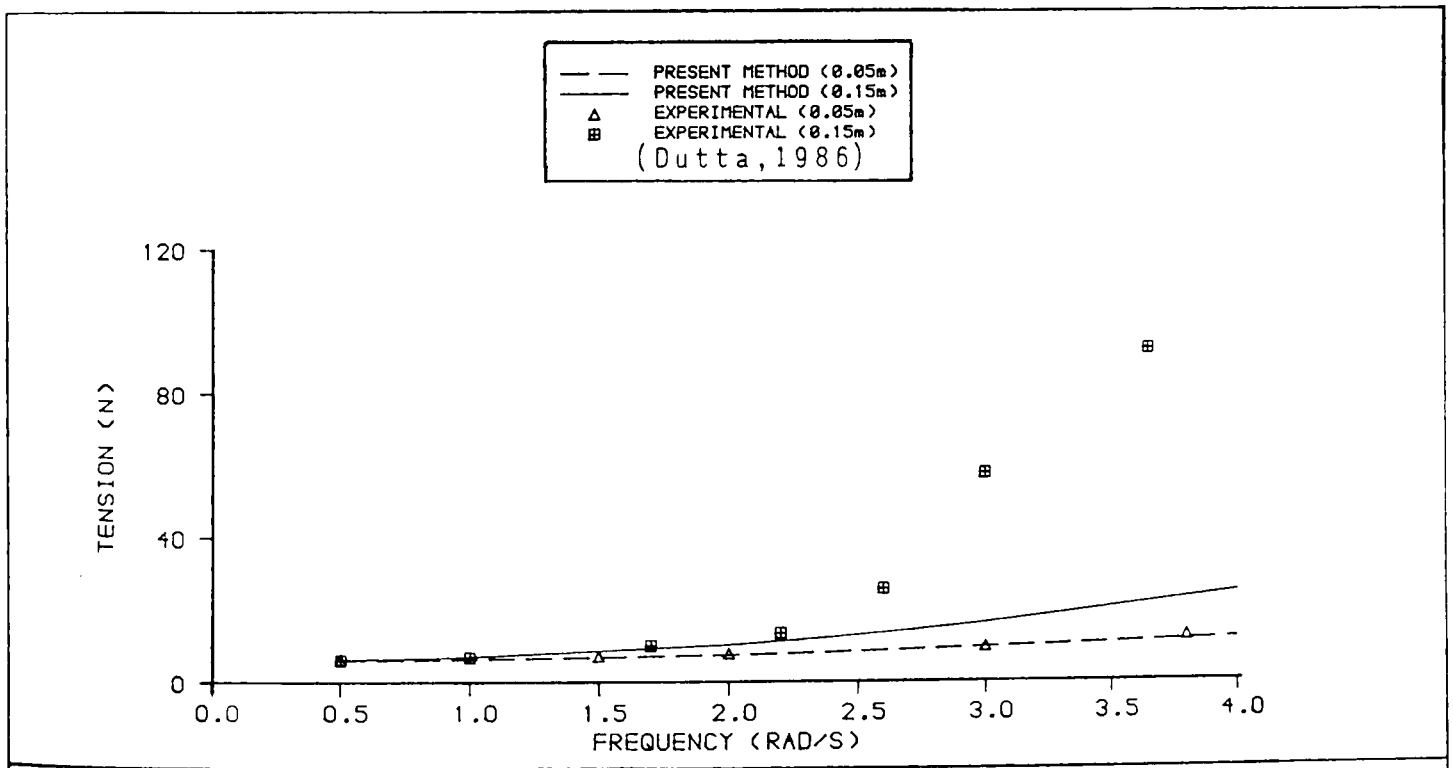

COMPARISON OF THEORETICAL AND EXPERIMENTAL RESULTS
WITH SSU SUBMERGED IN WATER (3mm PRESTRETCHED ROPE)
CIRCULAR MOTION AT TOP (AMPLITUDE: 0.05m and 0.15m)

Figure 4.5

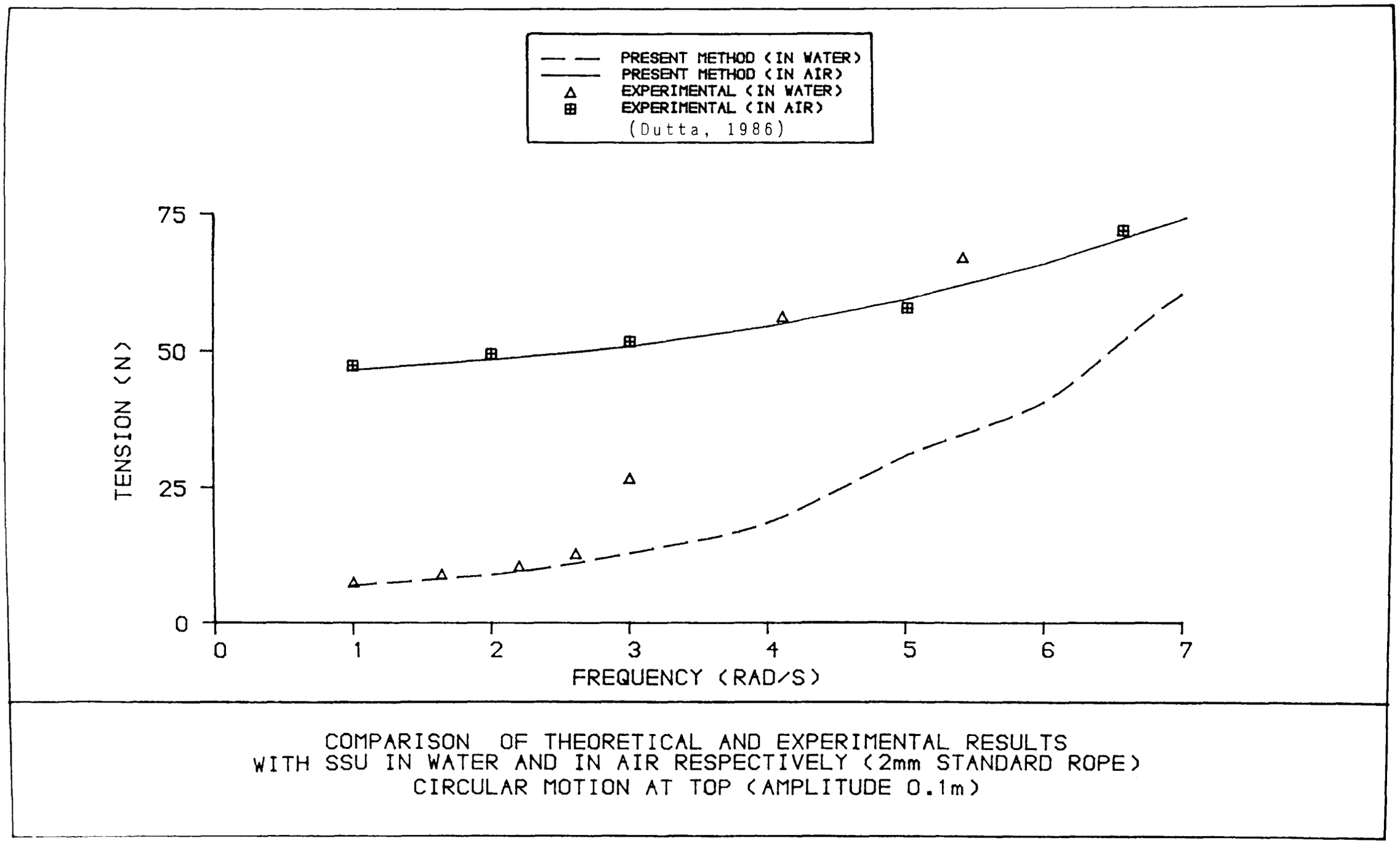

COMPARISON OF THEORETICAL AND EXPERIMENTAL RESULTS
WITH SSU IN WATER AND IN AIR RESPECTIVELY (2mm STANDARD ROPE)
CIRCULAR MOTION AT TOP (AMPLITUDE 0.1m)

Figure 4.6

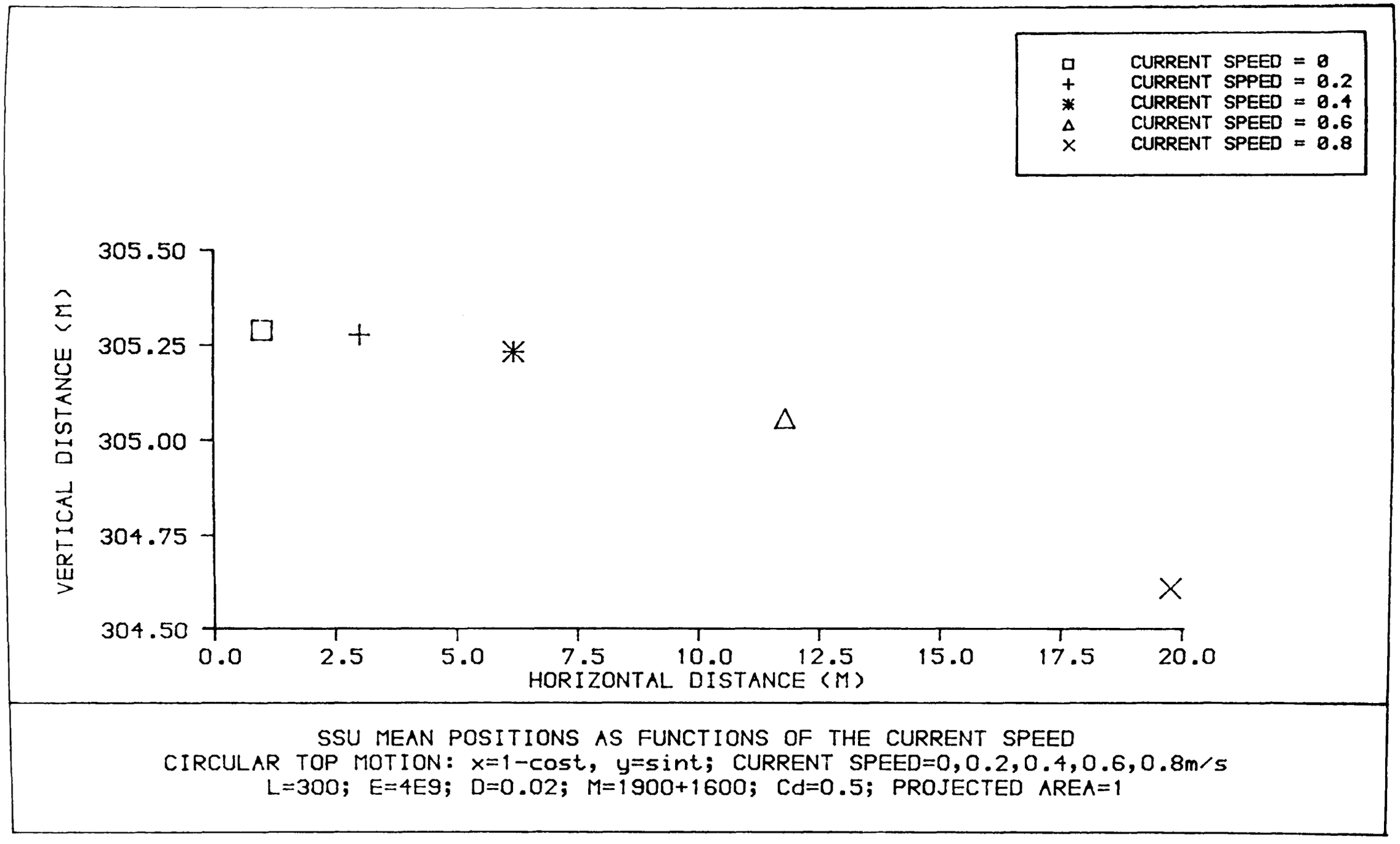

SSU MEAN POSITIONS AS FUNCTIONS OF THE CURRENT SPEED
CIRCULAR TOP MOTION: x=1-cost, y=sint; CURRENT SPEED=0,0.2,0.4,0.6,0.8m/s
L=300; E=4E9; D=0.02; M=1900+1600; Cd=0.5; PROJECTED AREA=1

Figure 4.7

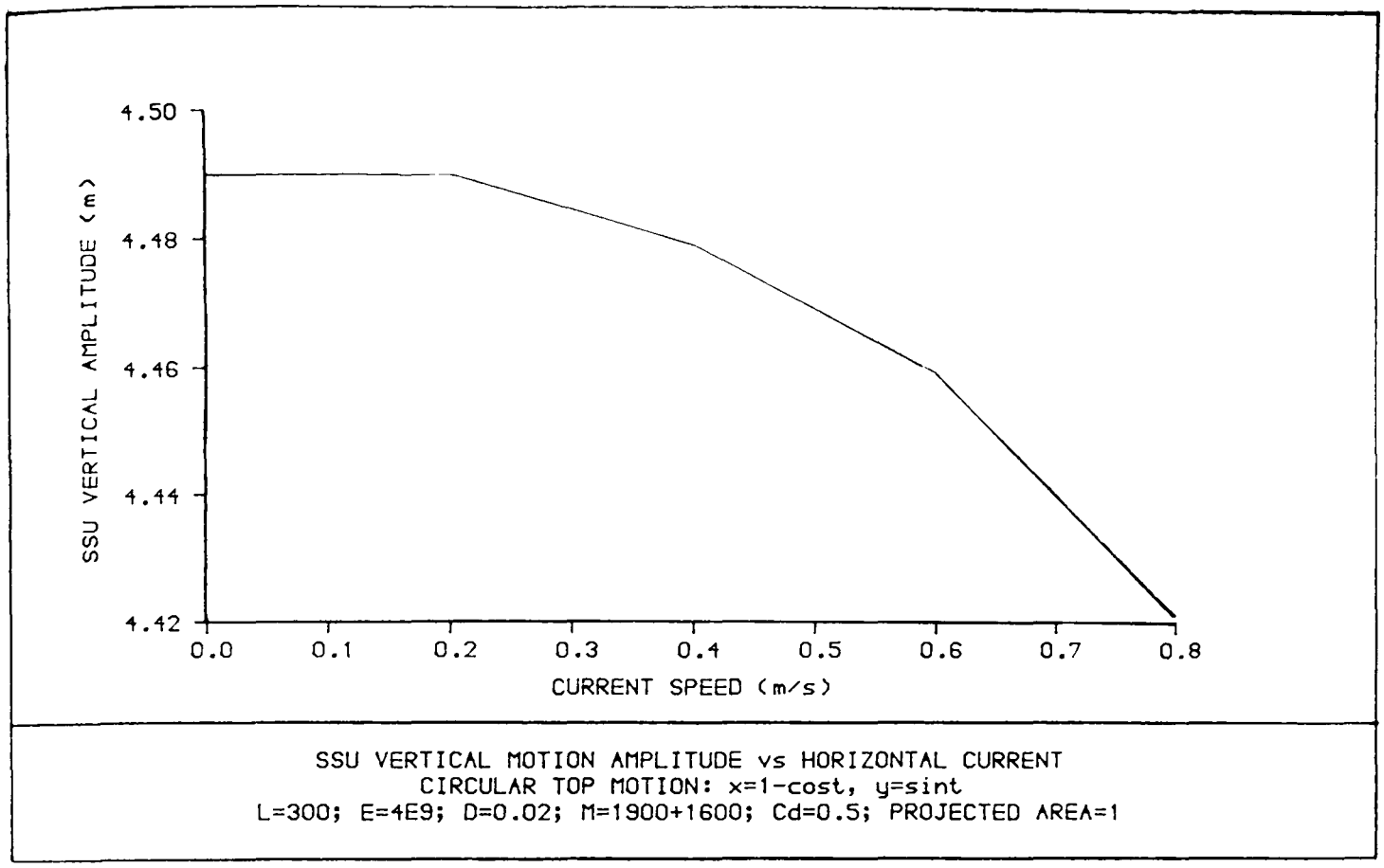

Figure 4.8

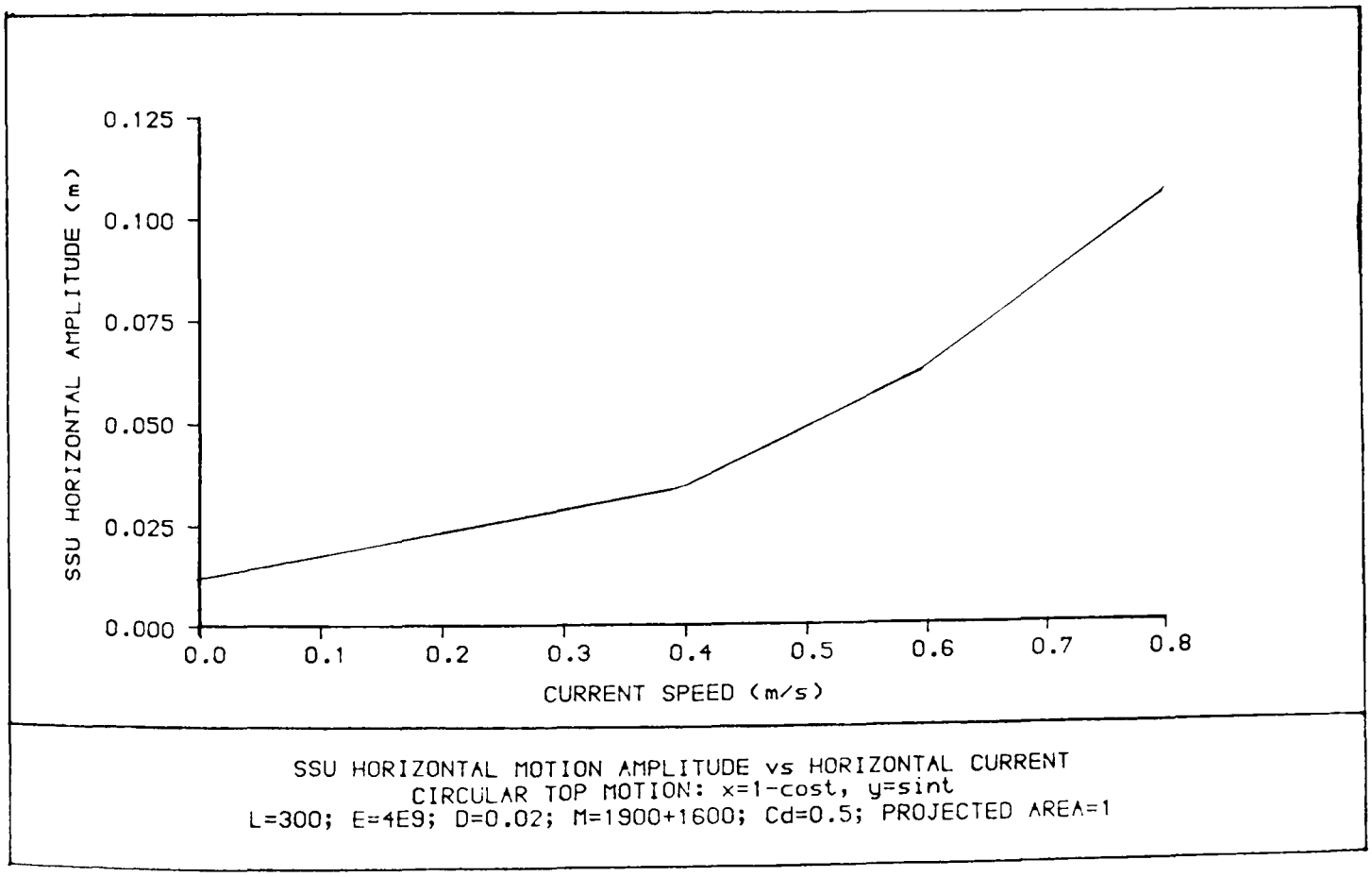

Figure 4.9

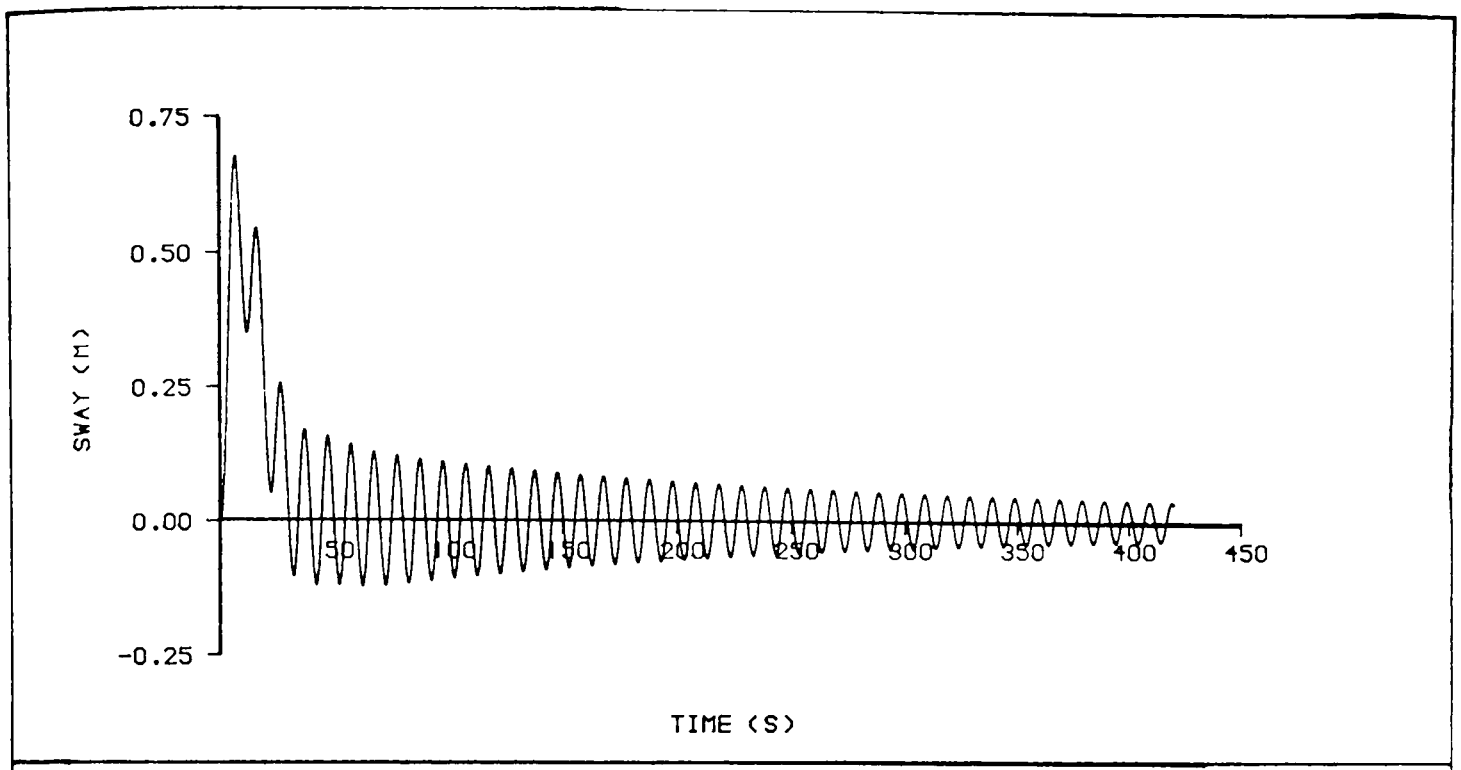

SSU SWAY RESPONSE DURING THE LAUNCH PROCESS
HORIZONTAL TOP MOTION x=5*Sin(0.628t); LAUNCH SPEED v=0.5m/s
L=200; E=9.05E9; D=0.047; M=1900+1600; Cd=0.5; PROJECTED AREA=1

Figure 4.10

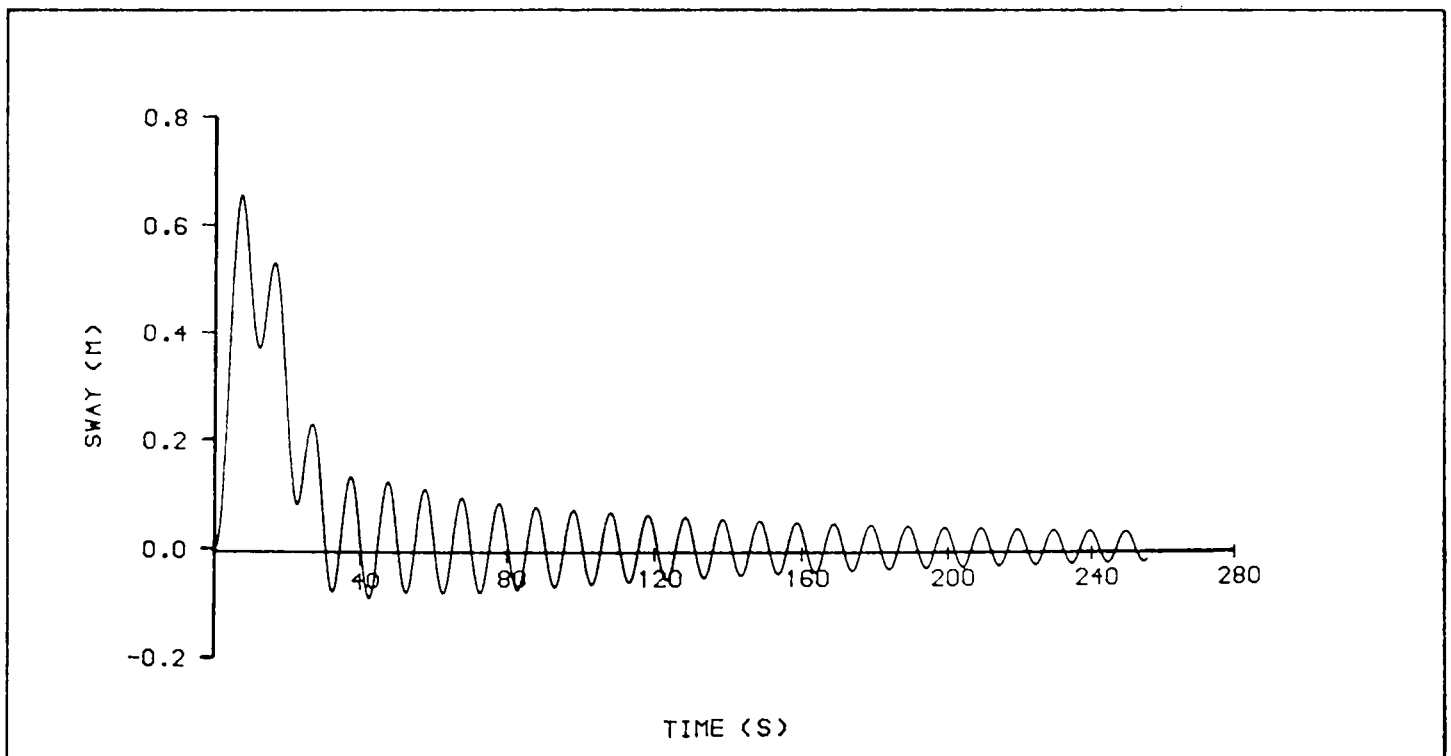

SSU SWAY RESPONSE DURING THE LAUNCH PROCESS
HORIZONTAL TOP MOTION x=5*Sin(0.628t); LAUNCH SPEED v=1m/s
L=200; E=9.05E9; D=0.047; M=1900+1600; Cd=0.5; PROJECTED AREA=1

Figure 4.11

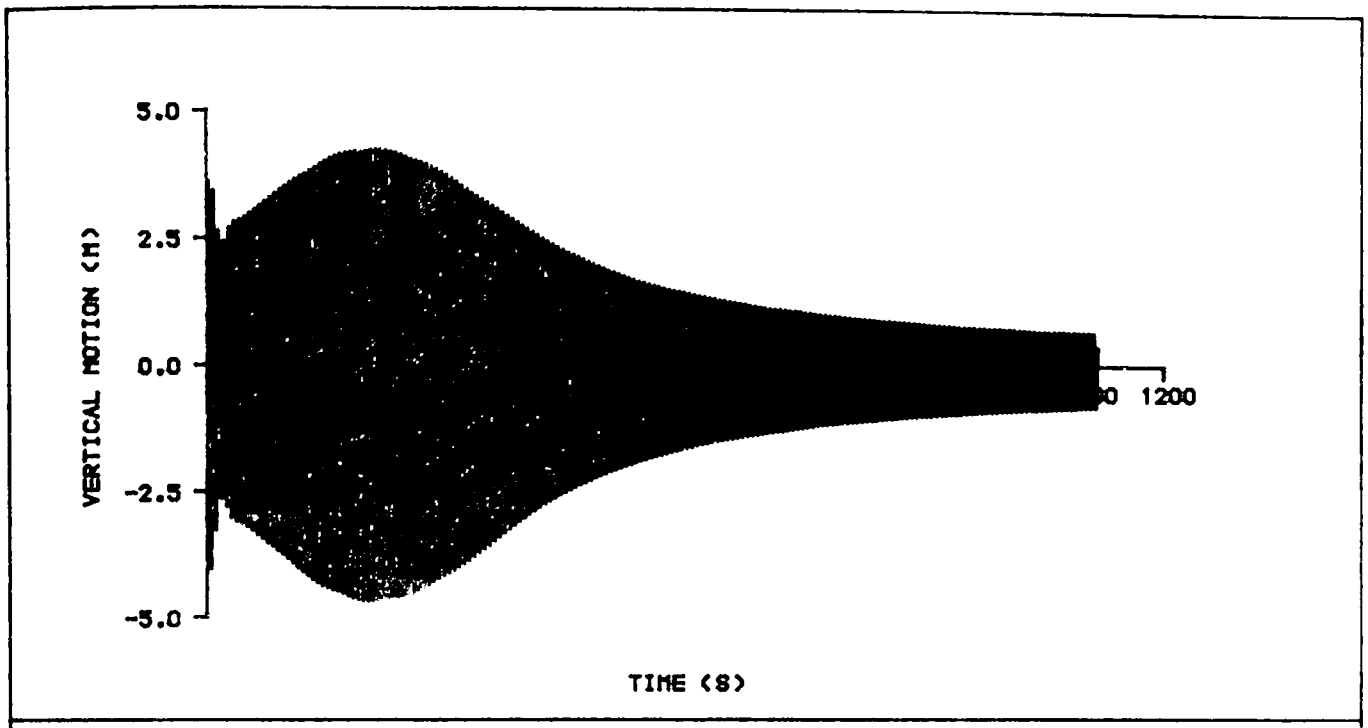

SSU VERTICAL MOTION DURING THE LAUNCH PROCESS
CIRCULAR TOP MOTION: x=1-cost, y=sint; LAUNCH SPEED V=0.5m/s
L=200; E=4E9; D=0.02; M=1900+1600; Cd=0.5; PROJECTED AREA=1

Figure 4.12

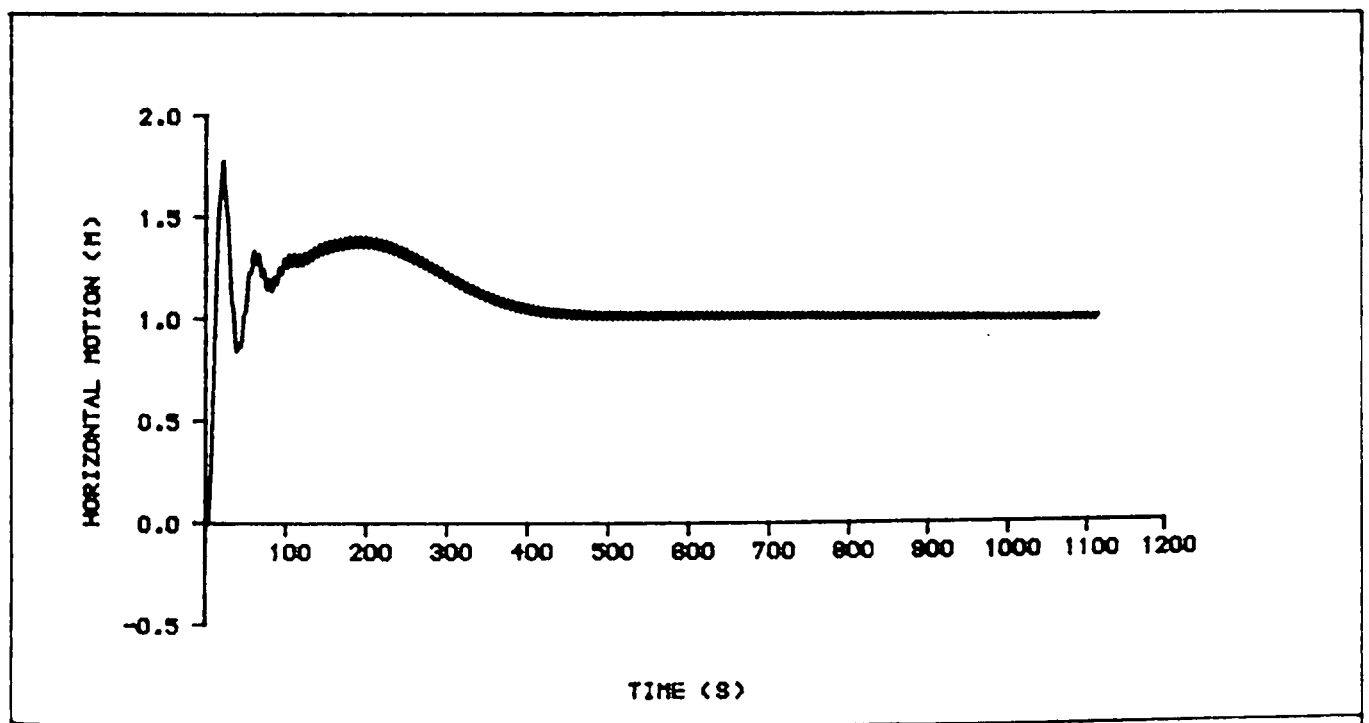

SSU HORIZONTAL MOTION DURING THE LAUNCH PROCESS
CIRCULAR TOP MOTION: x=1-cost, y=sint; LAUNCH SPEED V=0.5m/s
L=200; E=4E9; D=0.02; M=1900+1600; Cd=0.5; PROJECTED AREA=1

Figure 4.13

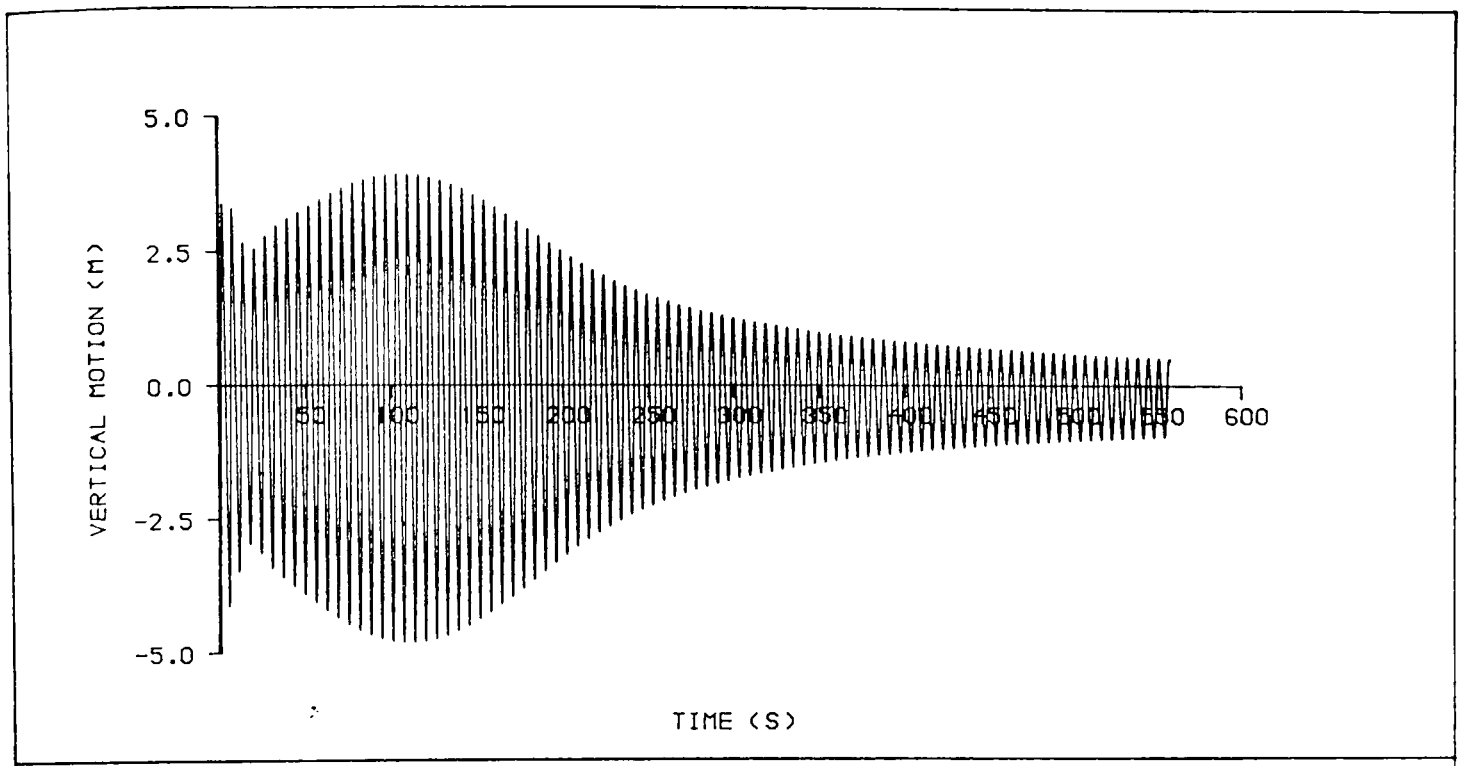

SSU VERTICAL MOTION DURING THE LAUNCH PROCESS
CIRCULAR TOP MOTION: x=1-cost, y=sint; LAUNCH SPEED V=1m/s
L=200; E=4E9; D=0.02; M=1900+1600; Cd=0.5; PROJECTED AREA=1

Figure 4.14

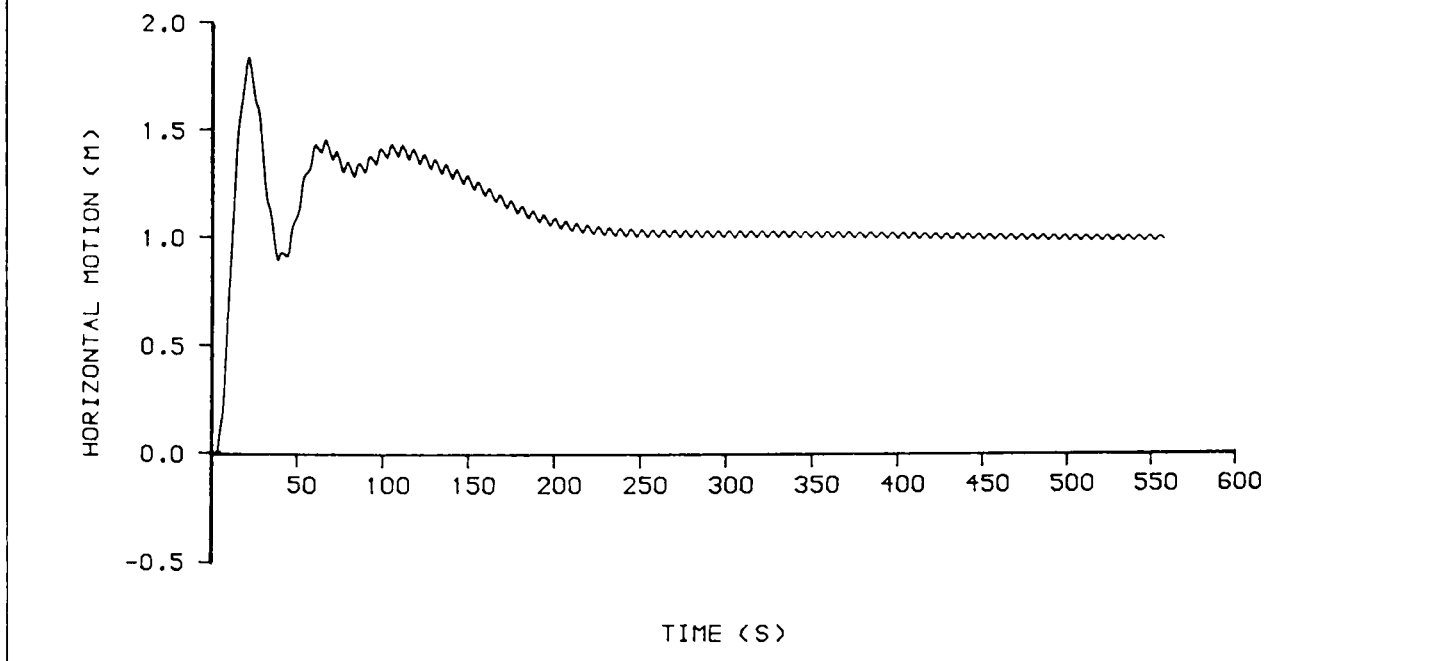

SSU HORIZONTAL MOTION DURING THE LAUNCH PROCESS
CIRCULAR TOP MOTION: x=1-cost, y=sint; LAUNCH SPEED V=1m/s
L=200; E=4E9; D=0.02; M=1900+1600; Cd=0.5; PROJECTED AREA=1

Figure 4.15

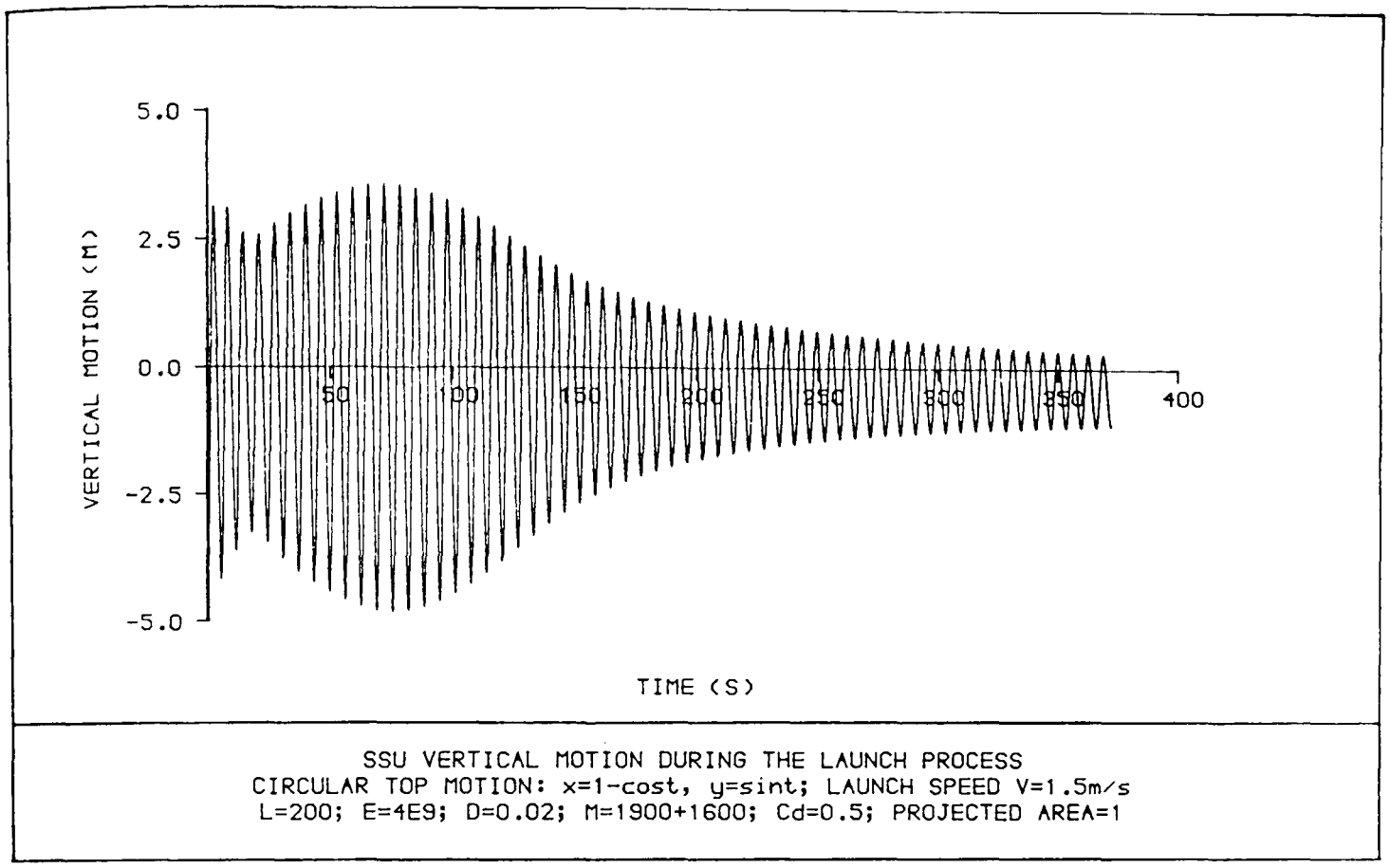

SSU VERTICAL MOTION DURING THE LAUNCH PROCESS
CIRCULAR TOP MOTION: x=1-cost, y=sint; LAUNCH SPEED V=1.5m/s
L=200; E=4E9; D=0.02; M=1900+1600; Cd=0.5; PROJECTED AREA=1

Figure 4.16

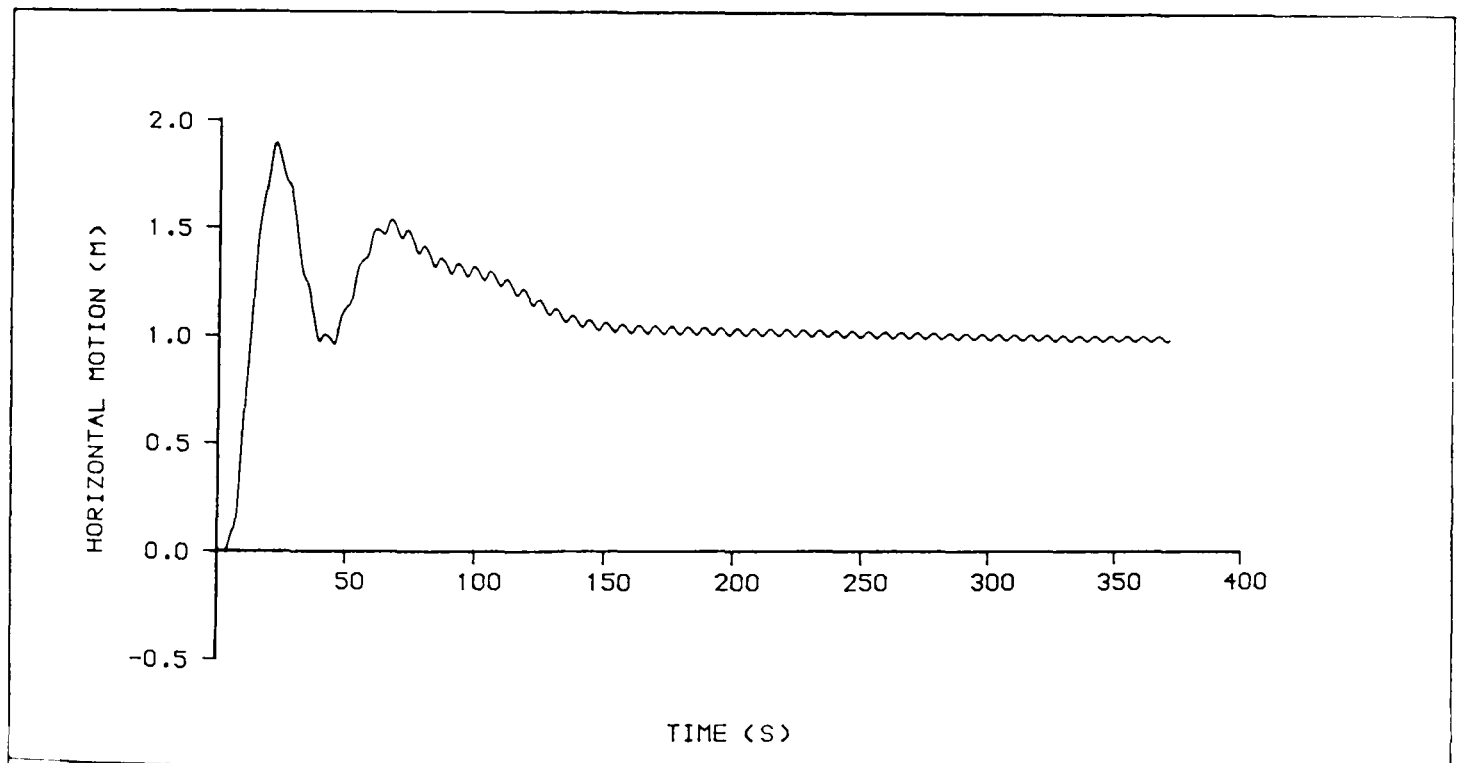

SSU HORIZONTAL MOTION DURING THE LAUNCH PROCESS
CIRCULAR TOP MOTION: x=1-cost, y=sint; LAUNCH SPEED V=1.5m/s
L=200; E=4E9; D=0.02; M=1900+1600; Cd=0.5; PROJECTED AREA=1

Figure 4.17

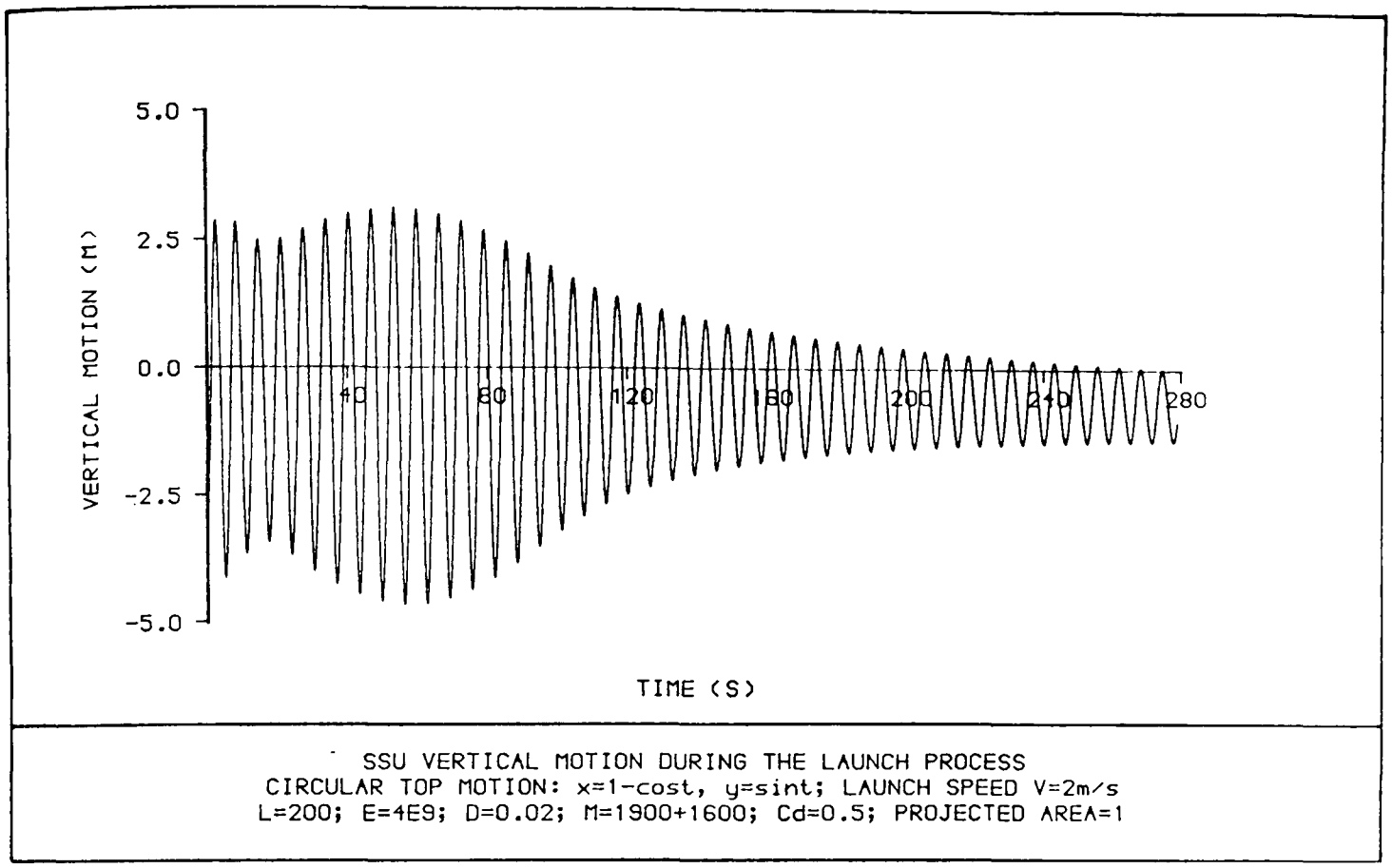

SSU VERTICAL MOTION DURING THE LAUNCH PROCESS
CIRCULAR TOP MOTION: x=1-cost, y=sint; LAUNCH SPEED V=2m/s
L=200; E=4E9; D=0.02; M=1900+1600; Cd=0.5; PROJECTED AREA=1

Figure 4.18

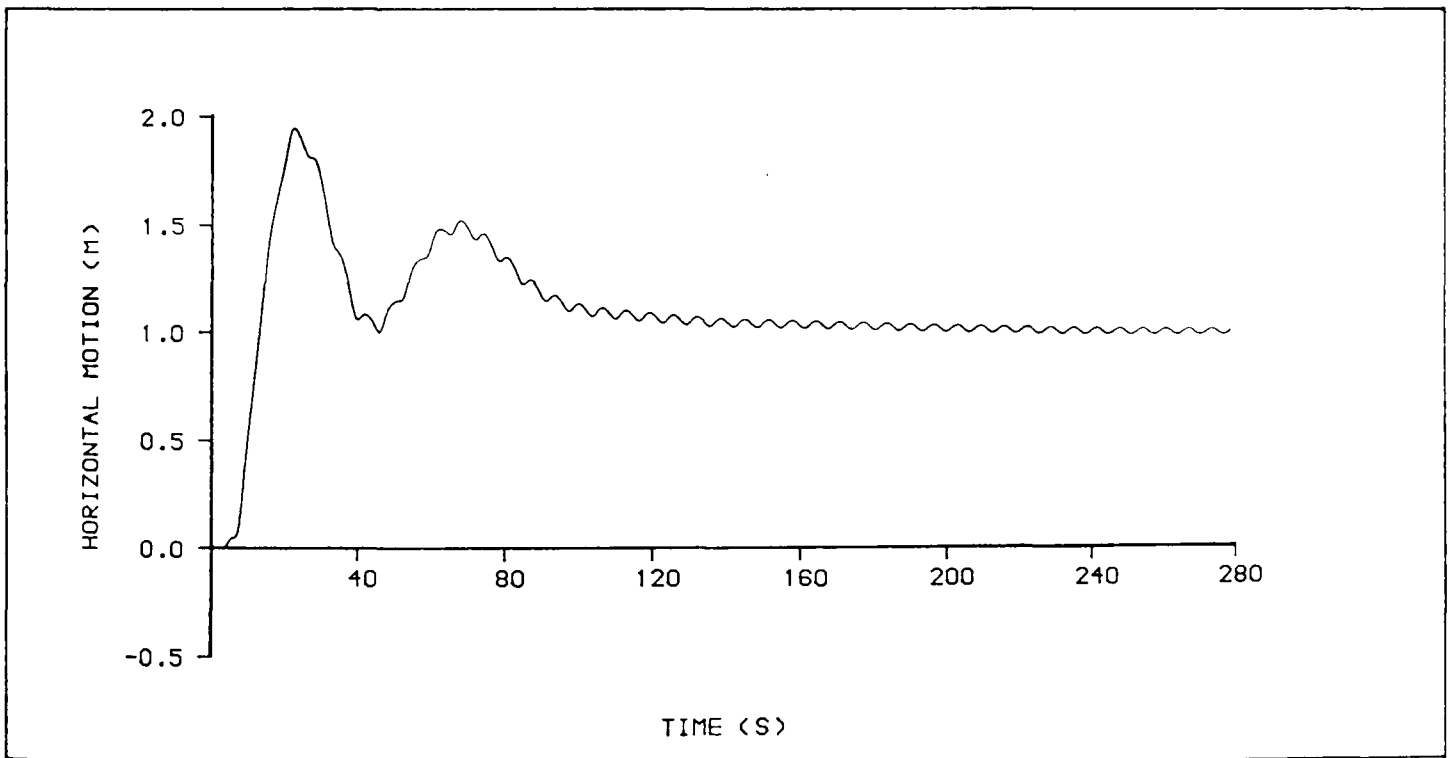

SSU HORIZONTAL MOTION DURING THE LAUNCH PROCESS
CIRCULAR TOP MOTION: x=1-cost, y=sint; LAUNCH SPEED V=2m/s
L=200; E=4E9; D=0.02; M=1900+1600; Cd=0.5; PROJECTED AREA=1

Figure 4.19

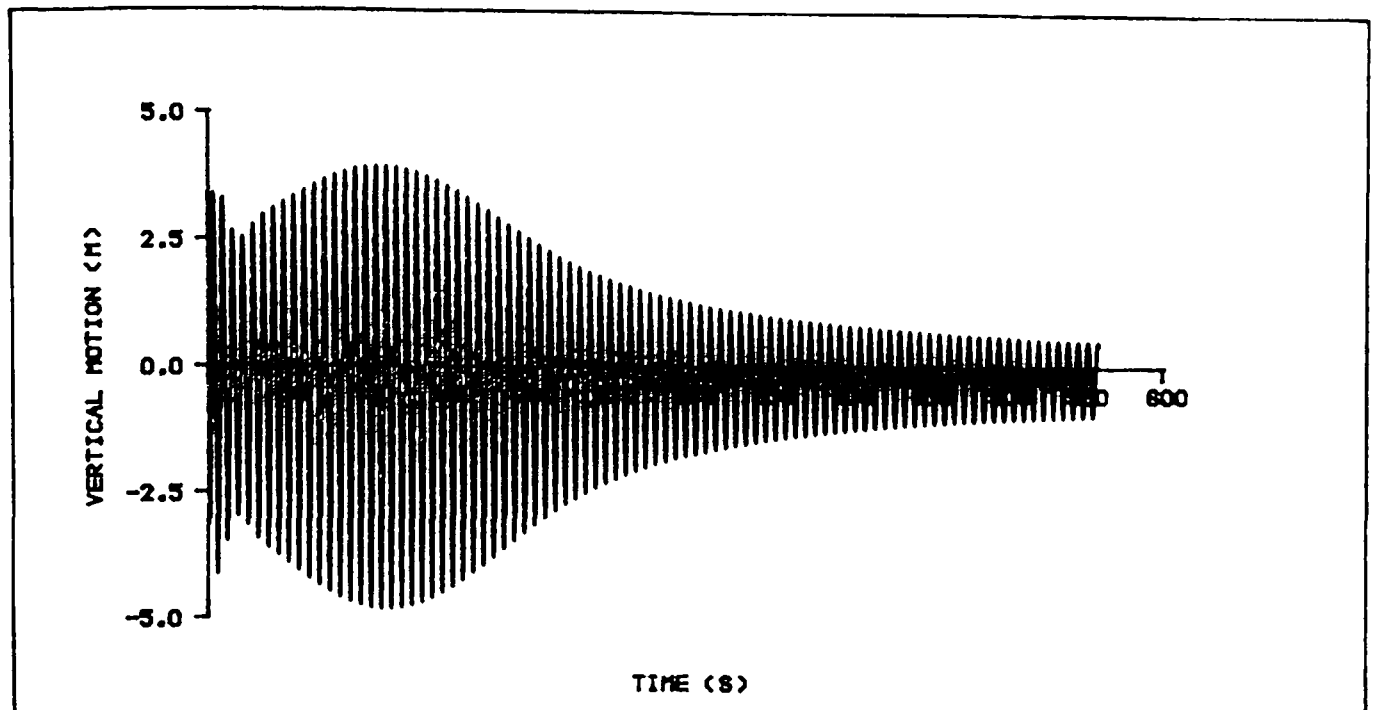

SSU VERTICAL MOTION DURING THE LAUNCH PROCESS
CIRCULAR TOP MOTION: x=1-cost, y=sint; LAUNCH SPEED V=1m/s; CURRENT=0.2m/s
L=200; E=4E9; D=0.02; M=1900+1600; Cd=0.5; PROJECTED AREA=1

Figure 4.20

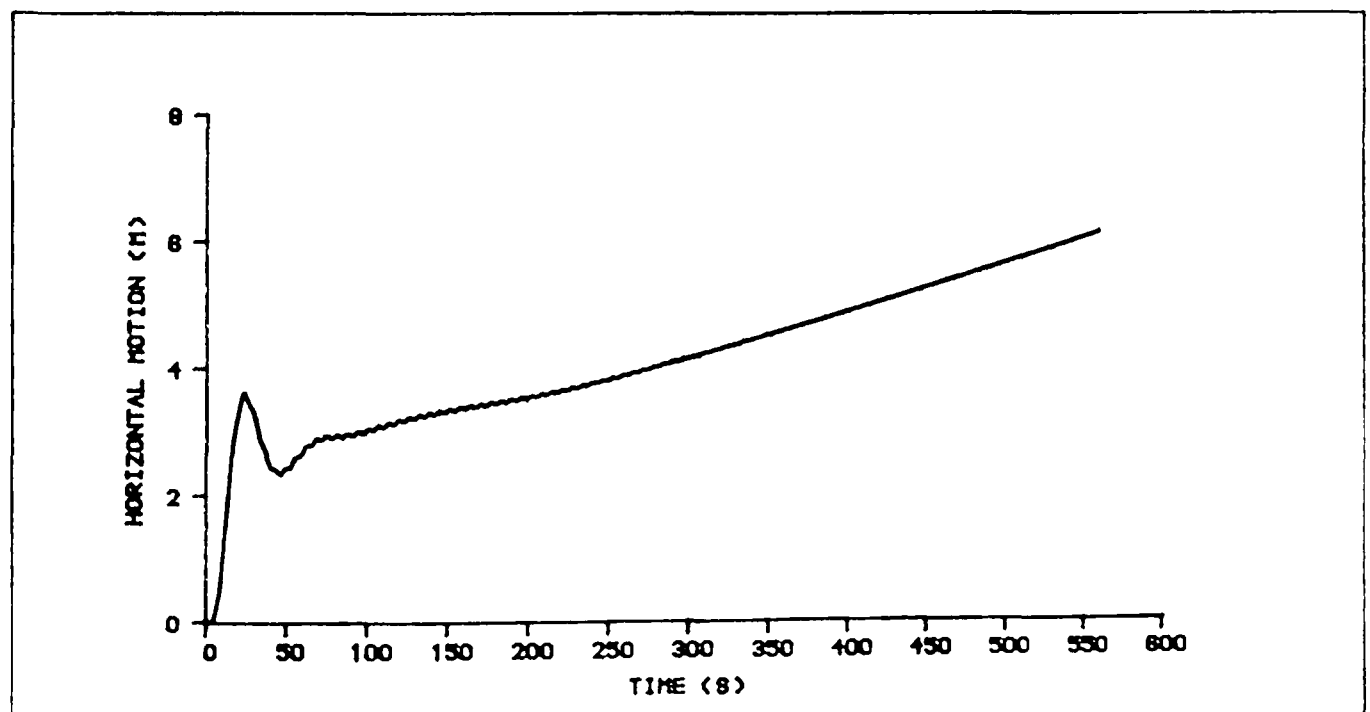

SSU HORIZONTAL MOTION DURING THE LAUNCH PROCESS
CIRCULAR TOP MOTION: x=1-cost, y=sint; LAUNCH SPEED V=1m/s; CURRENT=0.2m/s
L=200; E=4E9; D=0.02; M=1900+1600; Cd=0.5; PROJECTED AREA=1

Figure 4.21

Chapter 5

THREE DIMENSIONAL DYNAMICS

All good things are three.

A German proverb

5.1 GENERAL REMARKS

The marine environment continuously disturbs cable systems through the action of surface water waves, currents, subsurface turbulence, internal water waves, and other external disturbances such as the motions of the supporting vessel and subsystem. For that reason most marine cable systems must be operating three-dimensionally. Strictly speaking, one or two-dimensional cases are rare in practice. It is therefore decided to make further effort to simulate their dynamic response in a three-dimensional space domain.

In the previous two chapters, the cable was treated as a continuous system in the modelling, and only converted into discrete elements when the numerical solution of the partial differential governing equations was pursued. In this chapter, the cable will be discretised at the very beginning of modelling and replaced by jointed elements of finite lengths. This method is often termed the lump-mass-and-spring method. The resulting governing equations lead to a set of ordinary differential equations derived directly from Newton's law of motion or indirectly from Hamilton's principle.

The three-dimensional marine cable has not been tackled extensively yet. However, the basic concept that a cable may be represented as a series of finite inextensible or extensible elements joined at nodes has been widely adopted by many authors mainly for one- or two-dimensional dynamic analysis (Walton and Polacheck, 1960; Polachek et al, 1963; Dominguez and Smith, 1972; Winget and Huston, 1976; Wang, 1977; Nakajima, et al, 1982; van den Boom, 1985; Dutta, 1986; Nomoto and Hattori, 1986; Wang, 1988; Macgregor, 1990). The elements need not necessarily be straight. One way to improve accuracy is using curved elements with additional conditions to enforce the geometric continuity across the nodes (Ma et al, 1979; Lo and Leonard, 1982).

The lump-mass-and-spring method has the following advantages when compared with other methods such as the method of characteristics (Nath and Felix, 1970; Patton, 1972) and the method of perturbation expansion (Carrier, 1945 and 1949):

1. Straightforwardness

The modelling and mathematical formulation has clear physical interpretation. To understand it one need not wade through the esoteric mathematical morass.

2. Economy

   A moderate amount of computation time is needed.

3. Versatility

   Simple as it is, the method can solve many different types of problems including those of nonlinearity, unsteady state, nonuniform cable and oscillatory current.

However, while most investigators are satisfied with the success of the method, further theoretical work awaits to be done:

1. The hyperbolic wave equation and the ordinary differential equation are fundamentally different. A rigorous analysis is needed to prove that, in the limit, the resulting ordinary differential equations pass over into the continuous partial differential governing equations for the motion of a submerged cable.

2. There does not exist mathematical analysis on stability and convergence in most numerical investigations.

In this chapter, we are only concerned with the steady dynamics of a cable system where the length of cable is fixed.

5.2 MATHEMATICAL FORMULATION

The problem is formulated here in a general manner allowing the following:

1. Three-dimensional motion.

2. Large displacements. No linearization is made based upon the small amplitude motion assumption.

3. Inclusion of forces due to the weight of the cable, buoyancy, drag and virtual inertia of the fluid.

4. Non-uniform cables. The approach shall have the capacity to include any sub-systems, such as hanging weights on the cable.

5. Easy implementation of a variety of boundary conditions.

However, slack cable is excluded from this chapter.

5.2.1 Governing Equations

Figure 5.1 shows how a typical configuration of the system with the cable attached to a floating support vessel at one end and to a subsea unit at the other is replaced by a discretised model consisting of many point masses and massless elastic segments. All forces along the cable are assumed to be concentrated at the mass points which are numbered by i running from 0 at the subsea unit to N at the attachment to the support vessel.

The effect of added mass is assumed to be independent of the component of the motion parallel to the segment line. Thus only when an element of the cable has transverse acceleration, does it possess additional mass, whilst if it is accelerated longitudinally no hydrodynamic reaction due to inertia occurs.

By invoking Newton's law of motion for the i-th node on the line, we have

$$m_i \mathbf{a}_i + \frac{1}{2} e_{i+\frac{1}{2}} \mathbf{a}_{iN}|_{i+\frac{1}{2}} + \frac{1}{2} e_{i-\frac{1}{2}} \mathbf{a}_{iN}|_{i-\frac{1}{2}} = \mathbf{F}_i \tag{5.1}$$

where the mass m_i represents the mass of one cable segment. $\mathbf{a}_i$ is its acceleration. $e_{i+\frac{1}{2}}$ and $e_{i-\frac{1}{2}}$ are the added masses of the entrained fluid between the nodes $i, i+1$ and $i-1, i$ respectively. $\mathbf{a}_{iN}|_{i+\frac{1}{2}}$ and $\mathbf{a}_{iN}|_{i-\frac{1}{2}}$ are the components of the vector $\mathbf{a}_i$ on the normal directions of the two segments. The force vector $\mathbf{F}_i$ includes tension forces in the two segments, drag force, gravitational force and buoyant force. Any other external forces, if they are present, can be included in this term as well.

Let ϕ and θ represents the two rotational angles defined in Figure 5.2, and x_i, y_i and z_i three coordinates of the i-th node in a Cartesian coordinate system. In expanded form, the equation of motion can be written as (the dots indicating differentiation with respect to time):

$$\begin{bmatrix} A_{11} & A_{12} & A_{13} \\ A_{21} & A_{22} & A_{23} \\ A_{31} & A_{32} & A_{33} \end{bmatrix} \begin{bmatrix} \ddot{x}_i \\ \ddot{y}_i \\ \ddot{z}_i \end{bmatrix} = \begin{bmatrix} F_{xi} \\ F_{yi} \\ F_{zi} \end{bmatrix} \tag{5.2}$$

where

$$A_{11} = m_i + \frac{1}{2}[e_{i+\frac{1}{2}}(1 - sin^2\theta_{i+\frac{1}{2}} cos^2\phi_{i+\frac{1}{2}}) + e_{i-\frac{1}{2}}(1 - sin^2\theta_{i-\frac{1}{2}} cos^2\phi_{i-\frac{1}{2}})]$$

$$
\begin{aligned}
A_{22} &= m_i + \frac{1}{2}[e_{i+\frac{1}{2}}(1 - cos^2\theta_{i+\frac{1}{2}}cos^2\phi_{i+\frac{1}{2}}) + e_{i-\frac{1}{2}}(1 - cos^2\theta_{i-\frac{1}{2}}cos^2\phi_{i-\frac{1}{2}})] \\
A_{33} &= m_i + \frac{1}{2}(e_{i+\frac{1}{2}}cos^2\phi_{i+\frac{1}{2}} + e_{i-\frac{1}{2}}cos^2\phi_{i-\frac{1}{2}}) \\
A_{12} &= A_{21} = \\
&\quad -\frac{1}{2}(e_{i+\frac{1}{2}}sin\theta_{i+\frac{1}{2}}cos\theta_{i+\frac{1}{2}}cos^2\phi_{i+\frac{1}{2}} + e_{i-\frac{1}{2}}sin\theta_{i-\frac{1}{2}}cos\theta_{i-\frac{1}{2}}cos^2\phi_{i-\frac{1}{2}}) \\
A_{13} &= A_{31} = \\
&\quad -\frac{1}{2}(e_{i+\frac{1}{2}}sin\theta_{i+\frac{1}{2}}sin\phi_{i+\frac{1}{2}}cos\phi_{i+\frac{1}{2}} + e_{i-\frac{1}{2}}sin\theta_{i-\frac{1}{2}}sin\phi_{i-\frac{1}{2}}cos\phi_{i-\frac{1}{2}}) \\
A_{23} &= A_{32} = \\
&\quad -\frac{1}{2}(e_{i+\frac{1}{2}}cos\theta_{i+\frac{1}{2}}sin\phi_{i+\frac{1}{2}}cos\phi_{i+\frac{1}{2}} + e_{i-\frac{1}{2}}cos\theta_{i-\frac{1}{2}}sin\phi_{i-\frac{1}{2}}cos\phi_{i-\frac{1}{2}}) \\
e_{i+\frac{1}{2}} &= \rho k_{i+\frac{1}{2}} l_{i+\frac{1}{2}} \sigma_{i+\frac{1}{2}} \\
e_{i-\frac{1}{2}} &= \rho k_{i-\frac{1}{2}} l_{i-\frac{1}{2}} \sigma_{i-\frac{1}{2}} \\
m_i &= \frac{1}{2}(\mu_{i+\frac{1}{2}} l_{i+\frac{1}{2}} + \mu_{i-\frac{1}{2}} l_{i-\frac{1}{2}}) \\
F_{xi} &= T_{i+\frac{1}{2}}sin\theta_{i+\frac{1}{2}}cos\phi_{i+\frac{1}{2}} - T_{i-\frac{1}{2}}sin\theta_{i-\frac{1}{2}}cos\phi_{i-\frac{1}{2}} + \frac{1}{2}(F_{Dx}^{i+\frac{1}{2}} + F_{Dx}^{i-\frac{1}{2}}) \\
F_{yi} &= T_{i+\frac{1}{2}}cos\theta_{i+\frac{1}{2}}cos\phi_{i+\frac{1}{2}} - T_{i-\frac{1}{2}}cos\theta_{i-\frac{1}{2}}cos\phi_{i-\frac{1}{2}} + \frac{1}{2}(F_{Dy}^{i+\frac{1}{2}} + F_{Dy}^{i-\frac{1}{2}}) \\
F_{zi} &= T_{i+\frac{1}{2}}sin\phi_{i+\frac{1}{2}} - T_{i-\frac{1}{2}}sin\phi_{i-\frac{1}{2}} + \frac{1}{2}(F_{Dz}^{i+\frac{1}{2}} + F_{Dz}^{i-\frac{1}{2}}) \\
&\quad + \frac{1}{2}\rho g(l_{i+\frac{1}{2}}\sigma_{i+\frac{1}{2}} + l_{i-\frac{1}{2}}\sigma_{i-\frac{1}{2}}) - m_i g
\end{aligned}
$$

In these equations $T_{i+\frac{1}{2}}$ and $T_{i-\frac{1}{2}}$ stand for the tension forces in the cable segments which lie on either sides of the i-th node. Likewise, $k_{i+\frac{1}{2}}$ and $k_{i-\frac{1}{2}}$, $l_{i+\frac{1}{2}}$ and $l_{i-\frac{1}{2}}$, $\sigma_{i+\frac{1}{2}}$ and $\sigma_{i-\frac{1}{2}}$, $\mu_{i+\frac{1}{2}}$ and $\mu_{i-\frac{1}{2}}$, are respectively the added mass coefficients, lengths, cross section areas and cable densities of the two segments. ρ is the density of fluid, and g is the acceleration due to gravity.

The tensions are determined by the elastic properties of the cable and its deformation. By utilizing Hooke's law, the tensions $T_{i+\frac{1}{2}}$ and $T_{i-\frac{1}{2}}$ are given by:

$$T_{i+\frac{1}{2}} = \sigma_{i+\frac{1}{2}} E\left(\frac{\sqrt{(x_{i+1}-x_i)^2+(y_{i+1}-y_i)^2+(z_{i+1}-z_i)^2}}{l_{i+\frac{1}{2}}} - 1\right) \tag{5.3}$$

$$T_{i-\frac{1}{2}} = \sigma_{i-\frac{1}{2}} E\left(\frac{\sqrt{(x_i-x_{i-1})^2+(y_i-y_{i-1})^2+(z_i-z_{i-1})^2}}{l_{i-\frac{1}{2}}} - 1\right) \tag{5.4}$$

where E is Young's modulus.

The hydrodynamic drag on the i-th node has been expressed as one-half of each drag acting on the two segments lying on either side of that node, i.e., $\mathbf{F}_D^{i+\frac{1}{2}} = \{F_{Dx}^{i+\frac{1}{2}}, F_{Dy}^{i+\frac{1}{2}}, F_{Dz}^{i+\frac{1}{2}}\}$ and $\mathbf{F}_D^{i-\frac{1}{2}} = \{F_{Dx}^{i-\frac{1}{2}}, F_{Dy}^{i-\frac{1}{2}}, F_{Dz}^{i-\frac{1}{2}}\}$. The drag on each segment is assumed to be resolved into two components, namely, the normal one and tangential one, each as a function of the relative velocity in that direction. $\mathbf{F}_D^{i+\frac{1}{2}}$ is given by

$$\begin{aligned}\mathbf{F}_D^{i+\frac{1}{2}} &= -\frac{1}{2}\rho C_N^{i+\frac{1}{2}} l_{i+\frac{1}{2}} d_{i+\frac{1}{2}} |(\mathbf{V}_c - \mathbf{U})_N| (\mathbf{V}_c - \mathbf{U})_N \\ &\quad -\frac{\pi}{2}\rho C_\tau^{i+\frac{1}{2}} l_{i+\frac{1}{2}} d_{i+\frac{1}{2}} |(\mathbf{V}_c - \mathbf{U})_\tau| (\mathbf{V}_c - \mathbf{U})_\tau\end{aligned}$$

where $C_N^{i+\frac{1}{2}}$ and $C_\tau^{i+\frac{1}{2}}$ are the normal and the tangential drag coefficients. $d_{i+\frac{1}{2}}$ is the diameter of the segment. $\mathbf{U} = \{U_x, U_y, U_z\}$ is the underwater current which may vary in both direction and magnitude in the space domain and the time domain.

$$\begin{aligned}\mathbf{V}_c &= \{V_{cx}, V_{cy}, V_{cz}\} \\ &= \{\frac{1}{2}(\dot{x}_{i+1}+\dot{x}_i), \frac{1}{2}(\dot{y}_{i+1}+\dot{y}_i), \frac{1}{2}(\dot{z}_{i+1}+\dot{z}_i)\}\end{aligned}$$

$$(\mathbf{V}_c - \mathbf{U})_N = \mathbf{PV}$$

$$(\mathbf{V}_c - \mathbf{U})_\tau = \mathbf{QV}$$

$$\mathbf{P} = \begin{bmatrix} 1 - sin^2\theta_{i+\frac{1}{2}} cos^2\phi_{i+\frac{1}{2}} & -sin\theta_{i+\frac{1}{2}} cos\theta_{i+\frac{1}{2}} cos^2\phi_{i+\frac{1}{2}} & -sin\theta_{i+\frac{1}{2}} sino_{i+\frac{1}{2}} coso_{i+\frac{1}{2}} \\ -sin\theta_{i+\frac{1}{2}} cos\theta_{i+\frac{1}{2}} cos^2\phi_{i+\frac{1}{2}} & 1 - cos^2\theta_{i+\frac{1}{2}} cos^2\phi_{i+\frac{1}{2}} & -cos\theta_{i+\frac{1}{2}} sino_{i+\frac{1}{2}} coso_{i+\frac{1}{2}} \\ -sin\theta_{i+\frac{1}{2}} sin\phi_{i+\frac{1}{2}} cos\phi_{i+\frac{1}{2}} & -cos\theta_{i+\frac{1}{2}} sin\phi_{i+\frac{1}{2}} cos\phi_{i+\frac{1}{2}} & cos^2\phi_{i+\frac{1}{2}} \end{bmatrix}$$

$$\mathbf{Q} = \mathbf{I} - \mathbf{P}$$

$$\mathbf{V} = \begin{bmatrix} V_{cx} - U_x \\ V_{cy} - U_y \\ V_{cz} - U_z \end{bmatrix}$$

where $\mathbf{I}$ is the unit matrix.

A similar form may be derived for the drag $\mathbf{F}_D^{i-\frac{1}{2}}$.

5.2.2 Boundary Conditions

Boundary conditions must be given at both ends of the cable. Different types of boundary conditions may occur depending on the types of physical conditions at the two ends. The simplest case is that both ends are fixed. Here we are addressing one particular situation which is widely employed in offshore engineering where one end of the cable is attached to a surface supporting vessel and the other is connected to a powered or unpowered subsea unit.

Assuming the dynamic load on the vessel through the cable is negligible compared with other loads on the vessel such as the wave force, we can decouple the vessel's motion from the motion of the cable system. In this case the upper end conditions for the cable are:

$$x_N(t) = \bar{x}(t) \tag{5.5}$$

$$y_N(t) = \bar{y}(t)$$

$$z_N(t) = \bar{z}(t)$$

where $\bar{x}(t)$, $\bar{y}(t)$ and $\bar{z}(t)$ are the vessel's motions which are known functions of time.

At the lower end, boundary conditions can be specified by invoking Newton's law of motion. These are:

$$\begin{bmatrix} a_{11} & a_{12} & a_{13} \\ a_{21} & a_{22} & a_{23} \\ a_{31} & a_{32} & a_{33} \end{bmatrix} \begin{bmatrix} \ddot{x}_0 \\ \ddot{y}_0 \\ \ddot{z}_0 \end{bmatrix} = \begin{bmatrix} F_{x0} \\ F_{y0} \\ F_{z0} \end{bmatrix} \tag{5.6}$$

where

$$a_{11} = M_0 + m_0 + M_{ax} + \frac{1}{2}e_{\frac{1}{2}}(1 - sin^2\theta_{\frac{1}{2}}cos^2\phi_{\frac{1}{2}})$$

$$a_{22} = M_0 + m_0 + M_{ay} + \frac{1}{2}e_{\frac{1}{2}}(1 - cos^2\theta_{\frac{1}{2}}cos^2\phi_{\frac{1}{2}})$$

$$a_{33} = M_0 + m_0 + M_{az} + \frac{1}{2}e_{\frac{1}{2}}cos^2\phi_{\frac{1}{2}}$$

$$a_{12} = a_{21} = -\frac{1}{2}e_{\frac{1}{2}}sin\theta_{\frac{1}{2}}cos\theta_{\frac{1}{2}}cos^2\phi_{\frac{1}{2}}$$

$$a_{13} = a_{31} = -\frac{1}{2}e_{\frac{1}{2}}sin\theta_{\frac{1}{2}}sin\phi_{\frac{1}{2}}cos\phi_{\frac{1}{2}}$$

$$a_{23} = a_{32} = -\frac{1}{2}e_{\frac{1}{2}}cos\theta_{\frac{1}{2}}sin\phi_{\frac{1}{2}}cos\phi_{\frac{1}{2}}$$

$$m_0 = \frac{1}{2}\mu_{\frac{1}{2}}l_{\frac{1}{2}}$$

$$F_{x0} = T_{\frac{1}{2}}sin\theta_{\frac{1}{2}}cos\phi_{\frac{1}{2}} + \frac{1}{2}F_{Dx}^{\frac{1}{2}} + D_x$$

$$F_{y0} = T_{\frac{1}{2}}cos\theta_{\frac{1}{2}}cos\phi_{\frac{1}{2}} + \frac{1}{2}F_{Dy}^{\frac{1}{2}} + D_y$$

$$F_{z0} = T_{\frac{1}{2}}sin\phi_{\frac{1}{2}} + \frac{1}{2}F_{Dz}^{\frac{1}{2}} + \rho g(\frac{1}{2}l_{\frac{1}{2}}\sigma_{\frac{1}{2}} + V_0) - (M_0 + m_0)g + D_z$$

where M_0 and V_0 are the mass and the volume of the subsea unit. M_{ax}, M_{ay} and

M_{az} are its added masses. D_x, D_y and D_z are the components of the hydrodynamic drag on it. They are given by:

$$\begin{aligned} D_x &= -\frac{1}{2}\rho C_{Dx} S_x |\dot{x}_0 - U_x|(\dot{x}_0 - U_x) \\ D_y &= -\frac{1}{2}\rho C_{Dy} S_y |\dot{y}_0 - U_y|(\dot{y}_0 - U_y) \\ D_z &= -\frac{1}{2}\rho C_{Dz} S_z |\dot{x}_0 - U_z|(\dot{z}_0 - U_z) \end{aligned}$$

where C_{Dx}, C_{Dy} and C_{Dz} are the drag coefficients of the subsea unit in the three different directions. S_x, S_y and S_z are the projected areas accordingly.

5.2.3 Initial Conditions

To complete the formulation, a set of initial conditions must be specified for each node on the line. This includes both the initial positions and initial velocities, as required by the second order ordinary differential equations:

$$\begin{aligned} x_i(0) &= x_i^0 \\ y_i(0) &= y_i^0 \\ z_i(0) &= z_i^0 \end{aligned} \tag{5.7}$$

and

$$\begin{aligned} \dot{x}_i(0) &= \dot{x}_i^0 \\ \dot{y}_i(0) &= \dot{y}_i^0 \\ \dot{z}_i(0) &= \dot{z}_i^0 \end{aligned} \tag{5.8}$$

for all $i = 0, 1, 2, ..., N$. All the right hand sides of these equations are given beforehand.

5.3 PROBLEM CHARACTERISTICS

Though strictly speaking there is no such thing as a truly continuous system, the motion of cable is generally considered as a feature of a continuous system because the ultimate discontinuity due to the atomic structure is not obvious and the typical spacing involved is much less than the typical length of the motion. In the Appendix, a detailed analysis on cable dynamics is given assuming the cable is a continuous system. In this section, we shall investigate the relation between the formulation assuming the cable as a continuous system and the discrete formulation described in the previous section.

5.3.1 Governing Equations

Neglecting the effect of the added mass and assuming the lumped masses are initially equally spaced with a distance l between them, we can rewrite Eq. (5.2) in the following form

$$m\ddot{x}_i = T_{i+\frac{1}{2}} \frac{x_{i+1} - x_i}{l(1+\varepsilon_{i+\frac{1}{2}})} - T_{i-\frac{1}{2}} \frac{x_i - x_{i-1}}{l(1+\varepsilon_{i-\frac{1}{2}})} + \bar{F}_{xi} \tag{5.9}$$

$$m\ddot{y}_i = T_{i+\frac{1}{2}} \frac{y_{i+1} - y_i}{l(1+\varepsilon_{i+\frac{1}{2}})} - T_{i-\frac{1}{2}} \frac{y_i - y_{i-1}}{l(1+\varepsilon_{i-\frac{1}{2}})} + \bar{F}_{yi} \tag{5.10}$$

$$m\ddot{z}_i = T_{i+\frac{1}{2}} \frac{z_{i+1} - z_i}{l(1+\varepsilon_{i+\frac{1}{2}})} - T_{i-\frac{1}{2}} \frac{z_i - z_{i-1}}{l(1+\varepsilon_{i-\frac{1}{2}})} + \bar{F}_{zi} \tag{5.11}$$

where $\bar{F}_{xi}$, $\bar{F}_{yi}$ and $\bar{F}_{zi}$ represent the components of fluid drag forces, gravitational force and buoyant force.

To reduce this discrete description into a continuous approximation, we start with Taylor's theorem:

$$x_{i+1} - x_i = l\frac{\partial x}{\partial s}|_{i+\frac{1}{2}} + \frac{l^3}{3!2^2}\frac{\partial^3 x}{\partial s^3}|_{i+\frac{1}{2}} + \frac{l^5}{5!2^4}\frac{\partial^5 x}{\partial s^5}|_{i+\frac{1}{2}} + O(l^7) \tag{5.12}$$

$$x_i - x_{i-1} = l\frac{\partial x}{\partial s}|_{i-\frac{1}{2}} + \frac{l^3}{3!2^2}\frac{\partial^3 x}{\partial s^3}|_{i-\frac{1}{2}} + \frac{l^5}{5!2^4}\frac{\partial^5 x}{\partial s^5}|_{i-\frac{1}{2}} + O(l^7) \tag{5.13}$$

Similar expressions can be written for $y_{i+1} - y_i$, $y_i - y_{i-1}$, $z_{i+1} - z_i$ and $z_i - z_{i-1}$.

Let φ stand for any variable, we also have

$$\varphi_{i+\frac{1}{2}} - \varphi_{i-\frac{1}{2}} = l\frac{\partial \varphi}{\partial s}|_i + \frac{l^3}{3!2^2}\frac{\partial^3 \varphi}{\partial s^3}|_i + \frac{l^5}{5!2^4}\frac{\partial^5 \varphi}{\partial s^5}|_i + O(l^7) \tag{5.14}$$

Employing these relations, and taking the limit as $l \to 0$ after having divided both sides of Eqs. (5.9), (5.10) and (5.11) by l, we arrive at

$$\begin{aligned}
\mu\frac{\partial^2 x}{\partial t^2} &= \frac{\partial}{\partial s}(\frac{T}{1+\varepsilon}\frac{\partial x}{\partial s}) + \bar{F}_x \\
\mu\frac{\partial^2 y}{\partial t^2} &= \frac{\partial}{\partial s}(\frac{T}{1+\varepsilon}\frac{\partial y}{\partial s}) + \bar{F}_y \\
\mu\frac{\partial^2 z}{\partial t^2} &= \frac{\partial}{\partial s}(\frac{T}{1+\varepsilon}\frac{\partial z}{\partial s}) + \bar{F}_z
\end{aligned}$$

where $\mu = \frac{m}{l}$ as $l \to 0$, is the density distribution of the cable.

These equations are exactly the governing equations for cable dynamics when the cable is treated as a continuous system (Appendix).

5.3.2 Effects of the Discretisation

We have proved that in the limit the ordinary differential equations pass over into the continuous partial differential governing equations for the motion of a

cable. However, in implementing the lump-mass-and-spring method. the spacings between the masses must be always of finite lengths. The influence of discretisation is still to be examined.

Substituting Eqs. (5.12), (5.13) and (5.14) into (5.9), (5.10) and (5.11), and neglecting terms of order greater than $O(l^2)$, we have

$$\begin{aligned}\frac{m}{l}\frac{\partial^2 x}{\partial t^2} = \frac{\partial}{\partial s}\left(\frac{T}{1+\varepsilon}\frac{\partial x}{\partial s}\right) &+ \frac{l^2}{24}\frac{\partial}{\partial s}\left(\frac{T}{1+\varepsilon}\frac{\partial^3 x}{\partial s^3}\right) \\ &+ \frac{l^2}{24}\frac{\partial^3}{\partial s^3}\left(\frac{T}{1+\varepsilon}\frac{\partial x}{\partial s}\right) + \bar{F}_x\end{aligned}$$

$$\begin{aligned}\frac{m}{l}\frac{\partial^2 y}{\partial t^2} = \frac{\partial}{\partial s}\left(\frac{T}{1+\varepsilon}\frac{\partial y}{\partial s}\right) &+ \frac{l^2}{24}\frac{\partial}{\partial s}\left(\frac{T}{1+\varepsilon}\frac{\partial^3 y}{\partial s^3}\right) \\ &+ \frac{l^2}{24}\frac{\partial^3}{\partial s^3}\left(\frac{T}{1+\varepsilon}\frac{\partial y}{\partial s}\right) + \bar{F}_y\end{aligned}$$

$$\begin{aligned}\frac{m}{l}\frac{\partial^2 z}{\partial t^2} = \frac{\partial}{\partial s}\left(\frac{T}{1+\varepsilon}\frac{\partial z}{\partial s}\right) &+ \frac{l^2}{24}\frac{\partial}{\partial s}\left(\frac{T}{1+\varepsilon}\frac{\partial^3 z}{\partial s^3}\right) \\ &+ \frac{l^2}{24}\frac{\partial^3}{\partial s^3}\left(\frac{T}{1+\varepsilon}\frac{\partial z}{\partial s}\right) + \bar{F}_z\end{aligned}$$

The terms proportional to l^2 in the above equation can be regarded as the primary influences on the cable dynamics due to the discrete modelling. To show their effects, we drop out $\bar{F}_x$, $\bar{F}_y$ and $\bar{F}_z$ (the marine cable is moved into air), and assume

$$\begin{aligned}\varepsilon &\ll 1 \\ \frac{\partial T}{\partial s} &= 0\end{aligned}$$

This yields the following equations

$$\frac{m}{lT}\frac{\partial^2 x}{\partial t^2} = \frac{\partial^2 x}{\partial s^2} + \frac{l^2}{12}\frac{\partial^4 x}{\partial s^4}$$

$$\begin{aligned} \frac{m}{lT}\frac{\partial^2 y}{\partial t^2} &= \frac{\partial^2 y}{\partial s^2} + \frac{l^2}{12}\frac{\partial^4 y}{\partial s^4} \\ \frac{m}{lT}\frac{\partial^2 z}{\partial t^2} &= \frac{\partial^2 z}{\partial s^2} + \frac{l^2}{12}\frac{\partial^4 z}{\partial s^4} \end{aligned} \tag{5.15}$$

These are not the ideal wave equations for waves along the cable as they would be if the cable were modelled as a continuum. Nevertheless, we know that waves still can be transmitted; indeed, it is not difficult to show that the following sinusoidal waves are solutions to Eq. (5.15):

$$x = x_0 exp[\sqrt{-1}(\omega t - ks)]$$

$$y = y_0 exp[\sqrt{-1}(\omega t - ks)]$$

$$z = z_0 exp[\sqrt{-1}(\omega t - ks)]$$

provided the following relation holds

$$\omega = \sqrt{\frac{lT}{m}} k \sqrt{1 - \frac{l^2}{12}k^2} \tag{5.16}$$

The wave velocity is then given by

$$c = \frac{\omega}{k} = \sqrt{\frac{lT}{m}} \sqrt{1 - \frac{l^2}{12}k^2} \tag{5.17}$$

Eqs. (5.16) and (5.17) indicate:

1. The dependence of wave velocity c on wave number k shows that the wave is no longer non-dispersive as would exist in a continuous medium.

2. If $kl \ll 1$, that is, if the discretisation is fine enough or the wave length $\frac{2\pi}{k}$ is long enough in comparison to l, we have

$$c = \sqrt{\frac{lT}{m}} \approx \sqrt{\frac{T}{\mu}}$$

In this case, the discretisation has little effect.

3. The maximum frequency defined by Eq. (5.16) is

$$\omega_{max} = \omega(k = \frac{\sqrt{6}}{l}) = \sqrt{\frac{3T}{lm}}$$

If the excitation frequency $\omega > \omega_{max}$, there is no real solution of k from Eq. (5.16); this suggests that k shall become complex.

Putting

$$k = k_r + \sqrt{-1}k_i$$

and substituting it into Eq. (5.16), we have

$$k_r = \frac{1}{l}\sqrt{\omega\sqrt{\frac{3ml}{T}} + 3}$$

$$k_i = \pm\frac{1}{l}\sqrt{\omega\sqrt{\frac{3ml}{T}} - 3}$$

If k_i adopts the minus sign, the displacements become

$$x = x_0 exp(-|k_i|s)exp[\sqrt{-1}(\omega t - k_r s)]$$

$$y = y_0 exp(-|k_i|s)exp[\sqrt{-1}(\omega t - k_r s)]$$

$$z = z_0 exp(-|k_i|s)exp[\sqrt{-1}(\omega t - k_r s)]$$

This result indicates that the lump-mass-and-spring system exhibits a high-frequency cut-off. Waves of frequencies higher than ω_{max} will decrease exponentially as they are travelling along the lump-mass-and-spring cable. The higher the frequency, the more quickly the wave dies out.

On the other hand, if k_i assumes the plus sign, the waves theoretically become explosive. However, the existence of damping will prevent them from diverging into infinity, resulting in stable oscillations.

The former case reflects a genuine physical phenomenon; the latter one is purely mathematic but nevertheless has an implication on numerical aspect. It indicates the possibility of existence of parasitical motions at high frequencies.

The above analysis on effects of the discretisation is based upon the two key assumptions, namely, $\varepsilon \ll 1$ and $\frac{\partial T}{\partial s} = 0$, which can be viewed as linearizations. Interesting nonlinear analysis can be obtained by inclusion of nonlinear terms. For example, by retaining the nonlinear terms we have in the place of Eq. (5.15) the following equations:

$$\begin{aligned}
\frac{m}{lT}\frac{\partial^2 x}{\partial t^2} - \frac{\partial^2 x}{\partial s^2} - \frac{l^2}{12}\frac{\partial^4 x}{\partial s^4} &= \frac{1}{T}[\frac{\partial T}{\partial s}\frac{\partial x}{\partial s} + \frac{l^2}{24}(\frac{\partial^3 T}{\partial s^3}\frac{\partial x}{\partial s} + 3\frac{\partial^2 T}{\partial s^2}\frac{\partial^2 x}{\partial s^2} + 4\frac{\partial T}{\partial s}\frac{\partial^3 x}{\partial s^3})] \\
\frac{m}{lT}\frac{\partial^2 y}{\partial t^2} - \frac{\partial^2 y}{\partial s^2} - \frac{l^2}{12}\frac{\partial^4 y}{\partial s^4} &= \frac{1}{T}[\frac{\partial T}{\partial s}\frac{\partial y}{\partial s} + \frac{l^2}{24}(\frac{\partial^3 T}{\partial s^3}\frac{\partial y}{\partial s} + 3\frac{\partial^2 T}{\partial s^2}\frac{\partial^2 y}{\partial s^2} + 4\frac{\partial T}{\partial s}\frac{\partial^3 y}{\partial s^3})] \\
\frac{m}{lT}\frac{\partial^2 z}{\partial t^2} - \frac{\partial^2 z}{\partial s^2} - \frac{l^2}{12}\frac{\partial^4 z}{\partial s^4} &= \frac{1}{T}[\frac{\partial T}{\partial s}\frac{\partial z}{\partial s} + \frac{l^2}{24}(\frac{\partial^3 T}{\partial s^3}\frac{\partial z}{\partial s} + 3\frac{\partial^2 T}{\partial s^2}\frac{\partial^2 z}{\partial s^2} + 4\frac{\partial T}{\partial s}\frac{\partial^3 z}{\partial s^3})]
\end{aligned}$$

The terms on the right side can be regarded as the contribution of nonlinear effects. As long as l is small , the first terms on the right side will be the dominant ones. This provides the ground to discard all the second terms on the right side. By substituting the following relation into the above equation

$$\frac{\partial T}{\partial s} = EA\frac{\partial \varepsilon}{\partial s} = EA\frac{\frac{\partial x}{\partial s}\frac{\partial^2 x}{\partial s^2} + \frac{\partial y}{\partial s}\frac{\partial^2 y}{\partial s^2} + \frac{\partial z}{\partial s}\frac{\partial^2 z}{\partial s^2}}{\sqrt{(\frac{\partial x}{\partial s})^2 + (\frac{\partial y}{\partial s})^2 + (\frac{\partial z}{\partial s})^2}}$$

we have

$$\frac{m}{lT}\frac{\partial^2 x}{\partial t^2} - \frac{\partial^2 x}{\partial s^2} - \frac{l^2}{12}\frac{\partial^4 x}{\partial s^4} = \frac{(\frac{\partial x}{\partial s})^2\frac{\partial^2 x}{\partial s^2} + \frac{\partial x}{\partial s}\frac{\partial y}{\partial s}\frac{\partial^2 y}{\partial s^2} + \frac{\partial x}{\partial s}\frac{\partial z}{\partial s}\frac{\partial^2 z}{\partial s^2}}{\varepsilon\sqrt{(\frac{\partial x}{\partial s})^2 + (\frac{\partial y}{\partial s})^2 + (\frac{\partial z}{\partial s})^2}} \tag{5.18}$$

Similar equations can be derived for the other two components.

Now consider a special case where $\frac{\partial^2 y}{\partial s^2} = \frac{\partial^2 z}{\partial s^2} = 0$ and $\frac{\partial y}{\partial s} \neq 0$, $\frac{\partial z}{\partial s} \neq 0$, Eq. (5.18) yields:

$$\frac{\partial^2 x}{\partial t^2} = \frac{Tl}{m}[\frac{\partial^2 x}{\partial s^2} + \frac{1}{\varepsilon}(\frac{\partial x}{\partial s})^2\frac{\partial^2 x}{\partial s^2} + \frac{l^2}{12}\frac{\partial^4 x}{\partial s^4}] \tag{5.19}$$

This equation is very similar to the celebrated Boussinesq equation. We assume that in a region of the space-time domain, the variational functions T and ε vary slightly and therefore can be treated as constants. By means of a change of variables and a scaling transformation

$$\begin{aligned} s' &= e(s - ct) \\ t' &= e^3 t \\ x' &= \frac{\partial x}{\partial s'} \\ c &= \sqrt{\frac{Tl}{m}} \end{aligned}$$

where $e \ll 1$, Eq. (5.19) is simplified to

$$2\sqrt{\frac{m}{Tl}}\frac{\partial x'}{\partial t'} + \frac{1}{\varepsilon}x'^2\frac{\partial x'}{\partial s'} + \frac{l^2}{12}\frac{\partial^3 x'}{\partial s'^3} = 0 \tag{5.20}$$

This is the Modified Korteweg-de Vries equation (MKdV). The relation between the KdV equation and the MKdV equation can be found in Miura (1968).

The KdV equation was first derived in 1895 in connection with long water waves in shallow channels. Eq. (5.19) suggests that the transverse wave can travel along the lumped mass cable in the same way as the solitary wave in shallow water, first recorded in 1834 by the Scottish scientist and engineer John Scott Russell six miles from the centre of Edingburgh (Russell, 1840; Whitham, 1974; Dodd et al, 1982; Taniuti and Nishihara, 1983).

5.4 FINITE-DIFFERENCE SOLUTION IN TIME DOMAIN

The basic idea is to divide the continuous time into a set of discrete steps $t = j \triangle t (j = 0, 1, 2, ...)$. Assuming everything is known before and at a time step $t = j \triangle t$, the question is how to find out the unknowns at the next time step $t = (j+1) \triangle t$ via the governing equations complemented by the boundary conditions.

By invoking the following finite-difference equivalents:

$$
\begin{aligned}
\ddot{x}_i^j &= \frac{1}{\triangle t^2}(x_i^{j+1} + x_i^{j-1} - 2x_i^j) \\
\ddot{y}_i^j &= \frac{1}{\triangle t^2}(y_i^{j+1} + y_i^{j-1} - 2y_i^j) \\
\ddot{z}_i^j &= \frac{1}{\triangle t^2}(z_i^{j+1} + z_i^{j-1} - 2z_i^j) \\
\dot{x}_i^j &= \frac{1}{\triangle t}(x_i^j - x_i^{j-1}) \\
\dot{y}_i^j &= \frac{1}{\triangle t}(y_i^j - y_i^{j-1}) \\
\dot{z}_i^j &= \frac{1}{\triangle t}(z_i^j - z_i^{j-1})
\end{aligned}
$$

and linearizing Eqs. (5.3) and (5.4) as

$$
\begin{aligned}
(\frac{T^{j+1}_{i+\frac{1}{2}}}{\sigma_{i+\frac{1}{2}}E}+1)l^2_{i+\frac{1}{2}}(\frac{T^{j}_{i+\frac{1}{2}}}{\sigma_{i+\frac{1}{2}}E}+1) &= (x_{i+1}-x_i)^{j+1}(x_{i+1}-x_i)^j + \\
&\quad (y_{i+1}-y_i)^{j+1}(y_{i+1}-y_i)^j + \\
&\quad (z_{i+1}-z_i)^{j+1}(z_{i+1}-z_i)^j \\
(\frac{T^{j+1}_{i-\frac{1}{2}}}{\sigma_{i-\frac{1}{2}}E}+1)l^2_{i+\frac{1}{2}}(\frac{T^{j}_{i-\frac{1}{2}}}{\sigma_{i-\frac{1}{2}}E}+1) &= (x_i-x_{i-1})^{j+1}(x_i-x_{i-1})^j + \\
&\quad (y_i-y_{i-1})^{j+1}(y_i-y_{i-1})^j + \\
&\quad (z_i-z_{i-1})^{j+1}(z_i-z_{i-1})^j
\end{aligned}
$$

we can now approximate the governing equation (5.2) at the time step $t = j \triangle t$ by the following finite difference equation:

$$
\frac{1}{\triangle t^2}\mathbf{A}\begin{bmatrix} x_i \\ y_i \\ z_i \end{bmatrix}^{j+1} + \mathbf{BC}\begin{bmatrix} x_{i-1} \\ y_{i-1} \\ z_{i-1} \\ x_i \\ y_i \\ z_i \\ x_{i+1} \\ y_{i+1} \\ z_{i+1} \end{bmatrix}^{j+1} = \begin{bmatrix} f_{ix} \\ f_{iy} \\ f_{iz} \end{bmatrix}^{j} - \frac{\mathbf{A}}{\triangle t^2}\begin{bmatrix} x_i \\ y_i \\ z_i \end{bmatrix}^{j-1} +
$$

$$\frac{\mathbf{2}}{\triangle t^2}\mathbf{A}\left[\begin{array}{c} x_i \\ y_i \\ z_i \end{array}\right]^j + \mathbf{B}\left[\begin{array}{c} \sigma_{i-\frac{1}{2}}E \\ \sigma_{i+\frac{1}{2}}E \end{array}\right] \quad (5.21)$$

where

$$\begin{aligned} \mathbf{A} &= |A_{mn}|^j_{3\times 3} \\ \mathbf{B} &= |B_{mn}|^j_{3\times 2} \\ \mathbf{C} &= |C_{mn}|^j_{2\times 9} \end{aligned}$$

with

$$\begin{aligned} B_{11} &= sin\theta_{i-\frac{1}{2}}cos\phi_{i-\frac{1}{2}} \\ B_{21} &= cos\theta_{i-\frac{1}{2}}cos\phi_{i-\frac{1}{2}} \\ B_{31} &= sin\phi_{i-\frac{1}{2}} \\ B_{12} &= -sin\theta_{i+\frac{1}{2}}cos\phi_{i+\frac{1}{2}} \\ B_{22} &= -cos\theta_{i+\frac{1}{2}}cos\phi_{i+\frac{1}{2}} \\ B_{32} &= -sin\phi_{i+\frac{1}{2}} \end{aligned}$$

and

$$
\begin{aligned}
C_{11} &= -\sigma_{i-\frac{1}{2}} E(x_i - x_{i-1})/q_1; & C_{21} &= 0 \\
C_{12} &= -\sigma_{i-\frac{1}{2}} E(y_i - y_{i-1})/q_1; & C_{22} &= 0 \\
C_{13} &= -\sigma_{i-\frac{1}{2}} E(z_i - z_{i-1})/q_1; & C_{23} &= 0 \\
C_{14} &= -C_{11}; & C_{24} &= -\sigma_{i+\frac{1}{2}} E(x_{i+1} - x_i)/q_2 \\
C_{15} &= -C_{12}; & C_{25} &= -\sigma_{i+\frac{1}{2}} E(y_{i+1} - y_i)/q_2 \\
C_{16} &= -C_{13}; & C_{26} &= -\sigma_{i+\frac{1}{2}} E(z_{i+1} - z_i)/q_2 \\
C_{17} &= 0; & C_{27} &= -C_{24} \\
C_{18} &= 0; & C_{28} &= -C_{25} \\
C_{19} &= 0; & C_{29} &= -C_{26}
\end{aligned}
$$

$$
q_1 = l_{i-\frac{1}{2}}^2 \left(\frac{T_{i-\frac{1}{2}}}{\sigma_{i-\frac{1}{2}} E} + 1\right)
$$

$$
q_2 = l_{i+\frac{1}{2}}^2 \left(\frac{T_{i+\frac{1}{2}}}{\sigma_{i+\frac{1}{2}} E} + 1\right)
$$

and

$$
\begin{aligned}
f_{ix} &= \frac{1}{2}(F_{Dx}^{i+\frac{1}{2}} + F_{Dx}^{i-\frac{1}{2}}) \\
f_{iy} &= \frac{1}{2}(F_{Dy}^{i+\frac{1}{2}} + F_{Dy}^{i-\frac{1}{2}}) \\
f_{iz} &= \frac{1}{2}(F_{Dz}^{i+\frac{1}{2}} + F_{Dz}^{i-\frac{1}{2}}) + \frac{1}{2}\rho g(l_{i+\frac{1}{2}}\sigma_{i+\frac{1}{2}} + l_{i-\frac{1}{2}}\sigma_{i-\frac{1}{2}}) - m_i g
\end{aligned}
$$

The boundary condition Eq. (5.6) can be approximated in a similar manner. As a result, there are $3 \times N$ algebraic equations for the $3 \times N$ unknowns, namely x_i^{j+1}, y_i^{j+1} and $z_i^{j+1} (i = 1, 2, ..., N)$. The tension is calculated through Eq. (5.3) or Eq. (5.4) once the solution of the $3 \times N$ unknowns is obtained.

5.5 STABILITY OF THE NUMERICAL SCHEME

The presence of round-off errors or any other computational errors may lead to numerical instability. In this section the stability of the finite difference equation Eq. (5.21) is investigated.

A useful method of finding a stability criterion is to examine the propagating effect of a small disturbance (Lax and Richtmyer, 1956; Ames, 1969). The criterion for stability is the condition which guarantees that this small disturbance will not become unbounded with successive time steps. Here to simplify the investigation of the stability, all the terms involving virtual inertia and drag are omitted.

We introduce the following disturbances to the variables x, y and z at different positions and on different time steps:

$$\begin{aligned}
\tilde{x}_{i-1}^{j+1} &= x_{i-1}^{j+1} + \delta x_{i-1}^{j+1} \\
\tilde{y}_{i-1}^{j+1} &= y_{i-1}^{j+1} + \delta y_{i-1}^{j+1} \\
\tilde{z}_{i-1}^{j+1} &= z_{i-1}^{j+1} + \delta z_{i-1}^{j+1} \\
\tilde{x}_{i}^{j+1} &= x_{i}^{j+1} + \delta x_{i}^{j+1} \\
\tilde{y}_{i}^{j+1} &= y_{i}^{j+1} + \delta y_{i}^{j+1} \\
\tilde{z}_{i}^{j+1} &= z_{i}^{j+1} + \delta z_{i}^{j+1} \\
\tilde{x}_{i+1}^{j+1} &= x_{i+1}^{j+1} + \delta x_{i+1}^{j+1} \\
\tilde{y}_{i+1}^{j+1} &= y_{i+1}^{j+1} + \delta y_{i+1}^{j+1} \\
\tilde{z}_{i+1}^{j+1} &= z_{i+1}^{j+1} + \delta z_{i+1}^{j+1}
\end{aligned}$$

$$
\begin{aligned}
\tilde{x}_i^j &= x_i^j + \delta x_i^j \\
\tilde{y}_i^j &= y_i^j + \delta y_i^j \\
\tilde{z}_i^j &= z_i^j + \delta z_i^j \\
\tilde{x}_i^{j-1} &= x_i^{j-1} + \delta x_i^{j-1} \\
\tilde{y}_i^{j-1} &= y_i^{j-1} + \delta y_i^{j-1} \\
\tilde{z}_i^{j-1} &= z_i^{j-1} + \delta z_i^{j-1}
\end{aligned}
$$

Substituting in Eq. (5.21) we have

$$
\begin{aligned}
&\frac{1}{\triangle t^2}\mathbf{A}\begin{bmatrix} \tilde{x}_i \\ \tilde{y}_i \\ \tilde{z}_i \end{bmatrix}^{j+1} + (\mathbf{B}+\delta\mathbf{B})(\mathbf{C}+\delta\mathbf{C})\begin{bmatrix} \tilde{x}_{i-1} \\ \tilde{y}_{i-1} \\ \tilde{z}_{i-1} \\ \tilde{x}_i \\ \tilde{y}_i \\ \tilde{z}_i \\ \tilde{x}_{i+1} \\ \tilde{y}_{i+1} \\ \tilde{z}_{i+1} \end{bmatrix}^{j+1} = -\frac{\mathbf{A}}{\triangle t^2}\begin{bmatrix} \tilde{x}_i \\ \tilde{y}_i \\ \tilde{z}_i \end{bmatrix}^{j-1} \\
&\qquad + \frac{\mathbf{2}}{\triangle t^2}\mathbf{A}\begin{bmatrix} \tilde{x}_i \\ \tilde{y}_i \\ \tilde{z}_i \end{bmatrix}^{j} + (\mathbf{B}+\delta\mathbf{B})\begin{bmatrix} \sigma_{i-\frac{1}{2}}E \\ \sigma_{i+\frac{1}{2}}E \end{bmatrix} \qquad (5.22)
\end{aligned}
$$

Subtracting Eq. (5.21) from the above one and linearizing the resulting equation to the first order, we have the governing equation for the propagation of the

small disturbance:

$$\frac{1}{\triangle t^2}\mathbf{A}\begin{bmatrix}\delta x_i\\ \delta y_i\\ \delta z_i\end{bmatrix}^{j+1} + \mathbf{BC}\begin{bmatrix}\delta x_{i-1}\\ \delta y_{i-1}\\ \delta z_{i-1}\\ \delta x_i\\ \delta y_i\\ \delta z_i\\ \delta x_{i+1}\\ \delta y_{i+1}\\ \delta z_{i+1}\end{bmatrix}^{j+1} + (\mathbf{B}\delta\mathbf{C}+\mathbf{C}\delta\mathbf{B})\begin{bmatrix}x_{i-1}\\ y_{i-1}\\ z_{i-1}\\ x_i\\ y_i\\ z_i\\ x_{i+1}\\ y_{i+1}\\ z_{i+1}\end{bmatrix}^{j+1} =$$

$$-\frac{\mathbf{A}}{\triangle t^2}\begin{bmatrix}\delta x_i\\ \delta y_i\\ \delta z_i\end{bmatrix}^{j-1} + \frac{\mathbf{2}}{\triangle t^2}\mathbf{A}\begin{bmatrix}\delta x_i\\ \delta y_i\\ \delta z_i\end{bmatrix}^{j} + \delta\mathbf{B}\begin{bmatrix}\sigma_{i-\frac{1}{2}}E\\ \sigma_{i+\frac{1}{2}}E\end{bmatrix} \tag{5.23}$$

A solution of the above equations can be obtained in the form:

$$\begin{aligned}\delta x_i^j &= \Gamma_x^j e^{\sqrt{-1}i\beta}\\ \delta y_i^j &= \Gamma_y^j e^{\sqrt{-1}i\beta}\\ \delta z_i^j &= \Gamma_z^j e^{\sqrt{-1}i\beta}\end{aligned} \tag{5.24}$$

Assuming

$$\begin{bmatrix}\Gamma_x^{j+1}\\ \Gamma_y^{j+1}\\ \Gamma_z^{j+1}\end{bmatrix} = \lambda\begin{bmatrix}\Gamma_x^{j}\\ \Gamma_y^{j}\\ \Gamma_z^{j}\end{bmatrix} = \lambda^2\begin{bmatrix}\Gamma_x^{j-1}\\ \Gamma_y^{j-1}\\ \Gamma_z^{j-1}\end{bmatrix} \tag{5.25}$$

and substituting Eqs. (5.24) and (5.25) into Eq. (5.23), we have a system of linear homogeneous equations for Γ_x^{j-1}, Γ_y^{j-1} and Γ_z^{j-1}. For non-trivial solution, the determinant of the coefficients must be identically zero, which gives the characteristic equation for the amplification factor λ.

To facilitate the following analysis, we assume:

$$x_i - x_{i-1} \ll z_i - z_{i-1}$$

$$x_{i+1} - x_i \ll z_{i+1} - z_i$$

$$y_i - y_{i-1} \ll z_i - z_{i-1}$$

$$y_{i+1} - y_i \ll z_{i+1} - z_i$$

Also we assume that within a small region of the space-time domain, variational functions vary slightly, hence they can be denoted by

$$T_{i+\frac{1}{2}} = T_{i-\frac{1}{2}} = T$$

$$\sigma_{i+\frac{1}{2}} = \sigma_{i-\frac{1}{2}} = \sigma$$

$$l_{i+\frac{1}{2}} = l_{i-\frac{1}{2}} = l$$

$$m_{i+\frac{1}{2}} = m_{i-\frac{1}{2}} = m$$

Under these assumptions, $\delta\mathbf{B} = \delta\mathbf{C} = \mathbf{0}$, the characteristic equation can be written as

$$|(\mathbf{A} + \mathbf{BCD}\,\triangle t^2)\lambda^2 - 2\mathbf{A}\lambda + \mathbf{A}| = 0 \tag{5.26}$$

where

$$\mathbf{A} = \begin{bmatrix} m & 0 & 0 \\ 0 & m & 0 \\ 0 & 0 & m \end{bmatrix} \quad \mathbf{B} = \begin{bmatrix} 0 & 0 \\ 0 & 0 \\ 1 & -1 \end{bmatrix}$$

$$\mathbf{C} = \begin{bmatrix} 0 & 0 & -\frac{\sigma E}{l} & 0 & 0 & \frac{\sigma E}{l} & 0 & 0 & 0 \\ 0 & 0 & 0 & 0 & 0 & -\frac{\sigma E}{l} & 0 & 0 & \frac{\sigma E}{l} \end{bmatrix}$$

$$\mathbf{D} = \begin{bmatrix} exp(-\sqrt{-1}\beta) & 0 & 0 \\ 0 & exp(-\sqrt{-1}\beta) & 0 \\ 0 & 0 & exp(-\sqrt{-1}\beta) \\ 1 & 0 & 0 \\ 0 & 1 & 0 \\ 0 & 0 & 1 \\ exp(\sqrt{-1}\beta) & 0 & 0 \\ 0 & exp(\sqrt{-1}\beta) & 0 \\ 0 & 0 & exp(\sqrt{-1}\beta) \end{bmatrix}$$

Multiplying the elements of the determinant, we obtain the following solutions to λ:

$$\lambda_1 = \lambda_2 = \lambda_3 = \lambda_4 = 1$$

$$\lambda_{5,6} = \frac{1 \pm \sqrt{-4sin^2\frac{\beta}{2}\frac{\sigma E}{lm} \triangle t^2}}{1 + 4sin^2\frac{\beta}{2}\frac{\sigma E}{lm} \triangle t^2}$$

It is not difficult to show that all $|\lambda_i| \leq 1$, for $i = 1, 2, ..., 6$. Consequently the finite difference approximation Eq. (5.21) is unconditionally stable.

Though, generally speaking, stability is not drastically changed by boundary conditions, they do have influences. A more rigid analysis should take the boundary conditions into account, as well as the drag and the inertia effects, in addition to discarding all the assumptions made here.

5.6 COMPUTATIONAL ASPECTS

5.6.1 Procedure

The computational procedure is illustrated by Figure 5.3. It is recommended to start from a static equilibrium position of the cable in order to avoid transient behaviour. For the same reason, care needs to be taken for the upper end boundary conditions to avoid any impulsive loading to the system.

5.6.2 Geometrical Discretisation

The number of massless segments should be sufficient in order to describe the position of the cable satisfactorily and to achieve numerical convergence. Also, it should be fine enough to let genuine high frequency waves pass through and to prevent the occurrence of parasitic motions.

5.7 NUMERICAL EXAMPLES

Numerical simulations have been carried out to demonstrate the validity of the method and to investigate the effect of various factors on the motions of a

subsea unit such as the excitation frequency and the underwater current strength.

The particulars of a factual system of cable and subsea unit used in the following numerical investigations are:

diameter:	$0.047m$
length:	$300m$
Young's modulus:	$9\times10^9 N/m^2$
mass distribution:	5.4 kg/m
C_N and C_τ	1.2 and 0.01
mass of subsea unit	3000 kg
$\mathrm{M}_{ax}, M_{ay}, M_{az}$	3000 kg
$\mathrm{C}_{Dx}, C_{Dy}, C_{Dz}$	1.5
S_x, S_y, S_z	0.5 square metres
V_0	0.354 cubic metres

5.7.1 Convergence

Figure 5.4 shows the numerical convergence as the number of massless segments increases. In this case, the top end of the cable is subjected to the following forced motions:

$$\bar{x}(t) = sin(0.314t)$$

$$\bar{y}(t) = sin(0.314t)$$

$$\bar{z}(t) = sin(0.314t)$$

The calculation starts from a stationary unstrained cable configuration which lies on the z-axis. It can be seen that 20 segments are more than adequate to guarantee convergence.

An adequate number of the segments is not primarily dependent upon the length of cable under consideration. It is more dependent upon the transverse wave

length in the cable. In the following example, the same system of cable and subsea unit is subjected to excitations of higher frequency at its top end:

$$\bar{x}(t) = sin(1.256t)$$

$$\bar{y}(t) = sin(1.256t)$$

$$\bar{z}(t) = sin(1.256t)$$

The transverse wave length decreases. Consequently, at least 40 segments are needed to achieve the numerical convergence, as shown in Figure 5.5.

Other distinct features observed include:

1. As expected, the periods of the subsea unit motions are equal to the periods of the forced motions.

2. There is a transient vertical vibration due to the impulsive action of the gravitational force upon the system. This motion dies out quickly in a time of several periods.

3. Due to the viscous drag of the fluid medium, the transverse motion of the subsea unit is reduced in comparison with the transverse motion at the top end.

5.7.2 Effect of the Current

Figure 5.6 shows the results for the same system under the action of underwater current. In this case the top end excitations are:

$$\bar{x}(t) = sin(0.314t)$$

$$\bar{y}(t) = sin(0.314t)$$

$$\bar{z}(t) = sin(0.314t)$$

and a uniform current acts in the direction of the x-axis at a speed of 0.5m/s.

The effect of the current is clearly demonstrated here. It offsets the subsea unit away from its initial position to a new mean position, and attenuates the amplitude of transverse oscillation around this new mean position. Also the mean vertical position of the subsea unit has been raised slightly though the current has little effect on its vertical amplitude.

5.7.3 Effect of the Excitation Frequency

The conditions for Figure 5.7 are the same as the ones for the last example except that the forced vibration frequency has been increased to 0.628 rad/s. The transverse motion of the subsea unit has further attenuated though its mean position has hardly changed. This is as expected since the mean position is mainly determined by static parameters such as the strength of the time-invariant current and the gravitational forces. It is weakly related to dynamic parameters such as periods.

5.7.4 Loop Turn

The suite of programs is used to examine a loop turn manoeuvre. In still water the system starts moving from a static unstrained position with a towpoint speed of 4 m/s. The towpoint runs straight for 800 meters before tangentially turning through a circle of diameter 300 metres. After this 360 degree turn, it continues along

the straight line. The results are given in Figure 5.8.

Figure 5.9 shows the same loop turn manoeuvre except in this case the tow-point speed is 2 m/s. The effect of the speed is self evident.

Figure 5.10 shows the same system under the same manoeuvre in air (aerodynamic drag force is not considered). Unlike the previous cases where the drag force plays a significant role, the unit swings transversely once it enters into the circle. Also due to the lack of damping, the initial vibration, caused by the impulsive action of the gravitational force upon the system, persists.

5.8 CONCLUDING REMARKS

In this chapter, a mathematical analysis has been provided regarding various aspects of the lump-mass-and-spring method. The numerical approach results in a highly comprehensive and efficient method for analysing three-dimensional cable dynamics.

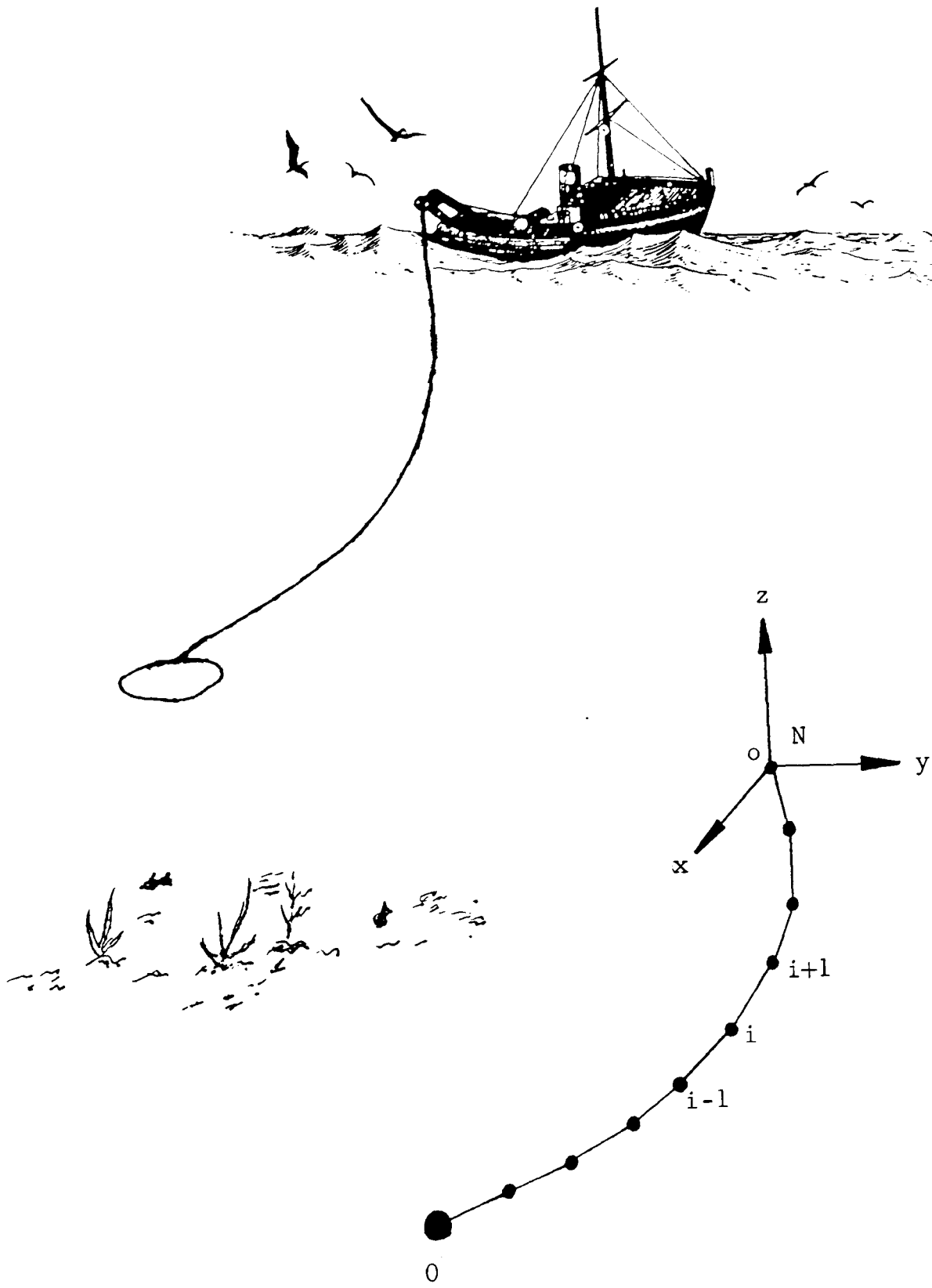

Figure 5.1

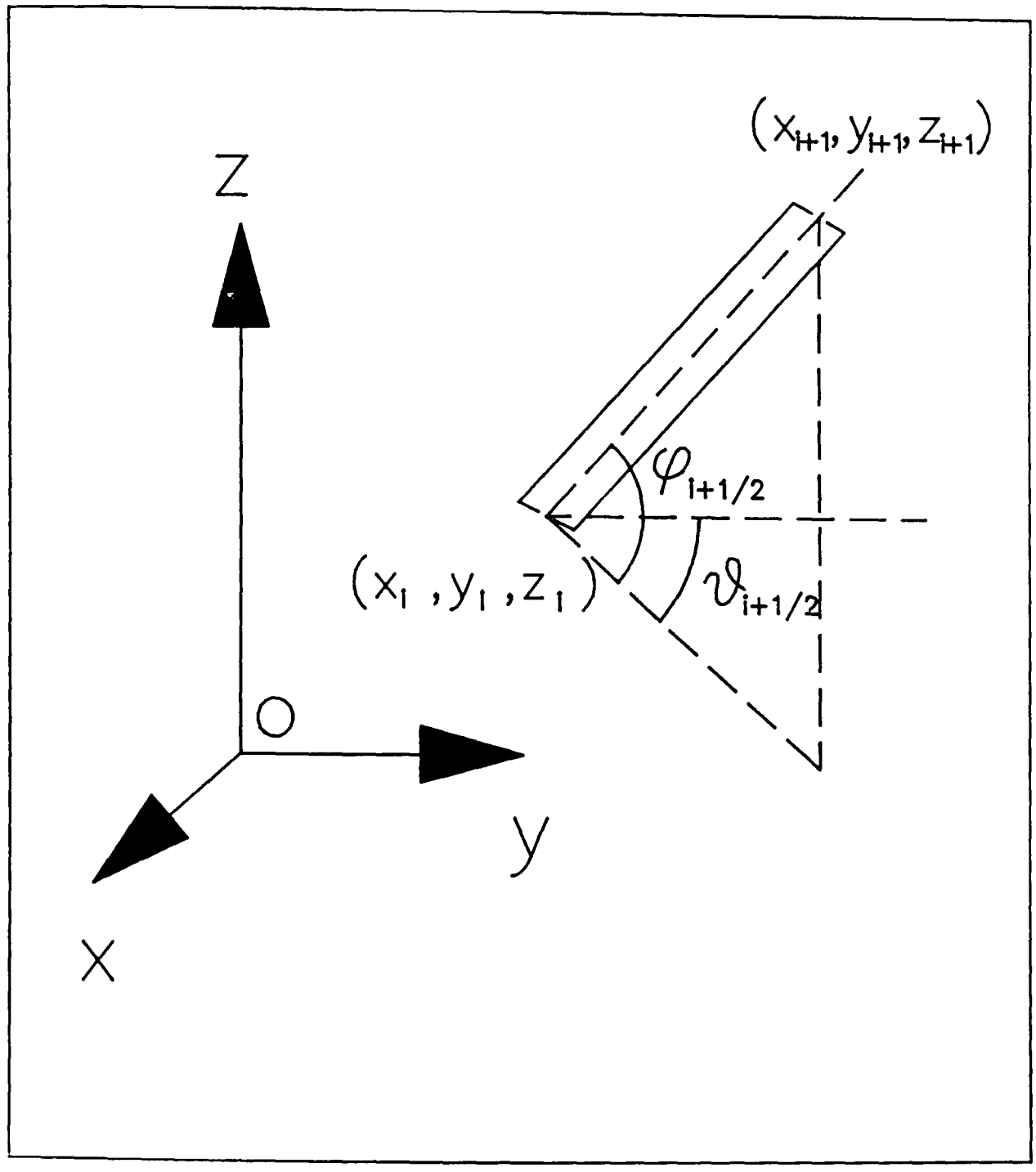

Figure 5.2

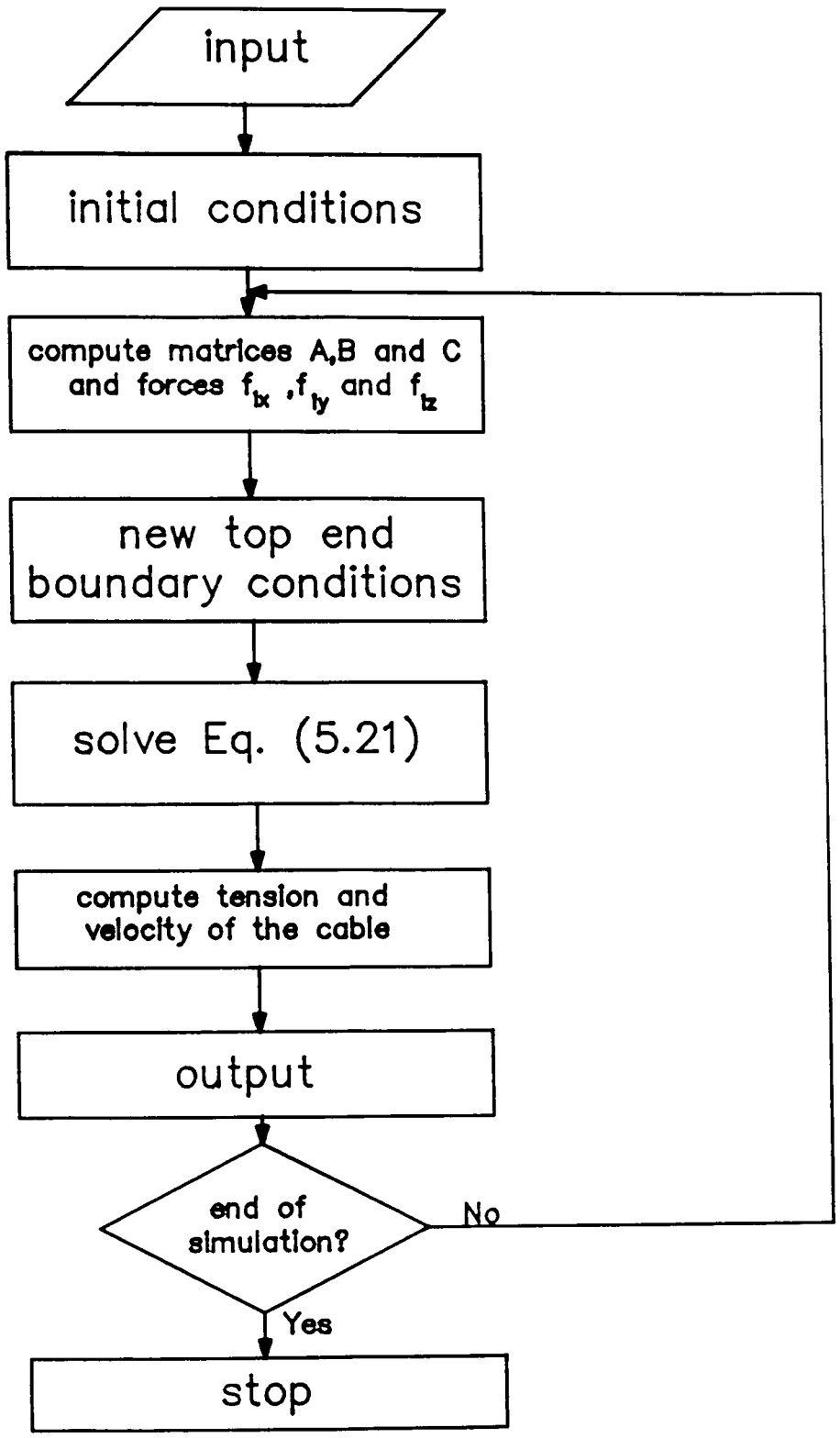
input
initial conditions
compute matrices A,B and C and forces f_{lx} ,f_{ly} and f_{lz}
new top end boundary conditions
solve Eq. (5.21)
compute tension and velocity of the cable
output
end of simulation?
No
Yes
stop

Figure 5.3

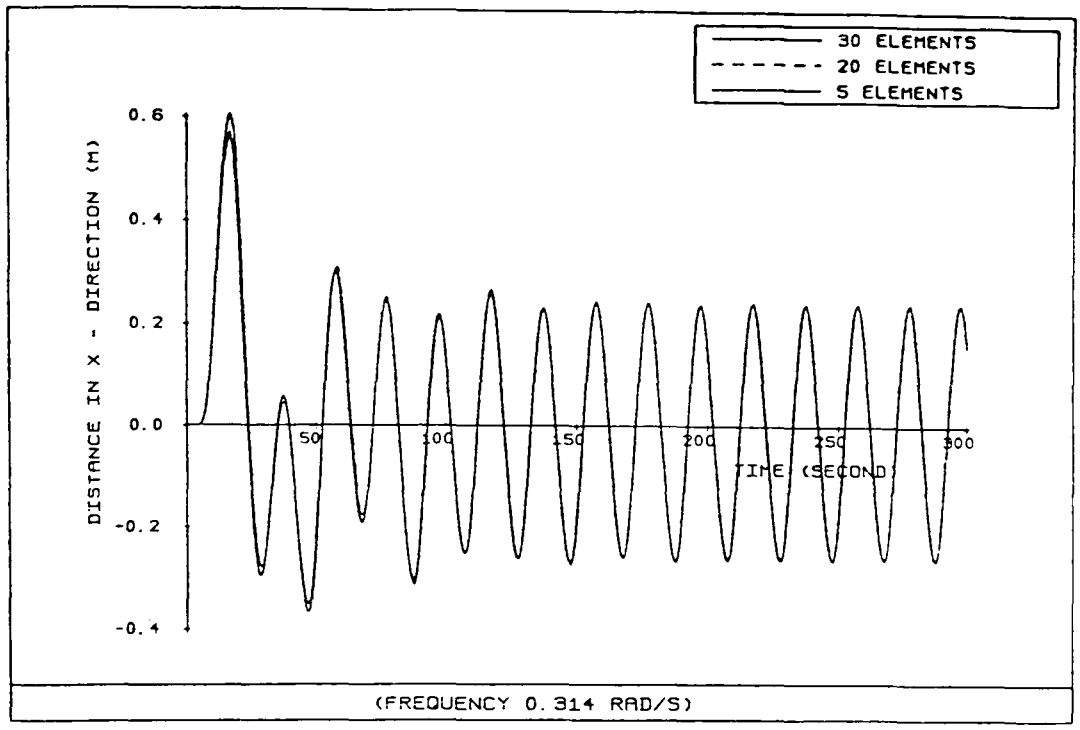
30 ELEMENTS
20 ELEMENTS
5 ELEMENTS
DISTANCE IN X - DIRECTION (M)
0.6
0.4
0.2
0.0
-0.2
-0.4
50
100
150
200
250
300
TIME (SECOND)
(FREQUENCY 0.314 RAD/S)

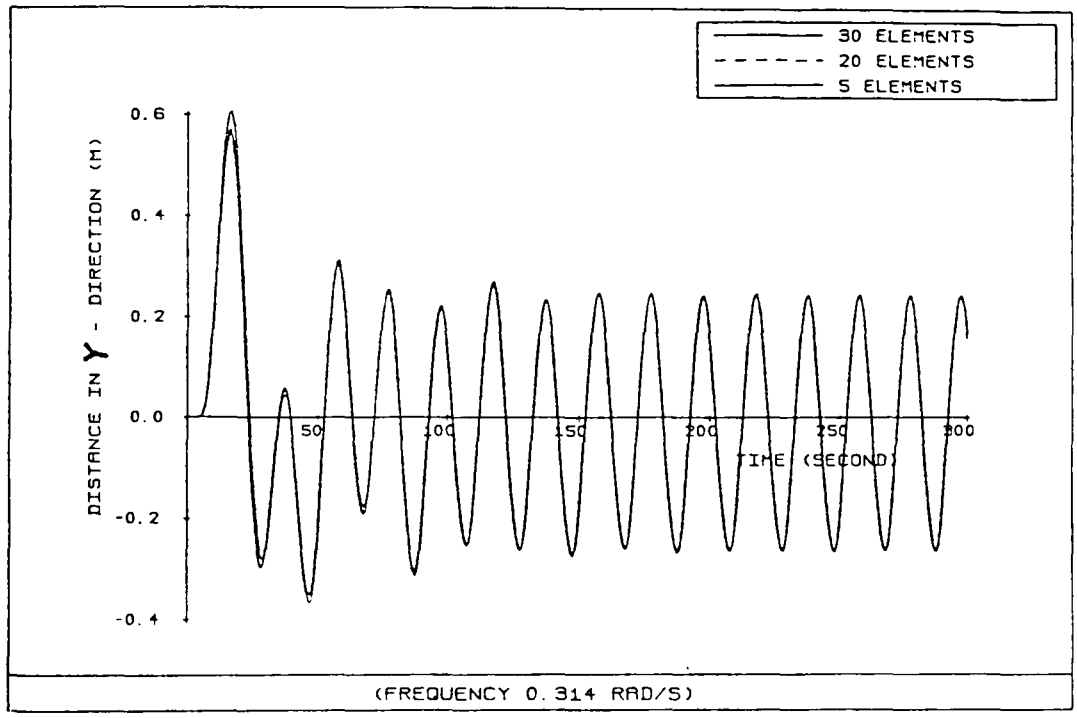
30 ELEMENTS
20 ELEMENTS
5 ELEMENTS
DISTANCE IN Y - DIRECTION (M)
0.6
0.4
0.2
0.0
-0.2
-0.4
50
100
150
200
250
300
TIME (SECOND)
(FREQUENCY 0.314 RAD/S)

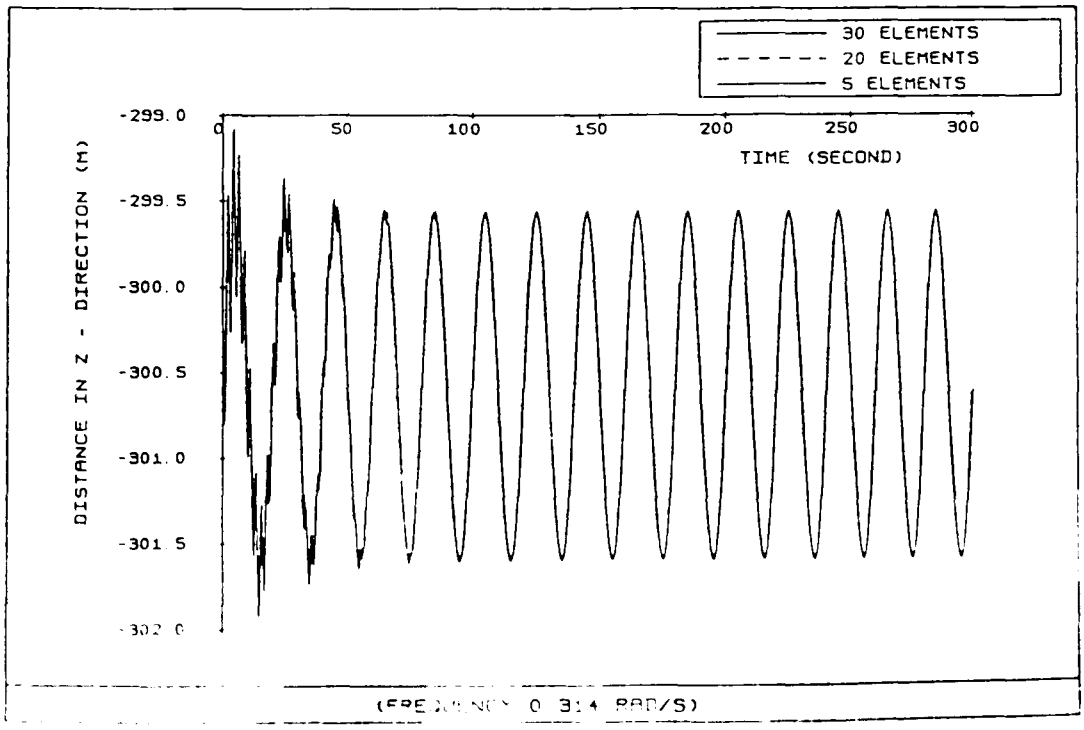
30 ELEMENTS
20 ELEMENTS
5 ELEMENTS
DISTANCE IN Z - DIRECTION (M)
-299.0
-299.5
-300.0
-300.5
-301.0
-301.5
-302.0
0
50
100
150
200
250
300
TIME (SECOND)
(FREQUENCY 0.314 RAD/S)

Figure 5.4

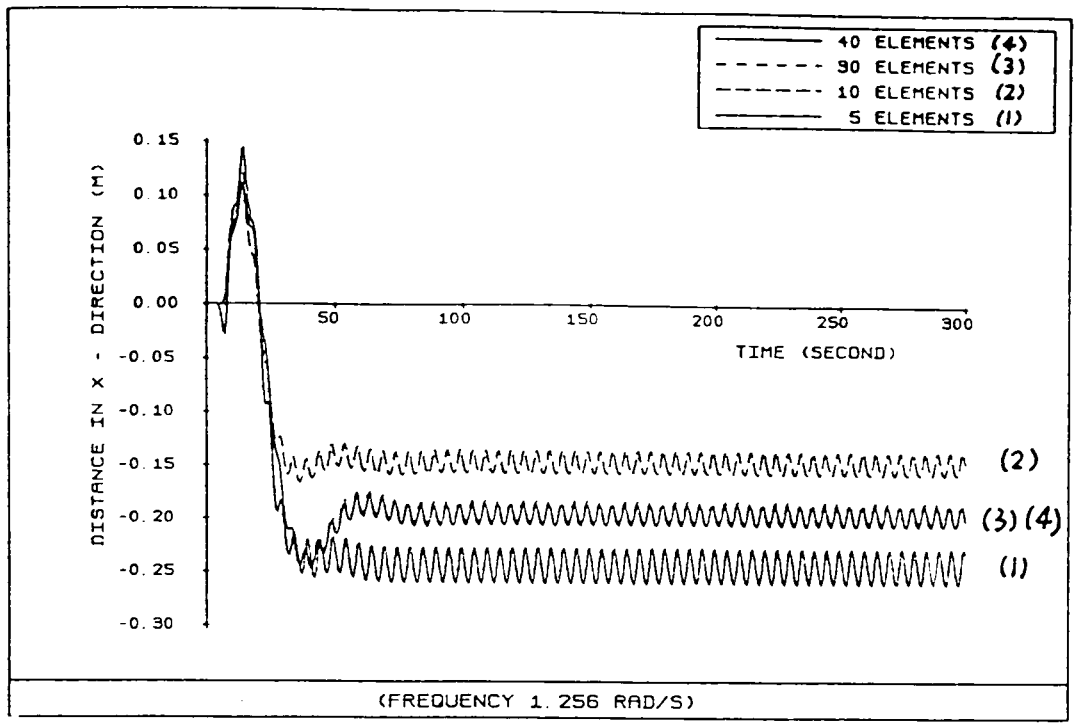
40 ELEMENTS (4)
30 ELEMENTS (3)
10 ELEMENTS (2)
5 ELEMENTS (1)
DISTANCE IN X - DIRECTION (M)
0.15
0.10
0.05
0.00
-0.05
-0.10
-0.15
-0.20
-0.25
-0.30
50
100
150
200
250
300
TIME (SECOND)
(2)
(3) (4)
(1)
(FREQUENCY 1.256 RAD/S)

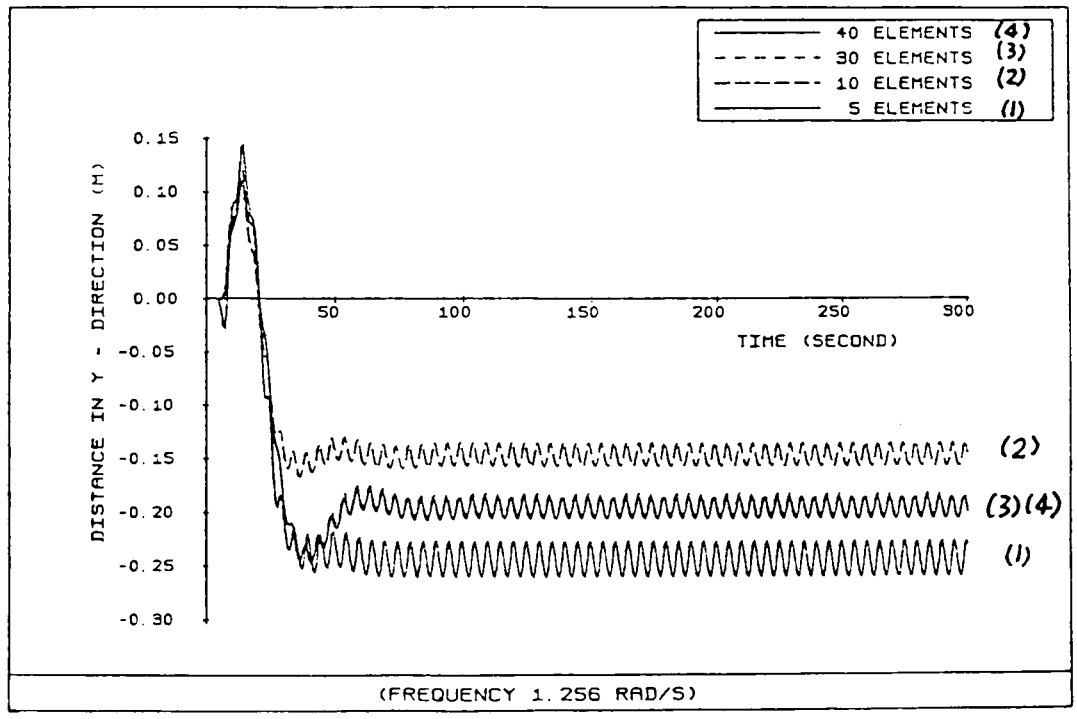
40 ELEMENTS (4)
30 ELEMENTS (3)
10 ELEMENTS (2)
5 ELEMENTS (1)
DISTANCE IN Y - DIRECTION (M)
0.15
0.10
0.05
0.00
-0.05
-0.10
-0.15
-0.20
-0.25
-0.30
50
100
150
200
250
300
TIME (SECOND)
(2)
(3)(4)
(1)
(FREQUENCY 1.256 RAD/S)

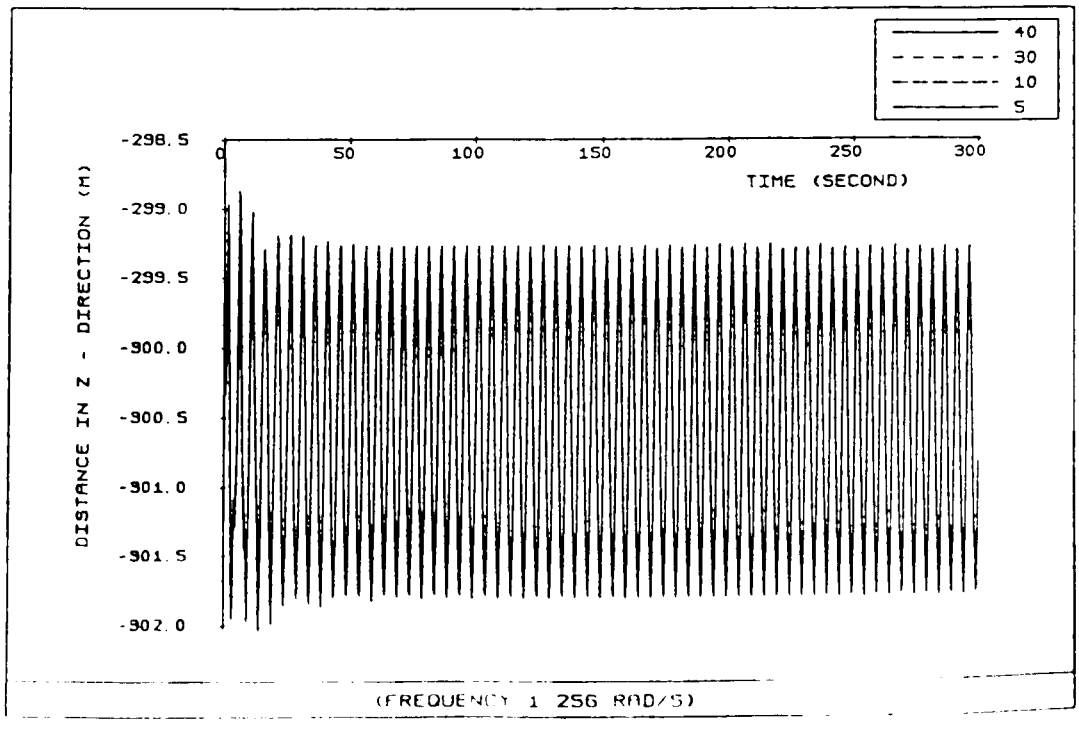
40
30
10
5
DISTANCE IN Z - DIRECTION (M)
-298.5
-299.0
-299.5
-300.0
-300.5
-301.0
-301.5
-302.0
0
50
100
150
200
250
300
TIME (SECOND)
(FREQUENCY 1.256 RAD/S)

Figure 5.

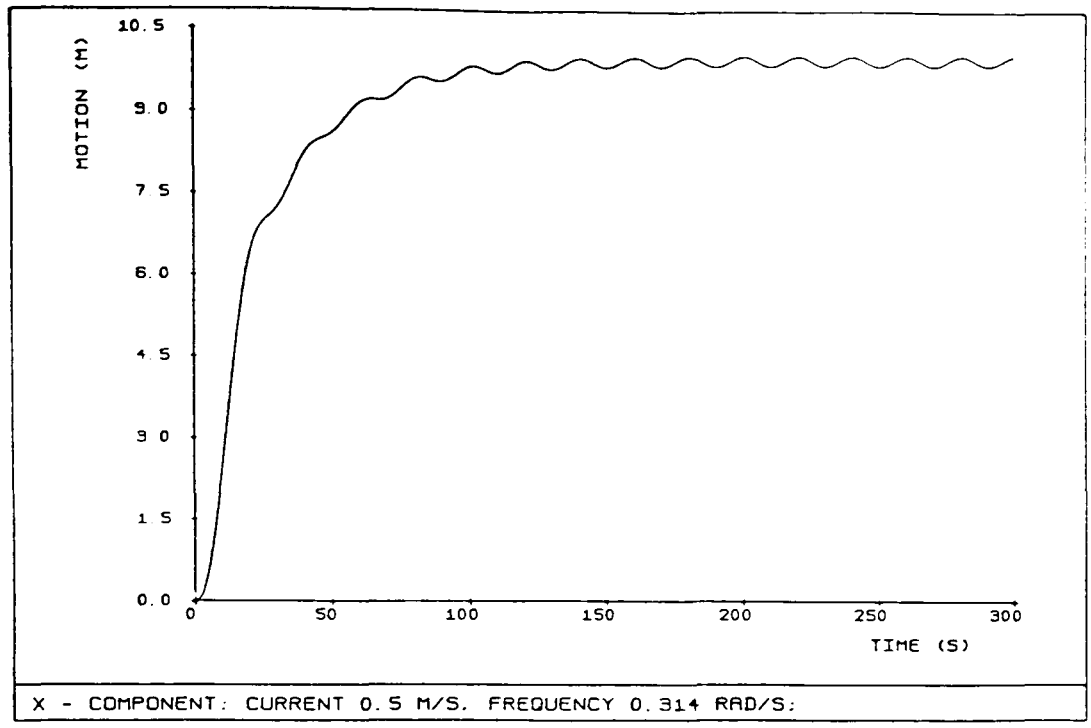

X - COMPONENT: CURRENT 0.5 M/S. FREQUENCY 0.314 RAD/S:

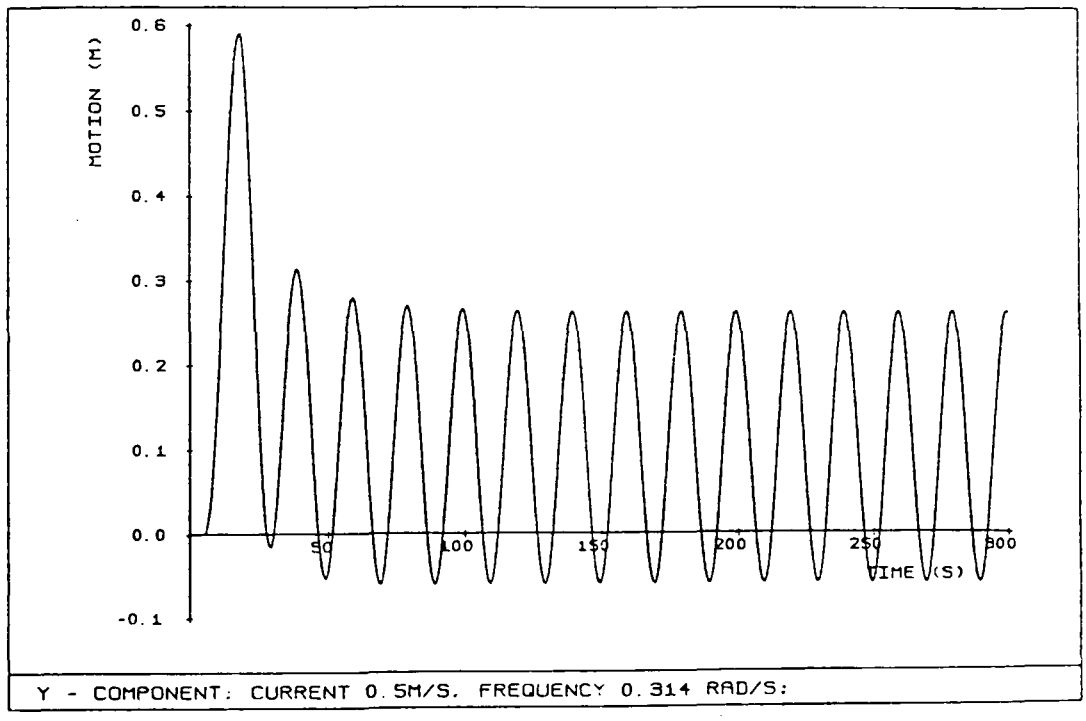

Y - COMPONENT: CURRENT 0.5M/S. FREQUENCY 0.314 RAD/S:

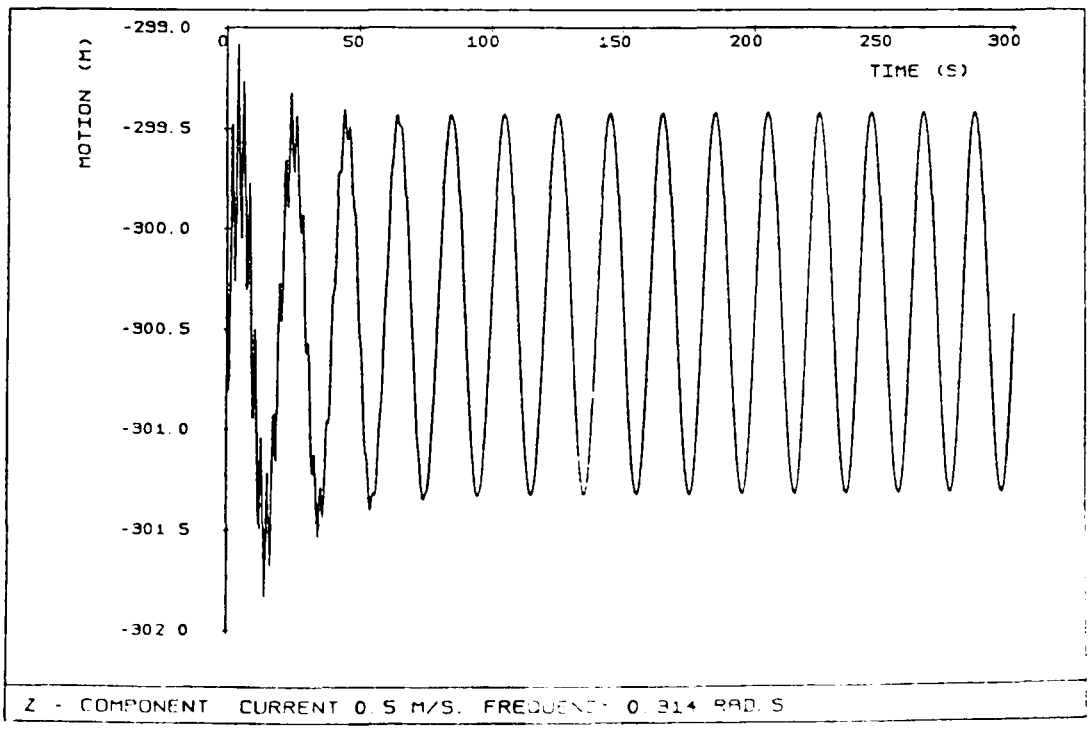

Z - COMPONENT CURRENT 0.5 M/S. FREQUENCY 0.314 RAD/S

Figure 5.6

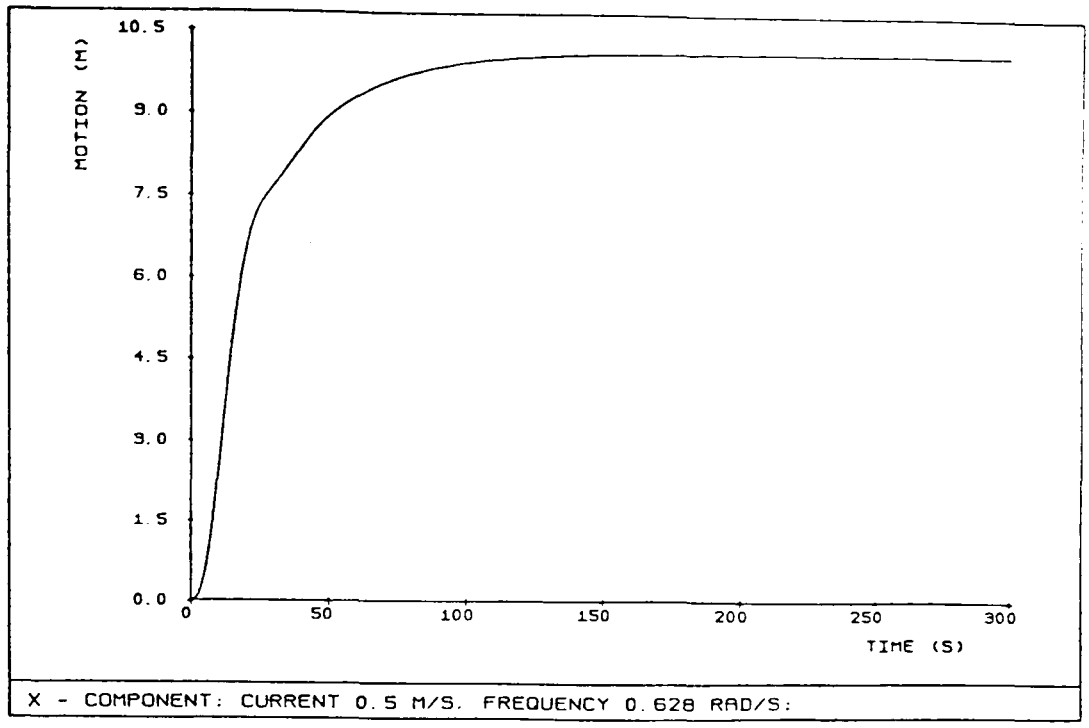
MOTION (M)
10.5
9.0
7.5
6.0
4.5
3.0
1.5
0.0
0
50
100
150
200
250
300
TIME (S)
X - COMPONENT: CURRENT 0.5 M/S. FREQUENCY 0.628 RAD/S:

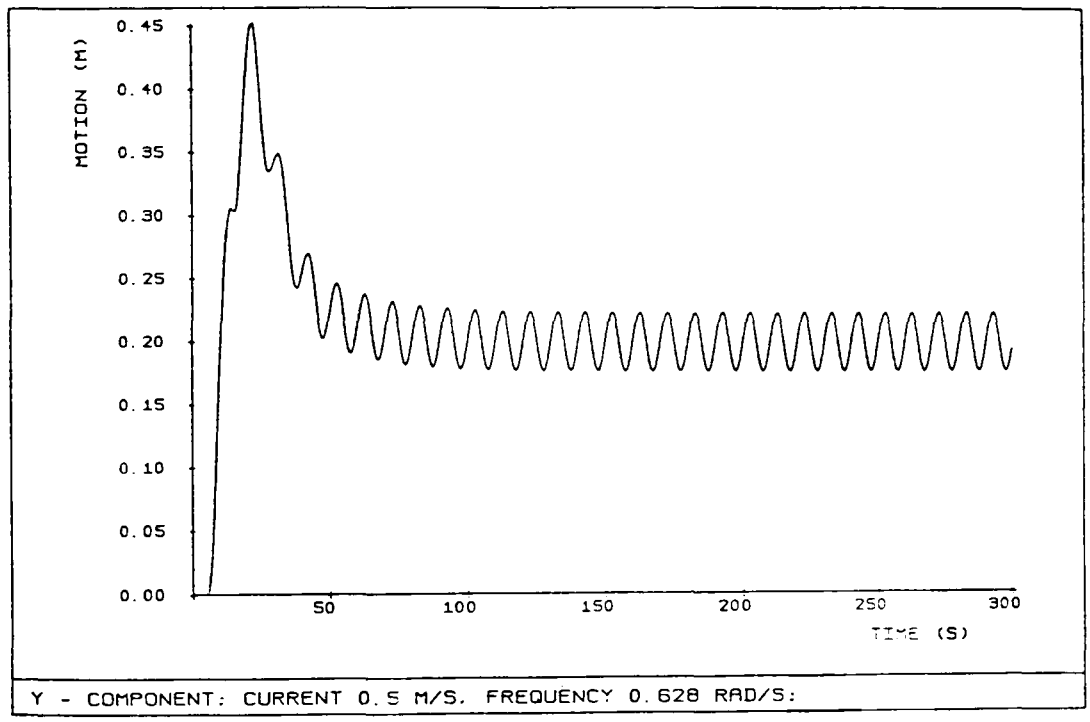
MOTION (M)
0.45
0.40
0.35
0.30
0.25
0.20
0.15
0.10
0.05
0.00
50
100
150
200
250
300
TIME (S)
Y - COMPONENT: CURRENT 0.5 M/S. FREQUENCY 0.628 RAD/S:

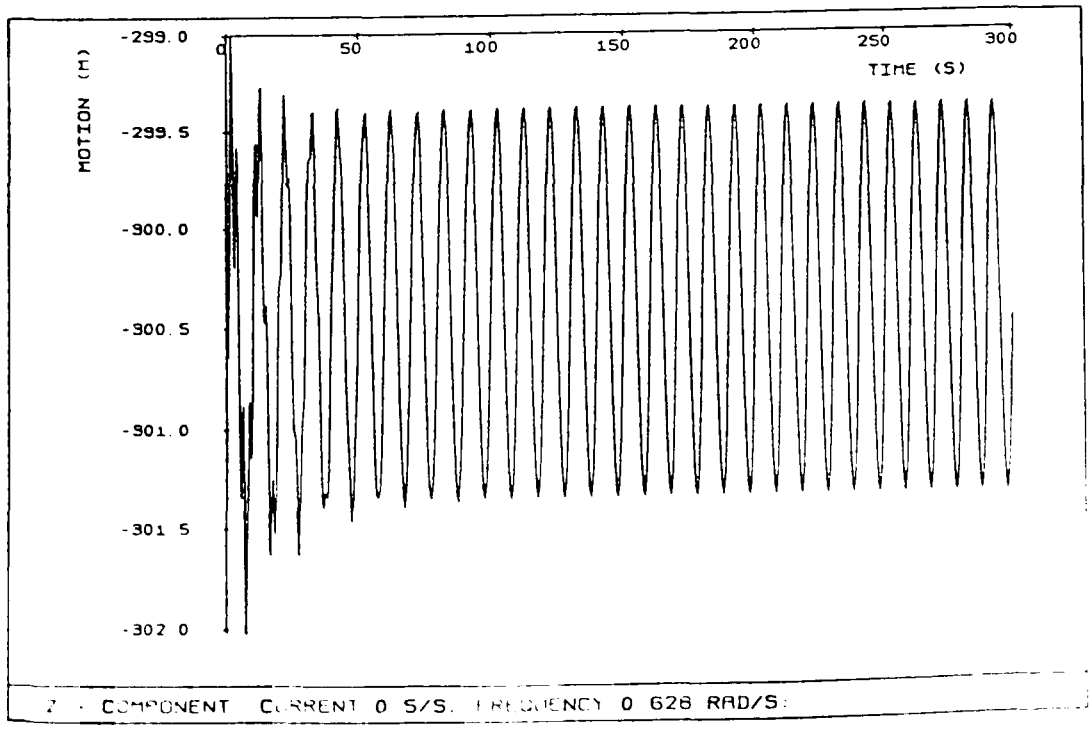
MOTION (M)
-299.0
-299.5
-900.0
-900.5
-901.0
-301.5
-302.0
0
50
100
150
200
250
300
TIME (S)

Figure 5.7

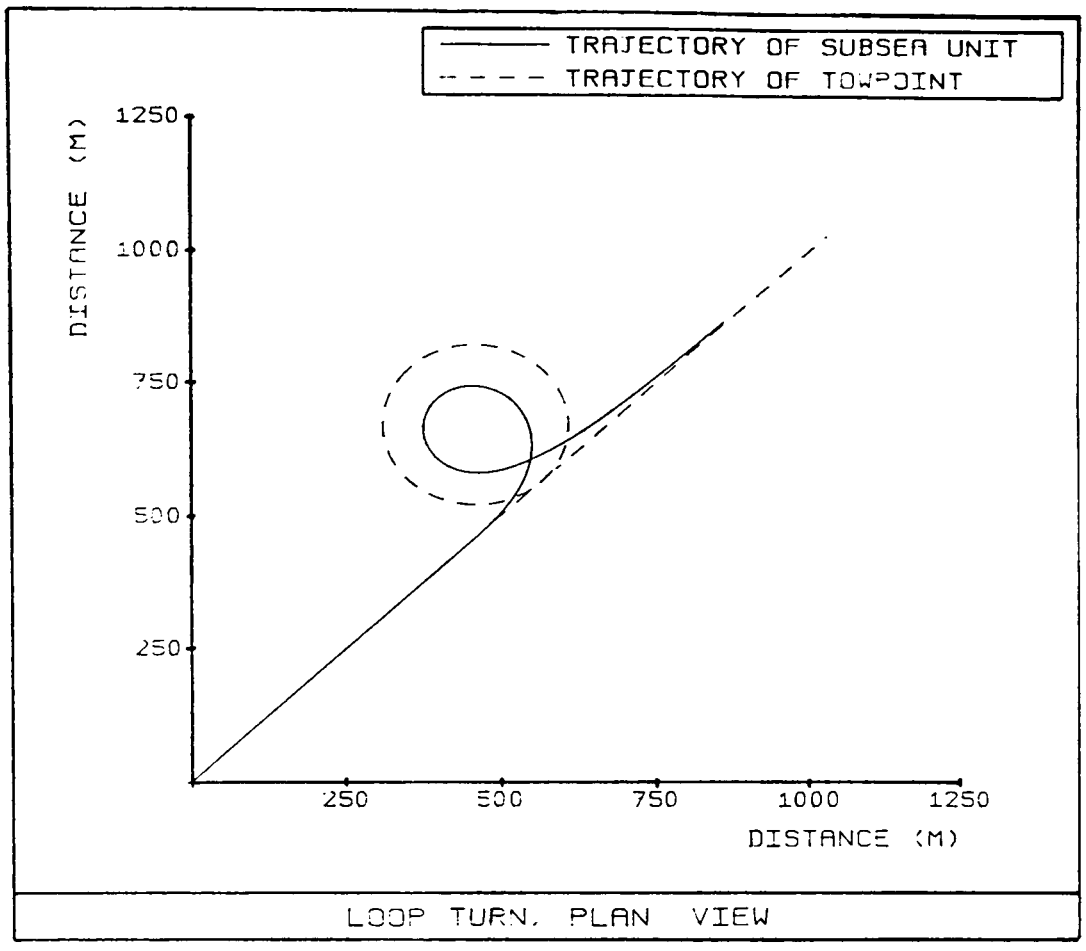
TRAJECTORY OF SUBSEA UNIT
TRAJECTORY OF TOWPOINT
DISTANCE (M)
1250
1000
750
500
250
250
500
750
1000
1250
DISTANCE (M)
LOOP TURN, PLAN VIEW

(a)

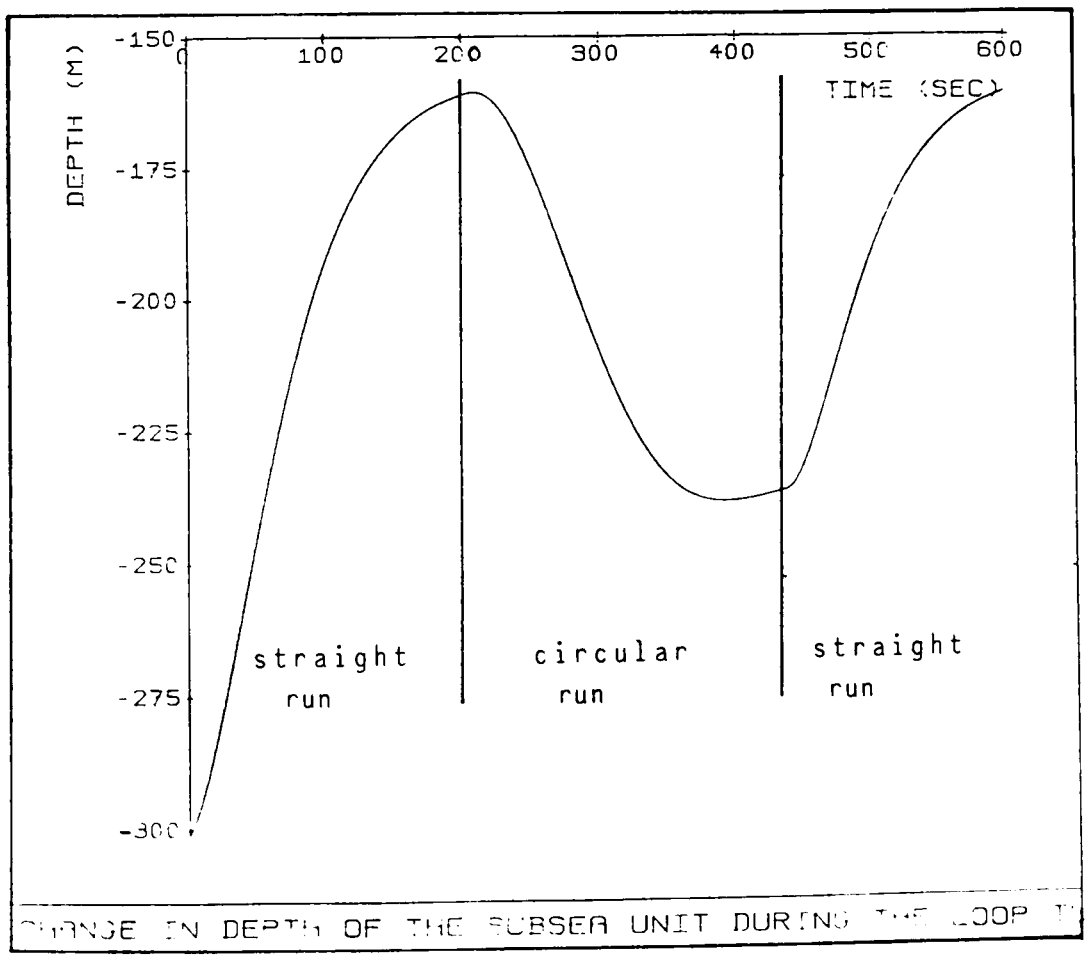
DEPTH (M)
-150
-175
-200
-225
-250
-275
-300
0
100
200
300
400
500
600
TIME (SEC)
straight run
circular run
straight run

(b)

Figure 5.5

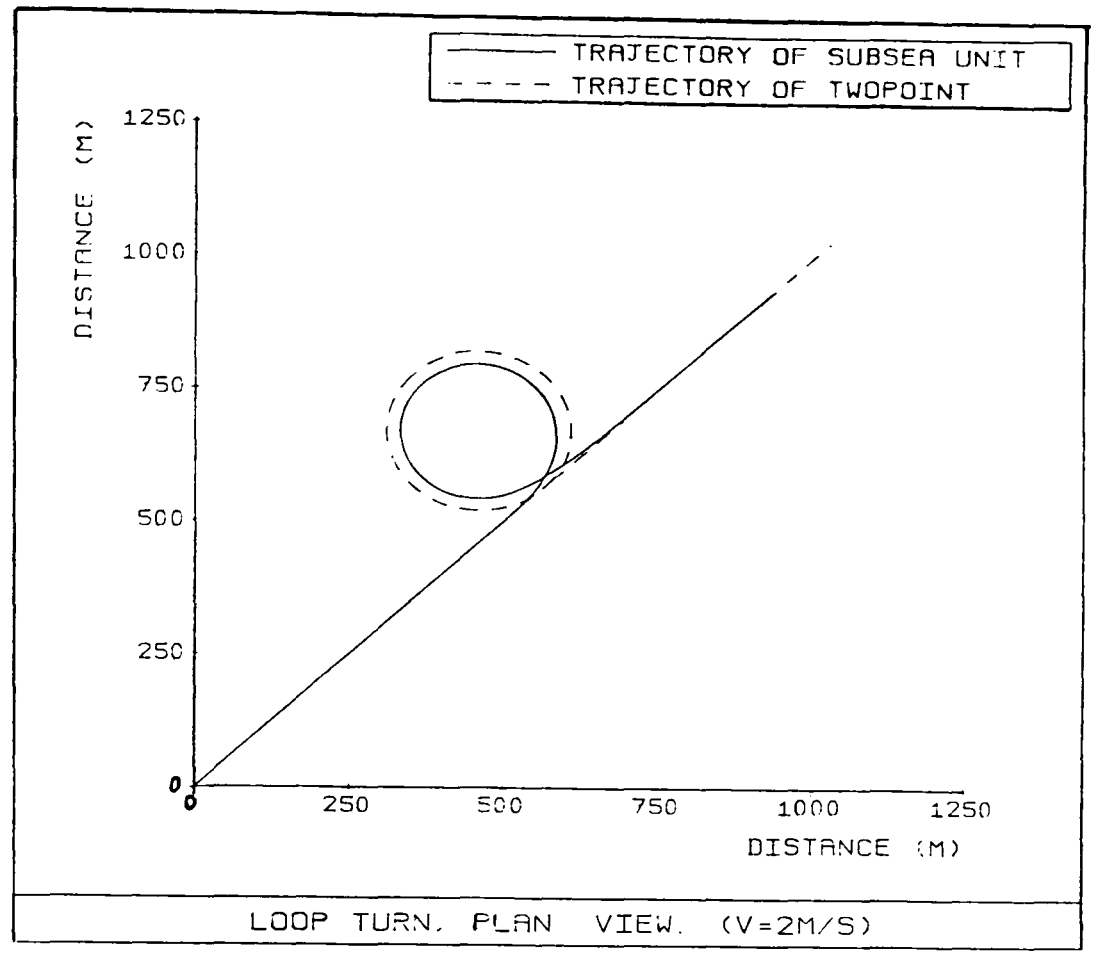
TRAJECTORY OF SUBSEA UNIT
TRAJECTORY OF TWOPOINT
DISTANCE (M)
1250
1000
750
500
250
0
0
250
500
750
1000
1250
DISTANCE (M)
LOOP TURN, PLAN VIEW. (V=2M/S)

(a)

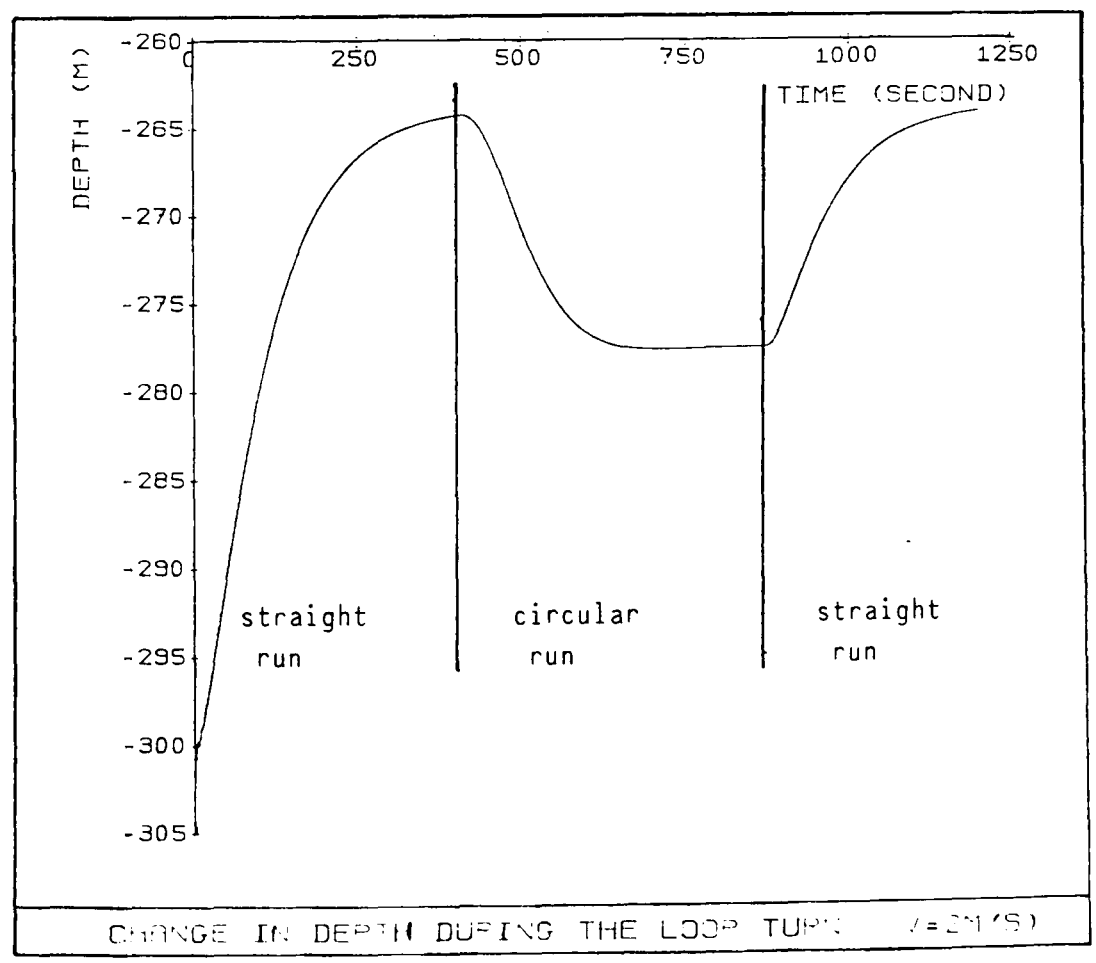
DEPTH (M)
-260
-265
-270
-275
-280
-285
-290
-295
-300
-305
0
250
500
750
1000
1250
TIME (SECOND)
straight run
circular run
straight run

(b)

Figure 5.9

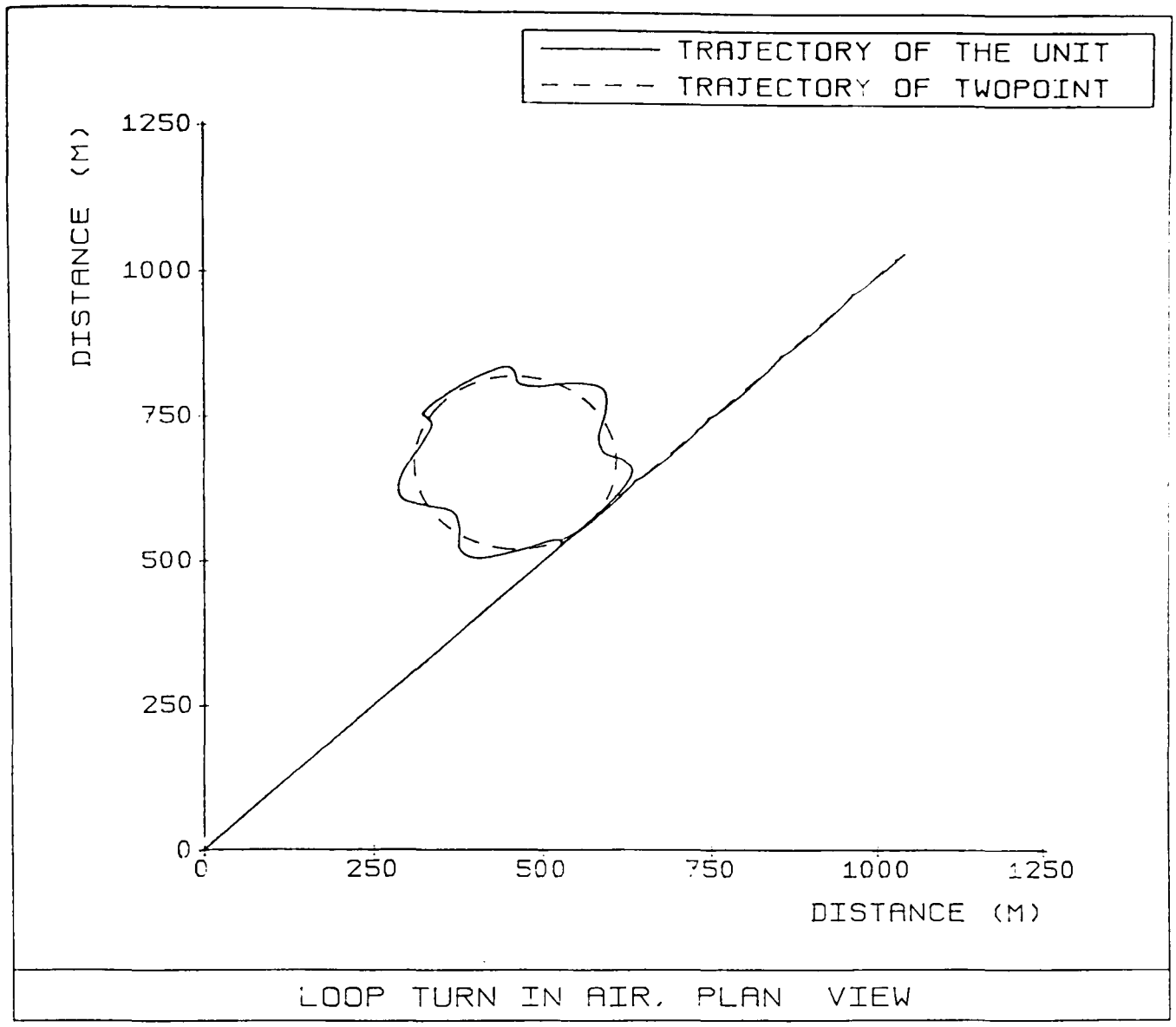

LOOP TURN IN AIR, PLAN VIEW

(a)

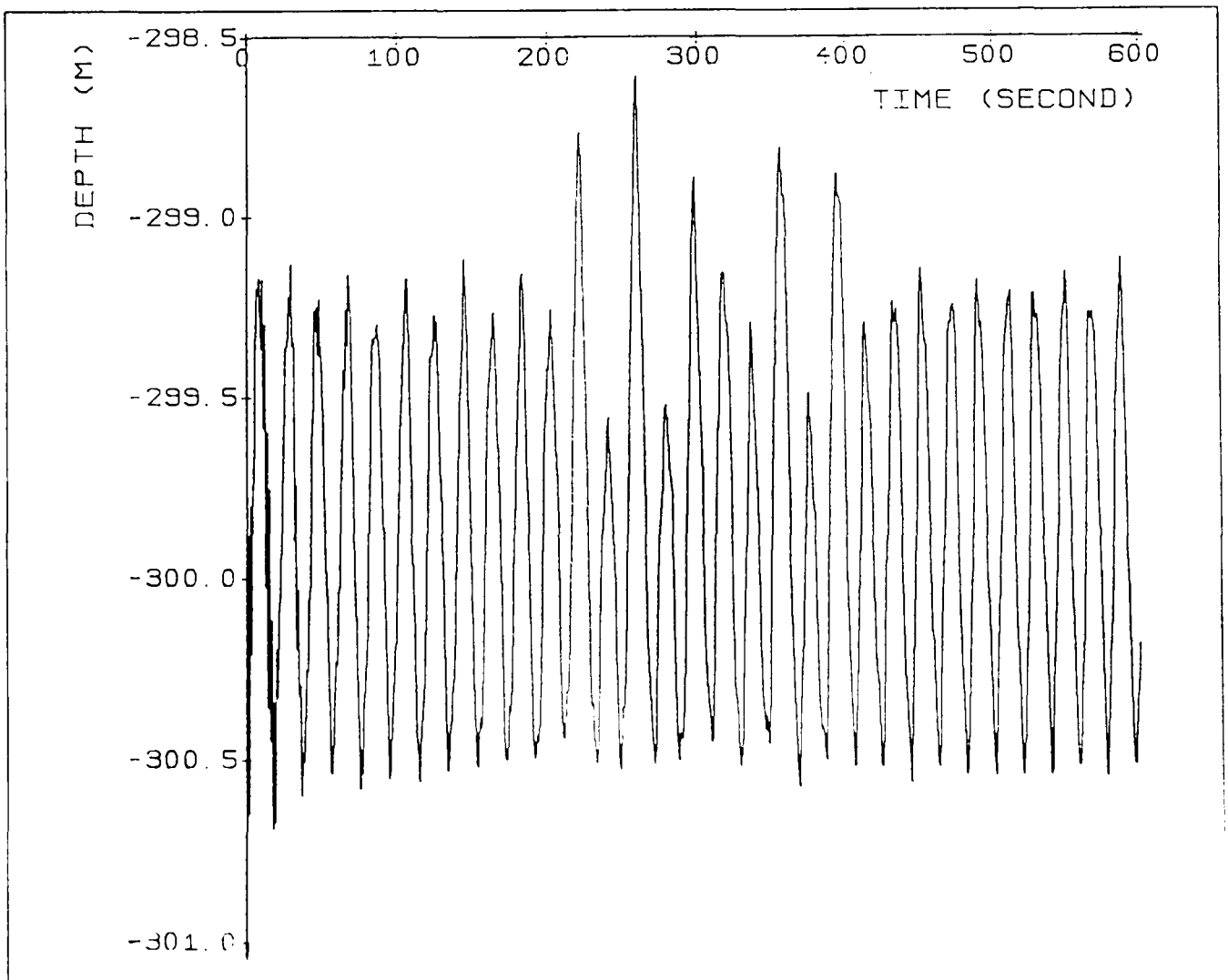

CHANGE IN DEPTH DURING THE LOOP TURN IN AIR

(b)

Chapter 6

HEAVE COMPENSATION

Once more upon the waters! yet once more!
And the waves bound beneath me as a steed
That knows his rider. Welcome to their roar!
Swift be their guidance, wheresoe'er it lead!

In K. Clark's *Civilization*

6.1 GENERAL REMARKS

6.1.1 Statement of the Problem

One of the key problems associated with subsea operation involving tethered subsea units is the motions of support vessels on the ocean surface which can be transmitted to the subsea unit through the cable and increase the tension. In general, environmentally induced responses of a support vessel can be divided into three frequency ranges:

1. Static offsets which include responses to steady current forces, mean wind forces and mean wave drift forces.

2. Low frequency motions which include motions due to wind, ocean current and the second order wave forces.

3. Wave frequency motions due to the first order wave forces.

The first two kinds of motions can be effectively counteracted by auxiliary vessel positioning systems such as mooring systems (Luo, 1990; Inoue, 1991) and dynamic positioning systems (Grimble et al, 1980; Fung et al, 1982; Lee et al, 1989). It is the third one that poses the most formidable challenges to the subsea intervention operations. The safety and performance of these operations are severely limited by the wave frequency vessel motions, and as a result, operations are often suspended during heavy weather. Curtailment of operation can be very costly, and possibly intolerable, as in the cases of military and rescue operations.

Also, there are some delicate subsea operations which require the ability to decouple the surface support vessel motions from the vessel-lowered tethered instruments. For example, the vertical ocean profiling of ocean parameters such as temperature and salinity can be seriously affected by the nonuniform drop rate caused by vessel motions (Kidera, 1983; Kidera and Mack, 1983).

The points at which the cable is normally attached to the vessel, namely the boom tip or the tip of an A-frame, have three translational motion components. Among these heave motion is likely the most hazardous. It is against this background

that the concept of heave compensation has been proposed.

6.1.2 Aim

The aim of heave compensation is to develop such a system that the tethered subsea unit working under the sea surface does not experience any heave motion transmitted through the umbilical cable, or that motion is attenuated as much as possible.

Though autonomous subsea unit systems have been proposed (Rodseth and Hallset, 1991), where no disturbances are transmitted through the removal of the umbilical link, they are not of our concern in this chapter.

6.1.3 Problem Characteristics

In this chapter we consider heave compensation, and assume that the problem can be regarded as one-dimensional. Neither lateral forces nor lateral motions are included in the analysis.

With reference to Figure 6.1, we denote the system of cable/subsea unit by S which is under the excitation of the input $I(t)$ producing the output $O(t)$. The input I is defined as the motion of a fixed point on the cable somewhere near the boom tip, whilst the output O represents the motion of the subsea unit. In a mathematical notation, we have

$$O(t) = S[I(t)]$$

A measure $d\{\cdot\}$ is defined on every $I(t)$ and $O(t)$ [1]. Under this measure intuitively we have

1. $d\{O(t)\} = 0$ if and only if $d\{I(t)\} = 0$.

2. $d\{O_2(t)\} > d\{O_1(t)\}$ if and only if $d\{I_2(t)\} > d\{I_1(t)\}$, where $O_2(t) = S[I_2(t)]$ and $O_1(t) = S[I_1(t)]$

3. $d\{O(t)\}$ is continuously dependent upon $d\{I(t)\}$

From the theory of function analysis, it is evident that the necessary and sufficient condition of reducing output $O(t)$ is to reduce the input $I(t)$, in the sense defined by the measure $d\{\cdot\}$.

The implication of this argument is that whatever heave compensation system is to be employed, either the boom tip heave motion has to be suppressed, or a continuous displacement has to be produced which opposes the boom tip heave motion. As a result, there must be a fixed point on the cable somewhere near its top end which is almost always in a horizontal plane.

6.1.4 Approaches

Various ideas relating to heave compensation can be conveniently divided into two groups:

1. Support vessel's stabilising systems (Figure 6.2)

[1] A general definition of the measure may be difficult to find. However, it can be defined if we are considering a specific subset. For example, in case that all $I(t)$ and $O(t)$ are sinusoidal functions of the same frequency, the measure can be defined as the amplitude.

The basic idea in this kind of system is to introduce some actively or passively controlled appendages or mechanisms which offer stabilising effects to the whole vessel or that part of it where the subsea unit is handled.

Such systems, for example, include bilge keels, fins, tank systems, moving weight systems, and submerged adjustable stabilising pontoons fitted to vertical columns sliding into trunks in the hull of the support vessel (Rawson and Tupper, 1986).

It is reported that with such systems, the vessel's heave motion can be reduced by 50%. In addition to providing a stable deck space for operation, this kind of system significantly improves the working conditions for personnel and reduces fatigue in the cable system. However, it does have drawbacks such as high cost and loss of efficiency in certain operational conditions. Such special purpose vessels are not always commercially viable.

2. Onboard mechanical system (Figure 6.3)

   There are several types of onboard system:

   - boom bobber system

     This system drives up and down the boom in such a way that the boom tip stays approximately in a horizontal plane. Surely this is not an economic system. In addition to the limitation imposed by the range of travel of the boom, it needs a great amount of power supply to drive up and down such a heavy structure.

- ram tensioner (Kozik et al, 1976; Woodall-Mason and Tilbe, 1978)

  Usually this is a passive compensator acting as a soft spring with a natural period significantly longer than the period of the boom tip motion. Though it is a reliable system, being able theoretically to maintain constant cable tension, and is widely used in industry, its performance becomes poorer when the period of the boom tip motion increases. Also this system often requires an unacceptably large number of gas accumulators.

- moonpool (Kuo, 1978; Lee 1982; Day, 1987)

  This system involves a vertical well in the support vessel and an enclosed space above the well with a pontoon floating on the water surface within the well. The handling system of the subsea unit is mounted on the pontoon whose heave motion is greatly reduced by the design of the well.

- winch system

  This system compensates the heave motion by means of an automatic winch control system. The winch pays out or hauls in the cable in such a way that a fixed point on the cable near its top end remains approximately in a horizontal plane. In order to create such a compensator, a fast responding drive system for the winch is required.

  The advantages of this system are its relatively small size, its compact structure and easy handling system. However, fatigue and reliability may cause problems in practical designs.

The inventory can be drawn up from a different point of view, that is, whether the device is actively controlled or passively actuated. An actively controlled system requires a measurement system and an extra energy supply. On the other hand, a passively controlled system operates without using any external energy supply. Instead it uses the potential energy generated by the current system response to control the system's subsequent response. It is easy to see that such a control action is limited depending as it does on the momentary potential energy of the system. Nevertheless, passive systems have the advantages of being reliable and can generally adequately compensate the heave motion at high frequencies where the potential energy is higher. Although, generally speaking, the active system costs more than the passive one, this economical disadvantage can be far outweighed by the advantages involved in its use: greater effectiveness, efficiency and flexibility.

It is envisaged at this stage that the future of heave compensation lies in a combination of the passive spring-like compensator and the actively controlled winch system. The passive component compensates a part of the heave motion and boosts the system's reliability while the active system removes the residual effect of the heave motion.

6.1.5 Concerns of the Chapter

In this chapter we are concerned with an actively controlled winch system for heave compensation during the operation process. The selection of this particular strategy is a natural outcome of the review carried out in the previous

subsection.

There are two different types of design philosophy involved in active winch heave compensation systems.

1. Feedforward System

   The idea of this system is illustrated in Figure 6.4. In this case, a sensor is mounted on the boom tip to measure its heave motion. The signal of the measurement is then fed into a controller and the winch is actuated accordingly. In so doing, the dynamics of the cable needs not be considered, thus the design of the system can be greatly simplified and becomes applicable to many situations in spite of diversity in cable/subsea unit systems.

2. Feedback System

   The idea of this system is illustrated in Figure 6.5. In this case, a sensor for measurement is mounted directly on the subsea unit, and based upon this signal the winch on deck is made to pay out or haul in the cable. Needless to say, in this case, a sensible design of the controller requires an understanding of the cable dynamics.

The following considerations allow us, in the remainder of this chapter, to confine ourselves to the second approach:

1. It is believed that the measurement of the state of the subsea unit can be more easily and more accurately achieved than the measurement of the position of

the boom tip.

2. The feedback system is more suitable in the presence of uncertainties in the applied boom tip motions and the system parameters.

3. The cable dynamics no longer imposes any formidable difficulties.

6.2 MODELLING AND DESIGN OF A REGULATOR

In this section, the automatic control theory is applied to control the action of the onboard winch. It is intended to develop a practically useful control mechanism with consideration given to the time-delay effect on the system performance.

6.2.1 An Explanation of the Problem

An active winch compensation system consists of hydraulic, mechanical, structural and electronic components. Nevertheless the system can be theoretically dissected into three basic components: cable, winch and controller. The dynamics of the first two components should be well investigated before the controller can be properly designed.

1. Modelling of the cable dynamics

   In the Appendix, rigorous mathematical formulation has shown that a second order non-linear hyperbolic equation will accurately model the cable dynamics. However this mathematical description is not in a form that can be easily used

for control system design. Assumptions are therefore made to simplify the model.

2. Modelling of the winch

   The winch plays a crucial role in the whole system. Whether it is possible to prevent transmission of the heave motion of the boom tip to the subsea unit depends on whether the winch can react as quickly as required. The winch can usually be modelled by an ordinary differential equation. The higher the order of the differential equation, the more accurate the model. The model normally contains parameters to be determined. For a specific hydraulic winch one has to rely on experimental information. The parameters can be determined either directly via the experiments or by system identification methods using experimental information.

3. Design of the controller

   Among the classic control techniques, the proportional integral differential (PID) controller finds wide application in process control systems. However, finding an optimal adjustment of the controller is often a troublesome task. Furthermore, the determination of the proportional gain, the integral gain and the differential gain is only dependent upon the input-output behaviour of the open-loop system. It can not take the internal structure of the system into account. On the basis of these considerations, the modern control theory is employed, namely, the state space method (Takahashi et al, 1970; Leipholz

and Abdel-Rohman, 1986; Borrie, 1986; Friedland, 1987; Furuta et al. 1988).

6.2.2 Modelling of the winch

The winch is a device for generating the control action under a power supply. A simple model for this device is depicted in Figure 6.6 (James et al. 1965).

The governing equation for this simple closed-loop mechanical system can be given by:

$$\dot{u} + Ku = Ku_0 \tag{6.1}$$

where u represents the output of the winch under the excitation of the input u_0. The dot indicates differentiation with respect to time.

It should be pointed out that this model has certain limitations. First of all, it does not exhibit the inertia effect which exists in any real servomechanism. Secondly, it assumes a linear relationship between the input and the output defined through the governing equation.

The behaviour of this model can be illustrated by subjecting it to the following two different types of inputs:

1. A step function (transient behaviour)

   In this case, u_0 is given by:

$$u_0 = \begin{cases} 0 & t < t_0 \\ u_I & t > t_0 \end{cases}$$

The solution then is

$$u = \begin{cases} 0 & t < t_0 \\ u_I\{1 - exp[-K(t - t_0)]\} & t > t_0 \end{cases}$$

As shown in Figure 6.7, the output approaches the input. The larger the value of K, the more quickly will the output approach the input.

2. A sinusoidal input (steady behaviour)

In this case,

$$u_0 = u_I sin(\omega t)$$

The output is given by

$$u = \frac{u_I}{\sqrt{\frac{\omega^2}{K^2} + 1}} sin(\omega t - tan^{-1}\frac{\omega}{K})$$

It is immediately evident, as shown in Figure 6.8, that if K is large enough, the output will be essentially equal to the input both in magnitude and in phase.

The physical implication of requiring a large value of K demands an ability to deliver an unlimited power supply at a high rate. However, in reality every control component exhibits the effect of saturation. For example, the range of signal (air pressure, electric current, etc.) used to operate a valve is bounded, as well as the valve stroke itself. The saturation sets a limit to K, and beyond this limit the relation between the output and the input becomes nonlinear.

6.2.3 Modelling of the cable

A simple second order linear model is proposed for the system of cable and subsea unit, given by

$$a\ddot{x} + b\dot{x} + x = x_0 \tag{6.2}$$

where x is the motion of the subsea unit, and x_0 is the motion of the boom tip.

The two coefficients a and b shall reflect the state of the system. They are determined by the system identification method, as illustrated in Figure 6.9. For a given cable and subsea unit, we first simulate, in the time domain, the subsea unit response to a given stochastic input of the boom tip motion using the method described in Chapter 3. The task of system identification is then performed to find the two coefficients a and b which provide the best fit for the response.

The iterative scheme of the system identification for determining a and b is described as follows. Letting $\begin{bmatrix} a \\ b \end{bmatrix}_k$ stand for the kth approximation of a and b, and the $(k+1)$th approximation be

$$\begin{bmatrix} a \\ b \end{bmatrix}_{k+1} = \begin{bmatrix} a \\ b \end{bmatrix}_k + \begin{bmatrix} \triangle a \\ \triangle b \end{bmatrix}_k$$

then the $\begin{bmatrix} \triangle a \\ \triangle b \end{bmatrix}_k$ is given by

$$\begin{bmatrix} \triangle a \\ \triangle b \end{bmatrix}_k = (\mathbf{X}_k^T \mathbf{X}_k)^{-1} \mathbf{X}_k^T \mathbf{e}_k$$

where

$$\mathbf{X}_k = \begin{bmatrix} x_{1a}^k(t_1) & x_{1b}^k(t_1) \\ x_{1a}^k(t_2) & x_{1b}^k(t_2) \\ \vdots & \vdots \\ x_{1a}^k(t_L) & x_{1b}^k(t_L) \end{bmatrix}$$

$$\mathbf{e}_k = \begin{bmatrix} z(t_1) - x^k(t_1) \\ z(t_2) - x^k(t_2) \\ \vdots \\ z(t_L) - x^k(t_L) \end{bmatrix}$$

The subsea unit motion at time equal to t_i is represented by $z(t_i), i = 1, 2, \cdots, L$ and is obtained by invoking the method described in Chapter 3, whilst $x^k(t_i), i = 1, 2, \cdots, L$ are the results found by solving Eq. (6.2) where a and b are set at their kth approximations. The elements in the matrix $\mathbf{X}_k$ are given by solving the following auxiliary ordinary differential equations:

$$\begin{aligned} \dot{x}_{1a} &= x_{2a} \\ \dot{x}_{2a} &= \frac{1}{a^2}(x_1 + bx_2 - x_0) - \frac{1}{a}x_{1a} - \frac{b}{a}x_{2a} \\ \dot{x}_{1b} &= x_{2b} \\ \dot{x}_{2b} &= -\frac{1}{a}x_2 - \frac{1}{a}x_{1b} - \frac{b}{a}x_{2b} \end{aligned}$$

subject to initial conditions:

$$\begin{bmatrix} x_{1a}(0) \\ x_{2a}(0) \\ x_{1b}(0) \\ x_{2b}(0) \end{bmatrix} = \mathbf{0}$$

A better model can be achieved by introducing nonlinear terms. For example, instead of Eq. (6.2), we propose

$$a\ddot{x} + b\dot{x}|\dot{x}| + x = x_0 \tag{6.3}$$

However, such a nonlinear model would cause considerable difficulties in the controller design. Hence, we confine ourselves throughout this chapter within the bounds of linearity.

For a detailed description of system identification, see Kalaba and Spingarn (1982).

6.2.4 Optimal control: the design of the control law

The open-loop consisting of the winch, cable/subsea unit is governed by

$$a\ddot{x} + b\dot{x} + x = x_0 + u \tag{6.4}$$

$$\dot{u} + Ku = Ku_0 \tag{6.5}$$

In a state-space form, the governing equations become

$$\frac{d}{dt}\begin{bmatrix} x \\ \dot{x} \\ u \end{bmatrix} = \begin{bmatrix} 0 & 1 & 0 \\ -\frac{1}{a} & -\frac{b}{a} & \frac{1}{a} \\ 0 & 0 & -K \end{bmatrix}\begin{bmatrix} x \\ \dot{x} \\ u \end{bmatrix} + \begin{bmatrix} 0 \\ 0 \\ K \end{bmatrix} u_0 + \begin{bmatrix} 0 \\ \frac{1}{a} \\ 0 \end{bmatrix} x_0 \tag{6.6}$$

or in a short form

$$\dot{\mathbf{x}} = \mathbf{A}\mathbf{x} + \mathbf{B}u_0 + \mathbf{C}x_0 \tag{6.7}$$

where

$$\mathbf{x} = \begin{bmatrix} x \\ \dot{x} \\ u \end{bmatrix} \quad \mathbf{B} = \begin{bmatrix} 0 \\ 0 \\ K \end{bmatrix} \quad \mathbf{C} = \begin{bmatrix} 0 \\ \frac{1}{a} \\ 0 \end{bmatrix}$$

$$\mathbf{A} = \begin{bmatrix} 0 & 1 & 0 \\ -\frac{1}{a} & -\frac{b}{a} & \frac{1}{a} \\ 0 & 0 & -K \end{bmatrix}$$

Since the objective in heave compensation is to strive for a zero steady state response, it becomes obvious that what we are concerned with is a regulator problem. In this case the performance index J of the optimal regulator control is defined by

$$J = \int_0^\infty [\mathbf{x}^T\mathbf{Q}\mathbf{x} + u_0\mathbf{R}u_0]dt \tag{6.8}$$

and the optimal control is obtained from

$$u_0 = \mathbf{G}\mathbf{x} \tag{6.9}$$

with the optimal gain in steady state given by

$$\mathbf{G} = -\mathbf{R}^{-1}\mathbf{B}^T\mathrm{M} \tag{6.10}$$

where $\mathbf{M}$ is the solution of the following Riccati matrix equation (Roberts, 1971; Denman, 1976; Balzer, 1980; Anderson, 1978; Friedland, 1987)

$$\mathbf{MA} + \mathbf{A}^T\mathbf{M} - \mathbf{MBR}^{-1}\mathbf{B}^T\mathbf{M} + \mathbf{Q} = 0$$

6.2.5 Account of the time delay

The control of the heave compensation system starts with measuring the subsea unit's response and then transmitting the signal into the winch. It ends up by actuating the winch according to the control law. This process involves a time delay between the instant of the measurement and that of applying the control action. In this subsection, we shall examine the effect of the time-delay (Hammarstrom and Gros, 1980; Leipholz and Abdel-Rohman, 1986).

We assume that most time delay in the system may be attributed to the winch. In this case, the equations of the dynamic behaviour of the system are:

$$a\ddot{x}(t) + b\dot{x}(t) + x(t) = x_0(t) + u(t) \tag{6.11}$$

$$\dot{u}(t) + Ku(t) = Ku_0(t - \tau) \tag{6.12}$$

where τ equals the delay.

By using Taylor's theorem, we have

$$u_0(t) = u_0(t - \tau) + \tau\dot{u}_0(t - \tau) + \frac{\tau^2}{2}\ddot{u}_0(t - \tau) + ...$$

This series is truncated to the second order, resulting in the following second order differential equation in terms of $u_0(t - \tau)$

$$\ddot{u}_0(t - \tau) = \frac{2}{\tau^2}u_0(t) - \frac{2}{\tau^2}u_0(t - \tau) - \frac{2}{\tau}\dot{u}_0(t - \tau) \tag{6.13}$$

Combining Eqs. (6.11), (6.12) and (6.13), we have the following system of equations in the state space form:

$$\frac{d}{dt}\begin{bmatrix} x \\ \dot{x} \\ u \\ u_0(t-\tau) \\ \dot{u}_0(t-\tau) \end{bmatrix} = \begin{bmatrix} 0 & 1 & 0 & 0 & 0 \\ -\frac{1}{a} & -\frac{b}{a} & \frac{1}{a} & 0 & 0 \\ 0 & 0 & -K & K & 0 \\ 0 & 0 & 0 & 0 & 1 \\ 0 & 0 & 0 & -\frac{2}{\tau^2} & -\frac{2}{\tau} \end{bmatrix} \begin{bmatrix} x \\ \dot{x} \\ u \\ u_0(t-\tau) \\ \dot{u}_0(t-\tau) \end{bmatrix} + \begin{bmatrix} 0 \\ 0 \\ 0 \\ 0 \\ \frac{2}{\tau^2} \end{bmatrix} u_0 + \begin{bmatrix} 0 \\ \frac{1}{a} \\ 0 \\ 0 \\ 0 \end{bmatrix} x_0 \tag{6.14}$$

or in a short form

$$\dot{\mathbf{x}}_c = \mathbf{A}_c\mathbf{x}_c + \mathbf{B}_c u_0 + \mathbf{C}_c x_0 \tag{6.15}$$

This equation is in the same form as Eq. (6.7), hence the same strategies can be used to design an optimal controller. In order to assess the effect of the time delay, the following indices are defined

$$J_d = \int_0^t x^2 dt \tag{6.16}$$

$$J_v = \int_0^t \dot{x}^2 dt \tag{6.17}$$

$$J_c = \sum_i G_i^2 \tag{6.18}$$

in which J_d involves the displacement of the subsea unit, J_v involves its velocity and J_c involves the control energy required. G_i are all elements of $\mathbf{G}$ defined by Eq. (6.10).

6.2.6 Numerical examples

An attempt to select factual cable/subsea unit parameters was made. The data chosen are:

cable length:	900m
cable diameter:	0.047m
Young's modulus:	9.09E9 N/m^2
cable weight in water:	54 N/m
cable mass distribution:	7.2 kg/m
tangential drag coefficient:	0.025
subsea unit weight in water:	50000 N
subsea unit projected area:	1 m^2
subsea unit effective mass:	125000 kg
drag coefficient of subsea unit:	1

In Figure 6.10, an artificial random time series is generated to represent the boom tip motion. The response of the subsea unit is then simulated and the result is given in Figure 6.11. Using the system identification method described in Section 6.2.3, we have the simple model defined by Eq. (6.2) with $a = 7.339769$ and $b = 0.1906759$. The response of the subsea unit is then reconstructed using the simple model, which gives the result in Figure 6.12.

A reasonably good agreement has been achieved between the results in Figures 6.11 and 6.12. It has been noticed that the values of a and b are scattered in a narrow band if the number of the points used in the least-squares estimation varies. In Figure 6.13, a better result is achieved by using the model defined by Eq. (6.3).

Having constructed a simple model for the cable/subsea unit system, we are now able to proceed with the design of the controller, as described in Section 6.2.4. The results are presented in Figure 6.14 to Figure 6.16. One observes a large reduction in the response of the subsea unit when the active control is introduced. As one would

expect, the output of the winch acts to oppose the boom tip motion. This conclusion was reached in Section 6.1.3.

The time-delay effect is depicted in Figures 6.17, 6.18 and 6.19. In Figure 6.17, the controlled and the uncontrolled responses are presented for the previous system, the only difference being that in this case a time-delay of $0.2s$ has been introduced. It can be seen that the controlled response can still be kept small. However, there is a significant increase in the control energy required which is manifested through the increase in magnitude of the gain. Indeed this may be observed in Figures 6.18 and 6.19 where the displacement index and the velocity index defined by Eqs. (6.16) and (6.17) respectively are plotted against the control energy index defined by Eq. (6.18). It is obvious that in order to achieve the same control effect, more control energy is required if the time-delay is present.

6.3 STOCHASTIC CONTROL: AN OVERALL APPROACH

It has been shown in the previous section that the heave compensation as a regulator problem is not dependent upon the characteristics of the boom tip motion. However, if the boom tip motion is known a priori and formulated into the state equations, presumably a better result can be obtained.

The stochastic control theory is applied here due to the fact that the boom tip motion is random in nature. In order to design a suitable optimal control law, it is necessary to be able to generate the boom tip motion by feeding an appropriate

filter with white noise. This demands the modelling of environmental factors such as sea wave and vessel dynamics, in addition to the modelling of the winch and the cable/subsea unit system described in the previous section. Once the filter is designed, finding an optimal stochastic control law becomes a straightforward problem (Athans, 1972; Friedland, 1987). A block diagram is shown in Figure 6.20 to illustrate the design procedure and the structure of the control system.

6.3.1 Modelling of sea waves

In this subsection, the stochastic wave elevation is approximated in such a way that the error between the wave spectrum and the approximated spectrum defined by the filter fed with white noise is minimized:

$$S_\omega \approx S_\omega^a = |H(\sqrt{-1}\omega)|^2 S_\omega^w \tag{6.19}$$

where S_ω is the wave spectrum. S_ω^a is a rational approximation. H is the transfer function of the filter. S_ω^w is the power spectral density of white noise:

$$S_\omega^w = 1$$

As an example, we use the Bretchneider wave spectrum

$$S_\omega = \frac{1.25}{4} H_{1/3}^2 \cdot \frac{\omega_m^2}{\omega^5} \cdot exp[-1.25(\frac{\omega_m}{\omega})^4] \tag{6.20}$$

where $H_{1/3}$ is the significant wave height, and ω_m is the modal frequency.

A rational approximation to this spectrum is given by (Triantaffyllou et al, 1983)

$$S_\omega^a = S_0 \cdot \frac{(\frac{\omega}{\omega_0})^4}{[1 + (\frac{\omega}{\omega_0})^4]^3} \tag{6.21}$$

where

$$S_0 = \frac{1.25}{4\omega_m} H_{1/3}^2 \cdot 1.8861$$

$$\omega_0 = 0.9538\omega_m$$

As the result, we have the following expression for the transfer function

$$H(s) = \sqrt{S_0} \cdot \frac{(\frac{s}{\omega_0})^2}{[1 + 1.414\frac{s}{\omega_0} + (\frac{s}{\omega_0})^2]^3} \tag{6.22}$$

The state space representation of the transfer function given in Eq. (6.22) can be expressed as

$$\dot{\mathbf{x}} = \mathbf{A}_s \mathbf{x}_s + \mathbf{B}_s \cdot w$$

$$\eta = \mathbf{C}_s \mathbf{x}_s \tag{6.23}$$

where η is the sea wave elevation, $\mathbf{x}_s$ represents the state variables of the model, and w is the white noise of unit power spectral density.

$$\mathbf{A}_s = \begin{bmatrix} 0 & 1 & 0 & 0 & 0 & 0 \\ -\omega_0^2 & -1.414\omega_0 & 0 & \omega_0^2 & 0 & 0 \\ 0 & 0 & 0 & 1 & 0 & 0 \\ 0 & 0 & -\omega_0^2 & -1.414\omega_0 & 0 & \omega_0^2 \\ 0 & 0 & 0 & 0 & 0 & 1 \\ 0 & 0 & 0 & 0 & -\omega_0^2 & -1.414\omega_0 \end{bmatrix}$$

$$\mathbf{B}_s = \begin{bmatrix} 0 \\ 0 \\ 0 \\ 0 \\ 0 \\ 1 \end{bmatrix}$$

$$\mathbf{C}_s = \begin{bmatrix} \sqrt{S_0} & 0 & 0 & 0 & 0 & 0 \end{bmatrix}$$

6.3.2 Modelling of vessel dynamics

It is desirable to have an accurate vessel model capable of providing theoretical prediction of the boom tip motion. However this is not an easy task. In the linear ship motion theory, the dynamics of the floating body consists of the solution of the following equation

$$(\mathbf{M} + \mathbf{\Theta})\ddot{\mathbf{q}} + \mathbf{B}\dot{\mathbf{q}} + \mathbf{C}\mathbf{q} = \mathbf{F} \tag{6.24}$$

where $\mathbf{q}$ is the vector of generalized coordinates describing the ship's position.

$\mathbf{M}$ is the generalized mass matrix.

$\mathbf{\Theta}$ is the added mass matrix due to the hydrodynamic forces.

$\mathbf{B}$ is the damping matrix due to the hydrodynamic forces.

$\mathbf{C}$ is the restoring matrix due to the hydrostatic effects.

$\mathbf{F}$ is the generalized wave excitation forces.

The ship dynamics can also been seen as a transfer function in the frequency domain. It takes a great deal of data and calculations to obtain the transfer function of our concern, namely the relation between the wave motion and the vertical motion of the boom tip, through solution of Eq. (6.24). In order to simplify the whole procedure, it is assumed that the relation can be approximated by a second order filter governed by

$$\ddot{x}_0 + 2\xi_v\omega_v\dot{x}_0 + \omega_v^2 x_0 = K_v\omega_v^2 \cdot \eta \tag{6.25}$$

where x_0 is the vertical coordinate of the boom tip. ξ_v, ω_v, and K_v are all parameters to be either determined empirically or derived from a sea-keeping program. The system identification method can be used here to determine the parameters.

In the state space form, Eq. (6.25) becomes

$$\dot{\mathbf{x}}_b = \mathbf{A}_b\mathbf{x}_b + \mathbf{B}_b \cdot \eta$$

$$x_0 = \mathbf{C}_b\mathbf{x}_b \tag{6.26}$$

where

$$\mathbf{A}_b = \begin{bmatrix} 0 & 1 \\ -\omega_v^2 & -2\xi_v\omega_v \end{bmatrix}$$

$$\mathbf{B}_b = \begin{bmatrix} 0 \\ 1 \end{bmatrix}$$

$$\mathbf{C}_b = \begin{bmatrix} K_v\omega_v^2 & 0 \end{bmatrix}$$

6.3.3 Modelling of the cable/subsea unit and the winch

The equations are rewritten here:

$$\dot{\mathbf{x}}_m = \mathbf{A}_m \mathbf{x}_m + \mathbf{B}_{m1} \cdot u_0 + \mathbf{B}_{m2} \cdot x_0$$

$$x = \mathbf{C}_m \mathbf{x}_m \tag{6.27}$$

where x is the vertical coordinate of the subsea unit,

$$\mathbf{A}_m = \begin{bmatrix} 0 & 1 & 0 \\ -\frac{1}{a} & -\frac{b}{a} & \frac{1}{a} \\ 0 & 0 & -K \end{bmatrix}$$

$$\mathbf{B}_{m1} = \begin{bmatrix} 0 \\ 0 \\ K \end{bmatrix} \quad \mathbf{B}_{m2} = \begin{bmatrix} 0 \\ \frac{1}{a} \\ 0 \end{bmatrix}$$

$$\mathbf{C}_m = \begin{bmatrix} 1 & 0 & 0 \end{bmatrix}$$

6.3.4 Stochastic optimal control design

Eqs. (6.23), (6.26) and (6.27) can be combined to yield one single system given by

$$\dot{\mathbf{x}} = \mathbf{A}\mathbf{x} + \mathbf{B}_1 \cdot u_0 + \mathbf{B}_2 \cdot w$$

$$x = \mathbf{C}\mathbf{x} \tag{6.28}$$

in which

$$\mathbf{A} = \left[\begin{array}{c|c|c} \mathbf{A}_m & \mathbf{B}_{m2}\mathbf{C}_b & \mathbf{0} \\ \hline \mathbf{0} & \mathbf{A}_b & \mathbf{B}_b\mathbf{C}_s \\ \hline \mathbf{0} & \mathbf{0} & \mathbf{A}_s \end{array}\right]$$

$$\mathbf{B}_1 = \left[\begin{array}{c} \mathbf{B}_{m1} \\ \hline \mathbf{0} \\ \hline \mathbf{0} \end{array}\right] \qquad \mathbf{B}_2 = \left[\begin{array}{c} \mathbf{0} \\ \hline \mathbf{0} \\ \hline \mathbf{B}_s \end{array}\right]$$

$$\mathbf{C} = \left[\begin{array}{c|c|c} \mathbf{C}_m & \mathbf{0} & \mathbf{0} \end{array}\right]$$

$$\mathbf{x} = \left[\begin{array}{c} \mathbf{x}_m \\ \hline \mathbf{x}_b \\ \hline \mathbf{x}_s \end{array}\right]$$

An objective function has to be specified in order to find an optimal control law. In the presence of random variables, the objective function is considered as a function of the average response and the control energy. Using a quadratic objective

function, we have

$$J = E\{\int_0^\infty [\mathbf{x}^\mathbf{T}\mathbf{Q}\mathbf{x} + u\mathbf{R}u]dt\} \tag{6.29}$$

where $\mathbf{Q}$ and $\mathbf{R}$ are non negative weighing matrices.

The optimal control law is given by

$$u_0 = -\mathbf{R}^{-1}\mathbf{B}_1^\mathbf{T}\mathbf{M}\mathbf{x} \tag{6.30}$$

where $\mathbf{M}$ is the solution of Riccati matrix equation.

The effectiveness of control is to be measured in terms of the mean square controlled response. To calculate the variances and covariances of the state variables, thereby to check the controlled mean square response, we need to solve the Lyapunov matrix equation:

$$\mathbf{A}_0\mathbf{P} + \mathbf{P}\mathbf{A}_0^T + \mathbf{B}_2\mathbf{B}_2^T = \mathbf{0} \tag{6.31}$$

where

$$\mathbf{P} = E\{\mathbf{x}\mathbf{x}^T\} = \begin{bmatrix} E\{x_1x_1\} & \dots & E\{x_1x_{11}\} \\ \dots & \dots & \dots \\ E\{x_{11}x_1\} & \dots & E\{x_{11}x_{11}\} \end{bmatrix}$$

$$\mathbf{A}_0 = \begin{cases} \mathbf{A} & \textit{uncontrolled} \\ \mathbf{A} - \mathbf{B}_1\mathbf{R}^{-1}\mathbf{B}_1^T\mathbf{M} & \textit{controlled} \end{cases}$$

6.3.5 Optimization

In the previous sections, emphasis was put on finding the optimal control law once the values of the parameters were given. However, one should realise that

to design an optimal system of heave compensation, optimization of the system parameters should also be considered.

When all the parameters in the Eqs. (6.28) and (6.29) have been specified, the optimal control law can be found through the algorithms presented in last section. Substituting Eq. (6.30) into Eq. (6.28), we obtain

$$\dot{\mathbf{x}} = \mathbf{A}_0\mathbf{x} + \mathbf{B}_2 \cdot w$$

$$x = \mathbf{C}\mathbf{x} \tag{6.32}$$

Since this equation's coefficients are time invariant, the Fourier transformation results in the following matrix equation

$$(\sqrt{-1}\omega\mathbf{I} - \mathbf{A}_0)\mathbf{X}(\sqrt{-1}\omega) = \mathbf{B}_2 W(\sqrt{-1}\omega)$$

where

$$\mathbf{X}(\sqrt{-1}\omega) = \mathcal{F}\{\mathbf{x}(t)\} = \int_{-\infty}^{+\infty} \mathbf{x}(t)e^{-\sqrt{-1}\omega t}dt$$

$$W(\sqrt{-1}\omega) = \mathcal{F}\{w(t)\} = \int_{-\infty}^{+\infty} w(t)e^{-\sqrt{-1}\omega t}dt$$

The relation between the input and the output in the frequency domain is

$$X(\sqrt{-1}\omega) = H(\sqrt{-1}\omega) \cdot W(\sqrt{-1}\omega)$$

where the transfer function H is given by

$$H(\sqrt{-1}\omega) = \mathbf{C}(\sqrt{-1}\omega\mathbf{I} - \mathbf{A}_0)^{-1}\mathbf{B}_2 \tag{6.33}$$

The power spectral density function of the random subsea unit response is then given as

$$S_\omega^r = H(-\sqrt{-1}\omega)S_\omega^w H(\sqrt{-1}\omega)$$

$$= |H(\sqrt{-1}\omega)|^2 \tag{6.34}$$

The standard deviation of the subsea unit response is given by

$$\sigma = \sqrt{\int_{-\infty}^{+\infty} |H(\sqrt{-1}\omega)|^2 d\omega} \tag{6.35}$$

In a real situation, parameters of the sea wave and the vessel are given beforehand. They can hardly be changed. To a certain extent, however, we can optimize the parameters of the winch or the cable in order to achieve better operation performances.

An optimal value of the parameter in question can be deduced by an optimization process consisting of the following steps:

1. Assume values for the parameter and design the optimal control law.
2. Evaluate the control energy consumed.
3. Calculate the standard deviation of the subsea unit response.
4. Find the optimal value of the parameter by plotting the control energy against the value of the parameter for a prescribed standard deviation.

It is clear that the deduced parameters are optimal in the sense that the least energy is required to meet certain criterion set beforehand for the subsea unit response. When minimising the energy consumption is not the only objective of the design, this optimization process ceases to be valid.

At this stage we can not calculate the real control energy consumption. However an index of the control energy for relative comparison may be given as, for

example,

$$energy\ index = \sqrt{\sum_i G_i^2}$$

6.3.6 Numerical examples

The values of the parameters selected are as follows:

1. environmental parameters: significant wave height $H_{1/3} = 10ft = 3.048m$, modal frequency $\omega_m = 0.785rad/s$. These values correspond to sea state 5. (Wind speed is about 20 knots)

2. ship dynamics parameters: $\omega_v = 0.393rad/s, \xi_v = 0.6, K_v = 0.5$

3. winch parameter: $K = 1$.

4. cable/subsea unit parameters: $a = 0.8959, b = 0.1658$

The subsea unit is assumed to have been at rest before the application of the wave. Under these conditions, the controlled and the uncontrolled responses of the subsea unit are determined. It is also assumed that continuous measurements are supplied to a Kalman filter which subsequently processes the signals and estimates state variables.

Figure 6.21 shows the rational approximation of the wave spectrum. Further improvement is needed here.

Figure 6.22 presents a realisation of the wave elevation.

Figure 6.23 shows the uncontrolled response of the subsea unit. The standard deviation, σ, is $0.255m$.

Figure 6.24 shows the controlled response where σ equals 2.96×10^{-4}m. The control effect is evident.

Figure 6.25 gives the optimization result for the winch parameter K_c. It has been stated that K is the parameter describing how quickly the output of the winch can approach the input to it. The larger the value of K, the more quickly the winch acts. Apparently a quicker winch is more desirable than a sluggish one, although it will cost more. The result here indicates that under a given situation and a prescribed standard deviation of subsea unit response, there exists a critical value of K_c. Any K which is greater than this critical value will not further improve the system in terms of reducing the control energy, while if K is less than this value the control energy will increase significantly.

6.4 DISCUSSION

The foregoing part of this chapter outlines the basic loop of an active control of the tethered subsea unit system which has as its purpose heave compensation. Numerical examples have shown the great potential of the proposed idea. In this section, relevant topics arising from previous sections are discussed.

1. Measurement. This chapter assumes continuous accurate measurements, from sensors mounted on the subsea unit, of its position and its velocity. The questions of what types of sensors to choose, which principles to be adopted as a basis for measurement, and how to transmit the signals, are beyond the scope

of this thesis. It is believed that these practical problems can be solved in one way or another.

The other information on the state of the system can be either measured directly or estimated by an optimal observer. The design of this observer should be straightforward.

2. The system identification method allows the determination of a and b provided that the particulars of cable and subsea unit are given. The reverse problem demands the ability to specify all particulars of the cable/subsea unit system once a and b are prescribed. The solution of this reverse problem will pave the way towards the optimisation of the cable/subsea unit system.

3. The paying out or reeling in of cable by the active winch will change the state of the cable/subsea unit system to some extent. The effect of this time-varying state can be neglected if the cable is relatively long.

4. This negligence ceases to be justifiable when we are considering the deployment or retrieval phase where in addition to the zero-mean paying out or reeling in there is a non-zero-mean change in the cable length. In this case, the system becomes a time-varying one, and the design of control system must be adapted accordingly.

6.5 CONCLUDING REMARKS

1. Based upon the work described above, it may be concluded that the active winch system appears to be a very promising solution to the problem of heave compensation.

2. Nevertheless, further work needs to be done before a comprehensive evaluation can be drawn up. This includes:

   - More accurate modelling of the winch. For this purpose, a second order ordinary differential equation should be considered.
   - A better rational approximation of the wave spectrum.
   - Feasibility studies of the active heave compensation. The feasibility shall be measured in terms of the magnitudes of the speed, acceleration and torque of the winch which generates the control action.

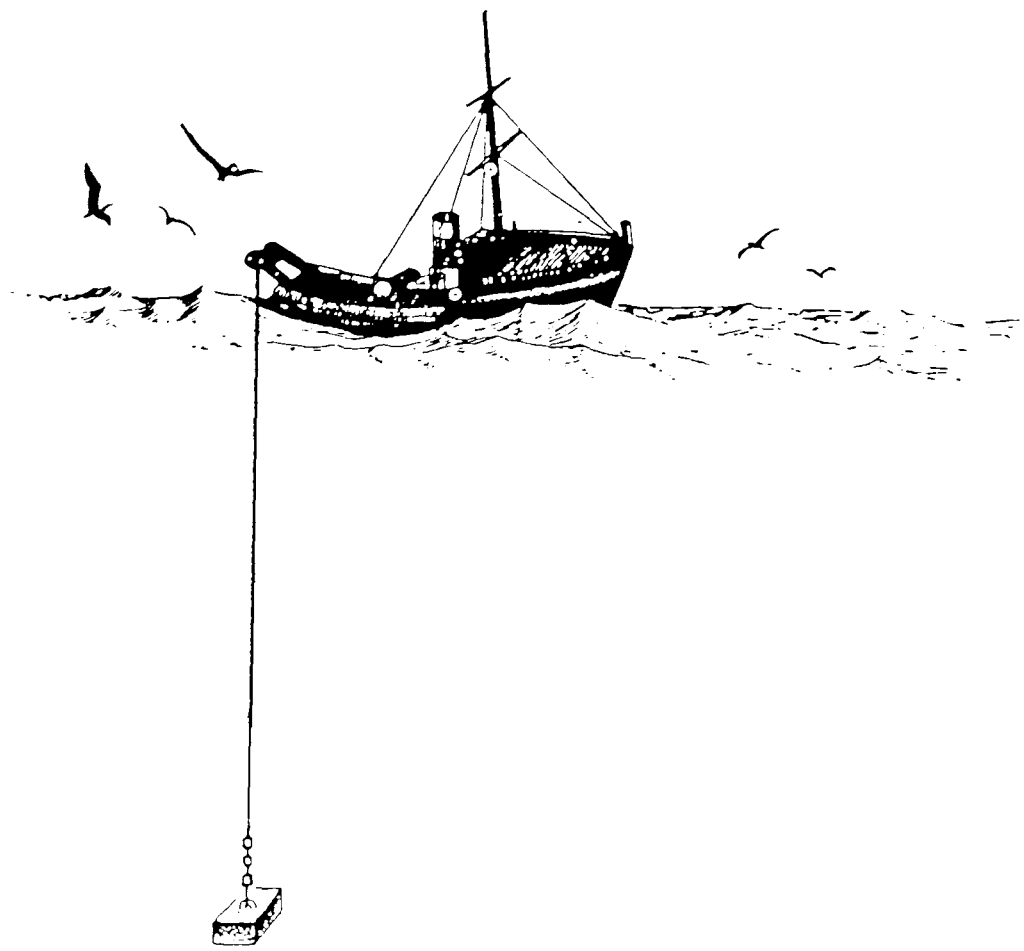

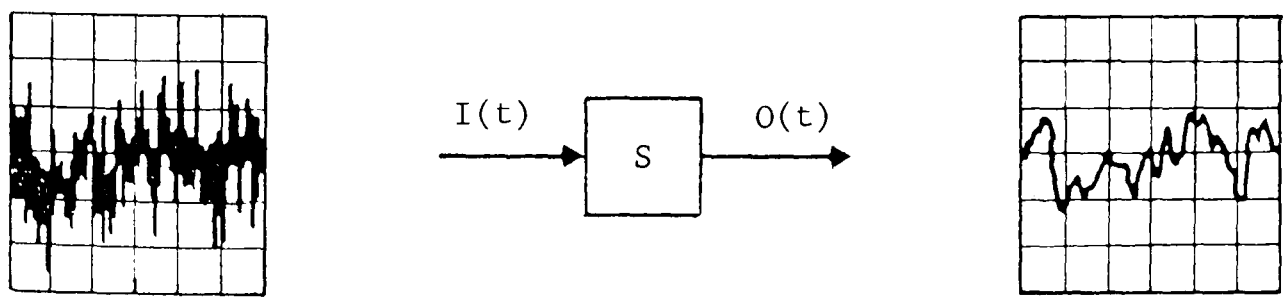

Figure 6.1

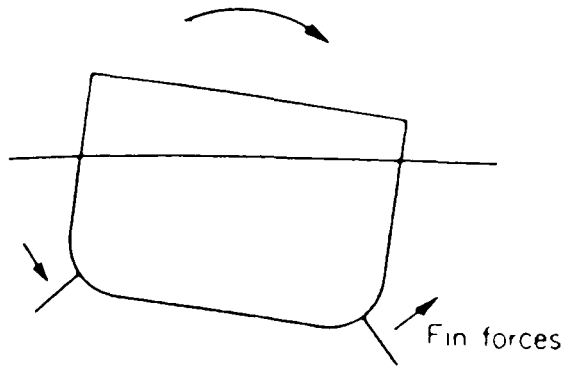
Fin forces

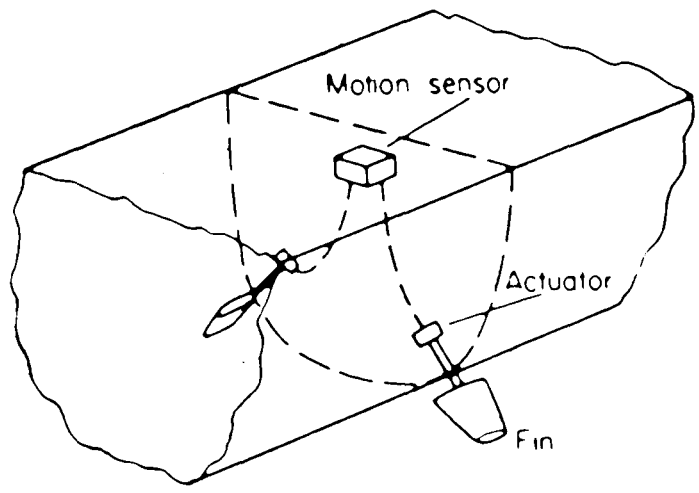
Motion sensor
Actuator
Fin

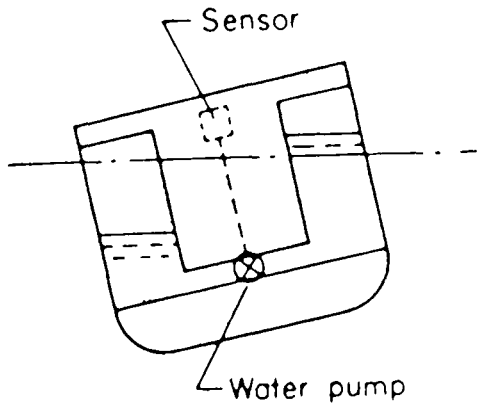
Sensor
Water pump

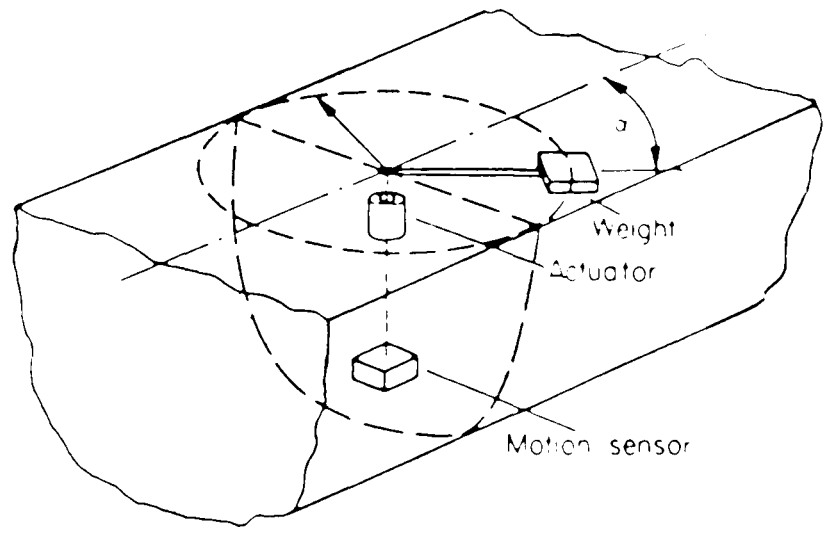
Weight
Actuator
Motion sensor

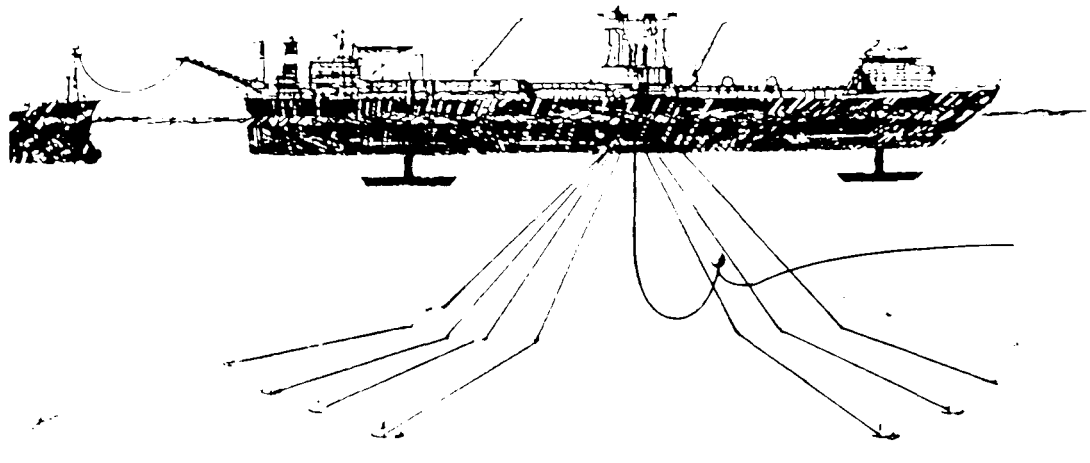

Figure 6.2

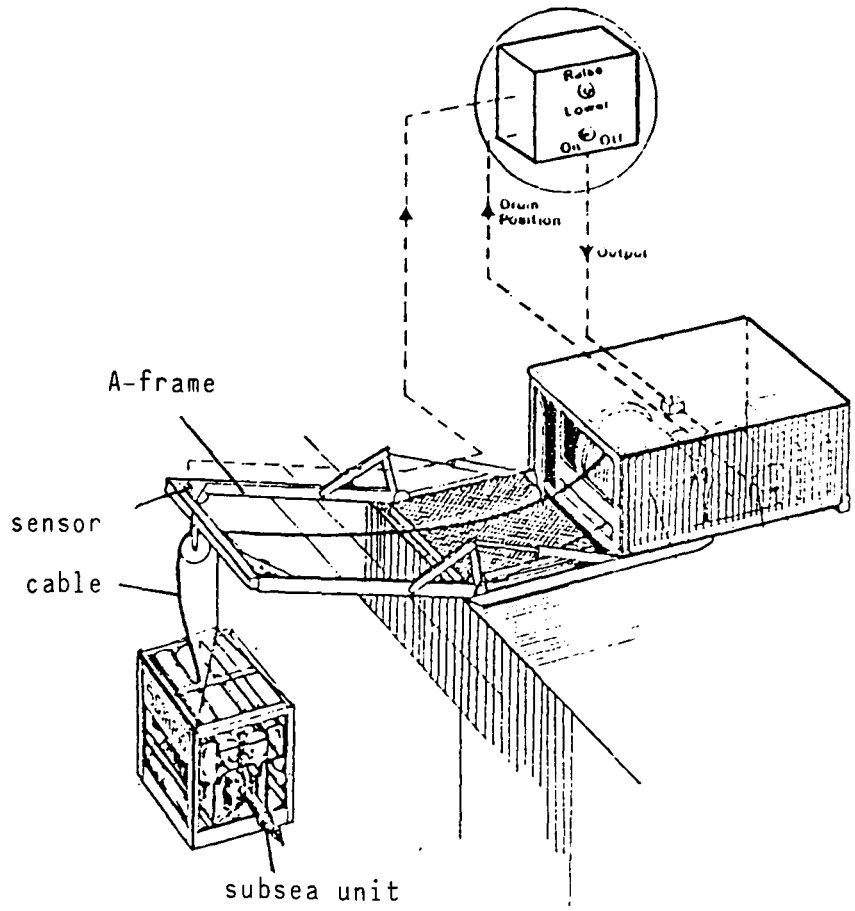
Raise
Lower
On
Off
Down
Position
Output
A-frame
sensor
cable
subsea unit

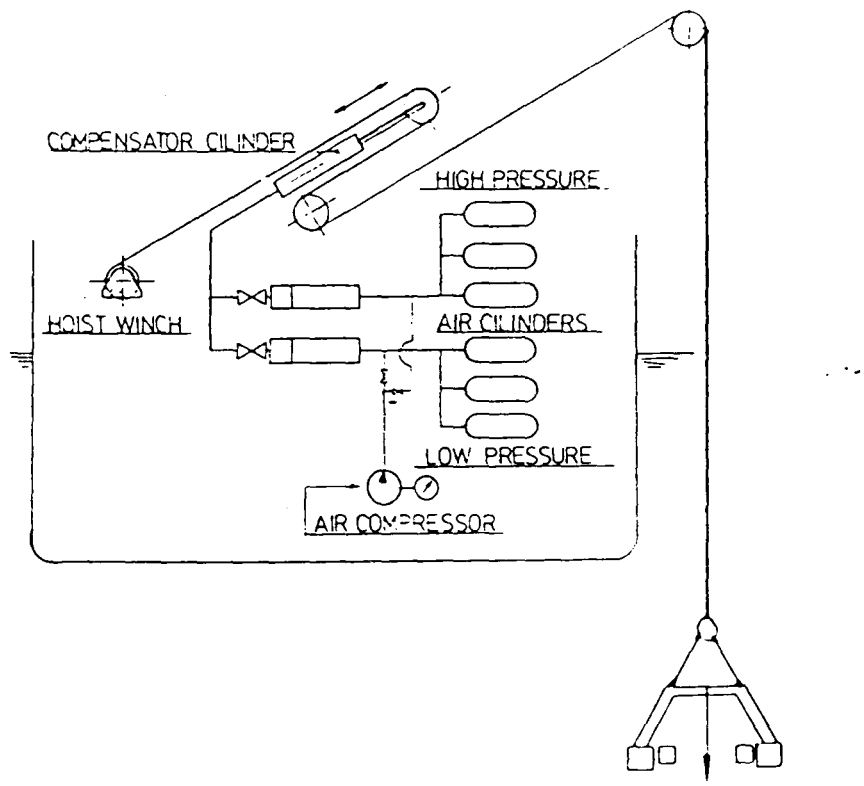
COMPENSATOR CILINDER
HIGH PRESSURE
HOIST WINCH
AIR CILINDERS
LOW PRESSURE
AIR COMPRESSOR

Figure 6.3

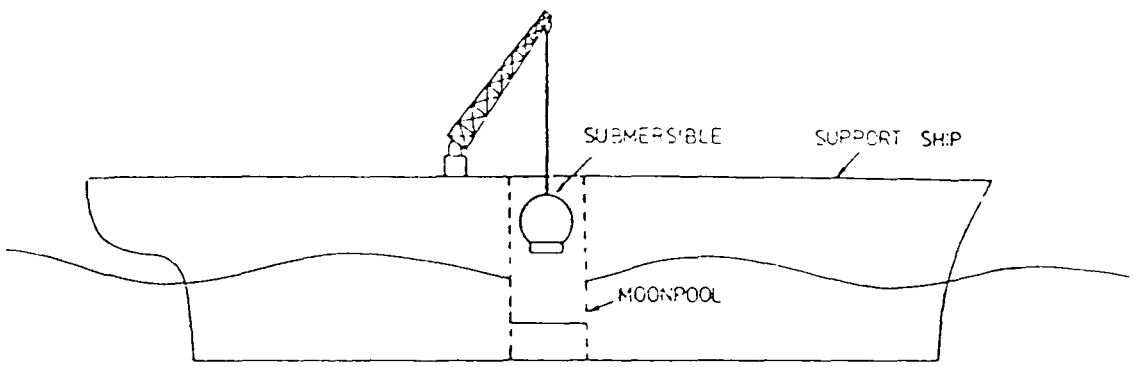

Figure 6.3 (continued)

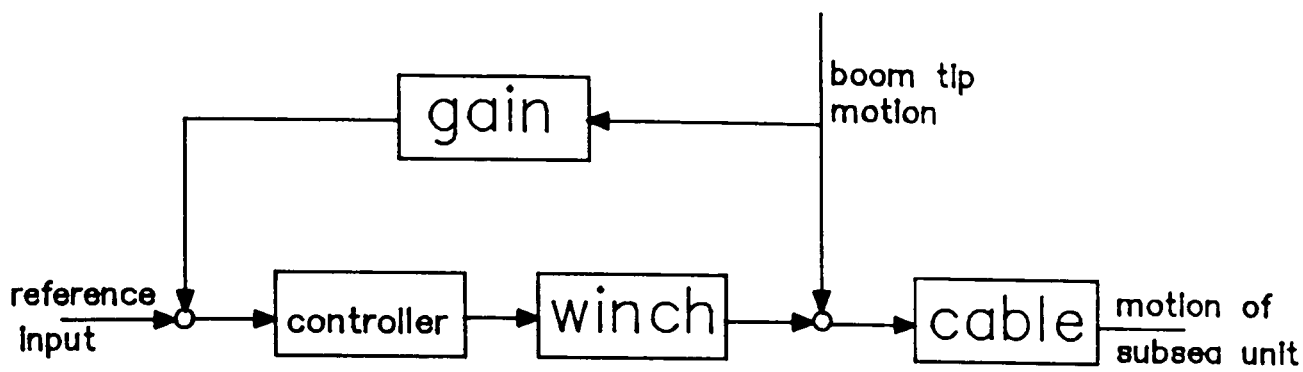

Figure 6.4

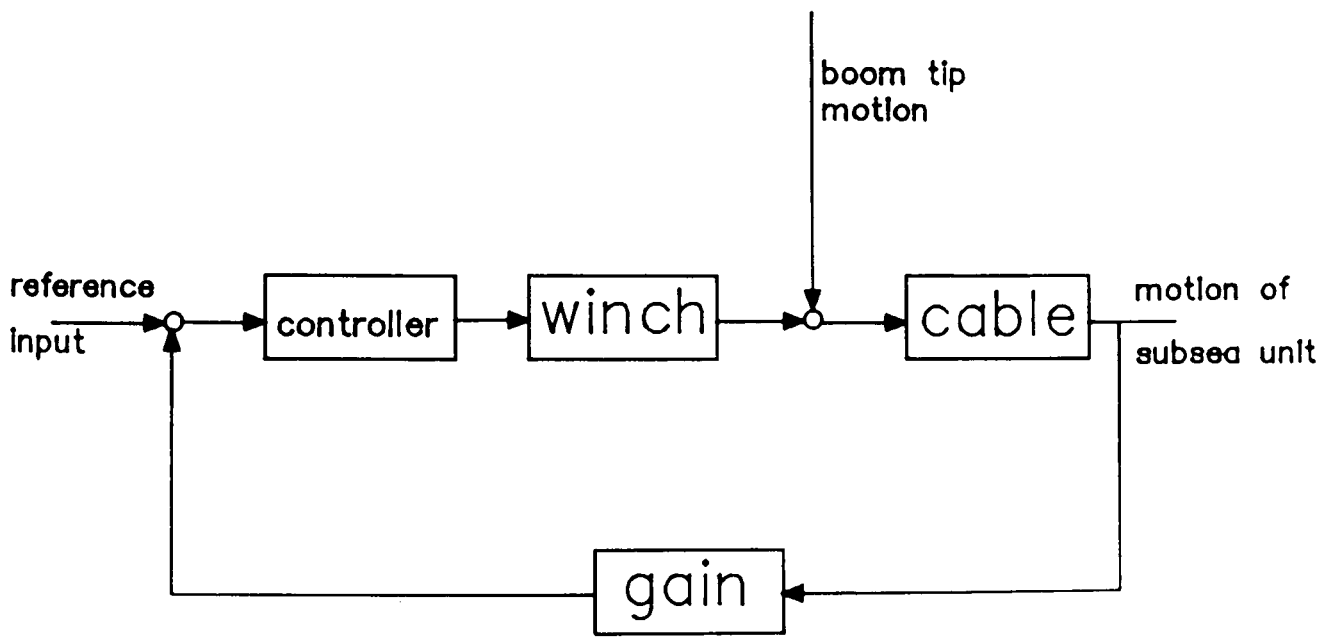

Figure 6.5

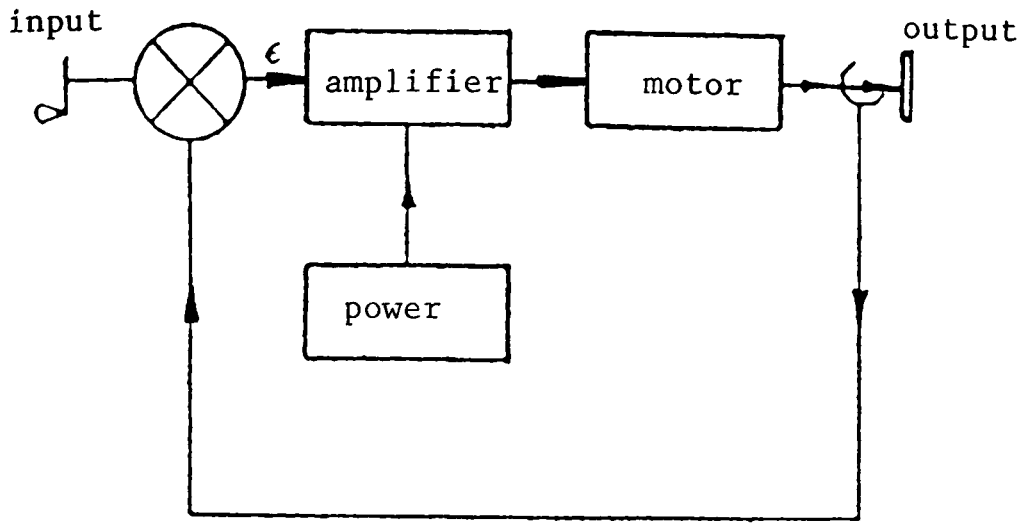

Figure 6.6

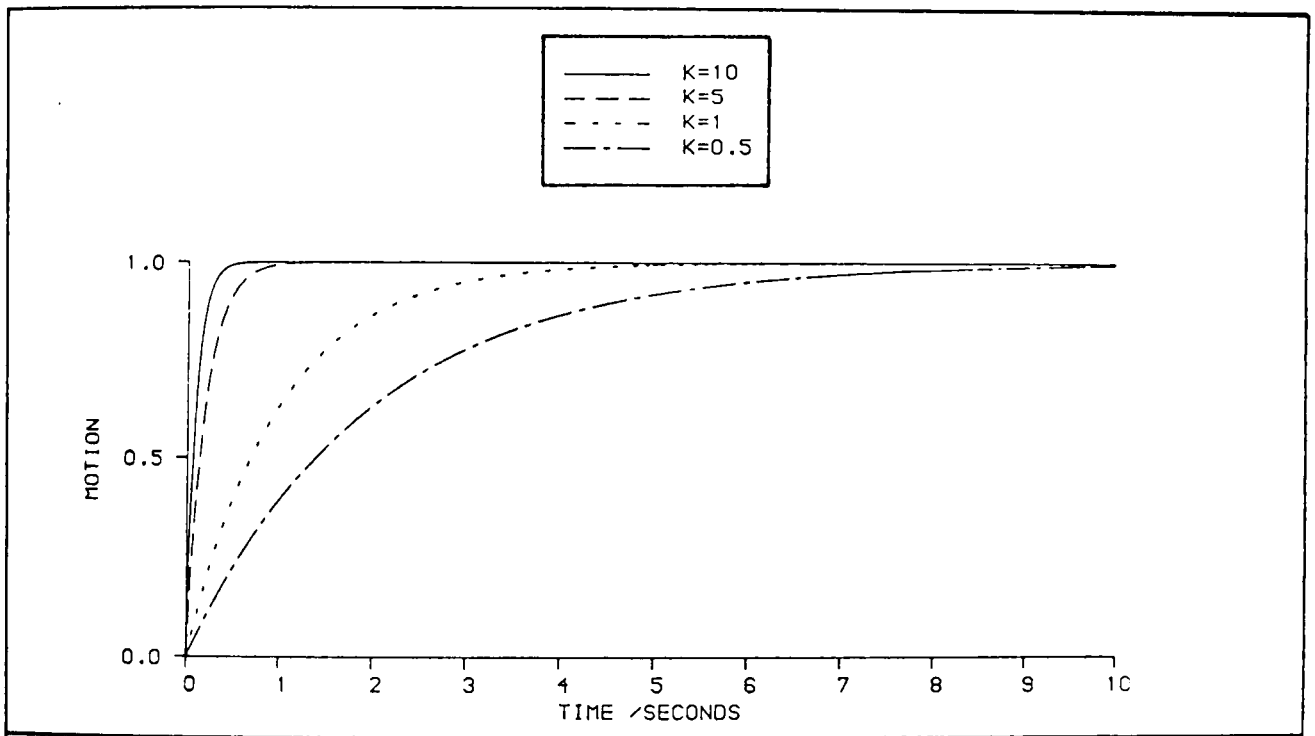

Figure 6.7 RESPONSE OF THE SIMPLE WINCH TO A STEP UNIT FUNCTION

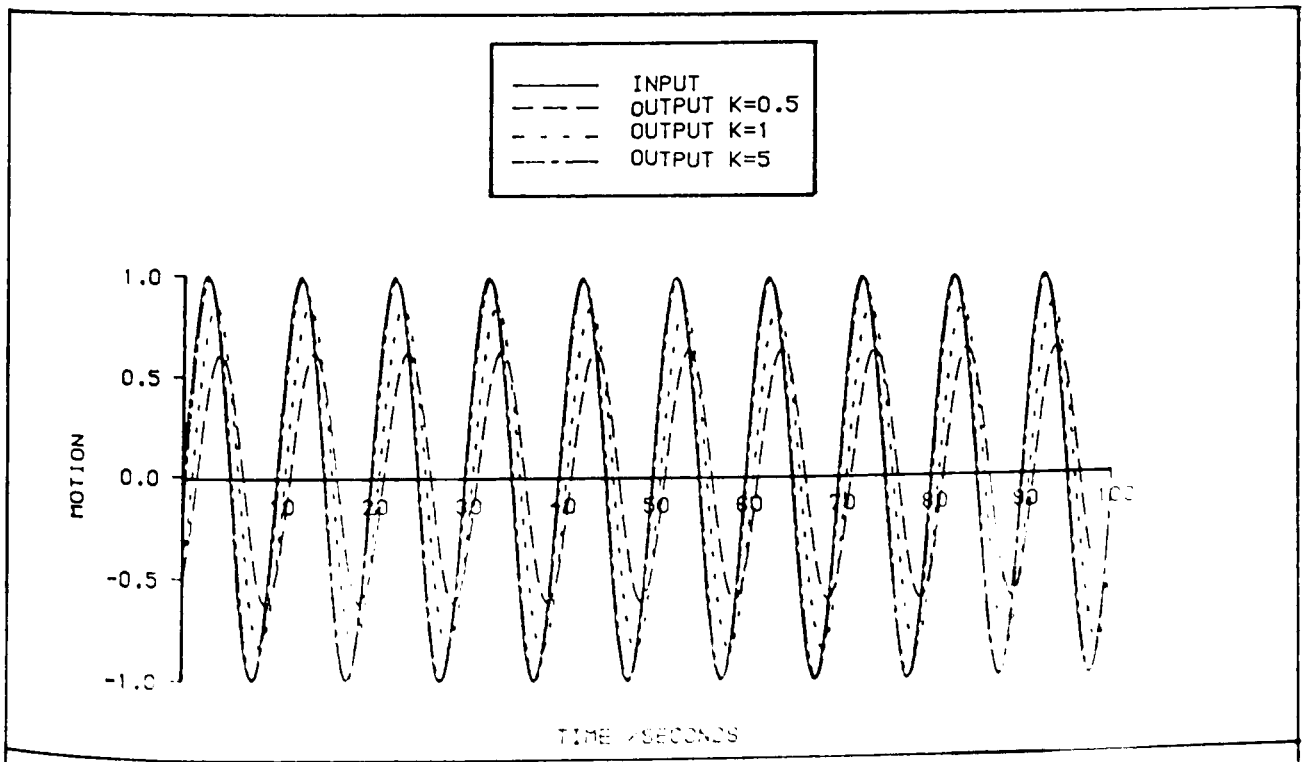

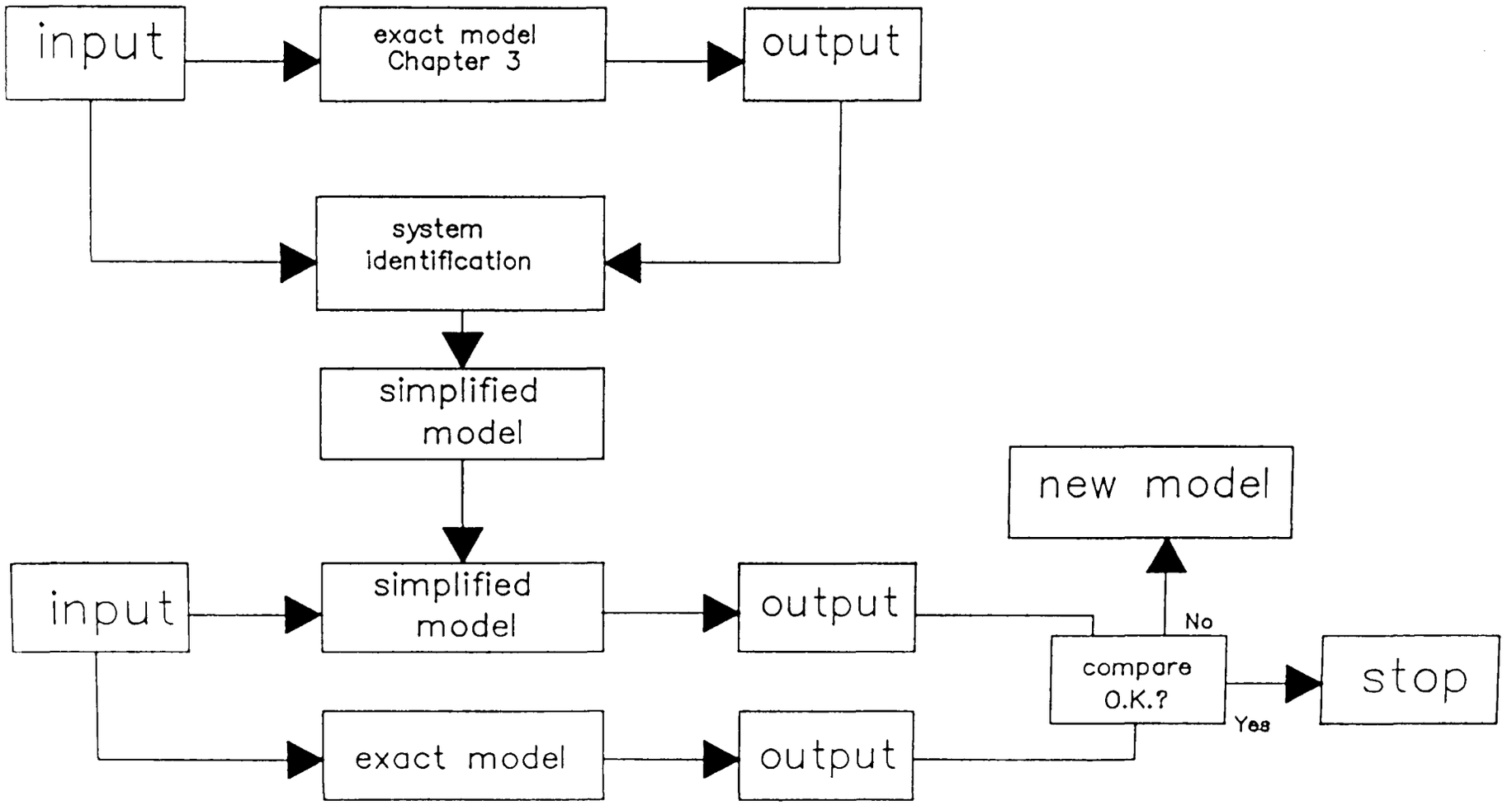
input
exact model
Chapter 3
output
system
identification
simplified
model
new model
input
simplified
model
output
No
compare
O.K.?
stop
Yes
exact model
output

Figure 6.9

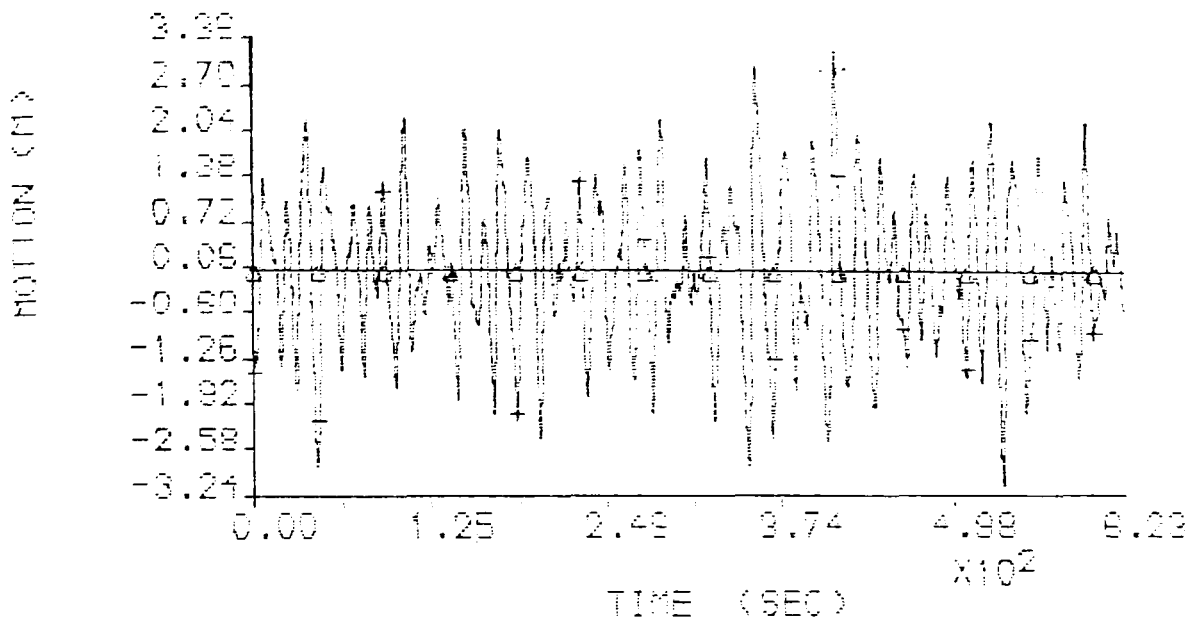

Figure 6.10

Boom tip motion defined by the Pierson-Moskowitz spectrum

(significant hight 6m: zero-crossing period 14s)

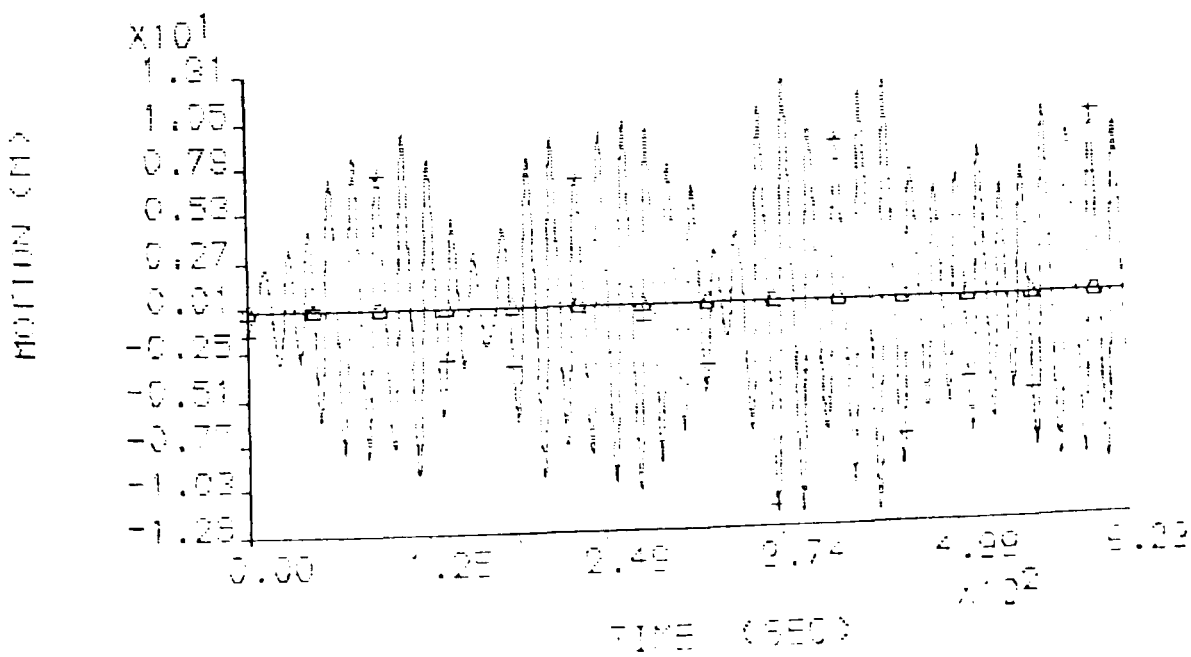

Figure 6.11

Response of the subsea unit calculated with a nonlinear hyperbolic equation

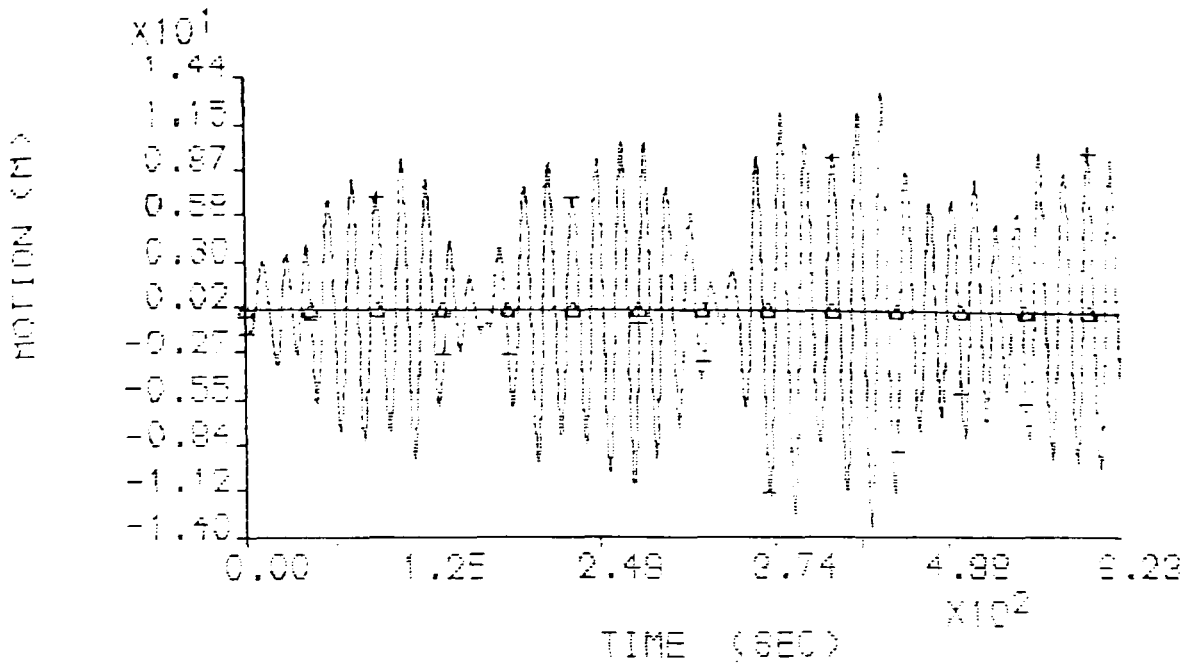

Figure 6.12

Reconstruction of the response

$7.339769\ddot{x} + 0.1996759\dot{x} + x = x_0$

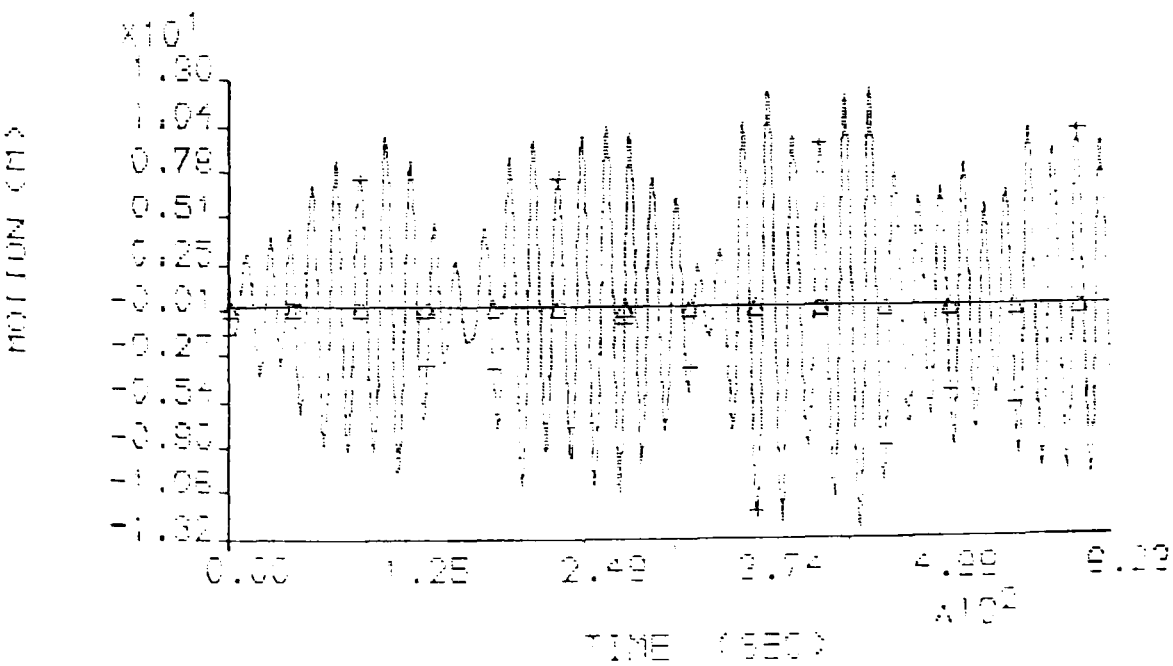

Figure 6.13

Reconstruction of the response

$7.3269444\ddot{x} + 0.0719096|\dot{x}|\dot{x} + x = x_0$

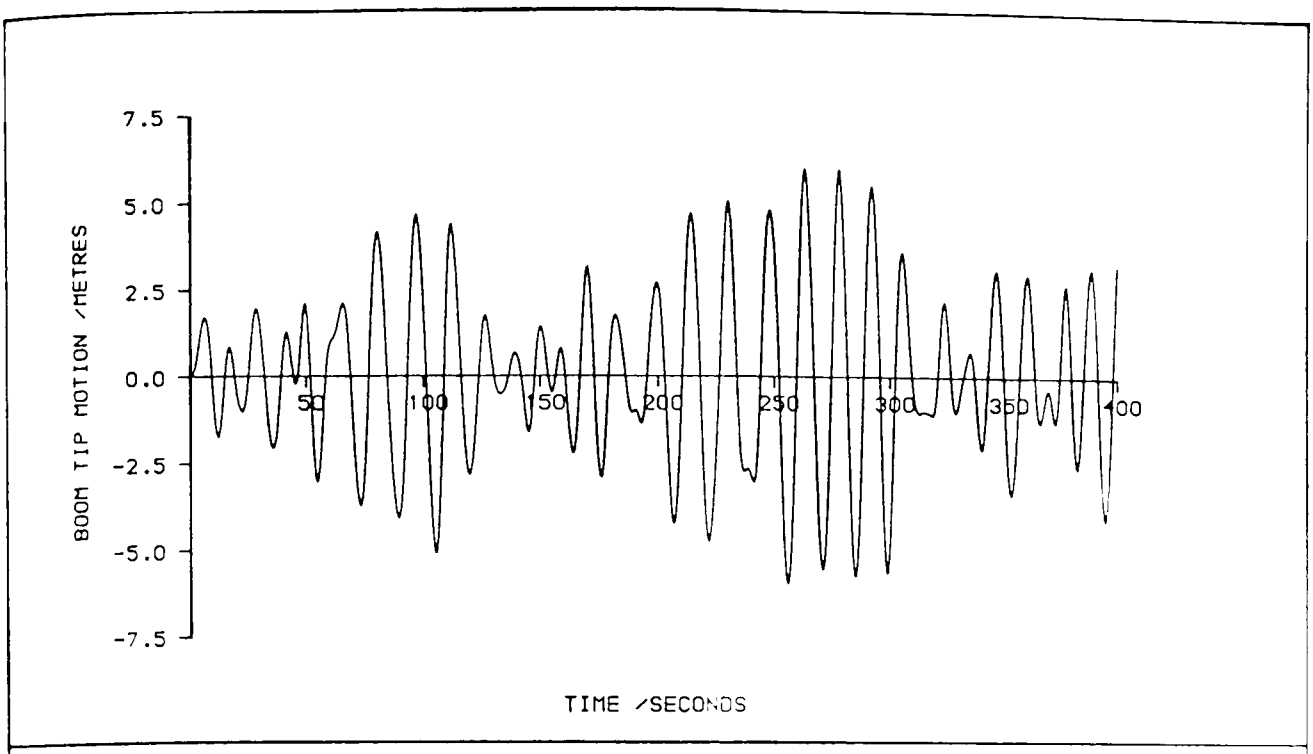

Figure 6.14 BOOM TIP MOTION

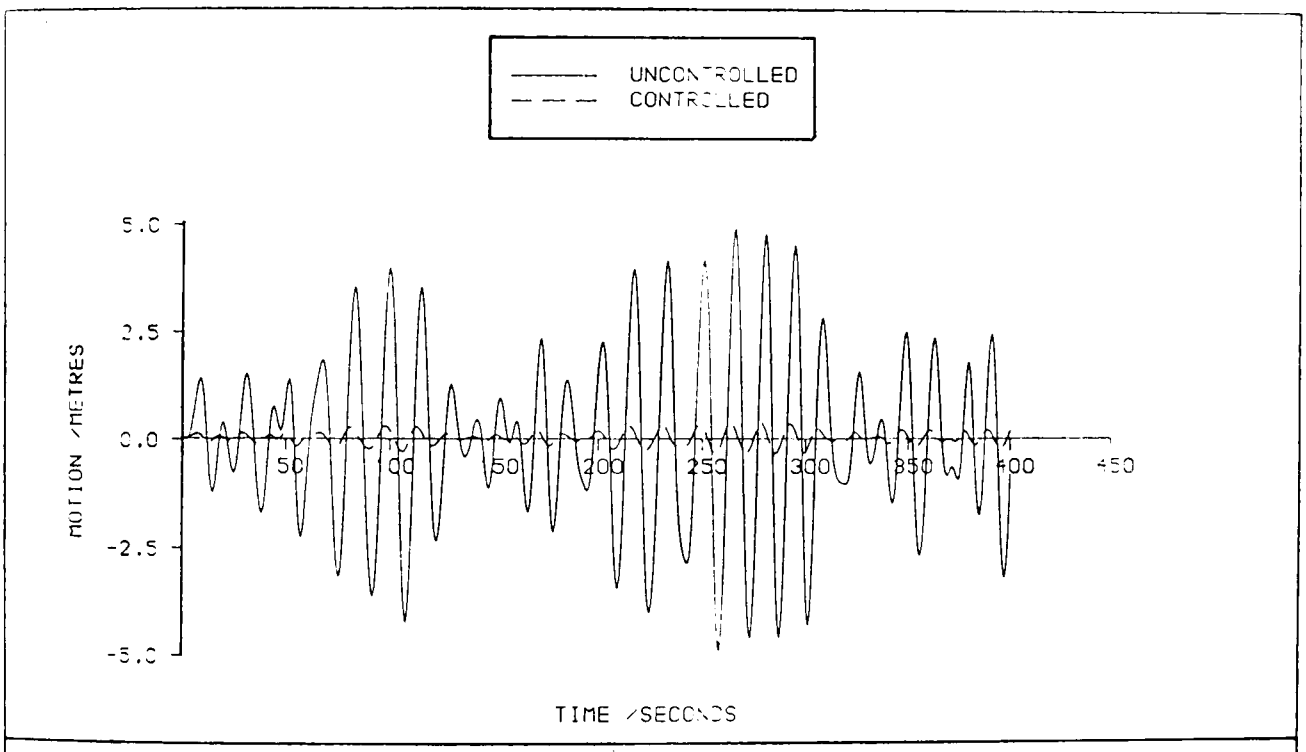

Figure 6.15 G=[93.944,41.41,5.166]

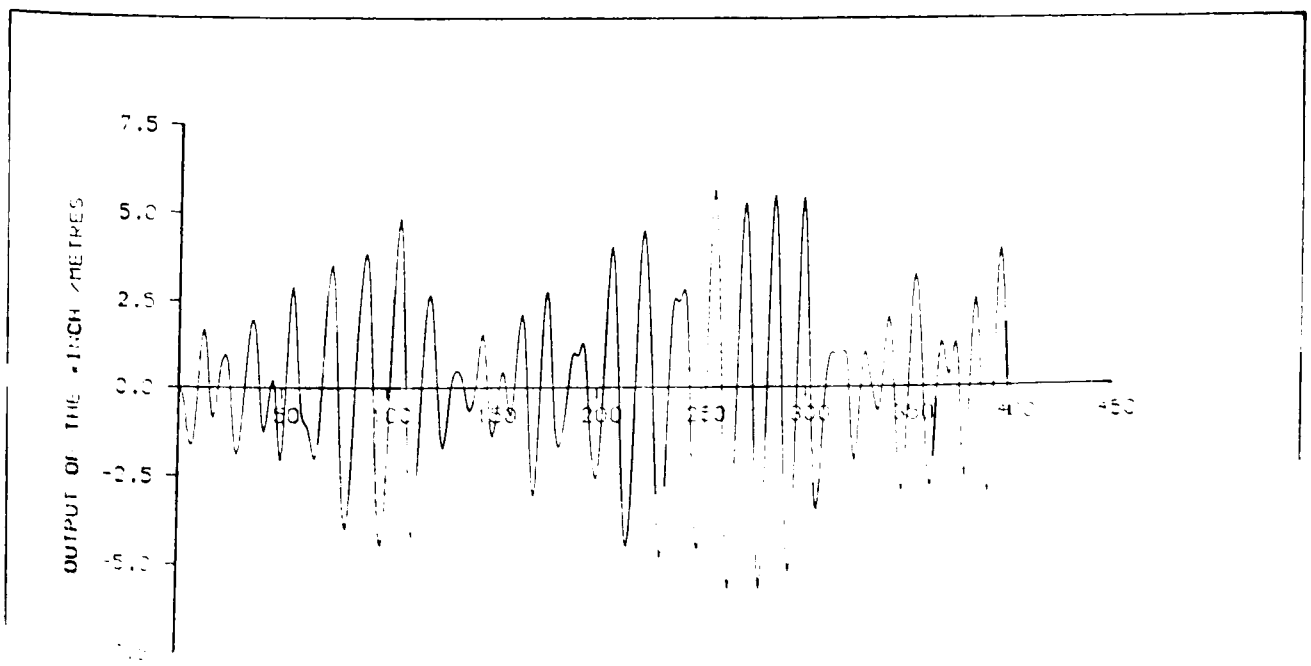

Figure 6.16 G=[93.944,41.41,5.166]

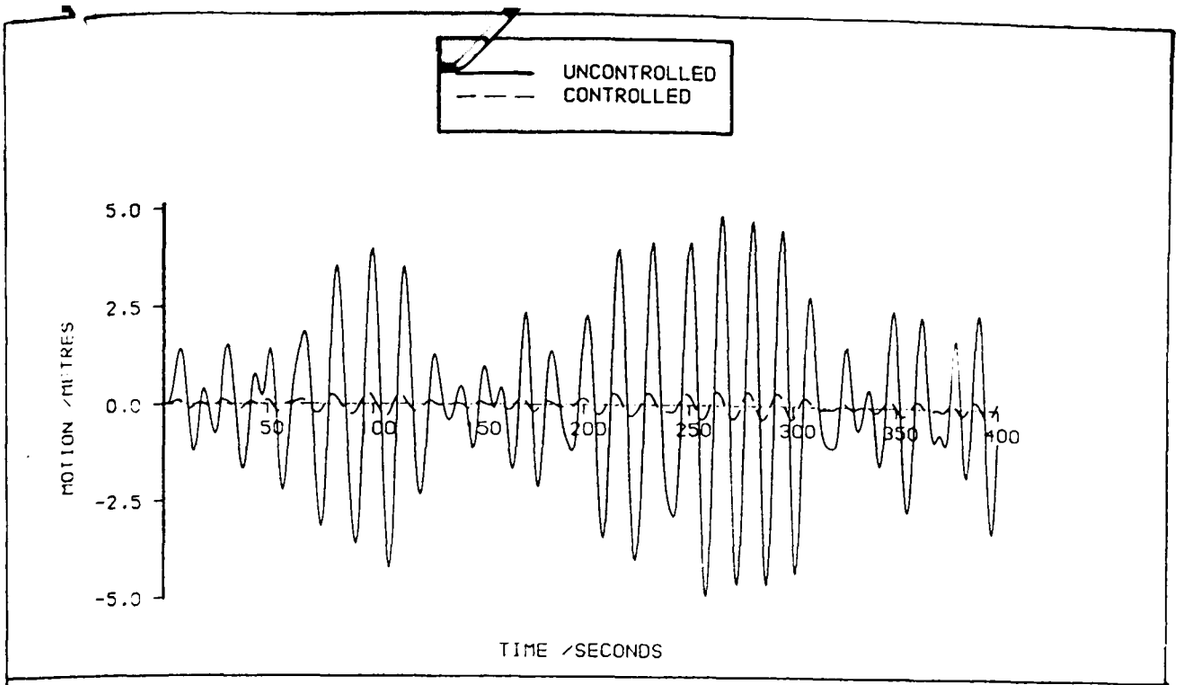

Figure 6.17 TIME DELAY = 0.2s; G=[296.97, 132.73, 15.95, 2.306, 0.164]

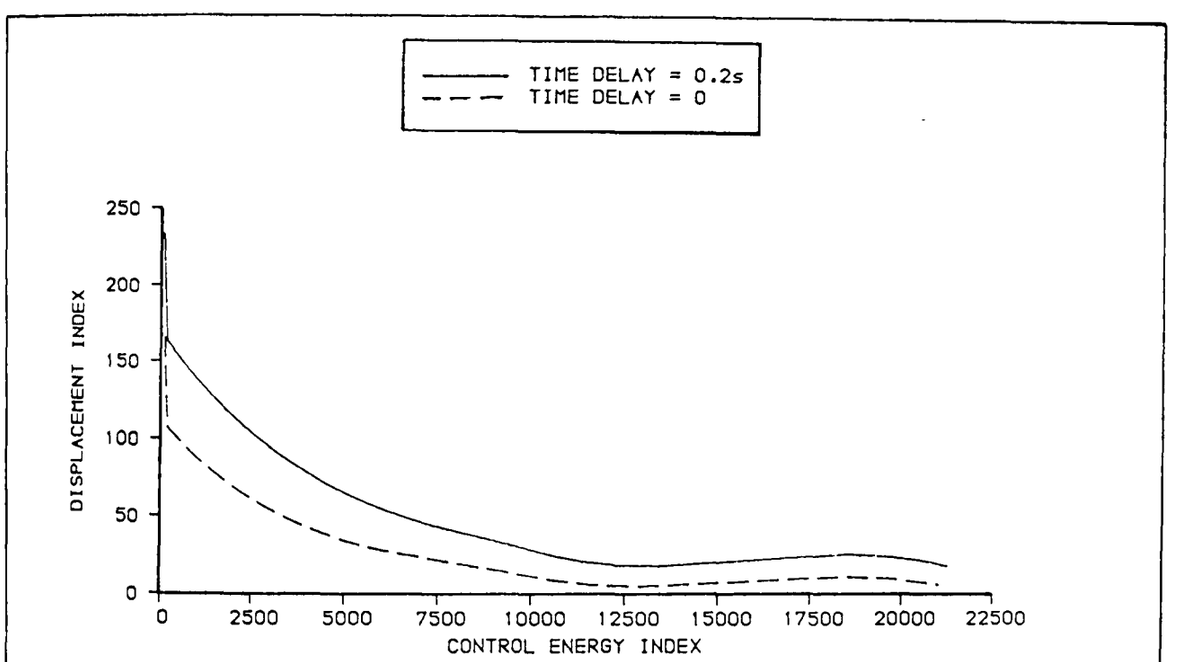

Figure 6.18 RELATION BETWEEN DISPLACEMENT AND CONTROL ENERGY INDICES

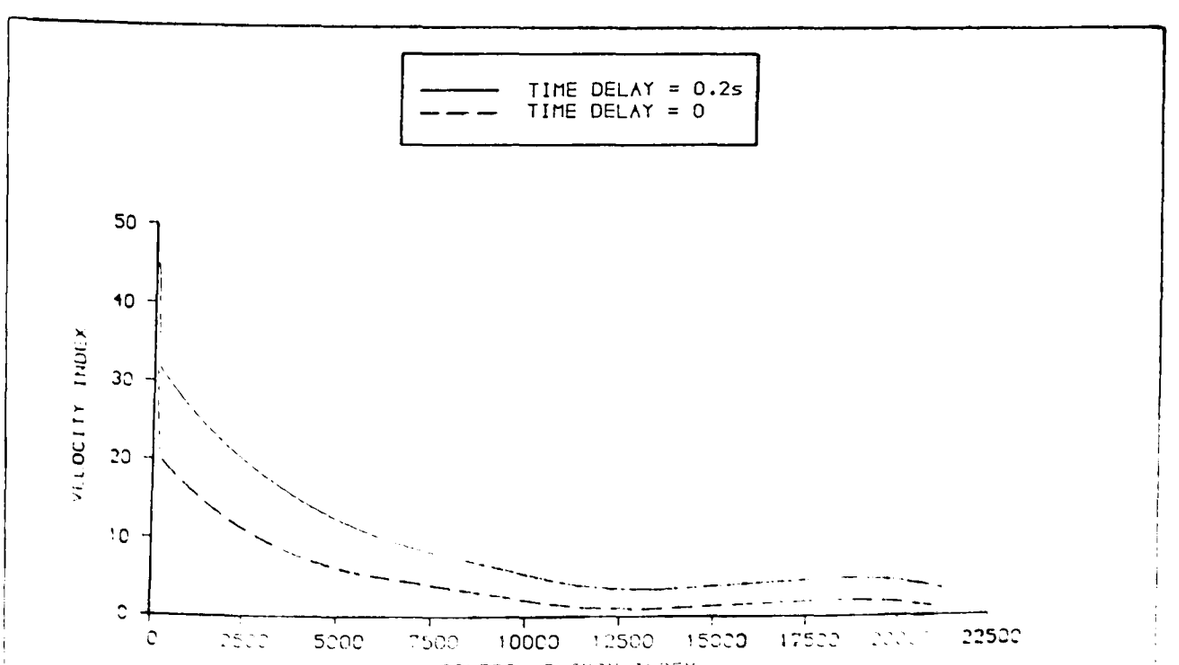

Figure 6.19 RELATION BETWEEN VELOCITY AND CONTROL ENERGY INDICES

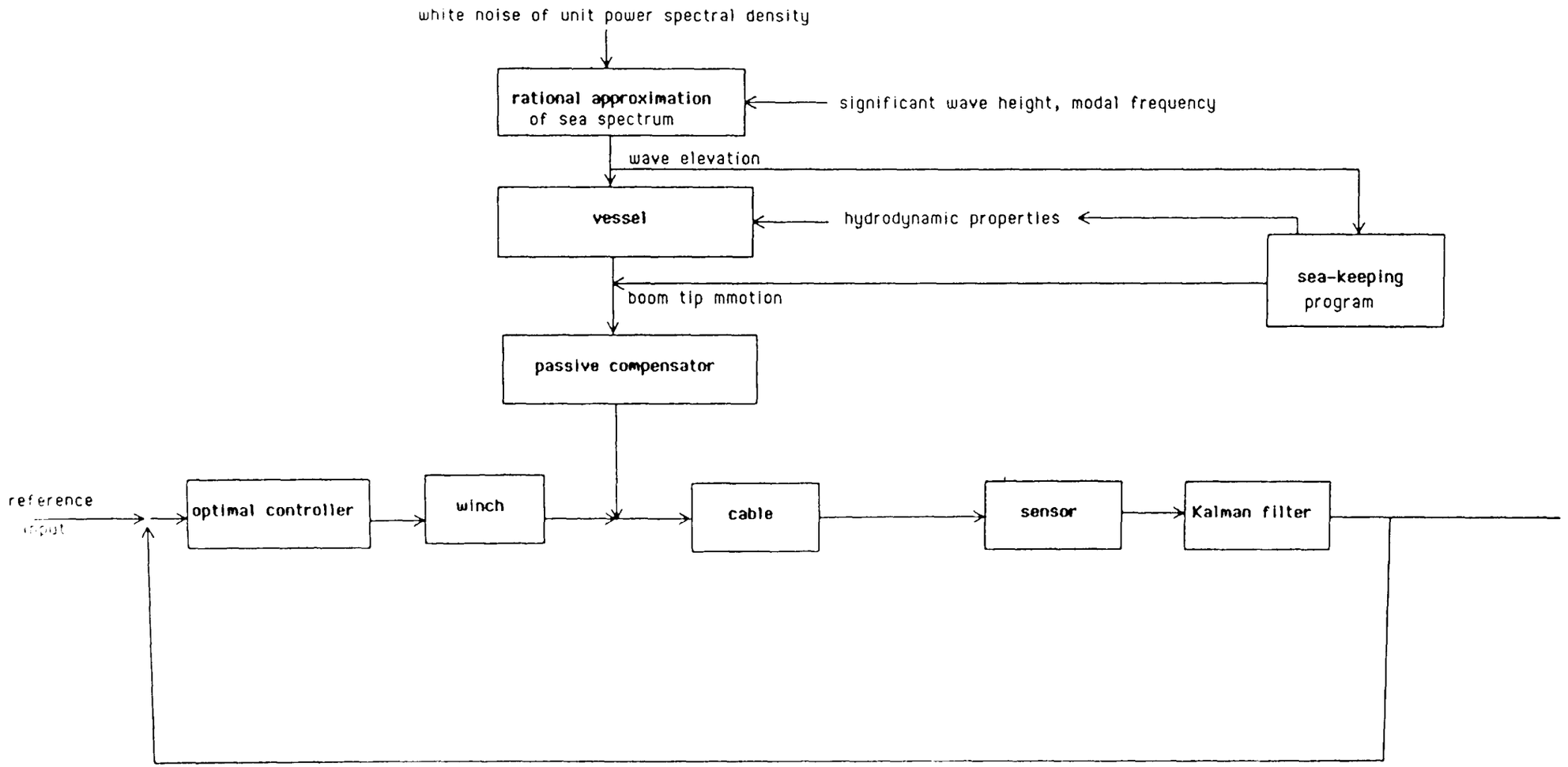
white noise of unit power spectral density
rational approximation of sea spectrum
significant wave height, modal frequency
wave elevation
vessel
hydrodynamic properties
sea-keeping program
boom tip mmotion
passive compensator
reference
optimal controller
winch
cable
sensor
Kalman filter

Figure 6.20

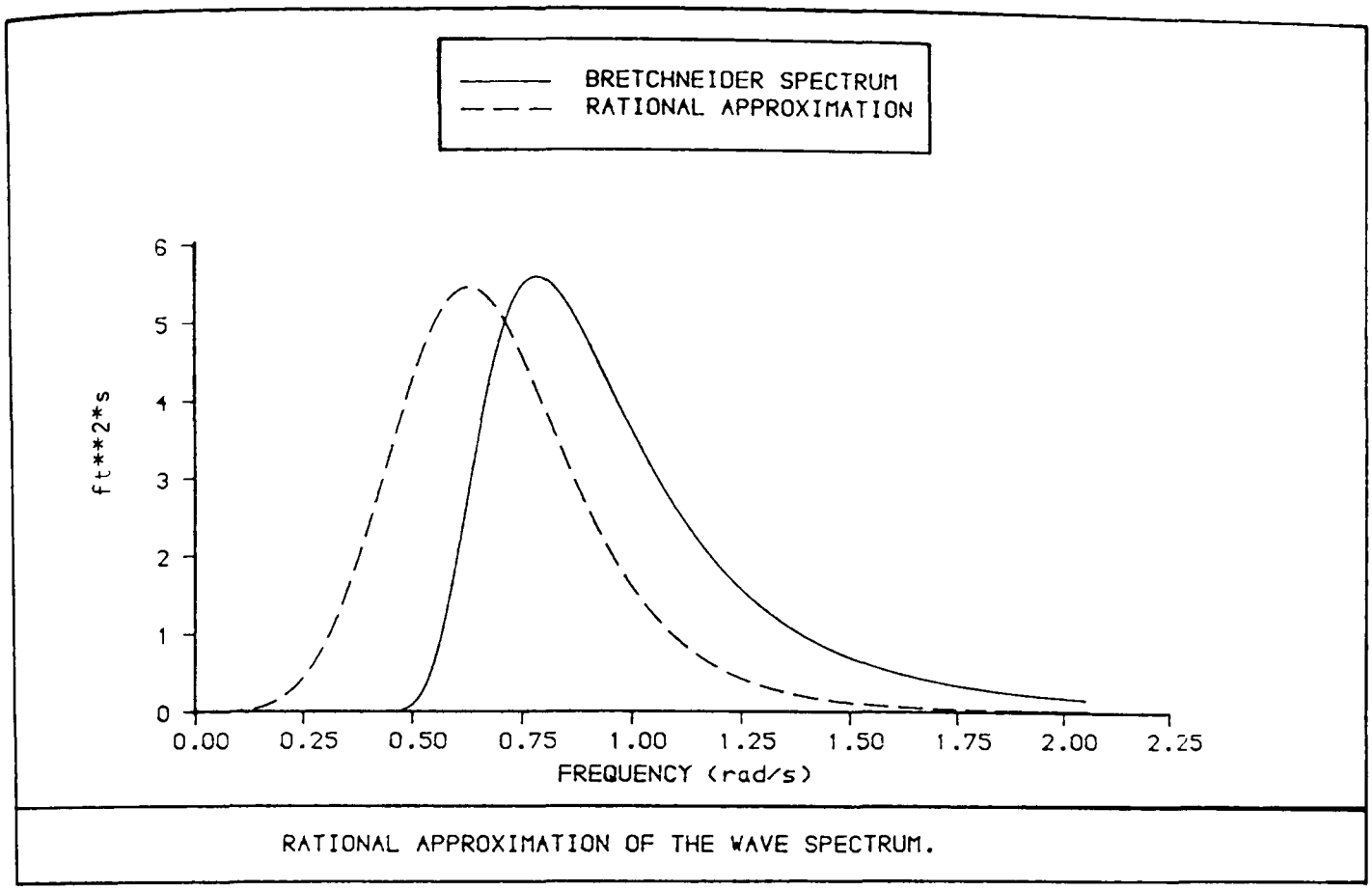

RATIONAL APPROXIMATION OF THE WAVE SPECTRUM.

Figure 6.21

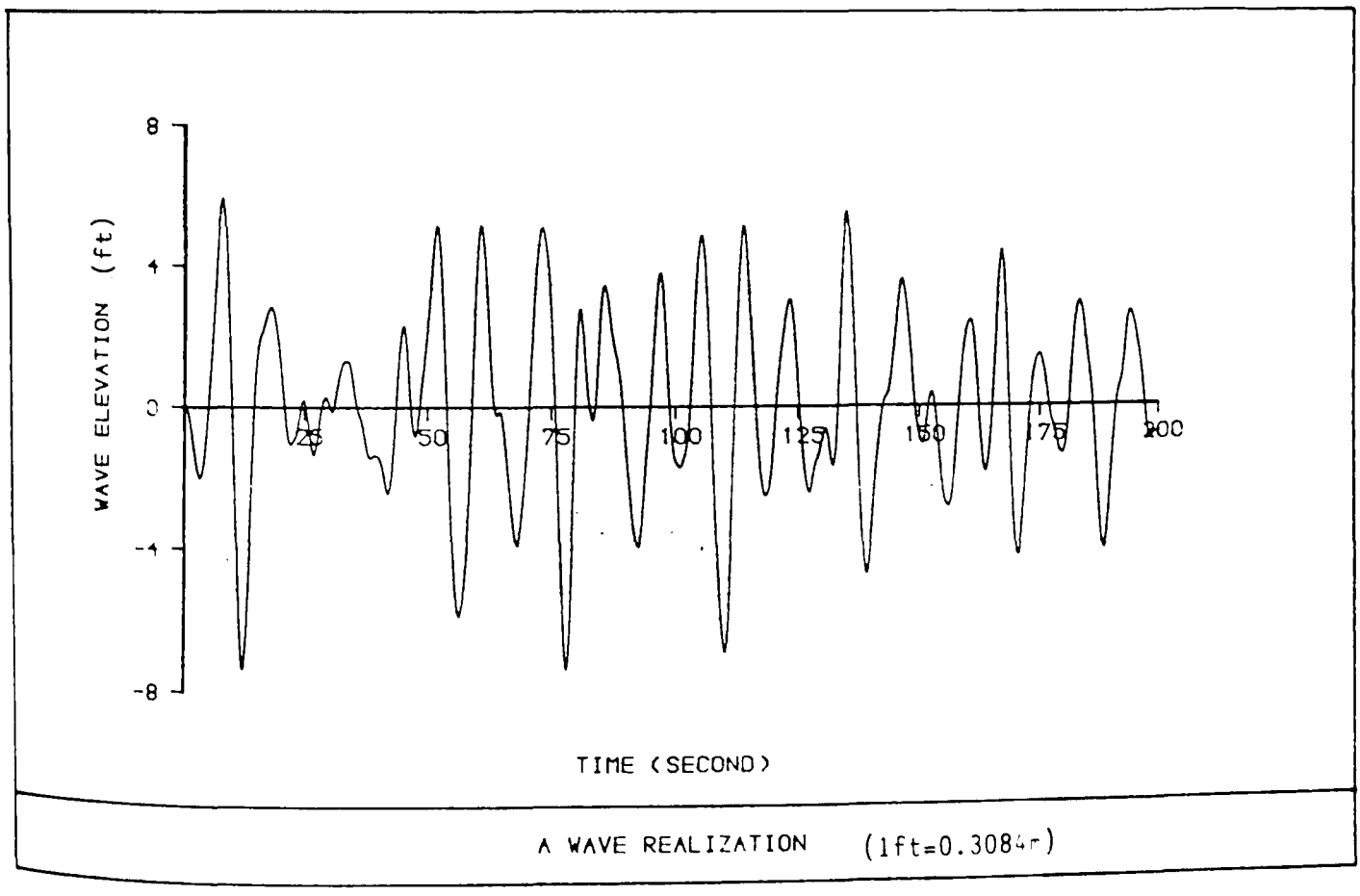

A WAVE REALIZATION (1ft=0.3084m)

Figure 6.22

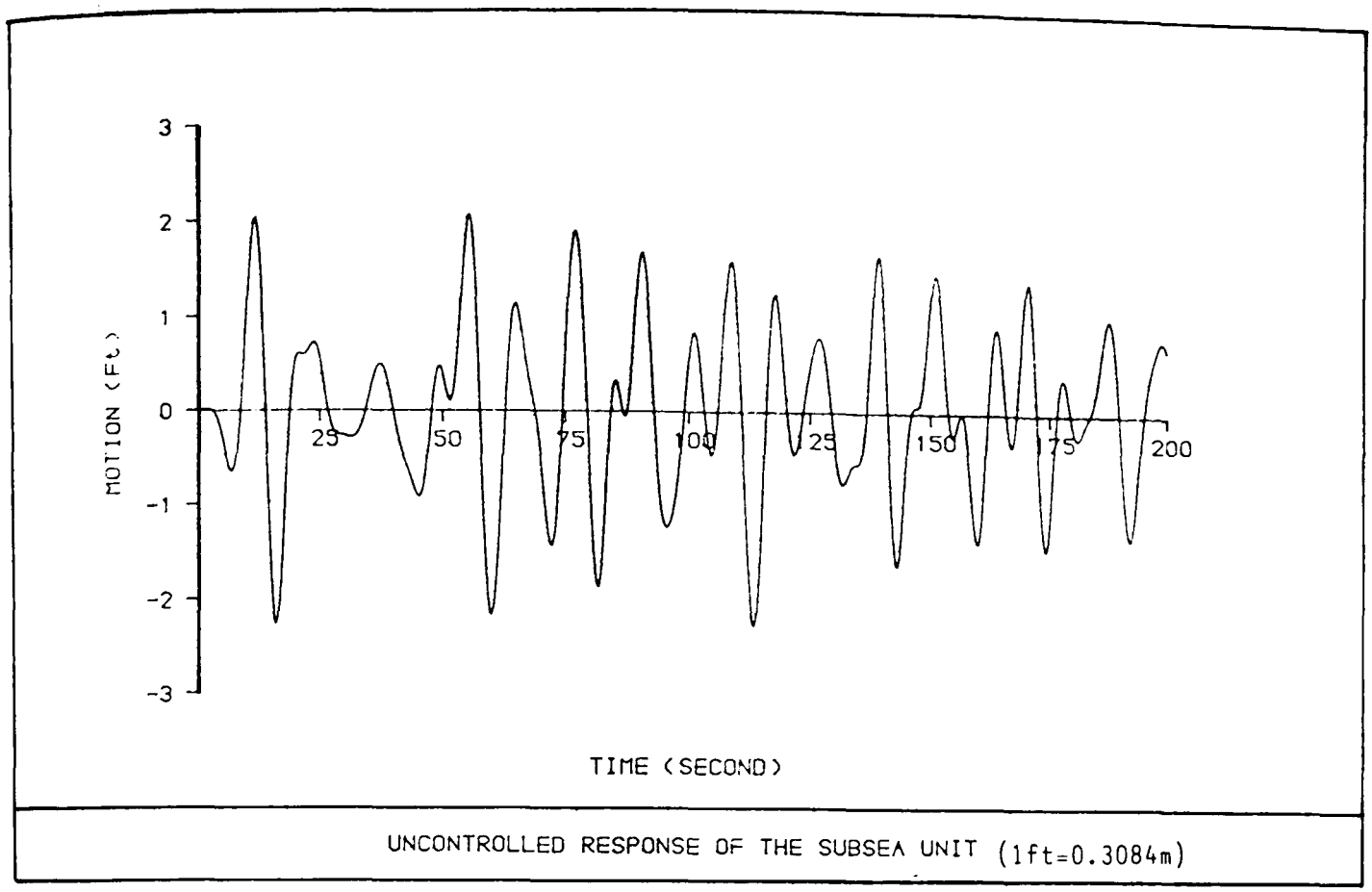

UNCONTROLLED RESPONSE OF THE SUBSEA UNIT (1ft=0.3084m)

Figure 6.23

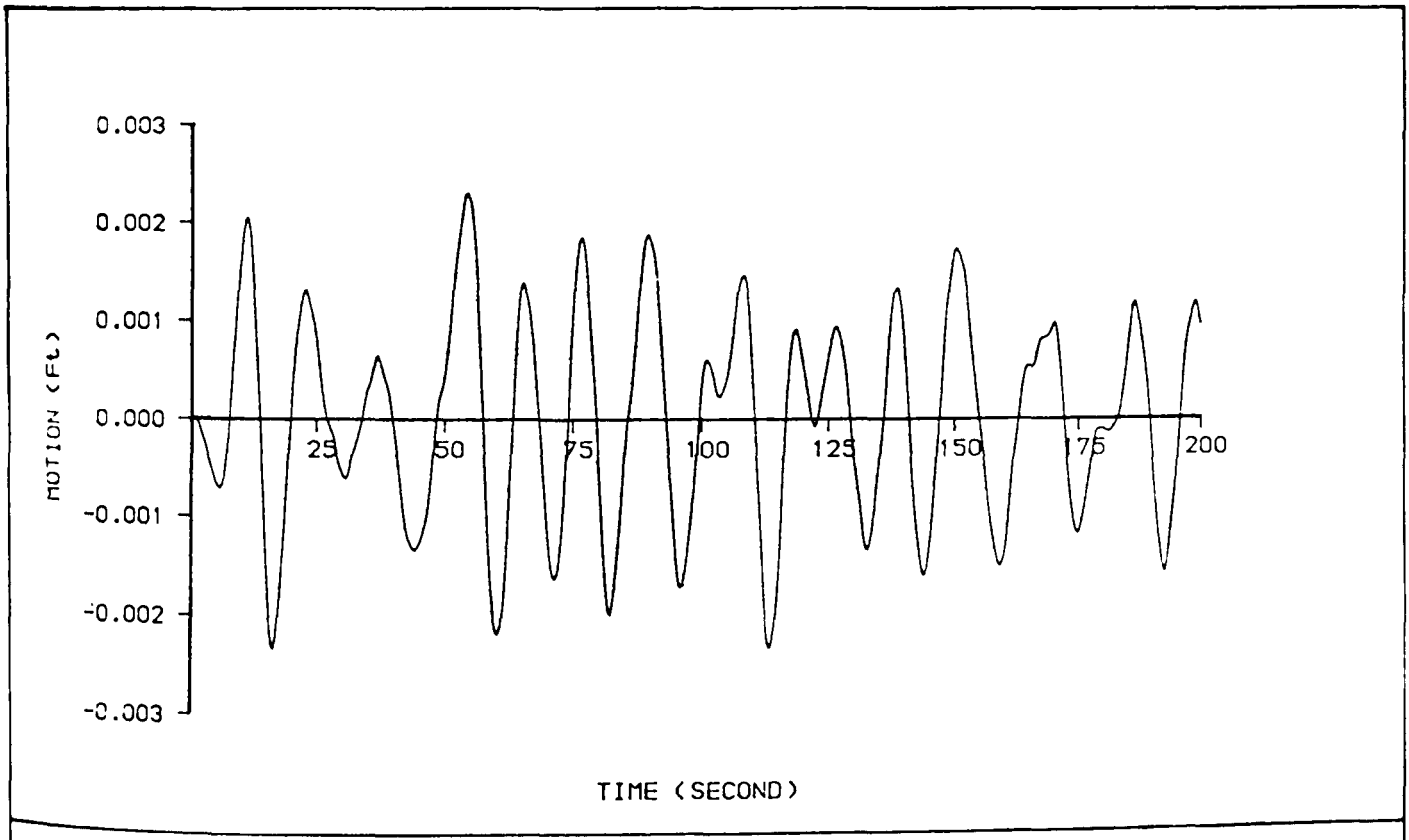

CONTROLLED RESPONSE OF THE SUBSEA UNIT (1ft=0.3084m)

Figure 6.24

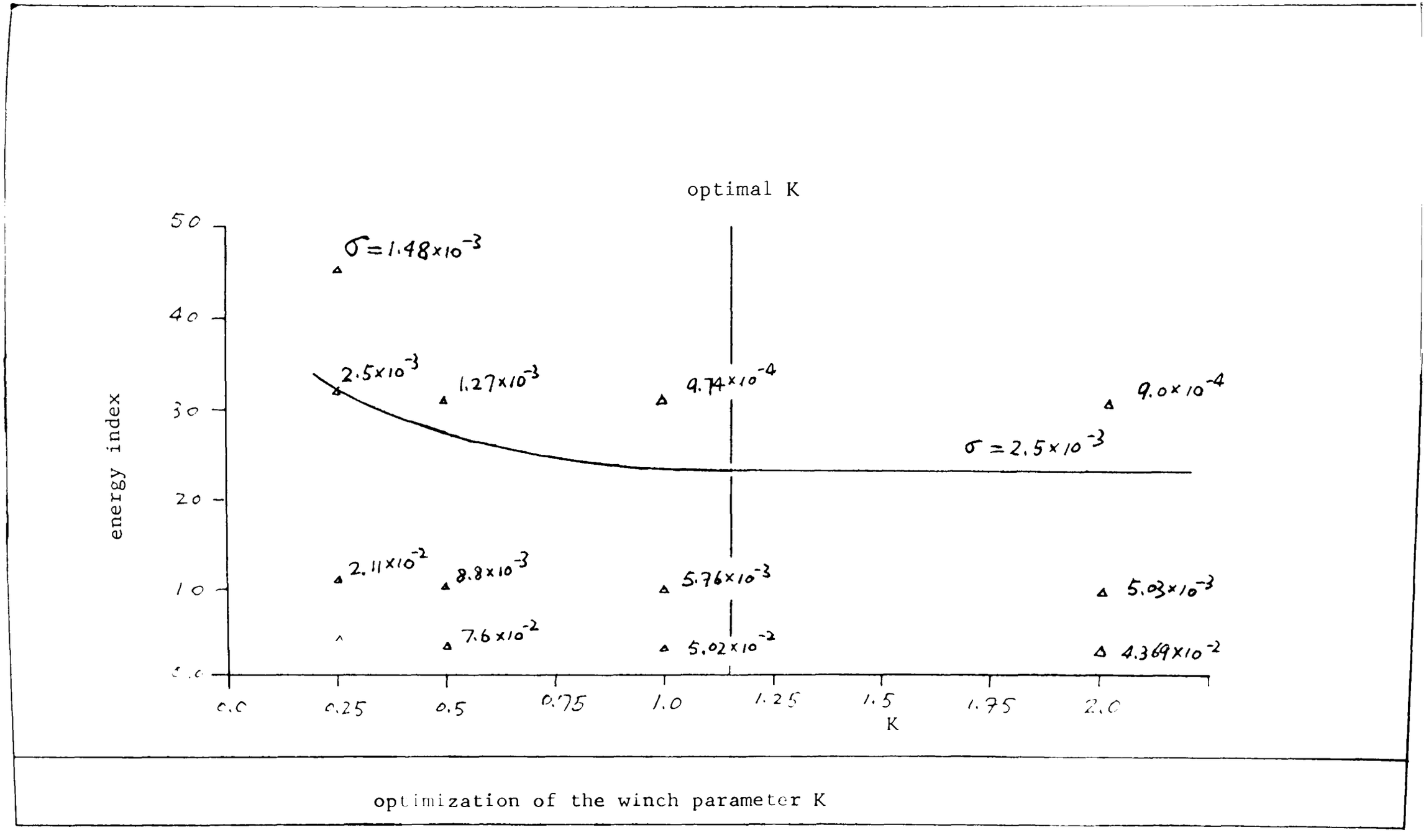

optimization of the winch parameter K

Figure 6.25

Chapter 7

DISCUSSION

A poem is never finished; it is only abandoned.

Paul Valéry

7.1 GENERAL REMARKS

From the beginning of this thesis, attention has been brought to focus upon the specific systems consisting of cables and subsea units which have wide applications in subsea intervention operations. Research work has then been carried out in this area, beginning with an assessment of the state of previous relevant work. This assessment has revealed an inadequate theoretical understanding towards the system on various aspects such as the unsteady dynamics and heave compensation.

It has been the aim of this thesis to improve our knowledge and provide some useful tools by which various aspects of the tethered-subsea-unit systems can be examined.

7.2 CONTRIBUTIONS OF THE THESIS

In the following areas lie the main contributions of this thesis:

7.2.1 Statics

The contribution in this area is of a technical rather than fundamental nature. The semi-analytic method developed in Chapter 2 has several advantages over others. In addition to its convenience in handling different types of boundary conditions, it uses less computational time and is highly accurate.

In the past, before the invention of the computer, researchers would try every mathematical tool available to find closed solutions to their problems. Since the computer entered daily research life, less and less attention has been paid towards analytical methods, numerical methods being adopted immediately after the establishment of governing equations. Just as school pupils indulging in the use of calculators find themselves poorer and poorer in the basics of arithmetic, this trend may prove detrimental to the advancement of research. A lot of successful examples have shown that a little more analytical consideration can make both the numerical computation easier and more effective, and the approach more beautiful.

7.2.2 Dynamics

The contribution in this area lies in the following aspects:

1. A Fresh start

   A general method, which has the capacity to handle both the steady and the

unsteady dynamics of a cable/subsea unit system, has been developed. This method gives an excellent quantitative understanding of the behaviour of the system. The method can be readily extended into three-dimensional space.

2. Rigorous analysis

   A rigorous analysis has been conducted to reveal fundamental characteristics of both the system and the mathematical models. Such analysis both enhances our understanding and is helpful in computation.

3. Package of software

   The suite of programs developed in the course of this thesis can be applied readily to various practical problems either to help in design or to supply information for operations.

7.2.3 Heave Compensation

The contribution of this thesis in this area lies in the novel idea of active heave compensation which can be put into practice in the near future. The research carried out in this thesis indicates the effectiveness of the method proposed.

7.3 RECOMMENDATIONS FOR FURTHER STUDIES

In addition to the refinement work suggested at the end of each chapter, the following topics are recommended for further studies:

1. As the current methods of estimating the hydrodynamic loadings upon both the cable and the subsea unit are mainly empirical and experimental, more theoretical research work should be directed towards this.

2. Naturally, further work can be done to extend the methodology presented in Chapters 3 and 4 into a three-dimensional case.

3. The problems of marine cable slack and the subsequent snap loading still remain unsolved. A possible approximation to this, which can be implemented into the present framework without significant alteration of the programs, is to propose a more general modulus Ξ in the place of the Young's modulus E by defining

$$\Xi = \begin{cases} E & tension > 0 \\ 10^{-20} & tension \leq 0 \end{cases}$$

4. In this thesis the main control parameter of the active heave compensation is the position of the subsea unit. The tension in the cable is not considered since we assume that high tension will be prevented by a passive compensator. Further work is needed to both investigate a passive compensator and integrate the passive one with the active one proposed here.

5. Work can be continued to extend the present methodology of heave compensation into the unsteady situation where the cable is being paid out or hauled in

at a constant speed.

6. Finally, endless effort can be made to refine the various numerical algorithms used in this thesis.

Chapter 8

CONCLUSIONS

Last scene of all,
That ends this strange eventful history,
Is second childishness and mere oblivion,
Sans teeth, sans eyes, sans taste, sans everything.

W. Shakespeare: *As you like it*

Based upon the investigations described in this thesis, the following conclusions can be drawn:

1. A highly accurate and efficient method has been developed which can be used to predict three-dimensional static configurations of marine cables. The method is based upon a semi-analytic solution of the governing equation.

2. A novel numerical approach has been developed which can be used to predict one-dimensional dynamic behaviour of systems of cables and subsea units. This method can handle the unsteady dynamics, where the length of cable varies, and

steady dynamics, where the length is fixed, in a uniform manner by introducing a coordinate transformation.

3. This idea of coordinate transformation has been further extended into more general two-dimensional cases. Theoretical analysis has revealed the relation between the one-dimensional and two-dimensional approximations.

4. In the three-dimensional case, dynamic behaviour of cable/subsea unit systems has been studied by a lumped-mass model. The proposed numerical integration scheme is unconditionally stable. Theoretical analysis has shown that the model exhibits high-frequency cut-off.

5. By applying modern control theories, an actively controlled heave compensation mechanism has been developed.

REFERENCES

1. Ablow, C. M. and Schechter, S., 'Numerical Simulation of Undersea Cable Dynamics', Ocean Engineering, Vol. 10, No. 6, 1983

2. Ahmadi-Kashani, K., 'Vibration of Hanging Cables', Computers & Structures, Vol.31, No.5, 1989

3. Airy, G. B., 'On the Mechanical Conditions of the Deposit of a Submarine Cable', Philosophical Magazine and Journal of Science, Fourth Series, Vol.16, No.14, 1858

4. Ali, S. A., 'Dynamic Response of Sagged Cable', Computers & Structures, Vol.23, 1986

5. Allgower, E. and Georg, K., Numerical Continuation Methods, Springer-Verlag, 1990

6. Ames, W. F., Numerical Methods for Partial Differential Equation, Thomas Nelson and Sons Ltd, 1969

7. Anderson, B. D. O., 'Second-Order Convergent Algorithms for the Steady-State Riccati Equation', International Journal of Control, Vol.28, No.2, 1978

8. Argyris, J. H., Angelopoulis, T. and Bichat, B., 'A General Method for the Shape Finding of Lightweight Tension Structures', Computer Methods in Applied Mechanics and Engineering, Vol.3, 1974

9. Athans, M., 'The Role and Use of the Stochastic Linear-Quadratic-Gaussian Problem in Control System Design', IEEE Transactions on Automatic Control, Vol. AC-16, No. 6, 1971

10. Balzer, L. A., 'Accelerated Convergence of the Matrix Sign Function Method of Solving Lyapunov, Riccati and Other Matrix Equations', International Journal of Control, Vol.32, No.6, 1980

11. Benedettini, F. and Rega, G., 'Nonlinear Dynamics of an Elastic Cable Under Plannar Excitation', International Journal of Non-linear Mechanics, Vol.22, No.6, 1987

12. Berteaux, H. O., Buoy Engineering, John Wiley & Sons, 1976

13. Bettles, R. W. and Chapman, D. A., 'The Experiment Verification of a Towed Body and Cable', Ocean Engineering, Vol.12, No.5, 1985

14. Borrie, J. A., Modern Control Systems: A Manual of Design Methods, Prentice/Hall International, 1986

15. Bryson, A. E. and Ho, Yu-chi, Applied Optimal Control, Hemisphere Publishing Corporation, 1975

16. Buchholdt, H. A., Introduction to Cable Roof Structures, Cambridge Universty Press, 1985

17. Burgess, J. J., 'Natural Modes and Impusive Motions of a Horizontal Shallow Sag Cable', Ph.D. Thesis, Department of Ocean Engineering, MIT, 1985

18. Burgess, J. J., 'Modeling of Undersea Cable Installation with a Finite Difference Method', Proceeding of International Offshore and Polar Engineering Conference, Edingburgh, 1991

19. Carrier, G. F., 'On the Non-linear Vibration Problem of Elastic String', Quarterly Journal of Applied Mathematics, Vol. 3, No. 2, 1945

20. Carrier, G. F., 'A Note on the Vibrating String', Quarterly Journal of Applied Mathematics, Vol. 7, No. 1, 1949

21. Choo, Y-I. and Casarella, M. J., 'A Survey of Analytical Methods for Dynamic Simulation of Cable-Body Systems', Journal of Hydronautics, Vol.7, No.4, 1973

22. Chung, J. S. and Whitney, A. K., 'Axial Stretching Osillation of an 18,000-ft Vertical Pipe in the Ocean', Journal of Energy Resources Technology, Vol.105, 1983

23. Courant, R., Issacson, E. and Rees, M., 'On the Solution of Nonlinear Hyperbolic Differential Equtaions by Finite Differences', Communications on Pure and Applied Mathematics, Vol.5, 1952

24. Crank, J., Free and Moving Boundary Problems, Clarendon Press, Oxford, 1984

25. Cristescu, N., Dynamic Plasticity, North-Holland Publishing Company, Amsterdam, 1967

26. Cruickshank, M. J. and Hess, H. D., 'Marine Sand and Gravel Mining', in R. E. Osgood (ed.), Toward a National Ocean Policy, John Hopkins University Press, Baltimore, 1976

27. Dand, I. and Every, M. J., 'An Overview of the Hydrodynamics of Umbilical Cables and Vehicles', Proceedings of SUBTECH'83, London, 1983

28. Davies, M. E., Daniel, A. P. and Osbourne, J., 'The Drag and Motion of a Model Umbilical Cable in a Steady Current', National Maritime Report, 1983

29. Day, A. H., 'An Integrated Approach to the Design of Moonpools for Subsea Operations', Ph.D. Thesis, Marine Technology Centre, University of Strathclyde, 1987

30. DeLaurier, J. D., 'A First Order Theory for Predicting the Stability of Cable Towed and Tethered Bodies Where the Cable Has a General Curvature

and Tension Variation', Technical Note 68, von Karman Institute for Fluid Dynamics, Belgium, 1970

31. Delmer, T. N., 'Numerical Simulation of Cable-Towed Acoustic Arrays', Ocean Engineering, Vol.15, No.6, 1988

32. Denman, E. D., 'The Matrix Sign Function and Computations in Systems', Applied Mathematics and Computation, Vol.2, 1976

33. Dodd, R. K., Eilbeck, J. C., Gibbon, J. D. and Morris, H. C., Solitons and Nonlinear Wave Equation, Academic Press, 1982

34. Dominguez, R. F. and Smith, D. E., 'Dynamic Analysis of Cable System', Journal of the Structural Division, ASCE, Vol.98, No.ST8, 1972

35. Dutta, D., 'Dynamics of Tethered Subsea Units During Launch/Recovery Through the Sea-Air Interface', Ph.D. Thesis, Marine Technology Centre, University of Strathclyde, 1986

36. Eames, M. C., 'Steady-State Theory of Towing Cable', Trans. RINA, Vol.110, 1968

37. Ertas, A. and Kozik, T. J., 'Numerical Solution Techniques for Dynamic Analysis for Marine Riser', Journal of Energy Resources Technology, Vol.109, 1987

38. Every, M. J., 'A Computer Program for the Static Analysis of Umbilical Cables to Undersea Remotely Operated Vehicles', BHRA Project 21708, The British Hydrodynamics Research Association, England, 1982

39. Ferriss, D. H., 'Numerical Determination of the Three-Dimensional Equilibrium Configuration of an Underwater Umbilical Subjected to Steady Hydrodynamic Loading', Report of National Physics Laboratory, England, 1979

40. Friedland, B., Control System Design. An Introduction of State-Space Methods, McGraw-Hill, 1987

41. Fung, D. T. K., Chen, Y. L. and Grimble, M. J., 'Dynamic Ship Positioning Control System Design Including Non-linear Thrusters and Dynamics', NATO Advanced Study Institute on Nolinear Stochastic Problem, Portugal, 1982

42. Furuta, K., Sano, A. and Atherton, D., State Variable Methods in Automatic Control, John-Wiley & Sons, 1988

43. Goeller, J. E. and Laura, P. A., 'Analytical and Experimental Study of the Dynamic Response of Segmented Cable Systems', Journal of Sound and Vibration, Vol.18, 1971

44. Goeller, J. E. and Laura, P. A., 'A Theoretical and Experimental Investigation of Impact Loads in Stranded Steel Cable During Longitudinal Excitation', Proceedings of the 5th Southeasten Conference on Theoretical and Applied Mechanics, North Caroline University and Duke University, 1970

45. Graham, J.R., Jones, K.M., Knorr, G.D. and Dixon, T.F., 'Design and Construction of the Dynamically Positioned Glomar Challenger', Marine Technology, Vol. 7, No. 2. 1970

46. Gravatt, W., 'On the Atlantic Cable', Philosophical Magazine and Journal of Science, Forth Series, Vol.16, 1858

47. Greenhow, M. and Yanboa, L., 'Added Mass for Circular Cylinders Near or Penetrating Fluid Boundaries; Review, Extension and Application to Water-Entry, -Exit and Slamming', Ocean Engineering, Vol.14, No.4, 1987

48. Griffin, O. M., Pattison, J. H., Skop, R. A., Ramberg, S. E. and Meggitt, D. J., 'Vortex-Excited Vibrations of Marine Cables', Journal of the Waterway, Port, Coastal and Ocean Division, ASCE, Vol.106, No.WW2, 1980

49. Grimble, M.J., Patton, R.J. and Wise, D.A., 'Use of Kalman Filtering Techniques in Dynamic Ship-Positioning', IEE Proceedings, Vol.127, Pt. D, No.3, 1980

50. Grimble, M.J. and Patton, R.J., 'The Design of Dynamic Ship Position Control Systems Using Stochastic Optimal Control Theory', Optimal Control Applications and Methods, Vol. 1, 1980

51. Gronan, D. S, Underwater Minerals, Academic Press, 1980

52. Hammarstrom, L.G. and Gros, K.S., 'Adaptation of Optimal Control Theory to System with Time Delays', International Journal of Control, Vol.32, No.2, 1980

53. Hartree, D. R., Numerical Analysis, Oxford University Press, 1958

54. Hover, F. S., Grosenbaugh, M. A. and Triantafyllou, M. S., 'Modelling the Dynamics of a Deeply-Towed Underwater Vehicle System', Proceedings of the First European Offshore Mechanics Symposium, Trondheim, Norway, 1990

55. Howell, C. T., 'Numerical Analysis of 2-D Nonlinear Cable Equations with Application to Low-Tension Problems', Proceeding of International Offshore and Polar Engineering Conference, Edingburgh, 1991

56. Inoue, Y., Miyabe, H., Xue, W. and Nakamura, M., 'Comparative Study on the Quasi-Static Analysis and Dynamic Simulations for Estimating the Maximum Tension of Mooring Lines', Proceeding of International Offshore and Polar Engineering Conference, Edingburgh, 1991

57. Irvine, H. M., Cable Structure, MIT Press, Cambridge, Massachussette and London, 1981

58. James. H. M., Nichols, N. B. and Phillips, R. S., Theory of Servomechanism, Dover Publications Inc., New York, 1965

59. Jeffrey, A. and Taniuti, T., Nonlinear Wave Propagation, Academic Press, 1964

60. Kabala, R. and Spingarn, K., Control, Identification and Input Optimization, Plenum Press, 1982

61. Kelvin (Lord), 'On Machinery for Lying Submarine Telegraph Cables', The Engineering, Vol.4, 1857

62. Kennedy, R. M. and Strahan, E. S., 'A Linear Theory of Transverse Cable Dynamics at Low Frequencies', NUSC Technical Report 6463, Naval Underwater Systems Centre, Connecticut, 1981

63. Kidera, E. H., 'A Motion-Compensated Launch/Recovery Crane', Ocean Engineering, Vol.10, No.4, 1983

64. Kidera, E. H. and Mack, S. A., 'Motion Compensation System for Ocean Profile', Ocean Engineering, Vol.10, No.3, 1983

65. Kojima, J., Shirasaki, Y. and Asakawa, K., 'Measurement and Analysis of Hydrodynamics of ROV's Tether Cable', Proceedings of ROV'86 Conference, Aberdeen, U.K., 1986

66. Kokarakis, J. E. and Bernitsas, M. M., 'Nonlinear Three-Dimensional Dynamic Analysis of Marine Risers', Journal of Energy Resources Technology, Vol.109, 1987

67. Kotera, T., 'Vibration of a String with Time-varying Length', Memoirs of the Faculty of Engineering, Kobe University, Japan, 1978

68. Kozik, T. T. and Noerager, J., 'Riser Tensioner Force Variation', Offshore Technology Conference, 1976

69. Kuo, C., 'A Controlled Handling Method for Effective Offshore Support Operations', Offshore Technology Conference 3318, Houston, Texas, 1978

70. Larsen, C. M. and Fylling, I. J., 'Dynamic Behaviour of Anchor Lines', Nowegian Maritime Research, No.3, 1982

71. Lax, P. D. and Richtmeyer, R. D., 'Survey of the Stability of Linear Finite Difference Equations', Communications on Pure and Applied Mathematics, Vol.9, 1956

72. Lee, B. S., 'On the Properties of Vertical Water Oscillations in a Moonpool', Ph.D. Thesis, Marine Technology Centre, University of Strathclyde, 1982

73. Lee, B. S., Kuo, C. and Chu, N., 'Wave-Feed-Forward', Report of Automation of Subsea Tasks, Project 2(6), Marine Technology Centre, University of Strathclyde, 1989

74. Leipholz, H. M. E. and Abdel-Rohman, M., Control of Structures, Martinus Nijhoff Publishers, Dordrecht, 1986

75. Lindsay, R. B., Mechnical Radiation, McGraw-Hill Book Company, Inc., 1960

76. Lo, A. and Leonard, J. W., 'Dynamic Analysis of Underwater Cables', Journal of the Engineering Mechanics Division, ASCE, Vol.108, No.EM4, 1982

77. Love, A. E. H., A Treatise on the Mathematical Theory of Elasticity, Cambridge University Press, 1927

78. Luo, Y., 'On Performance Analysis and Design of Offshore Catenary Mooring Systems', Ph.D. Thesis, Marine Technology Centre, Unversity of Strathclyde, 1990

79. Luyvers, L., Ocean Uses and Other Regulations, John Wiley & Sons, 1984

80. Ma., D. and Leonard, J. and Chu, K-H., 'Slack-Elasto-Plastic Dynamics of Cable Systems', Journal of the Engineering Mechanics Division, ASCE, Vol.105, No.EM2, 1982

81. Macgregor, P. G., 'The Statics and Dynamics of Deeply Submerged Directly Tethered Subsea Units', Ph.D. Thesis, Marine Technology Centre, University of Strathclyde, 1990

82. Miura, R. M., 'Korteweg-de Vries Equation and Generalization. I. A Remarkable Explicit Nonlinear Transformation', Journal of Mathematical Physics, Vol.9, 1968

83. Nakajima, T., Motora, S. and Fujino, M., 'On the Dynamic Analysis of Multicomponent Mooring Lines', Offshore Technology Conference, Paper 4309, 1982

84. Nath, J. H. and Felix, M. P., 'Dynamics of Single Point Mooring in Deep Water', Journal of the Waterways and Harbours Division, ASCE, Vol.96, No.WW4, 1970

85. Niedzwecki, J. M. and Thampi, S. K., 'Heave Response of Long Riserless Drill Strings', Ocean Engineering, Vol.15, No.5, 1988

86. Nomoto, M. and Hattori, M., 'A Deep ROV DOLPHIN 3K: Design and Performance Analysis', IEEE Journal of Oceanic Engineering, Vol.OE-11, No.3,

1986

87. Oritsland, O. and Lehn, E., 'Hydrodynamic Forces and Resulting Motion of Subsea Modules During Lifting in the Splashing Zone', Proceedings of 8th International Conference on Offshore Mechanics and Arctic Engineering, The Hague, 1989

88. Otto, F., Tensile Structures, Vol.1 and 2, The MIT Press, 1967

89. Patel, M., H., Dynamics of Offshore Structures, Butterworths, 1989

90. Patton, K. T., 'The Response of Cable-Moored Axisymmetric Buoys to Ocean Wave Excitation', Naval Underwater System Center, Report 4331, Connecticut, 1972

91. Pedersen, P. T., 'Equilibrium of Offshore Cables and Pipelines During Laying', International Shipbuilding Progress, Vol.22, No.236, 1975

92. Perkins, N. C., 'Plannar and Non-linear Response of a Suspended Cable Driven by Small Support Oscillations', Proceeding of International Offshore and Polar Engineering Conference, Edingburgh, 1991

93. Polachek, H., Walton, T. S., Mejia, R. and Dawson, C., 'Transient Motion of an Elastic Cable Immersed in a Fluid', Mathematical Tables and Other Aids to Computation, Vol.17, 1963

94. Ramberg, S. E. and Griffin, O. M., 'Free Vibration of Taut and Slack Marine Cables', Journal of Structure Division, ASCE, Vol.103, No.ST11, 1977

95. Rawson, K. J. and Tupper, E. C., Basic Ship Theory. Vol. 1 & 2, Longman Scientific & Technical, 1986

96. Rayleigh, (Lord), The Theory of Sound, New York Dover Publications, 1945

97. Roberts, J. D., 'Linear Model Reduction and Solution of the Algebraic Riccati Equation by Use of the Sign Function', CUED/B-CONTROL/TR13, University of Cambridge, 1971

98. Rodseth, O. J. and Hallset, J. O., 'ROV90 – A Prototype Autonomous Inspection Vehicle', Proceeding of International Offshore and Polar Engineering Conference, Edingburgh, 1991

99. Russell, J. S., 'Experimental Researches into the Law of Certain Hydrodynamic Phenomena That Accompany the Motion of Floating Bodies, and Have not Previously Been Reduced into Comformity with the Known Laws of the Resistance of Fluids', The Royal Society of Edingburgh Transaction, Vol.14, 1840

100. Sayer, P. G. and Brunt, S., 'A Parametric Survey of ROV Operational Footprints', Internal Report of Marine Technology Centre, University of Strathclyde, 1989

101. Schaffers, W. J., 'The Vibration of Shaft Ropes with Time-Variable Length, Treated by Means of Riemann's Method', Transactions of ASME, Series B, Vol.83, 1961

102. Schellin, T. E., Sharma, S. D. and Jiang, T., 'Crane Ship Response to Regular Waves: Linearized Frequency Domain Analysis and Nonlinear Time Domain Simulation', Proceedings of 8th International Conference on Offshore Mechanics and Arctic Engineering, The Hague, 1989

103. Smith, A., 'Initial Assessment of Phase 1 Conceptual Design: Active Winch Dynamic Analysis', Technical Report of Norson Power Ltd., 1988

104. Sparks, C. P., Cabillic, J. P. and Schawann, J. C., 'Longitudinal Resonant Behaviour of Very Deep Water Risers', Journal of Energy Resources Technology, Vol.105, 1983

105. Sterzenbach, M., 'Offshore Intervention Submarines, Advanced and Economic Submersible Support Vessels', Underwater Technology, Vol. 15, No. 3, 1990

106. Stricker, P. A., 'Active/Passive Motion Compensating Crane for Handling a Remote Unmanned Work System', Offshore Technology Conference, Paper 3236, Houston, Texas, 1978

107. Tagata, 'A Parametrically Driven Harmonic Analysis of a Non-linear Stretched String with Time Varying Length', Journal of Sound and Vibration, Vol. 87, No. 3, 1983

108. Takahashi, Y., Rabins, M. J. and Auslander, D. M., Control and Dynamic Systems, Addison-Wesley Publishing Company, 1970

109. Taniuti, T and Nishihara, K., Nonlinear Waves, Pitman Publishing Ltd. 1983

110. Triantafyllou, M. S., 'Preliminary Design of Mooring Systems', Journal of Ship Research, Vol.26, No.1, 1982

111. Triantafyllou, M. S. and Bliek, A., 'The Dynamics of Inclined Taut and Slack Marine Cables', Offshore Technology Conference, Paper 4498, Houston, Texas, 1983

112. Triantafyllou, M.S., Bodson, M. and Athans, M., 'Real Time Estimation of Ship Motions Using Kalman Filtering Techniques', IEEE Journal of Oceanic Engineering, Vol.OE-8, No. 1, 1983

113. Triantafyllou, M. S., Bliek, A., Burgess, J. and Shin, H., 'Mooring Dynamics for Offshore Application. Part I Theory and Part II Application', MITSG86-1 and -2, Massachusette Institute of Technology, 1986

114. van den Boom, H. J. J., 'Dynamic Behaviour of Mooring Lines', Behaviour of Offshore Structures, 1985

115. Walton, T. S. and Polachek, H., 'Calculation of Transient Motion of Submerged Cables', Mathematical Tables and Other Aids to Computation, Vol.14, 1960

116. Wang, A., 'Contribution a l'etude des Systemes D'elevage Mytilicole: Aspects Hydrodynamiques', These de Doctorat, Universite de Nants, France, 19xx

117. Wang, H. T., 'A FORTRAN IV Computer Program for the Time Domain Analysis of the Two-Dimensional Dynamic Motion of General Ship-Cable-Body System', David Taylor Naval Ship Research and Development Center,

Report 77-0046, 1977

118. Whitham, G. B., Linear and Nonlinear Waves, John Wiley & Sons, 1974

119. Wilson, B. W. and Carbaccio, D. H., 'Dynamics of Ship Anchor Lines in Waves and Currents', Journal of the Waterways and Harbours Divisions, ASCE, Vol.95, No.WW4, 1969

120. Winget, J. M. and Huston, R. L., 'Cable Dynamics – A Finite Segment Approach', Computer & Structures, Vol.6, 1976

121. Woodall-Mason, N. and Tilbe, J. R., 'Value of Heave Compensation to Floating Drill', Journal of Petroleum Technology, 1976

122. Woolhouse, W. S. B., 'On the Deposit of Submarine Cable', Philosophical Magazine and Journal of Science, Forth Series, Vol.19, 1860

123. Zajac, E. E., 'Dynamics and Kinematics of the Laying and Recovery of Submarine cable', The Bell System Technical Journal, September, 1957

124. Zajaczkowski, J. and Yamada, G., 'On the Further Results of Instability of the Motion of a Beam of Periodically Varying Length', Journal of Sound and Vibration, Vol.68, 1980

NOMENCLATURE

1. GENERAL CONVENTIONS

- Bold face letters represent either vectors or matrices.
- SI units are implicit.

2. LIST OF MAIN SYMBOLS

A	-	cross sectional area of the cable
B	-	buoyant force on an infinitesimal cable length
C_{Dx}, C_{Dy}, C_{Dz}	-	drag coefficients of the subsea unit
C_N, C_{DN}	-	normal drag coefficient of the cable
$C_\tau, C_{D\tau}$	-	tangential drag coefficient of the cable
d	-	diameter of the cable
D	-	drag force on an infinitesimal cable length
ϵ	-	a parameter of small quantity
$e_{i+\frac{1}{2}}, e_{i-\frac{1}{2}}$	-	added masses of the cable

E	-	Young's modulus
$E\{\ \}$	-	mean
F_x^i, F_y^i, F_z^i	-	drag force components on a cable segment
F_N, F_τ	-	normal and tangential drag components
g	-	gravitational acceleration
$\mathbf{G}$	-	gain matrix
H	-	transfer function
$H_{1/3}$	-	significant wave height
i	-	index
$\mathbf{i}, \mathbf{j}, \mathbf{k}$	-	unit vectors along the axes of a Cartesian coordinate system
I	-	moment of inertia
$\mathbf{I}$	-	unit matrix
	-	inertia force on an infinitesimal cable length
j	-	index
J	-	control index
k	-	wave number
K, K_c	-	winch parameter
$l, l_{i+\frac{1}{2}}, l_{i-\frac{1}{2}}$	-	lengths of cable segments
L	-	length of the cable
L_0	-	initial length of cable
m	-	mass distribution of the cable
m_{ap}, m_{aq}	-	added masses distribution due to the longitudinal and transverse motion of the cable

m_{ax}, m_{ay}, m_{az}	-	added masses distribution of the cable
M	-	bending moment
M_0, M_s	-	mass of the subsea unit
M_a, M_{ap}, M_{aq}	-	added masses of the subsea unit
M_{ax}, M_{ay}, M_{az}	-	added masses of the subsea unit
$O(t)$	-	horizontal component of the boom tip motion
p	-	arch length along the strained cable
	-	vertical displacement of the cable
q	-	horizontal displacement of the cable
$R(t)$	-	vertical component of the boom tip motion
$\mathbf{r}$	-	position vector of the cable
s	-	arch length of the unstrained cable
S_P	-	projected area of the subsea unit
S_x, S_y, S_z	-	projected areas of the subsea unit
S_ω	-	wave spectrum
S_ω^a	-	rational approximation of the wave spectrum
t	-	time
T	-	tension in the cable
	-	time
T_0	-	static tension in the cable
T_1	-	first order dynamic tension in the cable
T_2	-	second order dynamic tension in the cable

$T_{i+\frac{1}{2}}, T_{i-\frac{1}{2}}$ - tension in the cable

T_x, T_y, T_z - force components in a Cartesian coordinate system

$\mathbf{Tr}$ - transform matrix

u - vertical displacement of the cable

- output of the winch

u_0 - input of the winch

U_x, U_y, U_z - components of the current velocity

$\mathbf{U}$ - underwater current velocity vector

$\mathbf{U}_N$ - current velocity at cable's normal direction

$\mathbf{U}_\tau$ - current velocity at cable's longitudinal direction

v - deployment speed of the cable

V_0 - volume of the subsea unit

$\mathbf{V}_N$ - normal velocity of the cable

V_x, V_y, V_z - force components at one end of the cable

- velocity components of the cable in the natural coordinate system

$\mathbf{V}, \mathbf{V}_c$ - velocity of the cable

$\mathbf{V}_\tau$ - longitudinal velocity of the cable

w - white noise

w_1 - weight distribution of the cable in water

w_2 - subsea unit's weight in water

W - cable's weight in water

$\mathbf{W}$ - gravity force on an infinitesimal cable length

$\mathbf{x}$ - state vector

x, y, z	-	Cartesian coordinate system
x_L, y_L, z_L	-	coordinates
x', y', z'	-	natural coordinate system
β	-	wave number
ε	-	strain
ε_0	-	static strain of the cable
$\theta, \theta_{i+\frac{1}{2}}, \theta_{i-\frac{1}{2}}$	-	rotation angle of the cable
λ	-	engenvalue
	-	amplification factor
μ	-	mass (mass+added mass) distribution of the cable
$\mu_{i+\frac{1}{2}}, \mu_{i-\frac{1}{2}}$	-	added mass coefficients of the cable
ρ	-	density of the fluid medium
σ	-	standard deviation
$\sigma, \sigma_{i+\frac{1}{2}}, \sigma_{i-\frac{1}{2}}$	-	cross sectional areas of the cable
τ	-	shear force
$\phi, \phi_{i+\frac{1}{2}}, \phi_{i-\frac{1}{2}}$	-	rotation angle of the cable
ω	-	frequency
ω_m	-	modal frequency
Δt	-	time increment
Δy	-	space increment
$[\,]^T$	-	transposition of a matrix
$[\,]^{-1}$	-	inversion of a matrix

ACKNOWLEDGEMENT

I wish to express most sincere gratitude to my supervisor Dr. Dracos Vassalos for his support and stimulating supervision over the past three years.

APPENDIX:

INTRODUCTION TO

EQUATIONS OF MARINE

CABLE DYNAMICS

Introduction is seldom of any efficacy except in the happy cases
where it is almost superfluous.

E. Gibbon

12.1 GENERAL REMARKS

The purpose of this appendix is to provide a general mathematical formulation for marine cable dynamics.

The term 'general' refers to the following properties:

1. analysis conducted in three dimensions,

2. hydrodynamic forces included without any restrictions to the nature of the underwater current,

3. nonlinear stress-strain relation allowed.

However, some idealizations have been made. These include:

1. no bending stiffness and torsional stiffness,

2. the tension is strictly positive.

The mathematical modelling is based upon a distributed system. By equating the rate of change of momentum of an infinitesimal element of the cable to all the forces acting upon it, the equation of motion is derived in a vector form. This vector equation is then resolved in a Cartesian coordinate system and a natural coordinate system, followed by a rigid analysis in each coordinate system. For relevant references, see Cristescu (1967), Patton (1972) and Triantafyllou et al (1986).

12.2 FORCES ON A CABLE ELEMENT

Consider a strained cable element of an infinitesimal length ds' located at a point $\mathbf{r} = \{x, y, z\}$ in a Cartesian coordinate system, as shown in Figure A.1, where s' is a curvilinear coordinate along the strained cable from an arbitrary coordinate origin. The forces acting upon this element arise from:

- *Weight* The force due to the gravity is given by:

$$\mathbf{W} = -gm'ds'\mathbf{k}$$

where g is the gravity acceleration and m' the mass per unit length of the strained cable.

- *Buoyancy* The buoyant force is given by:

$$\mathbf{B} = \rho g A' ds' \mathbf{k}$$

where A' is the cross sectional area of the strained cable. [1]

- *Hydrodynamic drag force* Under the assumption of decomposition the drag force is given by:

$$\begin{aligned} \mathbf{D} &= \frac{1}{2}\rho C_{DN} d' |\mathbf{U}_N - \mathbf{V}_N|(\mathbf{U}_N - \mathbf{V}_N) ds' + \\ &\quad \frac{\pi}{2}\rho C_{D\tau} d' |\mathbf{U}_\tau - \mathbf{V}_\tau|(\mathbf{U}_\tau - \mathbf{V}_\tau) ds' \end{aligned}$$

where $\mathbf{U}$ is the current vector and

$$\mathbf{V} = \frac{\partial \mathbf{r}}{\partial t}$$

- *Hydrodynamic inertia force* The inertia force due to the added mass effect of the fluid media is given by:

$$\mathbf{I} = m_a'(\frac{\partial \mathbf{U}}{\partial t} - \frac{\partial \mathbf{V}}{\partial t}) ds'$$

where m_a' is the added mass per unit length of the strained cable.

- *Tension* The tension force at one end of the element is $\mathbf{T}(s')$ whilst at the other end the tension is $\mathbf{T}(s' + ds')$. In extensible, perfectly flexible cables, the tension in every point is always directed along the tangent to the cable.

[1] For a more accurate formulation, this term should be corrected for the lack of pressure at the ends of the infinitesimal element. This leads to a concept of effective tension. For details, see Pedersen (1975).

12.3 EQUATION OF MOTION

By applying Newton's law of motion, we have:

$$\begin{aligned} m^{'}ds^{'}\frac{\partial^2\mathbf{r}}{\partial t^2} &= -gm^{'}ds^{'}\mathbf{k}+\rho gA^{'}ds^{'}\mathbf{k}+ \\ &\frac{1}{2}\rho C_{DN}d^{'}|\mathbf{U}_N-\mathbf{V}_N|(\mathbf{U}_N-\mathbf{V}_N)ds^{'}+ \\ &\frac{\pi}{2}\rho C_{D\tau}d^{'}|\mathbf{U}_\tau-\mathbf{V}_\tau|(\mathbf{U}_\tau-\mathbf{V}_\tau)ds^{'}+ \\ &m_a^{'}(\frac{\partial\mathbf{U}}{\partial t}-\frac{\partial\mathbf{V}}{\partial t})ds^{'}+\mathbf{T}(s^{'}+ds^{'})-\mathbf{T}(s^{'}) \end{aligned} \tag{12.1}$$

Taking the limit as $ds^{'}\rightarrow 0$ and noticing the following relations of conservation between the strained and the unstrained cables: [2]

$$\begin{aligned} m^{'}ds^{'} &= m\cdot ds \\ m_a^{'}ds^{'} &= m_a\cdot ds \\ A^{'}ds^{'} &= A\cdot ds \end{aligned}$$

where s is an initial coordinate of the unstrained cable, Eq. (12.1) yields:

$$\begin{aligned} (m+m_a)\frac{\partial^2\mathbf{r}}{\partial t^2} &= -g(m-\rho A)\mathbf{k}+ \\ &\frac{1}{2}\rho C_{DN}d\sqrt{1+\varepsilon}|\mathbf{U}_N-\mathbf{V}_N|(\mathbf{U}_N-\mathbf{V}_N)+ \\ &\frac{\pi}{2}\rho C_{D\tau}d\sqrt{1+\varepsilon}|\mathbf{U}_\tau-\mathbf{V}_\tau|(\mathbf{U}_\tau-\mathbf{V}_\tau)+ \\ &m_a\frac{\partial\mathbf{U}}{\partial t}+\frac{\partial}{\partial s}(\frac{T}{1+\varepsilon}\frac{\partial\mathbf{r}}{\partial s}) \end{aligned} \tag{12.2}$$

[2]Strictly speaking, the volume conservation is not true for most materials. The ratio of an infinitesimal element of volume in the strained state to the corresponding infinitesimal element of volume in the unstrained state is often written as $1+\Delta$, where Δ is the cubical dilatation. When a cable is stretched longitudinally, $\Delta\approx(1-2\nu)\epsilon$, when ϵ is small. For most materials ν is about $\frac{1}{3}$ or $\frac{1}{4}$, not $\frac{1}{2}$ as required by the volume conservation. However, this conservation assumption only introduces very small errors into the following formulation.

where ε is given by:

$$\varepsilon = \frac{ds'}{ds} - 1 = |\frac{\partial \mathbf{r}}{\partial s}| - 1 \tag{12.3}$$

To this equation must be added a constitutive relation for the cable considered. The constitutive relation is dependent upon the type of material of the cable. Throughout this appendix, the relation is assumed to be of the form

$$T = T(\varepsilon) \tag{12.4}$$

where the function T is usually a monotonically increasing function of ε.

This assumption is better than Hooke's law in the sense that it allows nonlinear relations between the strain and the stress. Nevertheless, it still has the following restrictions:

1. The cable must not have a variable cross section area.

2. Plastic stretch resulting from the maximum stress exceeding the ultimate tensile strength of the material can not be taken into account.

3. The mechanical properties of the cable material must be independent of the rate of the dynamic loading.

12.4 ANALYSIS IN A CARTESIAN COORDINATE SYSTEM

12.4.1 Cable Equations

In a Cartesian coordinate system, Eq. (12.2) can be resolved into the following three components:

$$\begin{aligned}
(m+m_{ax})\frac{\partial^2 x}{\partial t^2} - \frac{\partial}{\partial s}(\frac{T}{1+\varepsilon}\frac{\partial x}{\partial s}) - F_x &= 0 \\
(m+m_{ay})\frac{\partial^2 y}{\partial t^2} - \frac{\partial}{\partial s}(\frac{T}{1+\varepsilon}\frac{\partial y}{\partial s}) - F_y &= 0 \\
(m+m_{az})\frac{\partial^2 z}{\partial t^2} - \frac{\partial}{\partial s}(\frac{T}{1+\varepsilon}\frac{\partial z}{\partial s}) - F_z &= 0
\end{aligned} \tag{12.5}$$

where

$$\begin{aligned}
F_x &= \frac{1}{2}\rho C_{DN} d\sqrt{1+\varepsilon}|\mathbf{U}_N - \mathbf{V}_N|(\mathbf{U}_N - \mathbf{V}_N)\cdot\mathbf{i} + \\
&\quad \frac{\pi}{2}\rho C_{D\tau} d\sqrt{1+\varepsilon}|\mathbf{U}_\tau - \mathbf{V}_\tau|(\mathbf{U}_\tau - \mathbf{V}_\tau)\cdot\mathbf{i} + m_{ax}\frac{\partial U_x}{\partial t} \\
F_y &= \frac{1}{2}\rho C_{DN} d\sqrt{1+\varepsilon}|\mathbf{U}_N - \mathbf{V}_N|(\mathbf{U}_N - \mathbf{V}_N)\cdot\mathbf{j} + \\
&\quad \frac{\pi}{2}\rho C_{D\tau} d\sqrt{1+\varepsilon}|\mathbf{U}_\tau - \mathbf{V}_\tau|(\mathbf{U}_\tau - \mathbf{V}_\tau)\cdot\mathbf{j} + m_{ay}\frac{\partial U_y}{\partial t} \\
F_z &= \frac{1}{2}\rho C_{DN} d\sqrt{1+\varepsilon}|\mathbf{U}_N - \mathbf{V}_N|(\mathbf{U}_N - \mathbf{V}_N)\cdot\mathbf{k} - g(m-\rho A) + \\
&\quad \frac{\pi}{2}\rho C_{D\tau} d\sqrt{1+\varepsilon}|\mathbf{U}_\tau - \mathbf{V}_\tau|(\mathbf{U}_\tau - \mathbf{V}_\tau)\cdot\mathbf{k} + m_{az}\frac{\partial U_z}{\partial t} \\
\varepsilon &= \sqrt{(\frac{\partial x}{\partial s})^2 + (\frac{\partial y}{\partial s})^2 + (\frac{\partial z}{\partial s})^2} - 1
\end{aligned} \tag{12.6}$$

12.4.2 Characteristics

Expanding Eq. (12.5) and taking into account the constitutive relation, Eq. (12.4), we have

$$\frac{T}{1+\varepsilon}\frac{\partial^2 x}{\partial s^2} - \mu_x \frac{\partial^2 x}{\partial t^2} + \frac{\partial x}{\partial s}\frac{(1+\varepsilon)T_\varepsilon - T}{(1+\varepsilon)^2}\frac{\partial \varepsilon}{\partial s} - F_x = 0 \qquad (12.7)$$

$$\frac{T}{1+\varepsilon}\frac{\partial^2 y}{\partial s^2} - \mu_y \frac{\partial^2 y}{\partial t^2} + \frac{\partial y}{\partial s}\frac{(1+\varepsilon)T_\varepsilon - T}{(1+\varepsilon)^2}\frac{\partial \varepsilon}{\partial s} - F_y = 0 \qquad (12.8)$$

$$\frac{T}{1+\varepsilon}\frac{\partial^2 z}{\partial s^2} - \mu_z \frac{\partial^2 z}{\partial t^2} + \frac{\partial z}{\partial s}\frac{(1+\varepsilon)T_\varepsilon - T}{(1+\varepsilon)^2}\frac{\partial \varepsilon}{\partial s} - F_z = 0 \qquad (12.9)$$

where

$$\begin{aligned}
\mu_x &= m + m_{ax} \\
\mu_y &= m + m_{ay} \\
\mu_z &= m + m_{az} \\
T_\varepsilon &= \frac{dT}{d\varepsilon} \\
\frac{\partial \varepsilon}{\partial s} &= \frac{1}{1+\varepsilon}\left[\frac{\partial x}{\partial s}\frac{\partial^2 x}{\partial s^2} + \frac{\partial y}{\partial s}\frac{\partial^2 y}{\partial s^2} + \frac{\partial z}{\partial s}\frac{\partial^2 z}{\partial s^2}\right]
\end{aligned} \qquad (12.10)$$

In order to analyse the system of Eqs. (12.7), (12.8) and (12.9), it is reduced into a equivalent first order quasi-linear system of partial differential equations

$$\frac{\partial \mathbf{Y}}{\partial t} + \mathbf{A}\frac{\partial \mathbf{Y}}{\partial s} + \mathbf{B} = \mathbf{0} \qquad (12.11)$$

where

$$\mathbf{Y} = \begin{bmatrix} x \\ y \\ z \\ x_s \\ y_s \\ z_s \\ x_t \\ y_t \\ z_t \end{bmatrix}$$

$$\mathbf{A} = \begin{bmatrix} 1 & 0 & 0 & 0 & 0 & 0 & 0 & 0 & 0 \\ 0 & 1 & 0 & 0 & 0 & 0 & 0 & 0 & 0 \\ 0 & 0 & 1 & 0 & 0 & 0 & 0 & 0 & 0 \\ 0 & 0 & 0 & 0 & 0 & 0 & -1 & 0 & 0 \\ 0 & 0 & 0 & 0 & 0 & 0 & 0 & -1 & 0 \\ 0 & 0 & 0 & 0 & 0 & 0 & 0 & 0 & -1 \\ 0 & 0 & 0 & J_1 & J_2 & J_3 & 0 & 0 & 0 \\ 0 & 0 & 0 & J_4 & J_5 & J_6 & 0 & 0 & 0 \\ 0 & 0 & 0 & J_7 & J_8 & J_9 & 0 & 0 & 0 \end{bmatrix}$$

$$\mathbf{B} = \begin{bmatrix} -x_t - x_s \\ -y_t - y_s \\ -z_t - z_s \\ 0 \\ 0 \\ 0 \\ \frac{F_x}{\mu_x} \\ \frac{F_y}{\mu_y} \\ \frac{F_z}{\mu_z} \end{bmatrix}$$

and

$$\begin{aligned}
J_1 &= -\frac{(1+\varepsilon)T_\varepsilon - T}{(1+\varepsilon)^3} x_s^2 - \frac{T}{\mu_x(1+\varepsilon)} \\
J_2 &= -\frac{(1+\varepsilon)T_\varepsilon - T}{(1+\varepsilon)^3} x_s y_s \\
J_3 &= -\frac{(1+\varepsilon)T_\varepsilon - T}{(1+\varepsilon)^3} x_s z_s \\
J_4 &= -\frac{(1+\varepsilon)T_\varepsilon - T}{(1+\varepsilon)^3} x_s y_s \\
J_5 &= -\frac{(1+\varepsilon)T_\varepsilon - T}{(1+\varepsilon)^3} y_s^2 - \frac{T}{\mu_y(1+\varepsilon)} \\
J_6 &= -\frac{(1+\varepsilon)T_\varepsilon - T}{(1+\varepsilon)^3} y_s z_s \\
J_7 &= -\frac{(1+\varepsilon)T_\varepsilon - T}{(1+\varepsilon)^3} x_s z_s \\
J_8 &= -\frac{(1+\varepsilon)T_\varepsilon - T}{(1+\varepsilon)^3} y_s z_s \\
J_9 &= -\frac{(1+\varepsilon)T_\varepsilon - T}{(1+\varepsilon)^3} z_s^2 - \frac{T}{\mu_z(1+\varepsilon)}
\end{aligned}$$

The system defined by Eq. (12.11) has nine equations for the nine un-

knowns $x, y, z, x_s, y_s, z_s, x_t, y_t$ and z_t. The notations $x_s, x_t, \cdots$ stand for $\frac{\partial x}{\partial s}, \frac{\partial x}{\partial t}, \ldots$, etc.

To simplify the analysis in what follows, it is assumed

$$\mu_x = \mu_y = \mu_z = \mu$$

The nine eigenvalues of Eq. (12.11) can be obtained through solving the following equation

$$\begin{vmatrix}
1-\lambda & 0 & 0 & 0 & 0 & 0 & 0 & 0 & 0 \\
0 & 1-\lambda & 0 & 0 & 0 & 0 & 0 & 0 & 0 \\
0 & 0 & 1-\lambda & 0 & 0 & 0 & 0 & 0 & 0 \\
0 & 0 & 0 & -\lambda & 0 & 0 & -1 & 0 & 0 \\
0 & 0 & 0 & 0 & -\lambda & 0 & 0 & -1 & 0 \\
0 & 0 & 0 & 0 & 0 & -\lambda & 0 & 0 & -1 \\
0 & 0 & 0 & J_1 & J_2 & J_3 & -\lambda & 0 & 0 \\
0 & 0 & 0 & J_4 & J_5 & J_6 & 0 & -\lambda & 0 \\
0 & 0 & 0 & J_7 & J_8 & J_9 & 0 & 0 & -\lambda
\end{vmatrix} = 0$$

It is evident that the first three eigenvalues are

$$\lambda_1 = \lambda_2 = \lambda_3 = 1$$

The rest are governed by the following polynomial of order six

$$\lambda^6 + (J_1 + J_5 + J_9)\lambda^4 + (J_5 J_9 - J_6 J_8 + J_1 J_5 - J_2 J_4 + J_1 J_9 - J_3 J_7)\lambda^2$$

$$+(J_1 J_5 J_9 + J_3 J_4 J_8 + J_2 J_6 J_7 - J_3 J_5 J_7 - J_1 J_6 J_8 - J_2 J_4 J_9) = 0$$

which gives

$$\lambda_{4,5} = \pm\sqrt{\frac{T_e}{\mu}}$$

$$\lambda_{6,7} = \lambda_{8,9} = \pm\sqrt{\frac{T}{(1+\varepsilon)\mu}}$$

It follows that Eq. (12.11) is hyperbolic since all the eigenvalues are real. Not all the eigenvalues have physical representation. Indeed the reduction can introduce redundant eigenvalues into the system.

Physically, the cable can propagate both longitudinal tensile waves and transverse flexural waves. The eigenvalues represent the velocities of waves travelling in the cable. It can be seen that the tensile wave velocity, represented by $\lambda_{4,5}$, and the transverse wave velocities, represented by $\lambda_{6,7}$ and $\lambda_{8,9}$, are functions of the state of the cable which changes in both the space and time domains.

Since for practical marine cables, $\varepsilon \ll 1$

$$\sqrt{1+\varepsilon} = 1 + \frac{\varepsilon}{2} - \frac{\varepsilon^2}{4} + \cdots \approx 1$$

we have

$$\lambda_{6,7} = \lambda_{8,9} = \pm\sqrt{\frac{T}{\mu}}$$

In Chapter 4, for the transverse waves of a two dimensional case, we have obtained the same result through perturbation analysis.

12.4.3 Ordinary Differential equations

The characteristic lines are defined by

$$(\frac{ds}{dt})_i = \lambda_i \quad i = 1, 2, \cdots, 9$$

It can be seen that with the exception of the first three, all the other characteristic lines are generally curved lines, whose slopes depend on the state of the cable.

It is well known that, according to the theory of hyperbolic equation, the original set of partial differential equations can be transformed into a set of ordinary differential equations along the characteristic lines.

The first three can be easily found. All are defined along the characteristic line $\frac{ds}{dt} = 1$, and given by

$$\begin{aligned} dx - (x_t + x_s)dt &= 0 \\ dy - (y_t + y_s)dt &= 0 \\ dz - (z_t + z_s)dt &= 0 \end{aligned}$$

To find the rest of the ordinary differential equations, we multiply Eq. (12.7) by x_s, Eq. (12.8) by y_s, Eq. (12.9) by z_s, and add them together. This operation results in

$$\begin{aligned} x_s(T_e\frac{\partial x_s}{\partial s} - \mu\frac{\partial x_t}{\partial t}) \quad & +y_s(T_e\tfrac{\partial y_s}{\partial s} - \mu\tfrac{\partial y_t}{\partial t}) \\ & +z_s(T_e\tfrac{\partial z_s}{\partial s} - \mu\tfrac{\partial z_t}{\partial t}) \quad -x_sF_x - y_sF_y - z_sF_z = 0 \end{aligned} \tag{12.12}$$

On the other hand, from the following relations

$$\begin{aligned} dx_s &= \frac{\partial x_s}{\partial s}ds + \frac{\partial x_s}{\partial t}dt \\ dx_t &= \frac{\partial x_t}{\partial s}ds + \frac{\partial x_t}{\partial t}dt \end{aligned}$$

we have

$$(\frac{ds}{dt})^2\frac{\partial x_s}{\partial s}-\frac{\partial x_t}{\partial t}=\frac{1}{dt}(\frac{ds}{dt}dx_s-dx_t) \tag{12.13}$$

Similarly we have

$$(\frac{ds}{dt})^2\frac{\partial y_s}{\partial s}-\frac{\partial y_t}{\partial t}=\frac{1}{dt}(\frac{ds}{dt}dy_s-dy_t) \tag{12.14}$$

$$(\frac{ds}{dt})^2\frac{\partial z_s}{\partial s}-\frac{\partial z_t}{\partial t}=\frac{1}{dt}(\frac{ds}{dt}dz_s-dz_t) \tag{12.15}$$

Thus from Eqs. (12.12) and (12.13), (12.14), (12.15), it is clear that along the characteristic line defined by $\frac{ds}{dt}=\sqrt{T_e/\mu}$, we have

$$\begin{aligned}x_s(\sqrt{\frac{T_e}{\mu}}dx_s-dx_t)\quad &+y_s(\sqrt{\tfrac{T_e}{\mu}}dx_s-dy_t)\\ &+z_s(\sqrt{\tfrac{T_e}{\mu}}dx_s-dz_t)\quad -\frac{dt}{\mu}(x_sF_x+y_sF_y+z_sF_z)=0\end{aligned}$$

and along characteristic line defined by $\frac{ds}{dt}=-\sqrt{T_e/\mu}$, we have

$$\begin{aligned}x_s(\sqrt{\frac{T_e}{\mu}}dx_s+dx_t)\quad &+y_s(\sqrt{\tfrac{T_e}{\mu}}dx_s+dy_t)\\ &+z_s(\sqrt{\tfrac{T_e}{\mu}}dx_s+dz_t)\quad +\frac{dt}{\mu}(x_sF_x+y_sF_y+z_sF_z)=0\end{aligned}$$

Further, substituting Eq. (12.12) into Eq. (12.7), we have

$$\frac{T}{1+\varepsilon}\frac{\partial x_s}{\partial s}-\mu\frac{\partial x_t}{\partial t}+\frac{x_s}{(1+\varepsilon)^2}[x_sF_x+y_sF_y+z_sF_z+$$

$$x_s(\frac{T}{1+\varepsilon}\frac{\partial x_s}{\partial s}-\mu\frac{\partial x_t}{\partial t})+y_s(\frac{T}{1+\varepsilon}\frac{\partial y_s}{\partial s}-\mu\frac{\partial y_t}{\partial t})+z_s(\frac{T}{1+\varepsilon}\frac{\partial z_s}{\partial s}-\mu\frac{\partial z_t}{\partial t})]-F_x=0 \tag{12.16}$$

Thus along $\frac{ds}{dt}=\sqrt{T/[\mu(1+\varepsilon)]}$, we have from Eq. (12.16)

$$\sqrt{\frac{T}{\mu(1+\varepsilon)}}dx_s-dx_t-\frac{dt}{\mu}F_x+\frac{x_s}{(1+\varepsilon)^2}[\frac{1}{\mu}(x_sF_x+y_sF_y+z_sF_z)+$$

$$x_s(\sqrt{\frac{T}{\mu(1+\varepsilon)}}dx_s - dx_t) + y_s(\sqrt{\frac{T}{\mu(1+\varepsilon)}}dy_s - dy_t) + z_s(\sqrt{\frac{T}{\mu(1+\varepsilon)}}dz_s - dz_t)] = 0$$

Along $\frac{ds}{dt} = -\sqrt{T/[\mu(1+\varepsilon)]}$, we have

$$-\sqrt{\frac{T}{\mu(1+\varepsilon)}}dx_s - dx_t - \frac{dt}{\mu}F_x + \frac{x_s}{(1+\varepsilon)^2}[\frac{1}{\mu}(x_sF_x + y_sF_y + z_sF_z) -$$

$$x_s(\sqrt{\frac{T}{\mu(1+\varepsilon)}}dx_s + dx_t) - y_s(\sqrt{\frac{T}{\mu(1+\varepsilon)}}dy_s + dy_t) - z_s(\sqrt{\frac{T}{\mu(1+\varepsilon)}}dz_s + dz_t)] = 0$$

Similarly, after substituting Eq. (12.12) into Eq. (12.8), we have the following two ordinary differential equations

$$\sqrt{\frac{T}{\mu(1+\varepsilon)}}dy_s - dy_t - \frac{dt}{\mu}F_y + \frac{y_s}{(1+\varepsilon)^2}[\frac{1}{\mu}(x_sF_x + y_sF_y + z_sF_z) +$$

$$x_s(\sqrt{\frac{T}{\mu(1+\varepsilon)}}dx_s - dx_t) + y_s(\sqrt{\frac{T}{\mu(1+\varepsilon)}}dy_s - dy_t) + z_s(\sqrt{\frac{T}{\mu(1+\varepsilon)}}dz_s - dz_t)] = 0$$

$$-\sqrt{\frac{T}{\mu(1+\varepsilon)}}dy_s - dy_t - \frac{dt}{\mu}F_y + \frac{y_s}{(1+\varepsilon)^2}[\frac{1}{\mu}(x_sF_x + y_sF_y + z_sF_z) -$$

$$x_s(\sqrt{\frac{T}{\mu(1+\varepsilon)}}dx_s + dx_t) - y_s(\sqrt{\frac{T}{\mu(1+\varepsilon)}}dy_s + dy_t) - z_s(\sqrt{\frac{T}{\mu(1+\varepsilon)}}dz_s + dz_t)] = 0$$

These two equations are defined respectively along the two characteristic lines given by

$$\frac{ds}{dt} = \pm\sqrt{\frac{T}{\mu(1+\varepsilon)}}$$

12.4.4 Propagation of Discontinuities

From the physical point of view, the characteristic lines represent wave fronts which define boundaries between the disturbed state and the undisturbed

state. In the undisturbed state any derivatives vanish whilst in the disturbed state they do not in general vanish. Therefore there exist discontinuities across the wave fronts (Jeffrey and Taniuti, 1964).

Some in-depth understanding may be obtained through examining these discontinuities. For this purpose we assume that the second order derivatives of displacements have jumps in crossing the wave fronts, while the first order and zero order derivatives remain continuous. A wave satisfying this criteria is called a smooth wave which excludes the shock wave whose fronts are travelling discontinuity boundaries even for the first order derivatives.

In what follows, the discussion will be confined to the neighbourhood of the wave fronts defined by the characteristic lines

$$(\frac{ds}{dt})_i = \lambda_i \quad i = 4, 5, \cdots, 9$$

Applying Eqs. (12.13), (12.14) and (12.15) to either side of any wave front and remembering that first order derivatives of displacements are continuous in crossing the front, we have

$$(\frac{ds}{dt})^2\langle\frac{\partial x_s}{\partial s}\rangle - \langle\frac{\partial x_t}{\partial t}\rangle = 0 \tag{12.17}$$

$$(\frac{ds}{dt})^2\langle\frac{\partial y_s}{\partial s}\rangle - \langle\frac{\partial y_t}{\partial t}\rangle = 0 \tag{12.18}$$

$$(\frac{ds}{dt})^2\langle\frac{\partial z_s}{\partial s}\rangle - \langle\frac{\partial z_t}{\partial t}\rangle = 0 \tag{12.19}$$

where $\langle\Psi\rangle$ denotes the jump of Ψ in crossing any wave front.

Also applying the governing equations (12.7), (12.8), (12.9) and the compatibility relation (12.10) to either side of any front, and taking Eqs. (12.17),

(12.18) and (12.19) into account, we obtain

$$[\frac{T}{1+\varepsilon}-\mu(\frac{ds}{dt})^2]\langle\frac{\partial x_s}{\partial s}\rangle+x_s\frac{(1+\varepsilon)T_\varepsilon-T}{(1+\varepsilon)^2}\langle\frac{\partial\varepsilon}{\partial s}\rangle=0$$

$$[\frac{T}{1+\varepsilon}-\mu(\frac{ds}{dt})^2]\langle\frac{\partial y_s}{\partial s}\rangle+y_s\frac{(1+\varepsilon)T_\varepsilon-T}{(1+\varepsilon)^2}\langle\frac{\partial\varepsilon}{\partial s}\rangle=0$$

$$[\frac{T}{1+\varepsilon}-\mu(\frac{ds}{dt})^2]\langle\frac{\partial x_s}{\partial s}\rangle+z_s\frac{(1+\varepsilon)T_\varepsilon-T}{(1+\varepsilon)^2}\langle\frac{\partial\varepsilon}{\partial s}\rangle=0$$

$$x_s\langle\frac{\partial x_s}{\partial s}\rangle+y_s\langle\frac{\partial y_s}{\partial s}\rangle+z_s\langle\frac{\partial z_s}{\partial s}\rangle-(1+\varepsilon)\langle\frac{\partial\varepsilon}{\partial s}\rangle=0$$

It is evident that in crossing the characteristic lines defined by

$$\frac{ds}{dt}=\pm\sqrt{\frac{T}{\mu(1+\varepsilon)}} \tag{12.20}$$

we have

$$\langle\frac{\partial\varepsilon}{\partial s}\rangle = 0 \tag{12.21}$$

$$\frac{x_s}{1+\varepsilon}\langle\frac{\partial x_s}{\partial s}\rangle+\frac{y_s}{1+\varepsilon}\langle\frac{\partial y_s}{\partial s}\rangle+\frac{z_s}{1+\varepsilon}\langle\frac{\partial z_s}{\partial s}\rangle = 0 \tag{12.22}$$

and in crossing the wave fronts defined by

$$\frac{ds}{dt}=\pm\sqrt{\frac{T_\varepsilon}{\mu}} \tag{12.23}$$

we have

$$\begin{aligned}\langle\frac{\partial x_s}{\partial s}\rangle &= \frac{x_s}{1+\varepsilon}\langle\frac{\partial\varepsilon}{\partial s}\rangle\\ \langle\frac{\partial y_s}{\partial s}\rangle &= \frac{y_s}{1+\varepsilon}\langle\frac{\partial\varepsilon}{\partial s}\rangle\\ \langle\frac{\partial z_s}{\partial s}\rangle &= \frac{z_s}{1+\varepsilon}\langle\frac{\partial\varepsilon}{\partial s}\rangle\end{aligned} \tag{12.24}$$

The physical meaning lying in Eqs. (12.20), (12.21) and (12.22) is that the transverse wave fronts affect the shape of the cable but do not affect the distribution

of the strain. On the other hand, from Eqs. (12.23) and (12.24), it follows that the longitudinal wave fronts affect the distribution of the strain in the cable but do not change its shape.

This conclusion only applies to the neighbourhood of the wave fronts. In the disturbed region, the longitudinal waves and the transverse waves interact with each other, and the propagation of a single type of wave is generally impossible.

12.4.5 Linearisation

The system defined by Eq. (12.5) is a non-linear one. The non-linearities arise as a consequence of the following system properties:

1. Material behaviour

2. Geometry

3. External forces

To linearise the system, we first assume that the cable material obeys Hooke's law, that is,

$$T = EA\varepsilon$$

Secondly, we assume the cable's motions can be decomposed into sums of small dynamic deviations and static equilibrium displacements. This is interpreted mathematically by

$$x = x_0 + ex_1$$

$$
\begin{aligned}
y &= y_0 + e y_1 \\
z &= z_0 + e z_1 \\
\varepsilon &= \varepsilon_0 + e \varepsilon_1 \\
F_x &= F_{x0} + e F_{x1} \\
F_y &= F_{y0} + e F_{y1} \\
F_z &= F_{z0} + e F_{z1}
\end{aligned}
$$

where $e \ll 1$.

Substituting these relations into Eq. (12.5), subtracting the static equation from the dynamic one, and neglecting the terms of second or higher orders of e, we have:

$$(m + m_{ax})\frac{\partial^2 x_1}{\partial t^2} - EA\frac{\partial}{\partial s}[\frac{\varepsilon_1}{(1+\varepsilon_0)^2}\frac{\partial x_0}{\partial s} + \frac{\varepsilon_0}{1+\varepsilon_0}\frac{\partial x_1}{\partial s}] - F_{x1} = 0 \qquad (12.25)$$

$$(m + m_{ay})\frac{\partial^2 y_1}{\partial t^2} - EA\frac{\partial}{\partial s}[\frac{\varepsilon_1}{(1+\varepsilon_0)^2}\frac{\partial y_0}{\partial s} + \frac{\varepsilon_0}{1+\varepsilon_0}\frac{\partial y_1}{\partial s}] - F_{y1} = 0 \qquad (12.26)$$

$$(m + m_{az})\frac{\partial^2 z_1}{\partial t^2} - EA\frac{\partial}{\partial s}[\frac{\varepsilon_1}{(1+\varepsilon_0)^2}\frac{\partial z_0}{\partial s} + \frac{\varepsilon_0}{1+\varepsilon_0}\frac{\partial z_1}{\partial s}] - F_{z1} = 0 \qquad (12.27)$$

$$\varepsilon_1 = \frac{1}{1+\varepsilon_0}(\frac{\partial x_0}{\partial s}\frac{\partial x_1}{\partial s} + \frac{\partial y_0}{\partial s}\frac{\partial y_1}{\partial s} + \frac{\partial z_0}{\partial s}\frac{\partial z_1}{\partial s}) \qquad (12.28)$$

where

$$\varepsilon_0 = \sqrt{(\frac{\partial x_0}{\partial s})^2 + (\frac{\partial y_0}{\partial s})^2 + (\frac{\partial z_0}{\partial s})^2} - 1$$

This set of equations is linear for the dynamic motions around the three dimensional static configuration.

One interesting feature of the linearised system is that if a cable has a two dimensional static configuration, the dynamics can be decoupled into a two-

dimensional in-plane motion and a one-dimensional out-of-plane motion. This conclusion can be demonstrated as follows.

Without losing generality, we can assume in this particular case

$$\frac{\partial z_0}{\partial s} = 0$$

It follows from Eq. (12.27) that we have

$$(m + m_{az})\frac{\partial^2 z_1}{\partial t^2} - EA\frac{\partial}{\partial s}(\frac{\varepsilon_0}{1+\varepsilon_0}\frac{\partial z_1}{\partial s}) - F_{z1} = 0$$

This indicates that the motion in this direction is completely independent of the motions in the other two directions, and that the reverse is also true, provided that there is not an interaction of the external forces.

In an even more extreme case, where the static configuration is a straight line, the three components of the motion become totally independent of each other, and each can be treated as an one-dimensional problem. This happens in cases such as a taut string, a hanging cable, etc.

The linearisation and decoupling greatly reduces the mathematical complexity of the original non-linear governing equations. However, general analytical solutions are still not accessible. The prominent difficulty involved is due to the variable coefficients in the linearised equations which are dependent upon the static state of the cable under consideration. Further geometric or constitutive simplifications must be made in order to pursue analytic solutions. Such special solutions under particular situations can be found in Irvine (1981) and Triantafyllou et al(1986).

So far, limited discussion has taken place regarding the external forces. Any linearisation would not be complete without linearising these terms. However, this proves to be a formidable task. The fluid drag force is one of the fundamental topics in fluid mechanics, involving tremendous complexities such as separation, turbulence, stability and fluid-surface interaction. It is no wonder to find that the current treatments of drag forces on cable are all semi-empirical.

We start with the acceptance of Eq. (12.6) as a valid account of the drag forces without questioning to what extent the expression reflects the mechanism of the fluid drag force. The following is concerned with its linearisation.

We assume that the tangential drag force is small in comparison to the normal one. This allows it to be dropped from the equations. Upon expansion, we have:

$$\mathbf{U}_N - \mathbf{V}_N =$$

$$\{U_x - \frac{\partial x}{\partial t} - \frac{1}{(1+\epsilon)^2}[(U_x - \frac{\partial x}{\partial t})\frac{\partial x}{\partial s} + (U_y - \frac{\partial y}{\partial t})\frac{\partial y}{\partial s} + (U_z - \frac{\partial z}{\partial t})\frac{\partial z}{\partial s}]\frac{\partial x}{\partial s}\}\mathbf{i}+$$

$$\{U_y - \frac{\partial y}{\partial t} - \frac{1}{(1+\epsilon)^2}[(U_x - \frac{\partial x}{\partial t})\frac{\partial x}{\partial s} + (U_y - \frac{\partial y}{\partial t})\frac{\partial y}{\partial s} + (U_z - \frac{\partial z}{\partial t})\frac{\partial z}{\partial s}]\frac{\partial y}{\partial s}\}\mathbf{j}+$$

$$\{U_z - \frac{\partial z}{\partial t} - \frac{1}{(1+\epsilon)^2}[(U_x - \frac{\partial x}{\partial t})\frac{\partial x}{\partial s} + (U_y - \frac{\partial y}{\partial t})\frac{\partial y}{\partial s} + (U_z - \frac{\partial z}{\partial t})\frac{\partial z}{\partial s}]\frac{\partial z}{\partial s}\}\mathbf{k}$$

Substituting x, y and z in the equation above with the sums of static components and dynamic components, and neglecting the effect of elastic strain on the drag force, we ultimately arrive at

$$F_{x0} = \frac{\rho}{2} C_{DN} da_x \sqrt{a_x^2 + a_y^2 + a_z^2}$$

$$F_{y0} = \frac{\rho}{2} C_{DN} da_y \sqrt{a_x^2 + a_y^2 + a_z^2}$$

$$
\begin{aligned}
F_{z0} &= \frac{\rho}{2} C_{DN} d a_z \sqrt{a_x^2 + a_y^2 + a_z^2} - g(m - \rho A) \\
F_{x1} &= \frac{\rho}{2} C_{DN} d (a_x \frac{a_x b_x + a_y b_y + a_z b_z}{\sqrt{a_x^2 + a_y^2 + a_z^2}} + b_x \sqrt{a_x^2 + a_y^2 + a_z^2}) \\
F_{y1} &= \frac{\rho}{2} C_{DN} d (a_y \frac{a_x b_x + a_y b_y + a_z b_z}{\sqrt{a_x^2 + a_y^2 + a_z^2}} + b_y \sqrt{a_x^2 + a_y^2 + a_z^2}) \\
F_{z1} &= \frac{\rho}{2} C_{DN} d (a_z \frac{a_x b_x + a_y b_y + a_z b_z}{\sqrt{a_x^2 + a_y^2 + a_z^2}} + b_z \sqrt{a_x^2 + a_y^2 + a_z^2})
\end{aligned}
$$

where

$$
\begin{aligned}
a_x &= U_x + \frac{\partial x_0}{\partial s}(U_x \frac{\partial x_0}{\partial s} + U_y \frac{\partial y_0}{\partial s} + U_z \frac{\partial z_0}{\partial s}) \\
a_y &= U_y + \frac{\partial y_0}{\partial s}(U_x \frac{\partial x_0}{\partial s} + U_y \frac{\partial y_0}{\partial s} + U_z \frac{\partial z_0}{\partial s}) \\
a_z &= U_z + \frac{\partial z_0}{\partial s}(U_x \frac{\partial x_0}{\partial s} + U_y \frac{\partial y_0}{\partial s} + U_z \frac{\partial z_0}{\partial s}) \\
b_x &= \frac{\partial x_1}{\partial s}(U_x \frac{\partial x_0}{\partial s} + U_y \frac{\partial y_0}{\partial s} + U_z \frac{\partial z_0}{\partial s}) - \frac{\partial x_1}{\partial t} + \\
&\quad \frac{\partial x_0}{\partial s}(U_x \frac{\partial x_1}{\partial s} + U_y \frac{\partial y_1}{\partial s} + U_z \frac{\partial z_1}{\partial s} - \frac{\partial x_1}{\partial t}\frac{\partial x_0}{\partial s} - \frac{\partial y_1}{\partial t}\frac{\partial y_0}{\partial s} - \frac{\partial z_1}{\partial t}\frac{\partial z_0}{\partial s}) \\
b_y &= \frac{\partial y_1}{\partial s}(U_x \frac{\partial x_0}{\partial s} + U_y \frac{\partial y_0}{\partial s} + U_z \frac{\partial z_0}{\partial s}) - \frac{\partial y_1}{\partial t} + \\
&\quad \frac{\partial y_0}{\partial s}(U_x \frac{\partial x_1}{\partial s} + U_y \frac{\partial y_1}{\partial s} + U_z \frac{\partial z_1}{\partial s} - \frac{\partial x_1}{\partial t}\frac{\partial x_0}{\partial s} - \frac{\partial y_1}{\partial t}\frac{\partial y_0}{\partial s} - \frac{\partial z_1}{\partial t}\frac{\partial z_0}{\partial s}) \\
b_z &= \frac{\partial z_1}{\partial s}(U_x \frac{\partial x_0}{\partial s} + U_y \frac{\partial y_0}{\partial s} + U_z \frac{\partial z_0}{\partial s}) - \frac{\partial z_1}{\partial t} + \\
&\quad \frac{\partial z_0}{\partial s}(U_x \frac{\partial x_1}{\partial s} + U_y \frac{\partial y_1}{\partial s} + U_z \frac{\partial z_1}{\partial s} - \frac{\partial x_1}{\partial t}\frac{\partial x_0}{\partial s} - \frac{\partial y_1}{\partial t}\frac{\partial y_0}{\partial s} - \frac{\partial z_1}{\partial t}\frac{\partial z_0}{\partial s})
\end{aligned}
$$

It can be seen that F_{x1}, F_{y1} and F_{z1} are all linear functions of the dynamic displacements x_1, y_1 and z_1. Further, the drag forces permit a decoupling of independent in-plane motion and out-of-plane motion if

1. the static configuration is two dimensional,

2. the current component perpendicular to the plane vanishes.

12.4.6 Effects of Bending Stiffness

Throughout this thesis, the cable is assumed to be perfectly flexible, that is, the cable can not sustain any forces other than the tension. However, our experience tells us that real cables, especially metal ones, when curved tend to straighten out even when unstretched. There must exist some return forces which are dependent upon the cable curvature, that is to say, bending stiffness exists.

This section does not set out to make a full account of the effect of bending stiffness on cable dynamics. A simple two dimensional case is examined to illustrate the consequences of incorporating the bending stiffness into the governing equation. For a more comprehensive three dimensional formulation of the governing equation, see Love (1927), Ertas and Kozik (1987), Kokarakis and Bernitsas (1987).

Consider a two dimensional cable element under the combined action of tension, bending moment, shear force and external force, as shown in Figure A.2 . From Newton's law, the equations of motion are

$$(m+m_{ax})\frac{\partial^2 x}{\partial t^2} - \frac{\partial}{\partial s}(\frac{T}{1+\varepsilon}\frac{\partial x}{\partial s}) - \frac{\partial}{\partial s}(\frac{\tau}{1+\varepsilon}\frac{\partial y}{\partial s}) - F_x = 0 \tag{12.29}$$

$$(m+m_{ay})\frac{\partial^2 y}{\partial t^2} - \frac{\partial}{\partial s}(\frac{T}{1+\varepsilon}\frac{\partial y}{\partial s}) + \frac{\partial}{\partial s}(\frac{\tau}{1+\varepsilon}\frac{\partial x}{\partial s}) - F_y = 0 \tag{12.30}$$

Neglecting the rotary inertia effect, we have the following relation between the bending moment M and the shear force τ

$$\frac{\partial M}{\partial s} = \tau(1+\varepsilon)$$

The bending moment is related to curvature by the following equation

$$M = \frac{EI}{(1+\varepsilon)^3}\left(\frac{\partial x}{\partial s}\frac{\partial^2 y}{\partial s^2} - \frac{\partial y}{\partial s}\frac{\partial^2 x}{\partial s^2}\right)$$

We now proceed with simplifications under the following special conditions

$$1+\varepsilon \approx 1$$

$$\frac{\partial T}{\partial s} = 0$$

$$\frac{\partial y}{\partial s} \ll \frac{\partial x}{\partial s} \approx 1$$

The physical meaning of these conditions is that we are considering a horizontally placed small sagged cable subject to constant tension. In this particular case, the lateral motion becomes

$$\mu\frac{\partial^2 y}{\partial t^2} - T\frac{\partial^2 y}{\partial s^2} + EI\frac{\partial^4 y}{\partial s^4} - F_y = 0 \qquad (12.31)$$

For the homogeneous solution ($F_y = 0$), assuming the cable can still support the wave motion

$$y = y_0 exp[\sqrt{-1}(\omega t - ks)]$$

we have

$$\omega = k\sqrt{\frac{T}{\mu} + \frac{EI}{\mu}k^2}$$

This indicates a feature of dispersion. As a result, a non-sinusoidal disturbance can not be propagated without change of its shape. Also the presence of the bending stiffness stiffens the system. This is manifested through an increase in the frequency for a specific wave number.

12.5 ANALYSIS IN A NATURAL COORDINATE SYSTEM

12.5.1 Cable Equations

Sometimes it is desirable to analyse cable dynamics in a natural coordinate system which is aligned normally and tangentially to the cable, for example, when the hydrodynamic forces are decomposed into normal and tangential components.

Let **Tr** be a transform matrix which transforms a vector from the Cartesian coordinate system $\{x, y, z\}$ to the natural coordinate system $\{x', y', z'\}$, as shown in Figure A.3. **Tr** is given by

$$\mathbf{Tr} = \begin{bmatrix} sin\theta & -cos\theta & 0 \\ sin\phi cos\theta & sin\phi sin\theta & -cos\phi \\ cos\phi cos\theta & cos\phi sin\theta & sin\phi \end{bmatrix} \tag{12.32}$$

where ϕ and θ are two rotation angles defined in the figure.

Since **Tr** is orthogonal, we have

$$\mathbf{Tr}^{-1} = \mathbf{Tr}^{T} = \begin{bmatrix} sin\theta & sin\phi cos\theta & cos\phi cos\theta \\ -cos\theta & sin\phi sin\theta & cos\phi sin\theta \\ 0 & -cos\phi & sin\phi \end{bmatrix} \tag{12.33}$$

The following part of this section shows how the cable equations in the Cartesian coordinate system can be transformed into equations in the natural coordinate system.

Firstly, consider the term $\frac{1}{1+\varepsilon}\frac{\partial \mathbf{r}}{\partial s}$, which is a unit vector tangent to the cable. In the natural coordinate system it must be equal to $[0\ 0\ 1]^T$, i.e.,

$$\mathbf{Tr}(\frac{1}{1+\varepsilon}\frac{\partial \mathbf{r}}{\partial s}) = \begin{bmatrix} 0 \\ 0 \\ 1 \end{bmatrix}$$

or

$$\frac{1}{1+\varepsilon}\begin{bmatrix} \frac{\partial x}{\partial s} \\ \frac{\partial y}{\partial s} \\ \frac{\partial z}{\partial s} \end{bmatrix} = \mathbf{Tr}^{-1}\begin{bmatrix} 0 \\ 0 \\ 1 \end{bmatrix}$$

which gives the following relations:

$$\begin{bmatrix} \frac{\partial x}{\partial s} \\ \frac{\partial y}{\partial s} \\ \frac{\partial z}{\partial s} \end{bmatrix} = (1+\varepsilon)\begin{bmatrix} cos\phi cos\theta \\ cos\phi sin\theta \\ sin\phi \end{bmatrix} \tag{12.34}$$

Secondly, let $F_{x'}$, $F_{y'}$ and $F_{z'}$ be forces per unit length acting upon the cable along the three axes of the natural coordinate system. We have

$$\begin{bmatrix} F_x \\ F_y \\ F_z \end{bmatrix} = \mathbf{Tr}^{-1}\begin{bmatrix} F_{x'} \\ F_{y'} \\ F_{z'} \end{bmatrix} \tag{12.35}$$

Finally, let $V_{x'}$, $V_{y'}$ and $V_{z'}$ be the velocity components of the cable along the three axes respectively. Their relation to the velocity components in the Cartesian

coordinate system is given by

$$\begin{bmatrix} \frac{\partial x}{\partial t} \\ \frac{\partial y}{\partial t} \\ \frac{\partial z}{\partial t} \end{bmatrix} = \mathbf{Tr}^{-1} \begin{bmatrix} V_{x'} \\ V_{y'} \\ V_{z'} \end{bmatrix} \tag{12.36}$$

Taking derivatives of both sides with respect to t, we have

$$\begin{bmatrix} \frac{\partial^2 x}{\partial t} \\ \frac{\partial^2 y}{\partial t} \\ \frac{\partial^2 z}{\partial t} \end{bmatrix} = \frac{\partial}{\partial t}(\mathbf{Tr}^{-1}) \begin{bmatrix} V_{x'} \\ V_{y'} \\ V_{z'} \end{bmatrix} + \mathbf{Tr}^{-1} \begin{bmatrix} \frac{\partial V_{x'}}{\partial t} \\ \frac{\partial V_{y'}}{\partial t} \\ \frac{\partial V_{z'}}{\partial t} \end{bmatrix} \tag{12.37}$$

Substituting Eqs. (12.34), (12.35) and (12.37) into Eq. (12.5), we have

$$\frac{\partial}{\partial t}(\mathbf{Tr}^{-1}) \begin{bmatrix} \mu_{x'} V_{x'} \\ \mu_{y'} V_{y'} \\ \mu_{z'} V_{z'} \end{bmatrix} + \mathbf{Tr}^{-1} \begin{bmatrix} \mu_{x'} \frac{\partial V_{x'}}{\partial t} \\ \mu_{y'} \frac{\partial V_{y'}}{\partial t} \\ \mu_{z'} \frac{\partial V_{z'}}{\partial t} \end{bmatrix} = \begin{bmatrix} \frac{\partial}{\partial s}(T cos\phi cos\theta) \\ \frac{\partial}{\partial s}(T cos\phi sin\theta) \\ \frac{\partial}{\partial s}(T sin\phi) \end{bmatrix} + \mathbf{Tr}^{-1} \begin{bmatrix} F_{x'} \\ F_{y'} \\ F_{z'} \end{bmatrix}$$

where

$$\begin{aligned} \mu_{x'} &= m + m_{ax'} \\ \mu_{y'} &= m + m_{ay'} \\ \mu_{z'} &= m + m_{az'} \end{aligned}$$

Multiplying both sides by $\mathbf{Tr}$ produces the equation

$$\begin{bmatrix} \mu_{x'} \frac{\partial V_{x'}}{\partial t} \\ \mu_{y'} \frac{\partial V_{y'}}{\partial t} \\ \mu_{z'} \frac{\partial V_{z'}}{\partial t} \end{bmatrix} + \mathbf{Tr} \frac{\partial}{\partial t}(\mathbf{Tr}^{-1}) \begin{bmatrix} \mu_{x'} V_{x'} \\ \mu_{y'} V_{y'} \\ \mu_{z'} V_{z'} \end{bmatrix} = \mathbf{Tr} \begin{bmatrix} \frac{\partial}{\partial s}(T cos\phi cos\theta) \\ \frac{\partial}{\partial s}(T cos\phi sin\theta) \\ \frac{\partial}{\partial s}(T sin\phi) \end{bmatrix} + \begin{bmatrix} F_{x'} \\ F_{y'} \\ F_{z'} \end{bmatrix} \tag{12.38}$$

After some mathematical manipulation, the two terms in the equation above can be simplified to

$$\mathbf{Tr}\frac{\partial}{\partial s}\begin{bmatrix} T cos\phi cos\theta \\ T cos\phi sin\theta \\ T sin\phi \end{bmatrix} = \begin{bmatrix} -T cos\phi \frac{\partial\theta}{\partial s} \\ -T\frac{\partial\phi}{\partial s} \\ \frac{\partial T}{\partial s} \end{bmatrix}$$

and

$$\mathbf{Tr}\frac{\partial}{\partial t}(\mathbf{Tr}^{-1}) = \begin{bmatrix} 0 & -sin\phi\frac{\partial\theta}{\partial t} & -cos\phi\frac{\partial\theta}{\partial t} \\ sin\phi\frac{\partial\theta}{\partial t} & 0 & -\frac{\partial\phi}{\partial t} \\ cos\phi\frac{\partial\theta}{\partial t} & \frac{\partial\phi}{\partial t} & 0 \end{bmatrix}$$

Substituting these expressions into Eq. (12.38), we obtain the following equations of motion in the natural coordinate system,

$$\begin{aligned} \mu_{x'}\frac{\partial V_{x'}}{\partial t} - \mu_{y'}V_{y'}sin\phi\frac{\partial\theta}{\partial t} - \mu_{z'}V_{z'}cos\phi\frac{\partial\theta}{\partial t} &= -T cos\phi\frac{\partial\theta}{\partial s} + F_{x'} \\ \mu_{y'}\frac{\partial V_{y'}}{\partial t} + \mu_{x'}V_{x'}sin\phi\frac{\partial\theta}{\partial t} - \mu_{z'}V_{z'}\frac{\partial\phi}{\partial t} &= -T\frac{\partial\phi}{\partial s} + F_{y'} \\ \mu_{z'}\frac{\partial V_{z'}}{\partial t} + \mu_{x'}V_{x'}cos\phi\frac{\partial\theta}{\partial t} + \mu_{y'}V_{y'}\frac{\partial\phi}{\partial t} &= \frac{\partial T}{\partial s} + F_{z'} \end{aligned}$$

Since the natural coordinate system, which is fixed on the cable, changes both in time and space, there is no apparent relationship such as Eq. (12.3) to define the strain by displacements. Geometrical relations need to be explored in order to provide more equations to enclose the system.

Taking the space derivative of both sides of Eq. (12.36), we obtain,

$$\frac{\partial}{\partial s}\begin{bmatrix} \frac{\partial x}{\partial t} \\ \frac{\partial y}{\partial t} \\ \frac{\partial z}{\partial t} \end{bmatrix} = \frac{\partial}{\partial s}(\mathbf{Tr}^{-1})\begin{bmatrix} V_{x'} \\ V_{y'} \\ V_{z'} \end{bmatrix} + \mathbf{Tr}^{-1}\begin{bmatrix} \frac{\partial V_{x'}}{\partial s} \\ \frac{\partial V_{y'}}{\partial s} \\ \frac{\partial V_{z'}}{\partial s} \end{bmatrix} \tag{12.39}$$

From Eq. (12.34) we have,

$$\frac{\partial}{\partial s}\begin{bmatrix} \frac{\partial x}{\partial t} \\ \frac{\partial y}{\partial t} \\ \frac{\partial z}{\partial t} \end{bmatrix} = \frac{\partial}{\partial t}\begin{bmatrix} \frac{\partial x}{\partial s} \\ \frac{\partial y}{\partial s} \\ \frac{\partial z}{\partial s} \end{bmatrix} = \frac{\partial}{\partial t}\begin{bmatrix} (1+\varepsilon)cos\phi cos\theta \\ (1+\varepsilon)cos\phi sin\theta \\ (1+\varepsilon)sin\phi \end{bmatrix}$$

Thus Eq. (12.39) becomes the following after multiplication of both sides by **Tr**,

$$\begin{bmatrix} \frac{\partial V_{x'}}{\partial s} \\ \frac{\partial V_{y'}}{\partial s} \\ \frac{\partial V_{z'}}{\partial s} \end{bmatrix} = \mathbf{Tr}\frac{\partial}{\partial t}\begin{bmatrix} (1+\varepsilon)cos\phi cos\theta \\ (1+\varepsilon)cos\phi sin\theta \\ (1+\varepsilon)sin\phi \end{bmatrix} - \mathbf{Tr}\frac{\partial}{\partial s}(\mathbf{Tr}^{-1})\begin{bmatrix} V_{x'} \\ V_{y'} \\ V_{z'} \end{bmatrix} \tag{12.40}$$

The two terms on the right side can be simplified to obtain,

$$\mathbf{Tr}\frac{\partial}{\partial t}\begin{bmatrix} (1+\varepsilon)cos\phi cos\theta \\ (1+\varepsilon)cos\phi sin\theta \\ (1+\varepsilon)sin\phi \end{bmatrix} = \begin{bmatrix} -(1+\varepsilon)cos\phi\frac{\partial\theta}{\partial t} \\ -(1+\varepsilon)\frac{\partial\phi}{\partial t} \\ \frac{\partial\varepsilon}{\partial t} \end{bmatrix}$$

and

$$\mathbf{Tr}\frac{\partial}{\partial s}(\mathbf{Tr}^{-1}) = \begin{bmatrix} 0 & -sin\phi\frac{\partial\theta}{\partial s} & -cos\phi\frac{\partial\theta}{\partial s} \\ sin\phi\frac{\partial\theta}{\partial s} & 0 & -\frac{\partial\phi}{\partial s} \\ cos\phi\frac{\partial\theta}{\partial s} & \frac{\partial\phi}{\partial s} & 0 \end{bmatrix}$$

Substituting the above into Eq. (12.40), we have,

$$\begin{aligned}
\frac{\partial V_{x'}}{\partial s} &= -(1+\varepsilon)cos\phi\frac{\partial\theta}{\partial t} + V_{y'}sin\phi\frac{\partial\theta}{\partial s} + V_{z'}cos\phi\frac{\partial\theta}{\partial s} \\
\frac{\partial V_{y'}}{\partial s} &= -(1+\varepsilon)\frac{\partial\phi}{\partial t} - V_{x'}sin\phi\frac{\partial\theta}{\partial s} + V_{z'}\frac{\partial\phi}{\partial s} \\
\frac{\partial V_{z'}}{\partial s} &= \frac{\partial\varepsilon}{\partial t} - V_{x'}cos\phi\frac{\partial\theta}{\partial s} - V_{y'}\frac{\partial\phi}{\partial s}
\end{aligned}$$

In summary, there are seven equations governing the cable dynamics in a natural coordinate system for the seven unknowns $\varepsilon, \phi, \theta, V_{x'}, V_{y'}, V_{z'}$ and T. They are as follows:

$$\begin{aligned}
\mu_{x'}\frac{\partial V_{x'}}{\partial t} - \mu_{y'}V_{y'}sin\phi\frac{\partial\theta}{\partial t} - \mu_{z'}V_{z'}cos\phi\frac{\partial\theta}{\partial t} + Tcos\phi\frac{\partial\theta}{\partial s} - F_{x'} &= 0 \\
\mu_{y'}\frac{\partial V_{y'}}{\partial t} + \mu_{x'}V_{x'}sin\phi\frac{\partial\theta}{\partial t} - \mu_{z'}V_{z'}\frac{\partial\phi}{\partial t} + T\frac{\partial\phi}{\partial s} - F_{y'} &= 0 \\
\mu_{z'}\frac{\partial V_{z'}}{\partial t} + \mu_{x'}V_{x'}cos\phi\frac{\partial\theta}{\partial t} + \mu_{y'}V_{y'}\frac{\partial\phi}{\partial t} - \frac{\partial T}{\partial s} - F_{z'} &= 0 \\
\frac{\partial V_{x'}}{\partial s} + (1+\varepsilon)cos\phi\frac{\partial\theta}{\partial t} - V_{y'}sin\phi\frac{\partial\theta}{\partial s} - V_{z'}cos\phi\frac{\partial\theta}{\partial s} &= 0 \\
\frac{\partial V_{y'}}{\partial s} + (1+\varepsilon)\frac{\partial\phi}{\partial t} + V_{x'}sin\phi\frac{\partial\theta}{\partial s} - V_{z'}\frac{\partial\phi}{\partial s} &= 0 \\
\frac{\partial V_{z'}}{\partial s} - \frac{\partial\varepsilon}{\partial t} + V_{x'}cos\phi\frac{\partial\theta}{\partial s} + V_{y'}\frac{\partial\phi}{\partial s} &= 0 \\
T - T(\varepsilon) &= 0
\end{aligned} \qquad (12.41)$$

12.5.2 Characteristics

In this section, basic properties associated with the system of nonlinear partial differential equations, Eq. (12.41), are examined. For brevity of notation, all primes are omitted.

We can rewrite Eq. (12.41) in the following form:

$$\mathbf{A}\frac{\partial \mathbf{Y}}{\partial t} + \mathbf{B}\frac{\partial \mathbf{Y}}{\partial s} + \mathbf{C} = \mathbf{0} \tag{12.42}$$

where

$$\mathbf{Y} = \begin{bmatrix} \varepsilon \\ \phi \\ \theta \\ V_z \\ V_y \\ V_x \end{bmatrix}$$

$$\mathbf{A} = \begin{bmatrix} 0 & \mu_y V_y & \mu_x V_x cos\phi & \mu_z & 0 & 0 \\ 0 & -\mu_z V_z & \mu_x V_x sin\phi & 0 & \mu_y & 0 \\ 0 & 0 & -\mu_y V_y sin\phi - \mu_z V_z cos\phi & 0 & 0 & \mu_x \\ -1 & 0 & 0 & 0 & 0 & 0 \\ 0 & 1+\varepsilon & 0 & 0 & 0 & 0 \\ 0 & 0 & (1+\varepsilon)cos\phi & 0 & 0 & 0 \end{bmatrix}$$

$$\mathbf{B} = \begin{bmatrix} -T_\varepsilon & 0 & 0 & 0 & 0 & 0 \\ 0 & T & 0 & 0 & 0 & 0 \\ 0 & 0 & Tcos\phi & 0 & 0 & 0 \\ 0 & V_y & V_x cos\phi & 1 & 0 & 0 \\ 0 & -V_z & V_x sin\phi & 0 & 1 & 0 \\ 0 & 0 & -(V_y sin\phi + V_z cos\phi) & 0 & 0 & 1 \end{bmatrix}$$

$$\mathbf{C} = \begin{bmatrix} -F_z \\ -F_y \\ -F_x \\ 0 \\ 0 \\ 0 \end{bmatrix}$$

Eq. (12.42) can be further transformed into a standard quasi-linear form:

$$\frac{\partial \mathbf{Y}}{\partial t} + \mathbf{A}^{-1}\mathbf{B}\frac{\partial \mathbf{Y}}{\partial s} + \mathbf{A}^{-1}\mathbf{C} = \mathbf{0} \tag{12.43}$$

To find the inversion of the matrix **A**, it is partitioned into the following form:

$$\mathbf{A} = \begin{bmatrix} \mathbf{D} & \mathbf{E} \\ \mathbf{F} & \mathbf{0} \end{bmatrix}$$

where **D**, **E** and **F** are all 3×3 matrices:

$$\mathbf{D} = \begin{bmatrix} 0 & \mu_y V_y & \mu_x V_x cos\phi \\ 0 & -\mu_z V_z & \mu_x V_x sin\phi \\ 0 & 0 & -\mu_y V_y sin\phi - \mu_z V_z cos\phi \end{bmatrix}$$

$$\mathbf{E} = \begin{bmatrix} \mu_z & 0 & 0 \\ 0 & \mu_y & 0 \\ 0 & 0 & \mu_x \end{bmatrix}$$

$$\mathbf{F} = \begin{bmatrix} -1 & 0 & 0 \\ 0 & 1+\varepsilon & 0 \\ 0 & 0 & (1+\varepsilon)cos\phi \end{bmatrix}$$

Denoting

$$\mathbf{A}^{-1} = \begin{bmatrix} \mathbf{A}_{11} & \mathbf{A}_{12} \\ \mathbf{A}_{21} & \mathbf{A}_{22} \end{bmatrix}$$

where $\mathbf{A}_{11}, \mathbf{A}_{12}, \mathbf{A}_{21}$ and $\mathbf{A}_{22}$ are all 3×3 matrices, we have

$$\begin{bmatrix} \mathbf{D} & \mathbf{E} \\ \mathbf{F} & \mathbf{0} \end{bmatrix} \begin{bmatrix} \mathbf{A}_{11} & \mathbf{A}_{12} \\ \mathbf{A}_{21} & \mathbf{A}_{22} \end{bmatrix} = \begin{bmatrix} \mathbf{I} & \mathbf{0} \\ \mathbf{0} & \mathbf{I} \end{bmatrix}$$

This is equivalent to the following:

$$\begin{aligned} \mathbf{D}\mathbf{A}_{11} + \mathbf{E}\mathbf{A}_{21} &= \mathbf{I} \\ \mathbf{D}\mathbf{A}_{12} + \mathbf{E}\mathbf{A}_{22} &= \mathbf{0} \\ \mathbf{F}\mathbf{A}_{11} &= \mathbf{0} \\ \mathbf{F}\mathbf{A}_{12} &= \mathbf{I} \end{aligned}$$

From this set of matrix equations, it is easy to derive the following results:

$$\begin{aligned} \mathbf{A}_{11} &= \mathbf{0} \\ \mathbf{A}_{12} &= \begin{bmatrix} -1 & 0 & 0 \\ 0 & \frac{1}{1+\epsilon} & 0 \\ 0 & 0 & \frac{1}{(1+\epsilon)cos\phi} \end{bmatrix} \end{aligned}$$

$$\mathbf{A}_{21} = \begin{bmatrix} \frac{1}{\mu_x} & 0 & 0 \\ 0 & \frac{1}{\mu_y} & 0 \\ 0 & 0 & \frac{1}{\mu_x} \end{bmatrix}$$

$$\mathbf{A}_{22} = \begin{bmatrix} 0 & -\frac{\mu_y V_y}{(1+\epsilon)\mu_x} & \frac{\mu_x V_x}{(1+\epsilon)\mu_x} \\ 0 & \frac{\mu_x V_x}{(1+\epsilon)\mu_y} & -\frac{\mu_x V_x tan\phi}{(1+\epsilon)\mu_y} \\ 0 & 0 & \frac{\mu_y V_y sin\phi + \mu_x V_x cos\phi}{(1+\epsilon)\mu_x cos\phi} \end{bmatrix}$$

Hence $\mathbf{A}^{-1}$ is given by:

$$\mathbf{A}^{-1} = \begin{bmatrix} 0 & 0 & 0 & -1 & 0 & 0 \\ 0 & 0 & 0 & 0 & \frac{1}{1+\epsilon} & 0 \\ 0 & 0 & 0 & 0 & 0 & \frac{1}{(1+\epsilon)cos\phi} \\ \frac{1}{\mu_x} & 0 & 0 & 0 & -\frac{\mu_y V_y}{(1+\epsilon)\mu_x} & \frac{\mu_x V_x}{(1+\epsilon)\mu_x} \\ 0 & \frac{1}{\mu_y} & 0 & 0 & \frac{\mu_x V_x}{(1+\epsilon)\mu_y} & -\frac{\mu_x V_x tan\phi}{(1+\epsilon)\mu_y} \\ 0 & 0 & \frac{1}{\mu_x} & 0 & 0 & \frac{\mu_y V_y sin\phi + \mu_x V_x cos\phi}{(1+\epsilon)\mu_x cos\phi} \end{bmatrix}$$

and $\mathbf{A}^{-1}\mathbf{B}$ and $\mathbf{A}^{-1}\mathbf{C}$ are given by:

$$\mathbf{A}^{-1}\mathbf{B} = \begin{bmatrix} 0 & -V_y & -V_x cos\phi & -1 & 0 & 0 \\ 0 & \frac{-V_x}{1+\epsilon} & \frac{V_x cos\phi}{1+\epsilon} & 0 & \frac{1}{1+\epsilon} & 0 \\ 0 & 0 & -\frac{V_y sin\phi + V_x cos\phi}{(1+\epsilon)cos\phi} & 0 & 0 & \frac{1}{(1+\epsilon)cos\phi} \\ -\frac{T_x}{\mu_x} & \frac{\mu_y V_y V_x}{(1+\epsilon)\mu_x} & J_1 & 0 & -\frac{\mu_y V_y}{(1+\epsilon)\mu_x} & -\frac{\mu_x V_x}{(1+\epsilon)\mu_x} \\ 0 & \frac{T}{\mu_y} - \frac{\mu_x V_x^2}{(1+\epsilon)\mu_y} & J_2 & 0 & \frac{\mu_x V_x}{(1+\epsilon)\mu_y} & -\frac{\mu_x V_x tan\phi}{(1+\epsilon)\mu_y} \\ 0 & 0 & J_3 & 0 & 0 & \frac{\mu_y V_y sin\phi + \mu_x V_x cos\phi}{(1+\epsilon)\mu_x cos\phi} \end{bmatrix}$$

where

$$J_1 = \frac{\mu_x V_x(V_y sin\phi + V_z cos\phi) - \mu_y V_y V_x sin\phi}{(1+\varepsilon)\mu_z}$$

$$J_2 = \frac{\mu_x V_x(V_y sin\phi + V_z cos\phi)tan\phi + \mu_z V_z V_x sin\phi}{(1+\varepsilon)\mu_y}$$

$$J_3 = \frac{T cos\phi}{\mu_x} - \frac{(\mu_y V_y sin\phi + \mu_z V_z cos\phi)(V_y sin\phi + V_z cos\phi)}{(1+\varepsilon)\mu_x cos\phi}$$

$$\mathbf{A}^{-1}\mathbf{C} = \begin{bmatrix} 0 \\ 0 \\ 0 \\ -\frac{F_z}{\mu_z} \\ -\frac{F_y}{\mu_y} \\ -\frac{F_x}{\mu_x} \end{bmatrix}$$

The eigenvalues of the system can be obtained by solving the following equation:

$$|\mathbf{A}^{-1}\mathbf{B} - \lambda\mathbf{I}| = 0 \tag{12.44}$$

i.e.,

$$\begin{vmatrix} -\lambda & -V_y & -V_x cos\phi & -1 & 0 & 0 \\ 0 & \frac{-V_z}{1+\epsilon} - \lambda & \frac{V_x cos\phi}{1+\epsilon} & 0 & \frac{1}{1+\epsilon} & 0 \\ 0 & 0 & -\frac{V_y sin\phi + V_z cos\phi}{(1+\epsilon)cos\phi} - \lambda & 0 & 0 & \frac{1}{(1+\epsilon)cos\phi} \\ -\frac{T_e}{\mu_z} & \frac{\mu_y V_y V_z}{(1+\epsilon)\mu_z} & J_1 & -\lambda & -\frac{\mu_y V_y}{(1+\epsilon)\mu_z} & -\frac{\mu_z V_z}{(1+\epsilon)\mu_z} \\ 0 & \frac{T}{\mu_y} - \frac{\mu_z V_z^2}{(1+\epsilon)\mu_y} & J_2 & 0 & \frac{\mu_z V_z}{(1+\epsilon)\mu_y} - \lambda & -\frac{\mu_z V_z tan\phi}{(1+\epsilon)\mu_y} \\ 0 & 0 & J_3 & 0 & 0 & \frac{\mu_y V_y sin\phi + \mu_z V_z cos\phi}{(1+\epsilon)\mu_x cos\phi} - \lambda \end{vmatrix} = 0$$

Taking the Laplace expansion of the first column, the determinant becomes:

$$-\lambda \begin{vmatrix} \frac{-V_z}{1+\epsilon} - \lambda & \frac{V_x cos\phi}{1+\epsilon} & 0 & \frac{1}{1+\epsilon} & 0 \\ 0 & -\frac{V_y sin\phi + V_z cos\phi}{(1+\epsilon)cos\phi} - \lambda & 0 & 0 & \frac{1}{(1+\epsilon)cos\phi} \\ \frac{\mu_y V_y V_z}{(1+\epsilon)\mu_z} & J_1 & -\lambda & -\frac{\mu_y V_y}{(1+\epsilon)\mu_z} & -\frac{\mu_z V_z}{(1+\epsilon)\mu_z} \\ \frac{T}{\mu_y} - \frac{\mu_z V_z^2}{(1+\epsilon)\mu_y} & J_2 & 0 & \frac{\mu_z V_z}{(1+\epsilon)\mu_y} - \lambda & -\frac{\mu_z V_z tan\phi}{(1+\epsilon)\mu_y} \\ 0 & J_3 & 0 & 0 & \frac{\mu_y V_y sin\phi + \mu_z V_z cos\phi}{(1+\epsilon)\mu_x cos\phi} - \lambda \end{vmatrix} +$$

$$\frac{T_e}{\mu_z} \begin{vmatrix} -V_y & -V_x cos\phi & -1 & 0 & 0 \\ \frac{-V_z}{1+\epsilon} - \lambda & \frac{V_x cos\phi}{1+\epsilon} & 0 & \frac{1}{1+\epsilon} & 0 \\ 0 & -\frac{V_y sin\phi + V_z cos\phi}{(1+\epsilon)cos\phi} - \lambda & 0 & 0 & \frac{1}{(1+\epsilon)cos\phi} \\ \frac{T}{\mu_y} - \frac{\mu_z V_z^2}{(1+\epsilon)\mu_y} & J_2 & 0 & \frac{\mu_z V_z}{(1+\epsilon)\mu_y} - \lambda & -\frac{\mu_z V_z tan\phi}{(1+\epsilon)\mu_y} \\ 0 & J_3 & 0 & 0 & \frac{\mu_y V_y sin\phi + \mu_z V_z cos\phi}{(1+\epsilon)\mu_x cos\phi} - \lambda \end{vmatrix}$$

Further expanding the determinant, we have,

$$(\lambda^2 - \frac{T_\varepsilon}{\mu_z}) \begin{vmatrix} \frac{-V_z}{1+\varepsilon} - \lambda & \frac{V_x cos\phi}{1+\varepsilon} & \frac{1}{1+\varepsilon} & 0 \\ 0 & -\frac{V_y sin\phi + V_z cos\phi}{(1+\varepsilon)cos\phi} - \lambda & 0 & \frac{1}{(1+\varepsilon)cos\phi} \\ \frac{T}{\mu_y} - \frac{\mu_z V_z^2}{(1+\varepsilon)\mu_y} & J_2 & \frac{\mu_z V_z}{(1+\varepsilon)\mu_y} - \lambda & -\frac{\mu_z V_x tan\phi}{(1+\varepsilon)\mu_y} \\ 0 & J_3 & 0 & \frac{\mu_y V_y sin\phi + \mu_z V_z cos\phi}{(1+\varepsilon)\mu_x cos\phi} - \lambda \end{vmatrix} = 0$$

Thus the first two eigenvalues are given by,

$$\lambda_{1,2} = \pm\sqrt{\frac{T_\varepsilon}{\mu_z}}$$

Continuing the process of Laplace expansion, we obtain the following two quadratic equations which allow us to determine the rest of the eigenvalues:

$$\begin{aligned} \frac{1}{1+\varepsilon}[\frac{T}{\mu_y} - \frac{\mu_z V_z^2}{(1+\varepsilon)\mu_y}] - [\frac{\mu_z V_z}{(1+\varepsilon)\mu_y} - \lambda](\frac{V_z}{1+\varepsilon} - \lambda) &= 0 \\ -[\frac{\mu_y V_y sin\phi + \mu_z V_z cos\phi}{(1+\varepsilon)\mu_x cos\phi} - \lambda][\frac{V_y sin\phi + V_z cos\phi}{(1+\varepsilon)cos\phi} + \lambda] - \frac{J_3}{(1+\varepsilon)cos\phi} &= 0 \end{aligned}$$

Consequently, the other four eigenvalues are given by

$$\begin{aligned} \lambda_{3,4} &= -\frac{V_z}{2(1+\varepsilon)}(1 - \frac{\mu_z}{\mu_y}) \pm \frac{1}{2}\sqrt{[\frac{V_z}{1+\varepsilon}(1 - \frac{\mu_z}{\mu_y})]^2 + \frac{4T}{(1+\varepsilon)\mu_y}} \\ \lambda_{5,6} &= -\frac{V_z(1 - \frac{\mu_z}{\mu_x}) + tan\phi V_y(1 - \frac{\mu_y}{\mu_x})}{2(1+\varepsilon)} \pm \\ & \quad \frac{1}{2}\sqrt{[\frac{V_z(1 - \frac{\mu_z}{\mu_x}) + tan\phi V_y(1 - \frac{\mu_y}{\mu_x})}{1+\varepsilon}]^2 + \frac{4T}{(1+\varepsilon)\mu_x}} \end{aligned}$$

A total of six real eigenvalues is obtained, so the system of Eq. (12.42) is hyperbolic.

If $\mu_x = \mu_y$, then

$$\lambda_{3,4} = \lambda_{5,6}$$

Moreover, if $\mu_x = \mu_y = \mu_z = \mu$, we have

$$\begin{aligned} \lambda_{1,2} &= \pm\sqrt{\frac{T_\varepsilon}{\mu}} \\ \lambda_{3,4} &= \pm\sqrt{\frac{T}{(1+\varepsilon)\mu}} \\ \lambda_{5,6} &= \pm\sqrt{\frac{T}{(1+\varepsilon)\mu}} \end{aligned}$$

12.5.3 Ordinary Differential Equations

In this section we assume

$$\mu_x = \mu_y = \mu_z = \mu$$

The results are given as follows:

1. Along the characteristic line defined by

$$\frac{ds}{dt} = \sqrt{\frac{T_\varepsilon}{\mu}}$$

which represents the travelling-down tensile wave, we have

$$-\sqrt{\frac{T_\varepsilon}{\mu}}d\varepsilon + V_y d\phi + V_x cos\phi d\theta + dV_z - \frac{1}{\mu}F_z dt = 0 \qquad (12.45)$$

2. Along the characteristic line defined by

$$\frac{ds}{dt} = -\sqrt{\frac{T_\varepsilon}{\mu}}$$

which represents the travelling-up tensile wave, we have

$$\sqrt{\frac{T_\varepsilon}{\mu}}d\varepsilon + V_y d\phi + V_x cos\phi d\theta + dV_z - \frac{1}{\mu}F_z dt = 0 \qquad (12.46)$$

3. Along the characteristic line defined by

$$\frac{ds}{dt} = \sqrt{\frac{T}{(1+\varepsilon)\mu}}$$

which represents the travelling-down transverse wave in the $y-z$ plane, we have

$$(\sqrt{\frac{T(1+\varepsilon)}{\mu}} - V_z)d\phi + V_x sin\phi d\theta + dV_y - \frac{1}{\mu}F_y dt = 0 \qquad (12.47)$$

4. Along the characteristic line defined by

$$\frac{ds}{dt} = -\sqrt{\frac{T}{(1+\varepsilon)\mu}}$$

which represents the travelling-up transverse wave in the $y-z$ plane, we have

$$-(\sqrt{\frac{T(1+\varepsilon)}{\mu}} + V_z)d\phi + V_x sin\phi d\theta + dV_y - \frac{1}{\mu}F_y dt = 0 \qquad (12.48)$$

5. Along the characteristic line defined by

$$\frac{ds}{dt} = \sqrt{\frac{T}{(1+\varepsilon)\mu}}$$

which represents the travelling-down transverse wave in the $x-z$ plane, we have

$$(\sqrt{\frac{T(1+\varepsilon)}{\mu}} cos\phi - V_y sin\phi - V_z cos\phi)d\theta + dV_x - \frac{1}{\mu}F_x dt = 0 \qquad (12.49)$$

6. Along the characteristic line defined by

$$\frac{ds}{dt} = -\sqrt{\frac{T}{(1+\varepsilon)\mu}}$$

which represents the travelling-up transverse wave in the $x-z$ plane, we have

$$-(\sqrt{\frac{T(1+\varepsilon)}{\mu}} cos\phi + V_y sin\phi + V_z cos\phi)d\theta + dV_x - \frac{1}{\mu}F_x dt = 0 \qquad (12.50)$$

As a consequence of their the dependence upon the state of the tension and strain of the cable, the characteristic lines of the transverse waves diverge in the space-time domain in contrast to the fixed parallel characteristic lines of the longitudinal tensile waves. This indeed casts disadvantages upon the natural numerical method of characteristics. Nevertheless, numerical methods of characteristics for this type of hyperbolic system are still available (Courant et al, 1952; Hartree, 1958; Jeffrey and Taniuti, 1964; Ames, 1969; Patton, 1972).

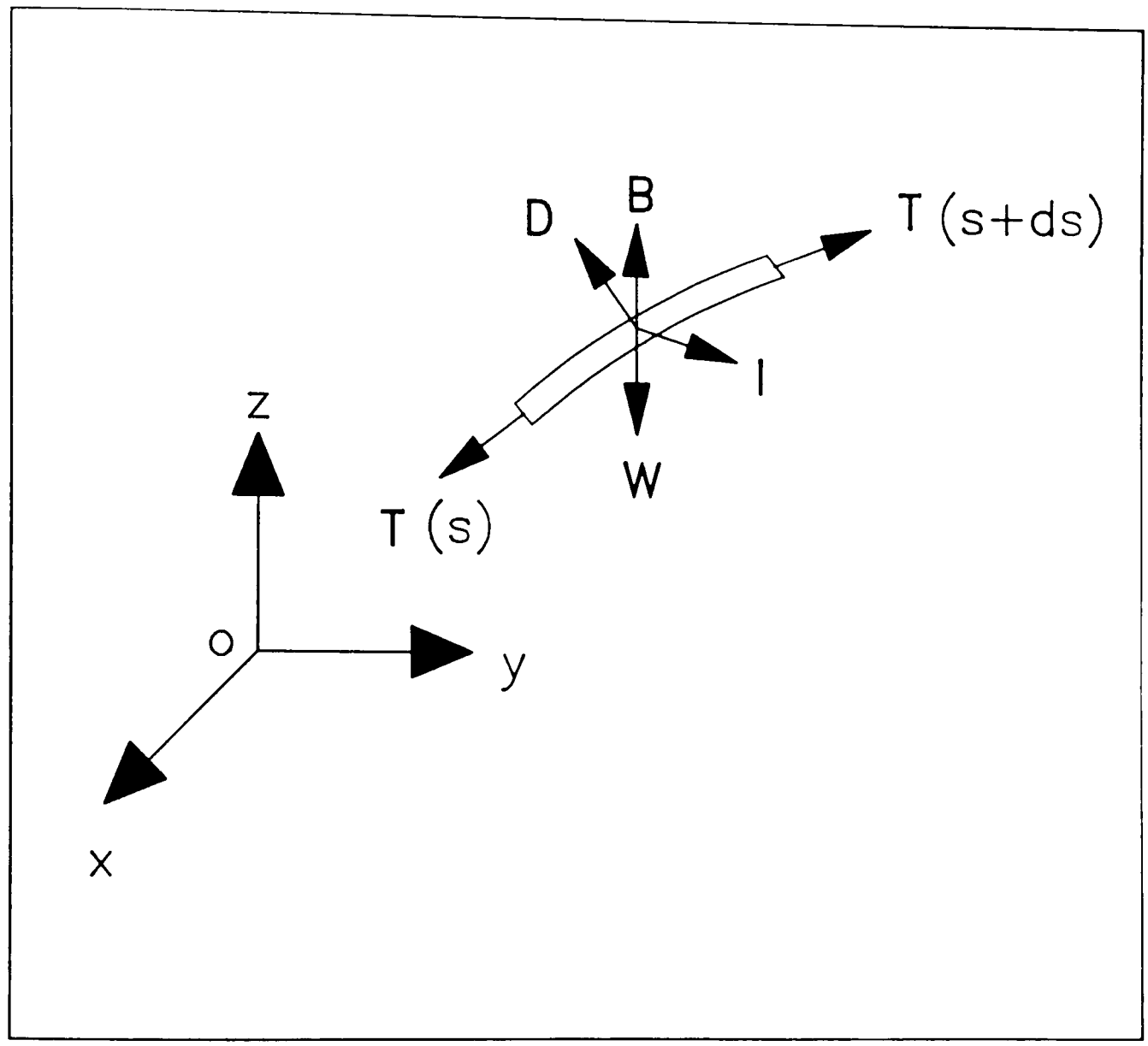

Figure A.1. Coordinate system and forces on a cable element

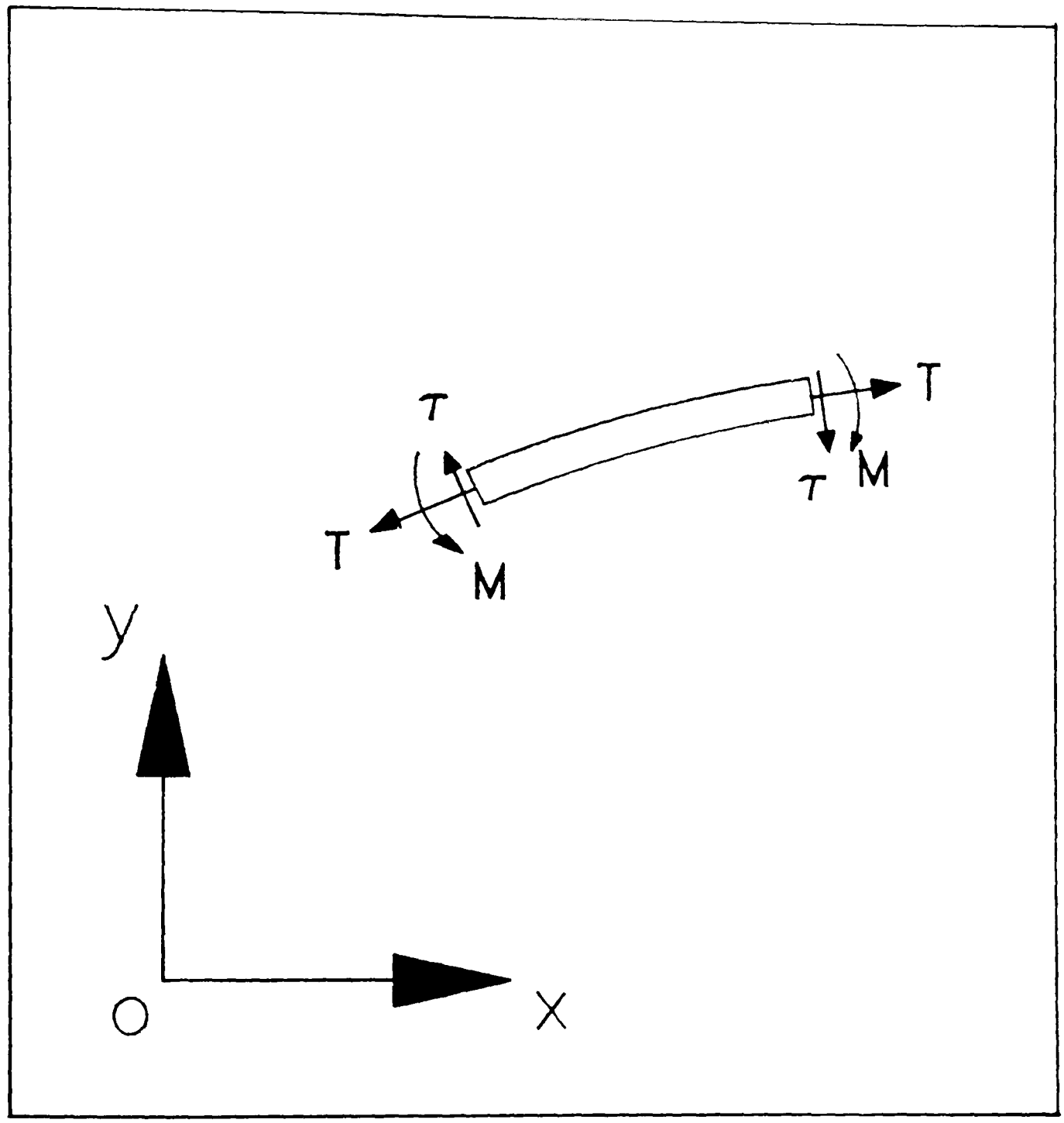

Figure A.2.

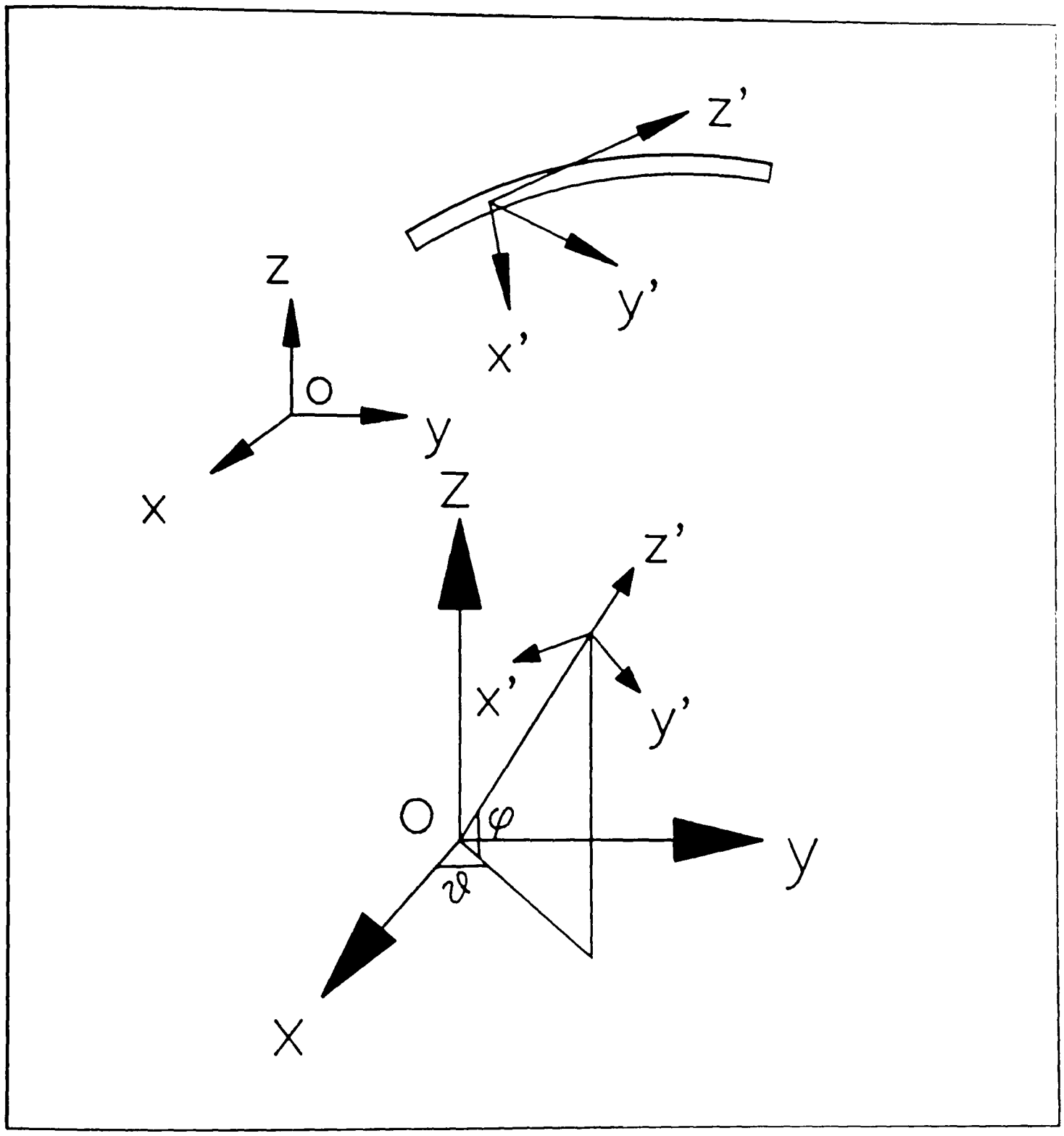

Figure A.3.